Investigation the relationship between increased intracellular branched chain amino acid concentrations and insulin-stimulated glucose uptake in muscle cells

QIONG YIN, BSc., MSc.

Thesis submitted to The University of Nottingham for the degree of Doctor of Philosophy, April 2019

Division of Food, Nutrition and Dietetics,
School of Biosciences
University of Nottingham
Sutton Bonington Campus
Lougborough
LE12 5RD

ABSTRACT

Type 2 diabetes is a metabolic disorder that result in high blood glucose level, due to the insulin resistance in insulin target tissue, such as skeletal muscle. In skeletal muscle, insulin resistance is manifested by decreased insulin-stimulated glucose transport and further a decline in glucose uptake. Branched chain amino acids (leucine, valine and isoleucine) are involved in protein synthesis and degradation and are crucial for growth. However, recent studies revealed a link between elevated circulating BCAAs and insulin resistance in obesity and normal weight subjects. Many studies pointed that this link was connected by mTOR, as both leucine and insulin seem to activate different signalling pathways that converge at mTOR. Previous studies have indicated that increased intracellular BCAA concentrations in muscle cells impair glucose uptake, purportedly through the activity of mTOR. However, this conclusion is controversial and the mechanisms are unclear. Therefore, the overall aim of this thesis was to investigate the relationship between increased intracellular BCAAs and glucose uptake in muscle cells and the mechanisms involved.

L6 myotubes displayed a 2-fold increase in glucose uptake in response to insulin, but C2C12 cells did not, suggesting that L6 myotubes are a better in vitro model system to investigate glucose uptake in muscle cells. Based on experiments in L6 myotubes, the results showed that rapamycin (mTOR inhibitor) and BCH (L-type amino acid transporter 1 inhibitor) reduced basal and insulin-stimulated glucose uptake. They also reduced phosphorylation of mTOR

and downstream target proteins (4E-BP1 and p70S6K) but had no effect on phosphorylation of Akt (upstream protein of mTOR). In addition, increased leucine concentrations were associated with increased glucose uptake by L6 myotubes after long-time treatment (24 and 48 hours), but there was little or no effect on insulin-induced glucose uptake. This effect was independent of phosphorylation of mTOR, downstream target proteins and Akt. After repeating the leucine experiments in C2C12 muscle cells, it showed similar results, increased leucine concentrations increased glucose uptake in C2C12 myotubes, but only in the absence of insulin, and this was more obvious after 48 hours treatment. In addition, the glucose uptake of C2C12 myotubes did not respond to insulin stimulation, but there was no difference between L6 and C2C12 cells in GLUT4 mRNA expression.

Together, this thesis reports that mTOR activity is associated with glucose uptake in L6 myotubes, but is independent of phosphorylation of Akt. Increased Leucine concentrations increased glucose uptake, with no effect on phosphorylation of mTOR and Akt. This might be because leucine increased GLUT4 translocation or expression of other glucose transporters.

ACKNOWLEDGEMENTS

Firstly, I would like to express my sincere gratitude to the University of Nottingham for sponsoring my three years PhD programme and my supervisors Prof. Tim Parr, Dr John Brameld and Dr Andrew Murton, for the continuous support of my PhD study and related research, for their patience, motivation, and immense knowledge. Their guidance helped me in all the time of research and writing of this thesis. I could not have imagined having the better supervisors for my PhD study.

Next, I would thank the technicians, Cathy Wells, Kirsty Jewell, Sarah Jones and Zoe Daniel, for training me in molecular and cell biology techniques. I really learned many techniques during these three years lab work. Besides, I am very grateful that Dr. Zoe Daniel who help me to do the qPCR experiment. The faculty members of Nutrition Science have been very kind enough to extend their help at various phases of this research, whenever I approached them, and I do hereby acknowledge all of them.

I would also like to thank my fellow PhD colleagues for making such a fun and friendly environment in the office or gym: Yihe (Lily), Amanda, Kimberley, Zoe, Kerensa, Maddy, Xiaoyi (Elaine), Rui and also my friends at Bei Jing for support and accompanying: Lei, Yaqi, Min (Zhao), Min (Yang), Xi, Siyuan, Xin, Nan, Deyu, Bante, Rundi and Yuxi.

Last but not the least, I would like to thank my family members: my parents Wenlan Wang and Huagang Yin who always stand by me and ask for nothing in return. In addition, I greatly thank to my boyfriend Hanxuan Wang, for all your listen, support and encouragement during my four years PhD study and thank you fly from China to UK every year to take care of me.

TABLE OF CONTENTS

List of Figures 10
List of Tables 14
List of Abbreviations 15
CHAPTER 1: INTRODUCTION 19
1.1. World prevalence of diabetes 20
1.2. Diabetes and glucose uptake 23
1.2.1. The classification of diabetes 23
1.2.2. Insulin and glucagon 23
1.2.3 Insulin resistance 26
1.2.4 Glucose uptake in skeletal muscle 29
1.2.5 Glucose metabolism in muscle cells 32
1.3 Branched-Chain Amino Acids (BCAAs) 34
1.3.1 BCAA metabolism 35
1.3.2 Linkage between BCAAs and insulin resistance 37
1.3.3 Why are BCAAs elevated with IR 41
1.4. The possible mechanisms underlying the relationship between circulating BCAAs and IR 43
1.4.1. mTORC1 and mTORC2 44
1.4.2. mTOR signalling pathways 47
1.4.3. mTOR and glucose homeostasis 53
1.4.4. mTOR, BCAAs and glucose uptake 54
1.5. Aim and Objectives 57
1.5.1. Hypothesis and Aim 57
1.5.2. Objectives 59
CHAPTER 2: GENERAL MATERIALS AND METHODS 60
2.1. General materials 61
2.2. Mammalian Cell Culture 61
2.2.1. Techniques for cell culture 61

2.2.2. L6 Cell line 61
2.2.3. C2C12 cell line 64
2.3 Adeno-Associated Viruses (AAV) 65
2.3.1 Preparing of samples and reagents 65
2.3.2 Determination of the MOI (multiplicity of infections) 67
2.3.3 Protocol for *in vitro* cell transduction 68
2.4 Glucose uptake Assay 69
2.4.1 Principle 69
2.4.2 Sample preparation 72
2.4.3 Reagent preparation 72
2.4.4 Procedure 72
2.5 Intracellular BCAAs Assay 73
2.5.1 Spectrophotometric Assay for Measuring Branched-Chain Amino Acids 74
2.5.2 BCAAs Assay kit (K564-100) 75
2.6. Western Blot 77
2.6.1. Preparing of reagents 77
2.6.2. Collecting cell samples for western blot analysis 79
2.6.3. Quantification of protein concentration by 2D Quant kit method 79
2.6.4. Polyacrylamide gel electrophoresis (PAGE) 81
2.6.5. Transfer gels to polyvinylidene difluoride membrane 81
2.5.8 Ponceau-S stain and Blocking 84
2.6.7. Primary and secondary antibody 85
2.6.8. Detection 86
2.6.9. Stripping 86
2.7. Real Time Quantitative Polymerase Chain Reaction (RTqPCR) 87
2.7.1. Collecting cell samples 87
2.7.2. RNA extraction methods 87
2.7.3. RevertAid RT First Strand cDNA Synthesis kit 88
2.7.4. Real time quantitative PCR (RTqPCR) 88
2.7.5. Primer designs and synthesis 88
2.8. Statistics 89

CHAPTER 3: EXAMINATION OF WHETHER ACUTELY INCREASED INTRACELLULAR BCAA CONCENTRATIONS INFLUENCE GLUCOSE UPTAKE IN CULTURED MUSCLE CELLS 90
3.1. Introduction 91
3.2. Materials and Methods 93
3.2.1. The treatment of C2C12 cells 94
3.2.2. Determination of intracellular BCAA concentrations 95
3.2.3. Western blot antibodies 95
3.2.4. L6 and C2C12 cells treated for glucose uptake and RTqPCR 96
3.2.5. Statistical Analyses 96
3.3. Results 96
3.3.1. Effects of 30 minutes CHX treatment on C2C12 cells 96
3.3.2. Intracellular BCAA concentrations in C2C12 myotubes after 30 minutes CHX treatment 99
3.3.3. Effects of 30 minutes CHX treatment on mTOR and downstream target proteins in C2C12 myotubes 101
3.3.4. Effects of 30 minutes CHX on Beta-actin in C2C12 myotubes 104
3.3.5. A comparison of insulin-stimulated glucose uptake between L6 and C2C12 Myotubes 105
3.3.6. The gene expressions of glucose transporters in L6 and C2C12 myotubes 107
3.4. Discussion and Conclusion 109
CHAPTER 4: EXAMINATION OF WHETHER mTOR IS INVOLVED IN GLUCOSE UPTAKE 115
4.1. Introduction 116
4.2. Methods 119
4.2.1. Effects of Rapamycin treatment on insulin-stimulated glucose uptake and mTOR signalling in L6 myotubes 119
4.2.2. Effects of Rapamycin and 3BDO treatments on insulin-stimulated glucose uptake and mTOR signalling in L6 myotubes 120
4.2.3. Effects of Rapamycin and BCH treatment on insulin-stimulated glucose uptake and mTOR signalling in L6 myotubes 121

4.2.4. Determination of Glucose uptake 122
4.2.5. Western blot analyses of mTOR signalling 122
4.2.6. Determination of intracellular BCAA concentrations 122
4.2.7. Statistical Analyses 123
4.3. Results 124
4.3.1. Effects of rapamycin treatment for different times on glucose uptake in L6 myotubes 124
4.3.2. Effects of 4 hours rapamycin treatment on mTOR and downstream target proteins in L6 myotubes 126
4.3.3. Effects of 4 hours rapamycin treatment on beta-actin in L6 myotubes 131
4.3.4. Effects of 4 hours 3BDO treatment on mTOR and downstream target proteins in L6 myotubes 132
4.3.5. Effects of 4 hours 3BDO treatment on beta-actin in L6 myotubes ……137
4.3.6. Effects of 4 hours 3BDO treatment on glucose uptake in L6 myotubes 138
4.3.7. Effects of 4 hours 3BDO treatment on Akt in L6 myotubes 139
4.3.8. Effects of 4 hours BCH treatment on mTOR and downstream target proteins in L6 myotubes 142
4.3.9. Effects of 4 hours BCH treatment on beta-actin in L6 myotubes ……..... 147
4.3.10. Effects of 4 hours BCH treatment on glucose uptake in L6 myotubes.. 148
4.3.11. Effects of 4 hours BCH treatment on Akt in L6 myotubes 150
4.3.12. Effects of 4 hours BCH treatment on intracellular BCAA concentrations in L6 myotubes 152
4.4. Discussion and Conclusion 154
CHAPTER 5: HOW DIFFERENT LEUCINE CONCENTRATIONS INFLUENCE GLUCOSE UPTAKE IN L6 MYOTUBES 162
5.1. Introduction 163
5.2. Materials and Methods 165
5.2.1. Effects of different leucine concentrations on insulin-stimulated glucose uptake and mTOR signalling in L6 and C2C12 myotubes 165
5.2.2. Glucose uptake testing for L6 and C2C12 myotubes 167

5.2.3. Western blot antibodies 167
5.2.4. Determination of intracellular BCAA concentrations 167
5.2.5. Statistical Analyses 167
5.3. Results 168
5.3.1. Effects of 24 hours treatment with different concentrations of leucine on mTOR and downstream target proteins in L6 myotubes..... 168
5.3.2. Effects of 48 hours treatment with different concentrations of leucine on mTOR and downstream target proteins in L6 myotubes..... 173
5.3.3. Effects of 24 hours treatment with different concentrations of leucine on glucose uptake in L6 myotubes 178
5.3.4. Effects of 48 hours treatment with different concentrations of leucine on glucose uptake in L6 myotubes 180
5.3.5. Effects of 24 hours treatment with different concentrations of leucine on Akt in L6 myotubes 182
5.3.6. Effects of 48 hours treatment with different concentrations of leucine on Akt in L6 myotubes 184
5.3.7. Effects of the 24 and 48 hours treatment with different concentrations of leucine on Beta-actin in L6 myotubes 186
5.3.8. Effects of 24 hours treatment with different concentrations of leucine on intracellular BCAA concentrations in L6 myotubes 187
5.3.9. Effects of 48 hours treatment with different concentrations of leucine on intracellular BCAA concentrations in L6 myotubes 189
5.3.10. Effects of 24 hours treatment with different concentrations of leucine on glucose uptake in C2C12 myotubes 191
5.3.11. Effects of 48 hours treatment with different concentrations of leucine on glucose uptake in C2C12 myotubes 193
5.4. Discussion and Conclusion 195
CHAPTER 6: EVALUATION OF SESTRIN 2 OVEREXPRESSION AS A STRATEGY TO INHIBIT mTOR FUNCTION AND ASCERTAIN ITS IMPACT ON GLUCOSE UPTAKE 206
6.1. Introduction..... 207
6.2 Methods..... 212
6.2.1 Cell culture and infections 212

6.2.2 Real Time Quantitative PCR analysis 213
6.3 Results 214
6.3.1 Fluorescence images at 7 days following AAV1-GFP infection in L6 cells. 214
6.3.2 Sestrin 2 mRNA level in L6 myotubes after infection with AAV1-mSESN2 216
6.4 Discussion and Conclusion 219
CHAPTER 7: GENERAL DISCUSSION AND CONCLUSIONS 222
7.1. General Discussion and Conclusions 223
7.2. Limitations .....错误!未定义书签。
7.3. Future works 234
CHAPTER 8: REFERENCES 238
CHAPTER 9: APPENDIXES 261

List of Figures

Figure 1.1The incidence and expected growth rate of world diabetics between 2017 and 2045..... 21
Figure 1.2The total global healthcare expenditure by people with diabetes .. 22
Figure 1.3 Glucagon and insulin regulate blood glucose. 25
Figure 1.4 Diagrammatic representation of the concept of insulin resistance. 27
Figure 1.5 Mechanism of GLUT4 translocation. 31
Figure 1.6 Regulation of glucose to glycogen. 34
Figure 1.7 BCAA metabolism pathway. 37
Figure 1.8 The structure of mTOR. 44
Figure 1.9 A diagram of the mTORC1 and mTORC2 protein complexes and their distinct cellular roles. 46
Figure 1.10 The Akt/mTOR signalling pathway. 51
Figure 1.11 The hypothesis of this research 58
Figure 2.1 The step of Glucose Uptake-Glo™ Assay technology. 71
Figure 2.2 The Organisation of the transfer cassette. 83
Figure 2.3 The example of Ponceau-S red stain. 84
Figure 3. 1 Timeline of different treatment groups 95
Figure 3. 2 Effects of 30 minutes CHX treatment on differentiated C2C12 cells 98
Figure 3. 3 Intracellular BCAA concentrations in C2C12 myotubes after 30 minutes CHX treatment 100
Figure 3. 4 Effects of CHX on the phosphorylation of mTOR 102
Figure 3. 5 Effects of CHX on the phosphorylation of 4E-BP1 and p70S6K 103
Figure 3. 6 Effects of 30 minutes CHX on Beta-actin in C2C12 myotubes .. 104
Figure 3. 7 Effects of insulin on glucose uptake in C2C12 and L6 skeletal muscle cell lines. 106

Figure 3. 8 mRNA expression of the different Glucose transporters in differentiated C2C12 and L6 muscle cells 108
Figure 3. 9 Balance of intracellular amino acids 110
Figure 4. 1 Conceptual schematic of 3BDO and mTOR action mechanism. 117
Figure 4. 2 Timeline of treatment groups. 119
Figure 4. 3 Timeline of treatment groups. 120
Figure 4. 4 Timeline of treatment groups. 121
Figure 4. 5 Effects of rapamycin (1h or 4h) +/- insulin on glucose uptake in L6 myotubes. 125
Figure 4. 6 Effects of rapamycin (4h) +/- insulin on mTOR activity in L6 myotubes. 128
Figure 4. 7 Effects of rapamycin (4h) +/- insulin on 4E-BP1 activity in L6 myotubes. 129
Figure 4. 8 Effects of rapamycin (4h) +/- insulin on p70S6K activity in L6 myotubes. 130
Figure 4. 9 Effects of rapamycin (4h) +/- insulin on Beta-actin in L6 myotubes. 131
Figure 4. 10 Effects of 4h rapamycin or 3BDO +/- 1h insulin on mTOR activity in L6 myotubes. 134
Figure 4. 11 Effects of 4h rapamycin or 3BDO +/- 1h insulin on 4E-BP1 activity in L6 myotubes. 135
Figure 4. 12 Effects of 4h rapamycin or 3BDO +/- 1h insulin on p70S6K activity in L6 myotubes. 136
Figure 4. 13 Effects of 4h rapamycin or 3BDO +/- 1h insulin on Beta-actin in L6 myotubes 137
Figure 4. 14 Effects of 4h rapamycin or 3BDO +/- insulin on glucose uptake in L6 myotubes. 139
Figure 4. 15 Effects of 4h rapamycin or 3BDO +/- 1h insulin on Akt activity in L6 myotubes. 141
Figure 4. 16 Effects of 4h rapamycin or BCH +/- 1h insulin on mTOR western blot in L6 myotubes. 144
Figure 4. 17 Effects of 4h rapamycin or BCH +/- 1h insulin on 4E-BP1 western

blot in L6 myotubes. 145
Figure 4. 18 Effects of 4h rapamycin or BCH +/- 1h insulin on p70S6K western blot in L6 myotubes. 146
Figure 4. 19 Effects of 4h rapamycin or BCH +/- 1h insulin on Beta-actin in L6 muscle cells 147
Figure 4. 20 Effects of 4h rapamycin or BCH +/- insulin on glucose uptake in L6 myotubes. 149
Figure 4. 21 Effects of 4h rapamycin or BCH +/- 1h insulin on Akt western blot in L6 myotubes. 151
Figure 4. 22 Effects of 4h rapamycin or BCH +/- insulin on intracellular BCAAs in L6 myotubes. 153
Figure 4. 23 Schematic of the relationship between mTORC1 and glucose uptake 161
Figure 5. 1 Timeline of treatment groups. 166
Figure 5. 2 Effects of 24 hours treatment with different concentrations of leucine +/- 1 hour insulin on mTOR activity in L6 myotubes 170
Figure 5. 3 Effects of 24 hours treatment with different concentrations of leucine +/- 1 hour insulin on 4E-BP1 activity in L6 myotubes 171
Figure 5. 4 Effects of 24 hours treatment with different concentrations of leucine +/- 1 hour insulin on p70S6K activity in L6 myotubes 172
Figure 5. 5 Effects of 48 hours treatment with different concentrations of leucine +/- 1 hour insulin on mTOR activity in L6 myotubes 175
Figure 5. 6 Effects of 48 hours treatment with different concentrations of leucine +/- 1 hour insulin on 4E-BP1 activity in L6 myotubes 176
Figure 5. 7 Effects of 48 hours treatment with different concentrations of leucine +/- 1 hour insulin on p70S6K activity in L6 myotubes 177
Figure 5. 8 Effects of 24 hours treatment with different concentrations of leucine +/- 1 hour insulin on glucose uptake in L6 myotubes 179
Figure 5. 9 Effects of 48 hours treatment with different concentrations of leucine +/- 1 hour insulin on glucose uptake in L6 myotubes 181

Figure 5. 10 Effects of 24 hours treatment with different concentrations of leucine +/- 1 hour insulin on Akt in L6 myotubes 183
Figure 5. 11 Effects of 48 hours treatment with different concentrations of leucine +/- 1 hour insulin on Akt in L6 myotubes 185
Figure 5. 12 Effects of the 24 and 48 hours treatment with different concentrations of leucine +/- 1 hour insulin on Beta-actin in L6 myotubes .. 186
Figure 5. 13 Effects of 24 hours treatment with different concentrations of leucine +/- 1 hour insulin on intracellular BCAA concentrations in L6 myotubes 188
Figure 5. 14 Effects of 48 hours treatment with different concentrations of leucine +/- 1 hour insulin on intracellular BCAA concentrations in L6 myotubes 190
Figure 5. 15 Effects of 24 hours treatment with different concentrations of leucine +/- 1 hour insulin on glucose uptake in C2C12 myotubes 192
Figure 5. 16 Effects of 48 hours treatment with different concentrations of leucine +/- 1 hour insulin on glucose uptake in C2C12 myotubes 194
Figure 5. 17 Schematic of the relationship between mTORC1, leucine and glucose uptake in L6 myotubes 205
Figure 6. 1 The diagram of how Sestrin 2 regulate AMPK/mTORC1 signalling pathway.. 209
Figure 6. 2 Diagram of how Sestrin 2 regulate mTORC1 via the GATOR complex.. 211
Figure 6. 3 GFP and Sestrin 2 vector map 212
Figure 6. 4 Bright-field and fluorescence photographs following 7 days infected with AAV1-GFP in L6 cells..... 215
Figure 6. 5 Mean Cp values for Sestrin 2 mRNA in L6 myotubes..... 217
Figure 6. 6 Mean Cp values of cyclophilin mRNA in L6 myotubes. 218
Figure 7. 1 Schematic of the relationship between mTORC1, leucine and glucose uptake 233
Figure 7. 2 Schematic of the mechanisms in the future works..... 237

List of Tables

Table 2.1 The seeding density of different plates in Cell Culture 64
Table 2.2 The information of AAV1-Sestrin2. 66
Table 2.3 The media needed for each MOI (250 µl/well) of GFP 68
Table 2.4 The media needed for each MOI (250 µl/well) of Sestrin 2 68
Table 2.5 Relative volumes of different components for detection reagent ... 73
Table 2.6 The components in 10ml 2XSDS 78
Table 2.7 The components of transfer buffer 82
Table 2.8 Volume of components for 10X TBS. 85
Table 2.9 RTqPCR primers for mouse genes measured. 89
Table 5. 1 Summary of effect of leucine on glucose uptake, mTOR/P70S6K and Akt signalling pathways……..203

List of Abbreviations

2DG: 2-Deoxy-D-glucose

2DG6P: 2-deoxyglucose-6-phosphate

3BDO: 3-Benzyl-5-((2-nitrophenoxy)methyl)-dihydrofuran-2(3H)-one

4E-BP1: Eukaryotic initiation factor 4E binding protein1

eIF4E: Eukaryotic translation initiation factor 4E

eIf-4F: Eukaryotic Initiation Factor-4F complex

AAV1: Adeno-Associated Viruses 1

ADP: Adenosine diphosphate

AICAR: 5-Aminoimidazole-4-carboxamide-1-beta-D-ribofuranoside

Akt/PKB: Protein kinase B

Alpha-MEM: α-Minimum Essential Medium

AMPK: Adenosine monophosphate-activated protein kinase

ANOVA: Analysis of variance

ATP: Adenosine triphosphate

BCAAs: Branched-Chain Amino Acids

BCAT: Branched-chain amino acid aminotransferase

BCH: 2-amino-3-norbane carboxylic acid

BCKAs: Branched chain α-keto acids

BCKD: Branched-chain α-keto acid dehydrogenase

BMI: Body mass index

BSA: Bovine Serum Albumin

C/EBPs: CCAAT-enhancer-binding proteins

cDNA: Complementary DNA

CHX: Cycloheximide

CoA-SH: Reduced coenzyme A

Cp: Crossing point

DEPTOR: DEP domain containing mTOR-interacting protein

DKA: Diabetic ketoacidosis

DM: Diabetes mellitus

DM: Differentiation media

DMEM: Eagle's minimal essential medium

DMSO: Dimethyl sulfoxide

DNA: Deoxyribonucleic acid

DTT: DL-Dithiothreitol

EAA: Essential amino acid

EDTA: Ethylenediaminetetraacetic acid

eIF4E: Eukaryotic translation initiation factor- 4E

FAT: a domain structure shared by FRAP, ATM and TRRAP

FATC: FAT C-terminus

FBS: Foetal Bovine Serum

FoxO1/3a: Forkhead box O1/3a

FRB: FKBP12/rapamycin binding domain.

FYVE: Fab1/YOTB/2K632.12/Vac1/EEA1 domain

G-1-p: Glucose 1-phosphate

G-6-p: Glucose 6-phosphate

G6PDH: Glucose-6-phosphate dehydrogenase

GAP: GTPase-activating protein

GDM: Gestational diabetes

GEF: Guanosine nucleotide exchange factor

GFP: Green fluorescent protein

GLUT1-4: Glucose transporter 1-4

GS: Glycogen synthase

GSK-3: Glycogen synthase kinase 3

HbA1c: Hemoglobin A1c

HOMA: Homeostatic model assessment

HUVECs: Human Umbilical Vein Endothelial Cells

IGF1: Insulin-like growth factor 1

IR: Insulin receptor

IR: Insulin resistance

IDF: International Diabetes Federation

IRS: Insulin receptor substrate

IRS-1: Insulin receptor substrate 1

KIC: a-ketoisocaproate

KIM: a-keto-b-methylglutarate

KIV: a-ketoisovalerate

LAT1: Large neutral amino acid transporter

LKB1: Liver kinase B1

mLST8/ GβL: mammalian lethal with sec-13

MOI: Multiplicity of infection

mRNA: Messenger RNA

mSin1: Mammalian stress-activated map kinase-interacting protein 1

mTOR: Mammalian Target of Rapamycin

mTORC1: mTOR complex 1

mTORC2: mTOR complex 2

NADH: Nicotinamide adenine dinucleotide

NADPH: Nicotinamide adenine dinucleotide phosphate

p/S: Penicillin/Streptomycin

p70S6 kinase/S6K1: S6 kinase beta-1

PAGE: Polyacrylamide gel electrophoresis

PBS: Phosphate buffer saline

PDCD4: programmed cell death protein 4

PDK1: Pyruvate dehydrogenase kinase 1

PDPK1: Phosphoinositide dependent protein kinase-1

PI3K: Phosphatidylinositol 3-kinase

PIP2: PtdIns(4,5)P2

PIP3: PtdIns(3,4,5)P3

PKC: Protein kinase C

PRAS40: Proline-rich Akt substrate 40kDa

Protor1/2: Protein observed with rictor 1 and 2

PX: Phox homology domain

RAPTOR: Regulatory-associated protein of mammalian target of rapamycin

R-CoA: acyl-CoA

Rheb: Ras-homolog enriched in brain

RICTOR: Rapamycin-insensitive companion of mTOR

RTqPCR: Real Time Quantitative Polymerase Chain Reaction

SDS: Sodium Dodecyl Sulfate

SEM: Standard error of means

SESN2: Sestrin2

T2D: Type 2 diabetes

TSC: Tuberous Sclerosis Complex

U: Unit (enzyme amount)

UDP-glucose: Uridine diphosphate glucose

WHO: World Health Organization

CHAPTER 1: INTRODUCTION

1.1. World prevalence of diabetes

Diabetes mellitus (DM), known commonly as diabetes, is a group of metabolic disorders characterised by high blood glucose levels over a prolonged period. If untreated, this condition may lead to many serious complications that will threaten a person's health and wellbeing. Specifically, abnormally high blood glucose concentrations can trigger acute complications including diabetic ketoacidosis (DKA), hyperosmolar coma, and death (Cho *et al.,* 2018; WHO, 2018). Furthermore, long-term high blood glucose concentrations can damage the heart, blood vessels, eyes, kidneys, and nerves, and increase the risk of cardiovascular disease and stroke. Likewise, damage to small blood vessels can compromise blood flow to various tissues, causing renal damage, retinopathy, and in conjunction with nerve damage (neuropathy) foot ulcers and infection, potentially culminating in amputation of the affected limb (Cho *et al.,* 2018; WHO,2018). These varied and chronic complications of diabetes demonstrate the need to devise effective treatment strategies that can reduce diabetes incidence.

With rapid developments in socioeconomics and the improvement of people's living standards, people spend more money on food, but not necessarily "healthy food" and tend to live a more sedentary lifestyle (IDF, 2017). International Diabetes Federation (IDF, 2017) indicated that the largest increase in diabetes incidence would take place in regions where economies are moving from low income to middle-income levels.

The World Health Organization (WHO) reported that in 1980, there were 108

million people living with diabetes and this number increased to 422 million worldwide in 2016 (WHO, 2016). In 2017, number of people with diabetes was 424.9 million, and is expected to increase further to 628.6 million in 2045 (Figure 1.1, IDF, 2017). The increase in incidence will be greatest in the Middle East/North Africa and remainder of Africa, where the increase is expected to be ~110% and 156%, respectively (Figure. 1.1. IDF, 2017).

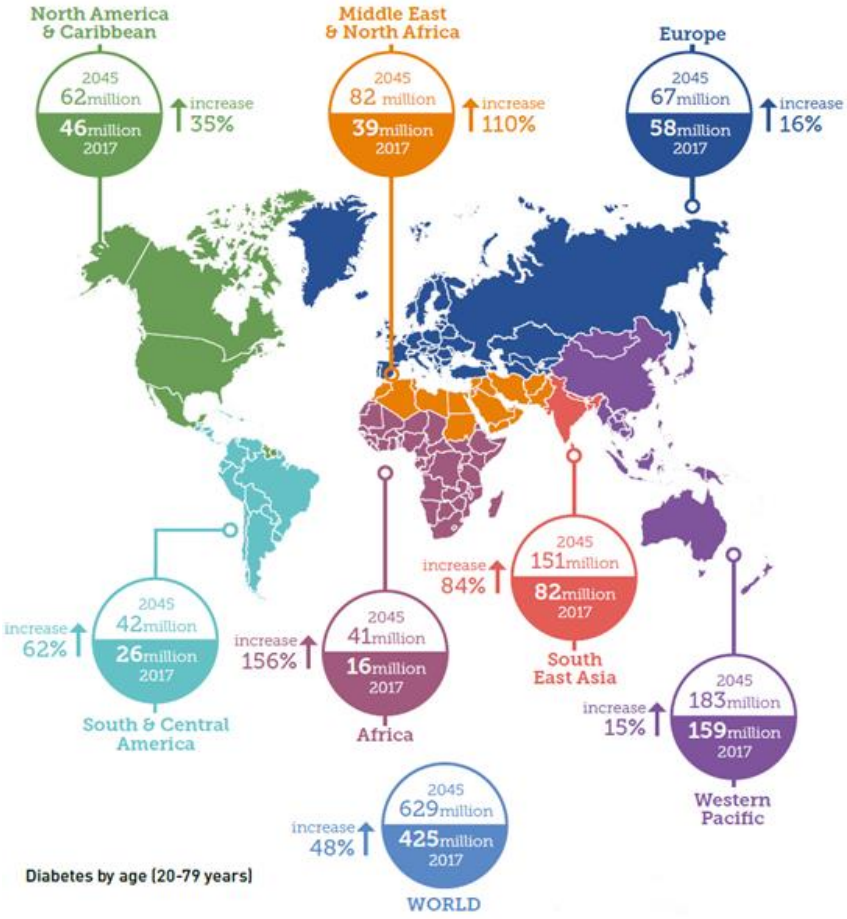


Figure 0.1The incidence and expected growth rate of world diabetics between 2017 and 2045. Reproduced from IDF 2017

Diabetes not only affects the quality of life but also increases healthcare expenditure. Because of the medication, inpatient and outpatient care, and regular clinical tests, a large economic burden is placed on the global health-care system and wider global economy by diabetes (WHO, 2018). Since 2006, the IDF started to track healthcare expenditure on diabetes. They noted that the cost has increased sharply, from 232 billion US dollars in 2007 to 727 billion US dollars in 2017 worldwide (expenditure associated with the care of people with diabetes, aged 20 to 79, Figure 1.2). It is projected this increase will continue to rise and may reach 776 billion dollars by 2045. When including people between 18 to 99 years old, the total healthcare expenditure could reach 958 billion dollars per year by 2045 (IDF, 2017).

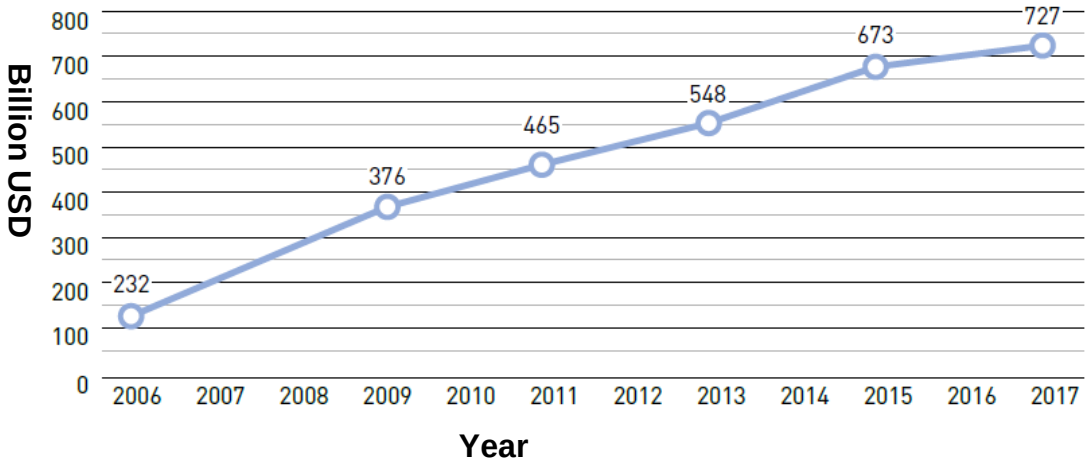


Figure 0.2The total global healthcare expenditure by people with diabetes (20-79 years). Reproduced from IDF 2017

Because of the huge financial burden of diabetes and the damage it can cause to human health, it is very important to understand the causes and consequences of diabetes, thereby allowing the development of more effective treatment strategies.

1.2. Diabetes and glucose uptake

1.2.1. The classification of diabetes

Normally, there are three types of diabetes: type 1 diabetes, characterized by deficient insulin production in the body, requiring people with type 1 diabetes to inject insulin to regulate the amount of glucose in their blood (WHO, 2018). Type 2 diabetes, which is the most common type of diabetes in the world, is where people cannot use insulin effectively, potentially coupled with inadequate production of insulin (WHO, 2018). The last one is Gestational diabetes (GDM), which only occurs in pregnancy. Worldwide, 90% of diabetes cases are type 2 diabetes, with most type 2 diabetes thought to be caused by overweight and obesity, unhealthy diet and/or physical inactivity (WHO, 2018).

1.2.2. Insulin and glucagon

The pancreas is a long, narrow gland located in the upper part of the abdomen, behind the stomach and in front of the spine. The pancreas has both exocrine and endocrine functions. The exocrine glands can produce enzymes, which can break down food into small molecules and help intestines to digest and absorb of nutrients (Go *et al.,* 1993; Falck, 2017). The enzymes include trypsin and chymotrypsin to digest proteins; amylase to digest carbohydrates; and lipase to break down fats (Falck, 2017). The mammalian endocrine pancreas consists of

groups of hormone-secreting cells. In 1869, Langerhans was the first to describe these cells. The hormones (such as insulin and glucagon) are produced and secreted from the islet cells (islets of Langerhans) and have been studied extensively in the context of diabetes (Da Silva Xavier, 2018). In human islet cells, about 30% are α-cells which produce glucagon, about 60% are β-cells which produce insulin, and the other 10% are made up of δ-cells (somatostatin-producing), γ- or PP cells (pancreatic polypeptide-producing), and ε-cells (ghrelin-producing) (Da Silva Xavier, 2018; Ionescu-Tirgoviste *et al.,* 2015, Ichii *et al.,* 2005; Taborsky, 2010).

Glucagon and insulin work together to regulate blood glucose homeostasis (Figure 1.3). After a meal, blood glucose concentrations will increase, stimulating the beta cells to secrete insulin, which in turn drives blood glucose uptake by insulin-sensitive peripheral tissues, such as muscle and adipose tissues. In parallel, insulin can also promote glycogenesis and glycolysis in liver and skeletal muscles. Through these three methods, insulin reduces blood glucose until homeostasis (3.9 to 5.4 mmol/L) has been restored. During fasting conditions, glucagon secretion by alpha cells will predominate. Glucagon stimulates hepatic glucose production through glycogenolysis and gluconeogenesis to increase blood glucose concentrations (Aronoff *et al,* 2004; Röder *et al.,* 2016).

Besides adjusting glucose homeostasis, insulin also can promote protein and fatty acid synthesis in muscle and adipose tissue; decrease fatty acid oxidation in muscle and liver and decrease protein degradation in muscle (Dimitriadis *et*

al., 2011).

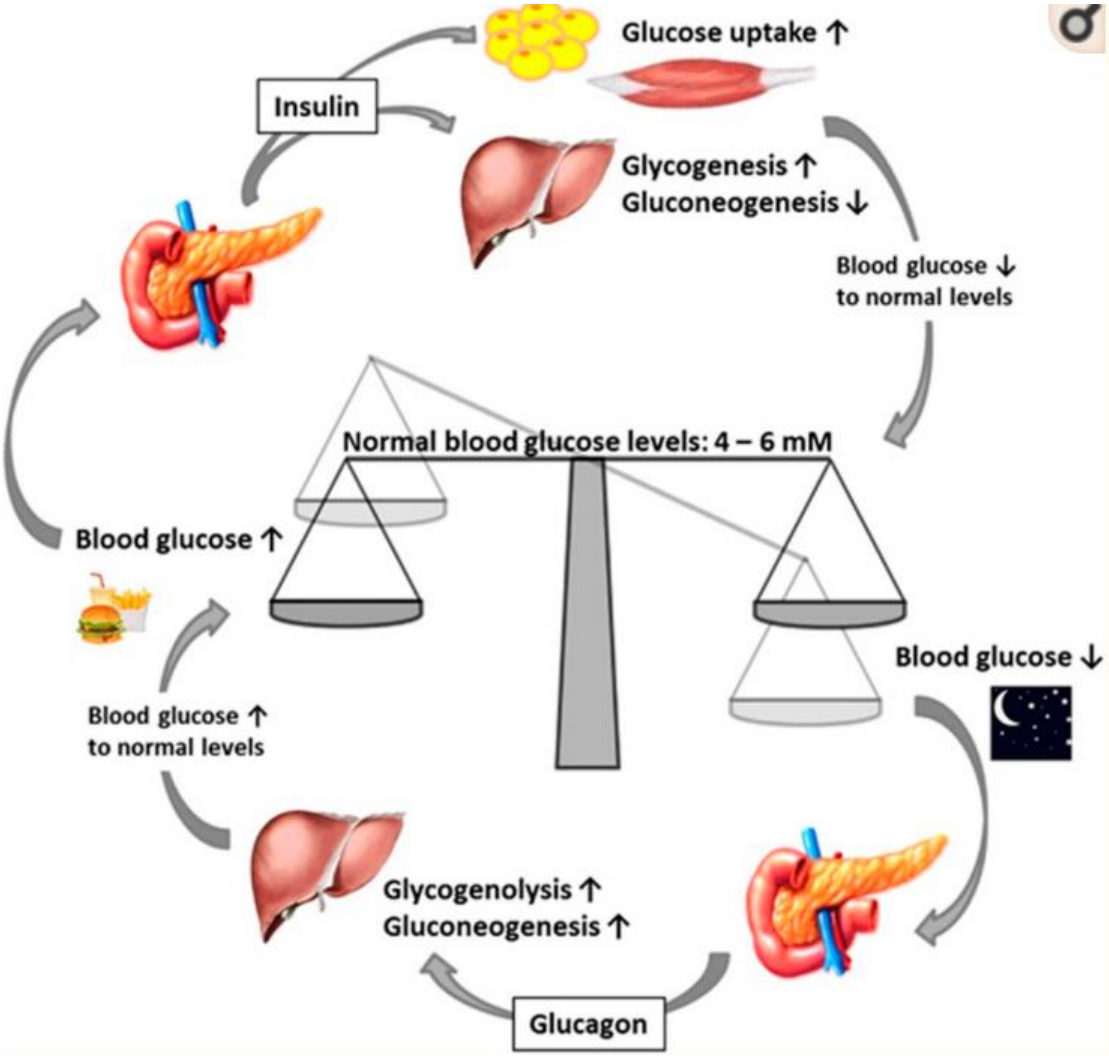


Figure 0.3 Glucagon and insulin regulate blood glucose. Reproduced from Röder *et al*., 2016

When blood glucose concentrations decrease, glucagon is released which in turn will break down liver glycogen through glycogenolysis. After consuming food, the blood glucose concentrations increase, insulin will stimulate glucose uptake in muscle cells and liver, and storage as glycogen through glycogenesis.

1.2.3 Insulin resistance

The main function of insulin is to keep the balance of blood glucose concentrations; however, in people who develop insulin resistance, key insulin sensitive organs including skeletal muscle, adipose tissue and liver, fail to respond to the action of insulin effectively (Figure 1.4). Systemic insulin resistance is because of impaired insulin action in target organs and can vary among individuals (Hardy, Czech and Corver; 2012). Because of insulin resistance, insulin-mediated glucose uptake and metabolism are impaired in skeletal muscle and adipose tissue, and hepatic glucose output is not sufficiently suppressed, leading to insulin requirements increasing to maintain blood glucose homeostasis (Lu *et al.,* 2013; Kahn and Flier, 2000).

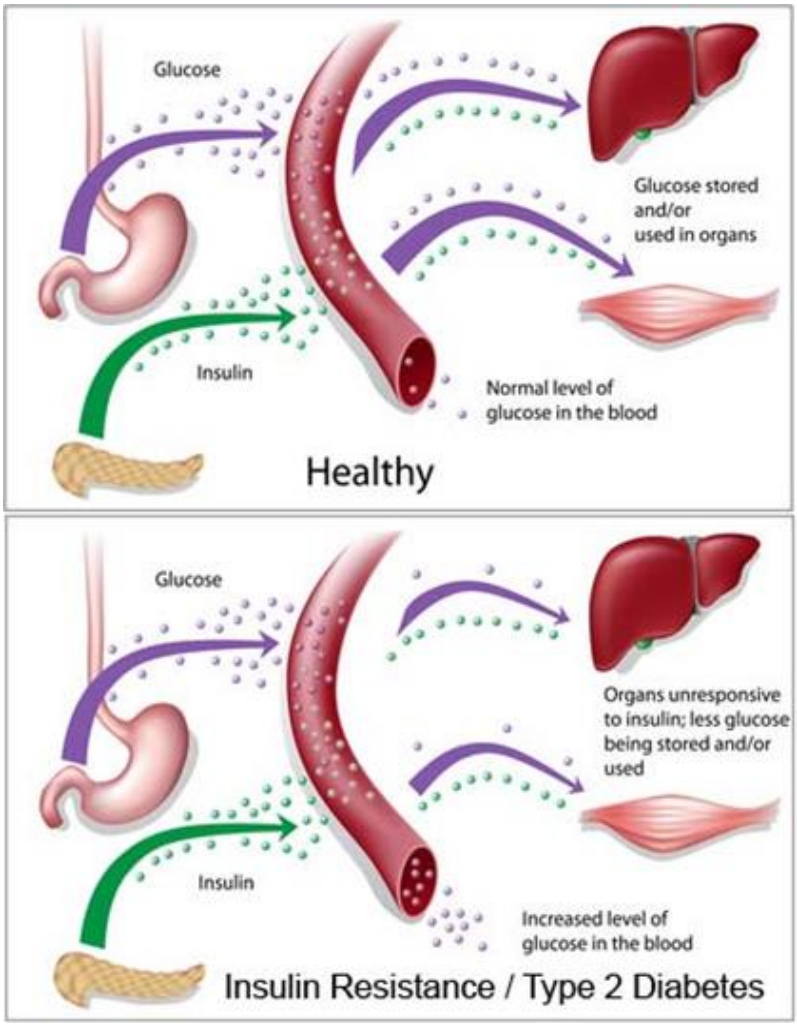


Figure 0.4 Diagrammatic representation of the concept of insulin resistance. Reproduced from good food eating, 2014.

For healthy people, insulin stimulates glucose in target organs where it is metabolized or stored as glycogen. However, in insulin resistance, the organs become unresponsive to insulin, less glucose is metabolized and/or stored, with blood glucose concentrations increasing as a result.

In mice with hepatic insulin resistance (impaired suppression of glucose production by insulin in hepatocytes), insulin fails to suppress gluconeogenesis but continues to activate lipogenesis, these lead to high blood level of glucose and triglyceridemia and then cause hyperglycemia and hypertriglyceridemia (Brown and Goldstein, 2008). High blood leveltriglyceride can activate PKC-δ in the liver, this in turn increase serine phosphlrylation of IRS-1 and then impair insulin singalling (Meshkani and Adeli, 2009). In adipose tissue, insulin resistance is manifested as impaired insulin-stimulated glucose transport, because the effect of insulin on glucose transporter-4 (GLUT-4) is blunted (Hardy, Czech and Corver; 2012). However, like in the liver, the insulin signalling in adipocytes also displays a divergence (Gonzalez *et al.,* 2011). In addition, insulin resistance in adipose tissue impairs the ability of insulin to inhibit lipolysis (Hardy, Czech and Corver; 2012). In skeletal muscle, insulin resistance is manifested by decreased insulin-stimulated glucose transport and a decline in muscle glycogen synthesis (Hardy, Czech and Corver; 2012). Besides, some papers contend that insulin resistance in diabetes is caused by deficiency in mitochondria in skeletal muscle (Lowell and Shulman, 2005; Morino *et al.,* 2006), however Hancock, *et al.,* (2008) argued this result. His team demonstrated that a high-fat diet that raises free fatty acids and induces insulin resistance, results in a gradual increase in mitochondria in rat skeletal muscle. Take together, in skeletal muscle, adipose tissue and liver, the mechanism of insulin resistance could be very different.

1.2.4 Glucose uptake in skeletal muscle

In the regulation of glucose uptake in skeletal muscle, the most important step is the transport of glucose through the cell membrane via the action of the glucose transporters (Lund, *et al.,* 1995). Under euglycemic hyperinsulinemic conditions, about 80% of glucose uptake occurs in skeletal muscle, making it the main site of glucose uptake and the predominant site of glycogen synthesis in the postprandial state in humans (DeFronzo and Tripathy, 2009). Therefore, it is essential to understand how glucose goes into skeletal muscle and after that, how glucose is metabolized in muscle cells.

In mammalian cells, glucose transport is controlled by a facilitative glucose transport system, which involves four glucose transporters—GLUT1 to GLUT4 (Gould and Holman, 1993). With different cell type and stimulus, the expression and localization of the glucose transporter is regulated in a variety of ways. Different glucose transporters are expressed in different sites. For example, GLUT1 is expressed mainly in the brain, GLUT2 is expressed at the liver, GLUT3 is expressed in brain and nerve cells and GLUT4 is expressed in adipose tissues, skeletal muscle and cardiac muscle (Gould and Holman, 1993).

Using muscle-specific GLUT4 knockout mice (muscle-G4KO mice), Zisman *et al.,* (2000) showed in muscle that GLUT4 is the major transporter for glucose after insulin stimulation. Comapre with the wild type mice, the muscle glucose uptake is reduced in muscle-G4KO mice ($p < 0.001$) and after insulin injection, glucose levels did not decrease in muscle-G4KO mice but in control mice glucose levels decreased. Utilizing isolated muscle tissue from the same

knockout animals, *ex vivo* glucose transport assays showed that basal glucose transport was reduced by 80% and insulin-stimulated glucose uptake was completely ablated (Gibbs *et al.,* 1995). Moreover, it has been shown that deficiency in glucose transport efficiency and GLUT4 activity results in insulin resistance (Petersen and Shulman 2006). In genetically induced diabetic mice *(db/db)*, overexpression of GLUT4 improved glycemic control and reduced insulin resistance (Gibbs *et al.,* 1995). Therefore, GLUT4 is a key protein in glucose uptake in muscle cells.

In the normal state (fasted non-insulin stimulated state), most of GLUT4 is located inside the cell, within tubulo-vesicular structures and multivesicular endosomes (Ploug *et al*., 1998) and crucially, not at the plasma membrane. After blood glucose concentrations increase (such as after a meal), insulin, secreted from β-cells of pancreas, binds the insulin receptor located on the surface of the muscle cell. The insulin receptor (IR) is a tetramer, which is composed of two extracellular α subunits and two transmembrane β subunits that are linked together by disulphide bonds (Guo, 2014). The binding of insulin to α subunits of the insulin receptor stimulates the tyrosine kinase activity of one of the two β subunits leading to rapid receptor auto-phosphorylation (Ryder, Chibalin and Zierath, 2001). Besides the auto-phosphorylation of the insulin receptor, tyrosine kinase activity also recruits various substrate adaptors including the insulin receptor substrate 1 (IRS-1, signalling adapter protein) family of proteins (Ryder, Chibalin and Zierath, 2001) (Figure 1.5).

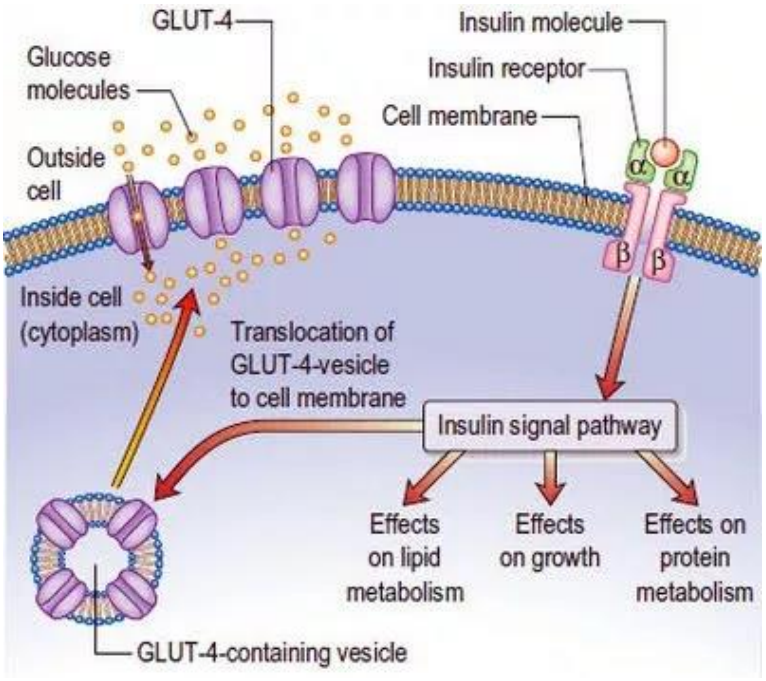


Figure 0.5 Mechanism of GLUT4 translocation. Reproduced from Chhabra, 2012

Insulin binds to its receptor (IR), then recruiting insulin receptor substrate 1, stimulating Akt and causing the glucose transporter 4 to translocate to the cell membrane, allowing glucose uptake in to the cell. **GLUT4:** glucose transporter 4

Phosphorylated IRS displays many binding sites for numerous signalling partners, and it can combine or activate proteins that have a SH2 domain structure, including phosphatidylinositol 3-kinase (PI3K) (Guo, 2014; Abdul-Ghani and DeFronzo, 2010). Activated PI3K catalyzes the addition of a phosphate group to the membrane lipid PtdIns(4,5)P2 (PIP2), thereby converting it to PtdIns(3,4,5)P3 (PIP3). PIP3 in turn binds with phosphoinositide dependent protein kinase-1 (PDPK1) to activate a key downstream effector of protein kinase B (PKB; also known as Akt) (Ryder, Chibalin and Zierath, 2001 Guo, 2014; Abdul-Ghani and DeFronzo, 2010). Akt is a serine/threonine kinase

that plays an important role in diverse cellular processes, including cancer progression and insulin-mediated metabolism. Akt has three related isoforms Akt1, Akt2, and Akt3, and these represent the major signalling arm of PI3K (Buller *et al*., 2008). Phosphorylated (activated) Akt stimulates translocation of GLUT4 from the cytosol to the cell surface, allowing glucose transport into the cell (Guo, 2014; Abdul-Ghani and DeFronzo, 2010; Khorami, Movahedi, and Sokhini, 2015). This process is called insulin-induced glucose uptake.

Besides insulin-induced glucose uptake, Richter (2013) pointined out the relationship between exercise, GLUT4 and muscle glucose uptake. During the exercise, the muscle contraction increased glucose uptake. This because exercise increase the translocation of GLUT4 from intracellular sites to the sarcolemma and T-tubules and maybe increase the GLUT4 inttrinsic activity. The result of *in vivo* exercise experiment showed that in muscle-specific GLUT4 deletion mice, muscle glucose uptake significantly reduced exercise tolercance (Fueger *et al.,* 2007).

1.2.5 Glucose metabolism in muscle cells

Glucose is stored as glycogen in the muscle cells, a process called glycogenesis. In the first step, glucose is phosphorylated to glucose 6-phosphate (G-6-p) by hexokinase (Richter and Hargreaves, 2013). Secondly, under physiologic conditions, about two-thirds of all glucose-6-phosphate is converted to glycogen, and one-third enters glycolysis (Abdul-Ghani and DeFronzo, 2010). Following formation, G-6-p is converted to glucose 1-

phosphate (G-1-p) in a reaction catalyzed by the enzyme phosphoglucomutase. With the enzyme uridine diphosphate glucose (UDP-glucose) pyrophosphorylase, glucose-1-phosphate is converted into UDP-glucose, producing pyrophosphate in the process, which is subsequently hydrolyzed by pyrophosphatase into two phosphate molecules (Gropper and Groff, 1999). Afterwards, UDP-glucose is incorporated into glycogen by the enzyme glycogen synthase, which requires the glycogen primer, glycogenin (Gropper and Groff, 1999). Glycogenin catalyzes the attachment of additional glucose residues to form chains of up to eight units, with glycogen synthase extending the glycogen chains further. Glycogen synthase (GS) is regulated in part by glycogen synthase kinase 3 (GSK-3). Insulin activates Akt, which in turn phosphorylates/inactivates GSK-3. Phosphorylation/activation of GSK-3 activates glycogen synthase (GS) leading to the increased synthesis of glycogen (Han *et al.,* 2016; Jensen *et al.,* 2011). Lastly, with the help of glycogen branching enzymes, the unbranched glycogen forms branched glycogen (Figure 1.6).

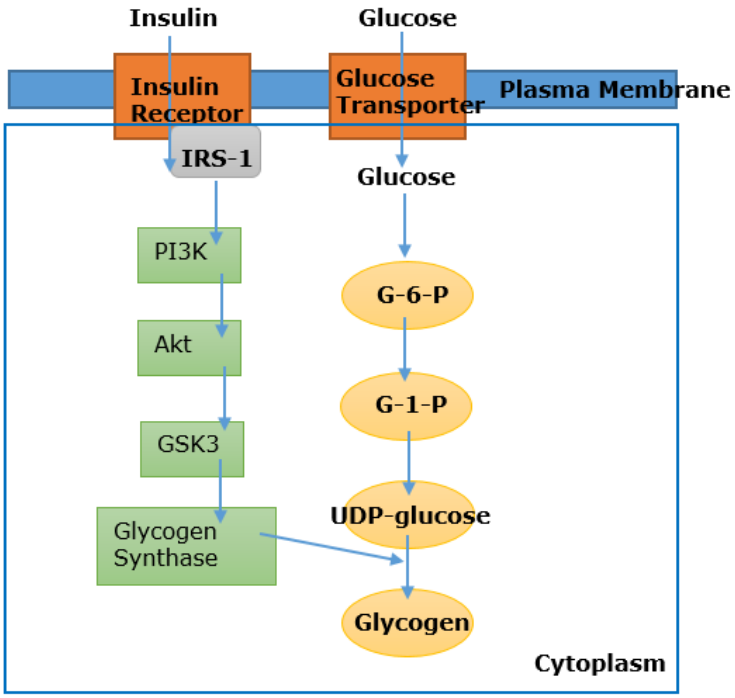


Figure 0.6 Regulation of glucose to glycogen. Adapted from Han *et al*., 2016 and Gropper and Groff, 1999

After glucose transfer into the cells, through several steps, it converts to glycogen and stored in the muscle cells. Glycogen synthase is the important enzyme to control glycogenesis, which in turn is under the control of Akt. **PI3-K:** Phosphoinositide 3-kinase. **Akt:** Protein kinase B (PKB). **GSK-3:** Glycogen synthase kinase 3. **G-6-p:** Glucose 6-phosphate. **G-1-p:** Glucose 1-phosphate. **UDP-glucose:** Uridine diphosphate glucose

1.3 Branched-Chain Amino Acids (BCAAs)

Amino acids are the building blocks of protein. There are twenty amino acids used to synthesize protein, nine of them including BCAAs (leucine, isoleucine

and valine) cannot be synthesized by human cells (Hutson, Sweatt, and LaNoue, 2005). Therefore, they must be obtained via diet and are classified as essential amino acids. The BCAAs account for 35% of the essential amino acids in muscle proteins and 40% of the preformed amino acids required by mammals (Shimomura *et al.,* 2004, Rietman *et al.,* 2014).

Branched-Chain Amino Acids (BCAAs) have become popular in the athletic community, especially leucine, as they can enhance muscle protein synthesis (Gannon, Schnuck and Vaughan, 2018). Furthermore, BCAAs are assumed to enhance cell metabolism, as they can activate several regulatory targets involved in increasing mitochondrial metabolism (Gannon, Schnuck and Vaughan, 2018). Despite BCAAs potentially helping to increase skeletal muscle mass and improving cellular energetics, recently, some research has showed that elevated circulating concentrations of BCAAs have been observed during metabolic pathologies including insulin resistance/diabetes (Newgard *et al.*, 2009, Tai *et al.,* 2010; Chen *et al.*, 2016; Huffman *et al.,*2009; Shaham *et al.,*2008; Floegel *et al*., 2013; Würtz *et al.,* 2012).

1.3.1 BCAA metabolism

The first step in the metabolism of BCAA is a reversible transamination reaction producing their respective branched-chain a-keto acids (BCKAs)—L-leucine--a-ketoisocaproate (KIC), L-isoleucine--a-keto-b-methylglutarate (KIM), and L-valine-a-ketoisovalerate (KIV) and glutamate (Naylor and Shows, 1980). This transamination reactions are readily reversible, and the equilibrium constant is close to 1. The enzyme branched-chain amino acid aminotransferase (BCAT)

is involved in this step. During this step, BCAAs can either be transformed into their cognate BCKAs or synthesized from their respective branched-chain a-keto acid. BCAT has two molecular isoforms, BCATm, which is located in mitochondria and BCATc, which is located in the cytosol (Naylor and Shows, 1980).

The second step of BCAA catabolism is an irreversible reaction, whereby the BCKA substrate is oxidatively decarboxylated by the branched-chain α-keto acid dehydrogenase (BCKD) complex, to produce NADH, CO_2, and CoA derivatives of the oxidized BCKAs (Adeva *et al*., 2012; Hutson, Sweatt, and LaNoue, 2005). The BCKD complex contains multiple copies of three enzymes—a branched-chain α-keto acid decarboxylase (E1), a dihydrolipoyl transacylase (E2), and a dihydrolipoyl dehydrogenase (E3) (Lu *et al*., 2013). Activities of the BCKDH complex are tightly regulated by phosphorylation/dephosphorylation of the E1α subunit (Harris *et al.,* 1997). Afterwards, metabolism of the individual BCAA diverge. Leucine, as a ketogenic amino acid can produce acetyl-CoA and acetoacetate. Valine, a glucogenic amino acid, can produce succinyl-CoA, and isoleucine being both a glucogenic and a ketogenic amino acid, can produce succinyl CoA and oxaloacetate (Figure 1.7) (Hutson, Sweatt, and LaNoue, 2005).

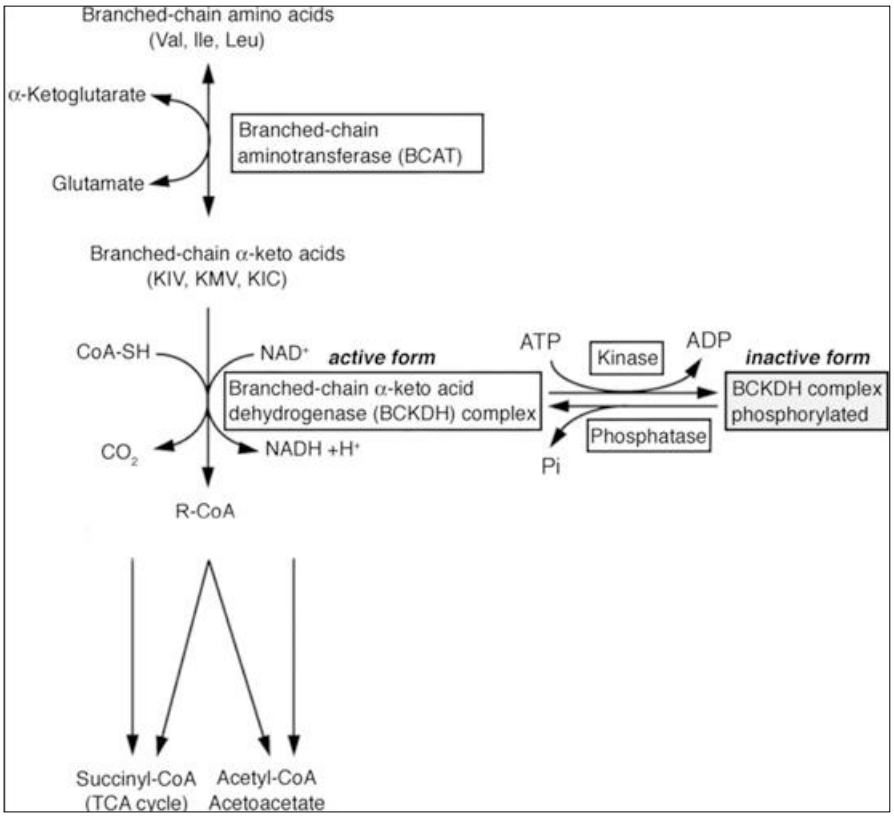


Figure 0.7 BCAA metabolism pathway. Reproduced from Brosnan and Brosnan, 2006

Through catalyzing by BCAT, the BCAAs produce BCKA. The second step is oxidative decarboxylation, catalyzed by the BCKD enzyme complex. After several steps, CoA derivatives can enter the TCA cycle to aid ATP resynthesis. **BCAT:** branched-chain amino acid aminotransferase. **BCKA:** branched-chain a-keto acids. **BCKD:** branched chain ketoacid dehydrogenase kinase. **ATP:** adenosine triphosphate. **ADP:** adenosine diphosphate. **CoA-SH**: reduced coenzyme A; **R-CoA**: acyl-CoA

1.3.2 Linkage between BCAAs and insulin resistance

The increased blood level of BCAAs in insulin resistant states or obesity has been noted for over 40 years (Felig, Marliss and Cahill, 1969; Caballero, Finer and Wurtman, 1988; Felig, 1970), however BCAAs have never been considered

as an important player in the modulation of insulin action, until the study conducted by Newgard *et al.,* (2009). He and his team demonstrated that BCAA-related metabolites show a significant linear relationship with insulin resistance ($r=0.58$, $p<0.001$) in humans, with insulin sensitivity assessed using homeostatic model assessment (HOMA, a method used to quantify insulin resistance and beta-cell function (Wallace, Levy and Matthews, 2004). Based on this work, he concluded that a high fat diet is not sufficient to induce insulin resistance, but requires additional factors such as elevated circulating BCAA concentrations. Huffman *et al.,* (2009) further validated the findings in a human cross-sectional study involving 73 sedentary, overweight to obese, dyslipidemic individuals. They found that besides the well-recognized risks for insulin resistance, elevated concentrations of large, neutral amino acids (including valine, leucine and isoleucine) were independently associated with insulin resistance. Following on from these reports, Chen *et al.,* (2016) found further evidence of the close correlation between BCAAs, insulin resistance, and future development of diabetes in Chinese populations. Specifically, baseline serum concentrations of five AAs (BCAAs plus the aromatic amino acids phenylalanine and tyrosine) were significantly elevated in those who were subsequently diagnosed with diabetes 10 years later. Among the five AAs, valine in particular stood out, with elevated concentrations associated with 251% increased odds (per s.d.) of developing diabetes in the future ($p< 0.001$). Secondly, the five AAs were found to be progressively increased in overweight/obese and diabetic subjects, and moreover, closely associated with multiple metabolic markers of

insulin resistance including HOMA-IR, BMI, and Hemoglobin A1c (HbA1c) (Chen *et al.,* 2016).

Importantly, those observations suggest that increased post-absorptive BCAA blood concentrations may be a causative feature in the development of insulin resistance. While the above investigations were performed in overweight or obese individuals where elevated plasma BCAA concentrations in the fasted state are commonly observed, the relationship between insulin resistance and BCAAs also can be observed in normal weight subjects. In Shaham *et al.,* (2008), a multivariate analysis of 191 metabolites examined in two groups of healthy individuals were measured by mass spectrometry. His team revealed that reductions in leucine/isoleucine concentrations during oral glucose tolerance tests represented the strongest predictor of insulin sensitivity. Another study from Tai *et al.,* (2010), who performed a large cross-sectional study in 263 non-obese Asian-Indian and Chinese men with a BMI of approximately 24 kg/m^2, confirmed again that BCAAs and related metabolites are associated with IR even in the absence of obesity (R^2=0.18, p=0.003). Moreover, traditional insulin resistance risk factors such as fatty acids and inflammatory cytokines could not discriminate between low HOMA and high HOMA subjects; in sharp contrast, increased concentrations of BCAAs and aromatic amino acids were significantly associated with IR. In an attempt to utilize this information as a prognostic tool, Wang *et al.,* (2011) executed a study to investigate whether BCAA metabolite profiles could predict the development of diabetes, using a nested case-control study (a retrospective study type that uses an existing cohort study) from Framingham Offspring Study. They demonstrated that

fasting concentrations of branched-chain and aromatic amino acids were elevated up to 12 years before the onset of diabetes; the risk of diabetes was increased at least fourfold in those with high plasma amino acid concentrations. These findings provide further evidence that BCAAs may be an early event responsible for eliciting metabolic changes that lead to the development of insulin resistance and if unresolved, diabetes. More recently, two large cohort studies proved the predictive value of BCAAs for IR/T2D (McCormack *et al.,* 2013; Floegel *et al.,* 2013). Analyzing the association between serum metabolites and risk of T2D in the European Prospective Investigation into Cancer and Nutrition (EPIC)-Potsdam (27,548 adults), they showed metabolic alterations, including BCAAs and aromatic amino acids were associated with a significant 3.82-fold increased risk of T2D (3.82 [2.64–5.52]) (Floegel *et al.,* 2013). Furthermore, in a cross-sectional cohort study involving 69 healthy subjects (ages 8–18 years), increased concentrations of BCAAs were significantly associated with body mass index (BMI) Z-score (Spearman's Rho=0.27, p= 0.03). In a subsequent longitudinal study, baseline BCAA concentrations were positively associated with the homeostasis model assessment for insulin resistance, measured 18 months later (p=0.046) (McCormack *et al.,* 2013).

To conclude, recent studies revealed a link between elevated circulating BCAAs and insulin resistance in obesity and normal weight subjects. It seems like BCAA metabolism and plasma concentration become the reliable and useful markers and act as a prognostic tool for IR and T2D development.

1.3.3 Why are BCAAs elevated with IR?

BCAAs as essential amino acids are obtained from our diet and cannot be synthesized endogenously within the human body. Consequently, plasma BCAA concentrations are heavily influenced by protein intake and show diurnal patterns of peaks and troughs based on meal consumption, subsequent digestion and uptake into bodily tissues. In a previous study, Newgard *et al.,* (2009) reported that there was no difference in protein consumption between obese (with IR) and lean subjects. In the later experiment of Tai *et al*., (2010), he confirmed that dietary protein intake did not differ between insulin-resistant (high HOMA) and sensitive individuals (low HOMA).

Another reason to explain why BCAAs are elevated along with IR condition could be accelerated protein degradation. Specifically, while insulin typically suppresses muscle proteolysis, with insulin resistance this fails to occur resulting in accelerated muscle protein degradation (Luzi, Castellino, and DeFronzo, 1996; Wang *et al.,* 2006).

Thirdly, evidences revealed that part of the reason for the higher levels of circulating BCAAs in insulin resistant states, including obesity, could be impaired BCAA oxidation in adipose tissue. The *in vitro* and *ex vivo* experiments suggested that adipose tissue is an important site for BCAA oxidation and can metabolize substantial amounts of BCAAs (Tischler and Goldberg, 1980; Rosenthal Angel and Farkas, 1974). Therefore, impaired BCAA oxidation in adipose tissue has been considered to be the primary reason for these observations. mRNA expression of mitochondrial BCAT and BCKDH complex

were reduced in adipose tissue of obese mice (ob/ob and Zucker rats) and in conjunction with increased plasma BCAAs concentrations, compared to lean mice (Suryawan *et al.,* 1998; She *et al.,* 2007A). She *et al*., (2007B) further demonstrated that in humans receiving surgical weight loss intervention (Roux-en-Y gastric bypass), plasma BCAA concentrations significantly decreased at post-surgery together with increased mitochondrial BCAT and total BCKD E1α (BCKD E1α subunit) in subcutaneous and visceral adipose tissue. Boulet *et al.,* (2015) showed that gene expression of BCKD-α and - β as well as BCAT2 were significantly decreased in visceral adipose tissue among women with a BMI ≥30 kg/m^2 compared with lean and overweight (BMI 25-30 kg/m^2) individuals ($p<0.05$ for all). In addition, the same authors showed that in obese women, increased plasma BCAAs occur independent of diet. A study analysing 14 pairs of monozygotic twins discordant for BMI, found that the BCAA catabolism pathway in adipose tissue was significantly downregulated in obese twins and correlated closely with IR (Pietiläinen *et al.,* 2008).

Interestingly, a few studies have suggested that increased BCAA could be a consequence of insulin resistance. As BCKD (enzyme in BCAA metabolism) activity is inhibited by insulin, BCAA catabolism also becomes inhibited in parallel (Adams, 2011; Adeva *et al.,* 2012). In insulin resistance subjects, increased plasma-free fatty acid levels are commonly associated with reduced BCKD activity (Adams, 2011). Therefore, it could be speculated that raised blood BCAA and BCKA concentrations in the obese, insulin-resistant state or in T2DM reflect reduced BCKD activity, and is a consequence rather than a cause

of insulin resistance. This conclusion is supported by *in vitro* data, but *in vivo* studies have shown that there is no decrease in leucine oxidation with hyperinsulinaemia (Heslin, *et al.,* 1992).

To conclude, these studies explain the correlation between increased plasma BCAA concentrations and degree of insulin resistance. Most, albeit not all, implicated decreased BCAAs oxidation, together with increased proteolysis in insulin resistance, as the source of the increased intracellular BCAA concentrations.

1.4. The possible mechanisms underlying the relationship between circulating BCAAs and IR

Amino acids are not only the building blocks of proteins, but also play an important role in activating and/or modulating signalling pathways. Recently, many compelling studies have shown that the extracellular BCAAs are transported into the cells through their respective transport mechanism, and then activate intracellular signalling pathways by stimulated intra-cellular amino acid sensor(s). The mTOR signalling pathway is one of the most studied signalling pathways in which the BCAAs are involved (Kim, 2009; Deldicque *et al.,* 2008; Tremblay*, et al.,* 2007a). Importantly, mTOR has been considered as the central signalling molecule mediating the crosstalk between amino acids and insulin. Both leucine and insulin seem to activate different signalling processes that converge at the mTOR complex (Adeva *et al.,* 2012).

1.4.1. mTORC1 and mTORC2

The mammalian Target of Rapamycin (mTOR) is a large (2549 amino acids) proline-directed serine threonine protein kinase, which belongs to the PI3K-related kinase family (Laplante and Sabatini, 2012). It contains 20 tandem HEAT repeats in the N-terminal. This repetitive structure is an important site for protein-protein interaction. FAT (FRAP, ATM, and TRRAP, all PIKK family members) and FRB (FKBP12/rapamycin binding) domains are followed by these HEAT repeats. The FATC (FAT C-terminus) domain is located at the end of the C-terminus of mTOR. The kinase domain is in the middle of the FATC and FRB domains (FKBP12/rapamycin), and located at the C-terminal (Figure 1.8). The protein mTOR is ubiquitously expressed, and can be found in cells such as the brain, skeletal system, reproductive system, and immune system (Vergès and Cariou, 2015).

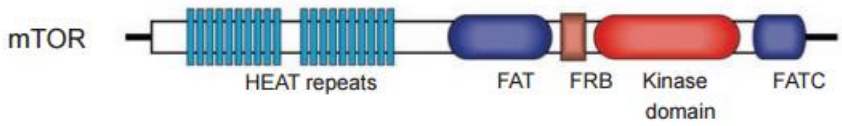


Figure 0.8 The structure of mTOR. Reproduced from Yang and Guan, 2007

There are five domains in mTOR. HEAT repeats: a protein-protein interaction structure. **FAT:** a domain structure shared by FRAP, ATM and TRRAP. **FRB:** FKBP12/rapamycin binding domain. **FATC:** FAT C-terminus

mTOR can form two different complexes, mTOR complex 1 (mTORC1) and

mTOR complex 2 (mTORC2) (Figure 1.9). Both mTORC1 and mTORC2 are very large and contain the same four subunits: mTOR subunit, mammalian lethal with sec-13 (mLST8, also known as GβL), DEP domain containing mTOR-interacting protein (DEPTOR), and the Tti1/Tel2 complex. However, the mTORC1 complex is distinct by incorporating regulatory-associated protein of mammalian target of rapamycin (RAPTOR) and proline-rich Akt substrate 40kDa (PRAS40). Conversely, only the mTORC2 complex includes the rapamycin-insensitive companion of mTOR (RICTOR), mammalian stress-activated map kinase-interacting protein 1 (mSin1), and protein observed with rictor 1 and 2 (protor1/2) (Vergès and Cariou, 2015; Laplante and Sabatini, 2012; Hara *et al.,* 2002; Kim *et al.,* 2002; Vander Haar *et al.,* 2007; Frias *et al.,* 2006). Figure 1.9 displays the details of each complex.

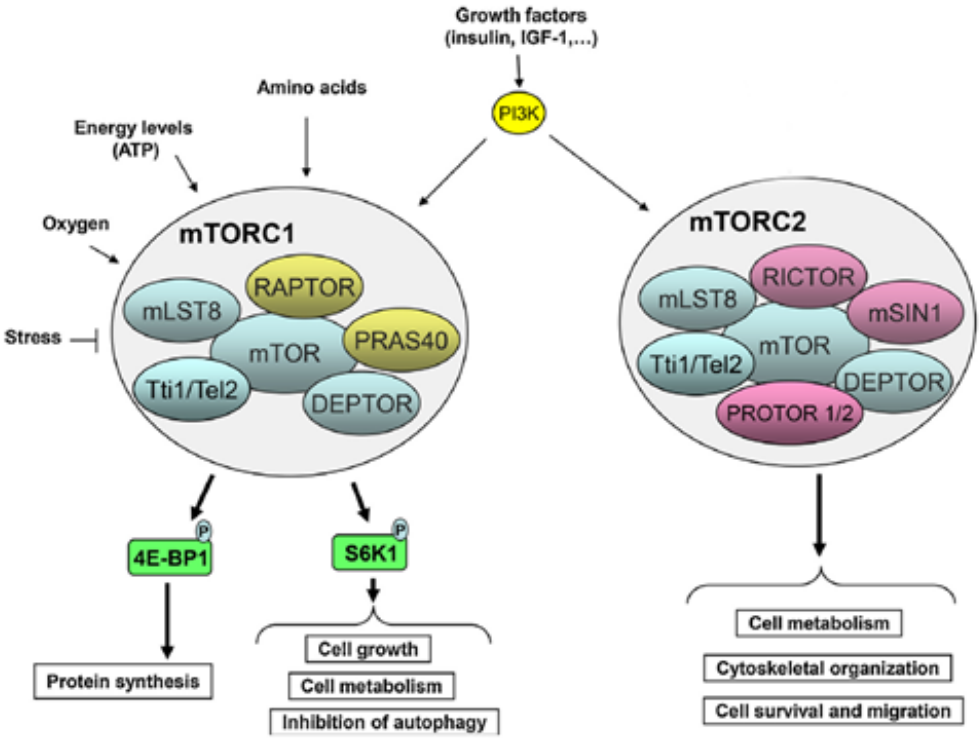


Figure 0.9 A diagram of the mTORC1 and mTORC2 protein complexes and their distinct cellular roles. Reproduced from: Vergès and Cariou, 2015

mTORC1 responds to amino acids, ATP, stress, and oxygen. It promotes protein synthesis, cell growth, and cell metabolism through regulated downstream proteins 4E-BP1and P70S6K. However, mTORC2 responds to growth factors and regulates cell survival, migration, and metabolism.

The RICTOR and RAPTOR proteins are thought to be primarily responsible for the different biological roles of the mTORC1 and mTORC2 protein complexes. As highlighted above and in Figure 1.9, the activity of both complexes is enhanced via PI3K signalling in response to growth factors including insulin. However, only mTORC1 is activated by amino acids, with mTORC2 insensitive to nutrients. While mTORC1 appears principally responsible for stimulating

protein synthesis, cell growth, cell metabolism and inhibiting processes associated with proteolysis through regulation of 4E-BP1 and p70S6K. mTORC2 has a wider role in regulating cellular metabolism and survival, but also in controlling cell metabolism, such as protein synthesis and glycolysis in skeletal muscle (via Akt activation) (Vergès and Cariou, 2015; Meng *et al.,* 2013; Zinzalla *et al.,* 2011).

1.4.2. mTOR signalling pathways

1.4.2.1. Downstream signalling pathway of mTORC1

In mammalian cells, mTOR directly phosphorylates the downstream proteins ribosomal protein S6 kinase beta-1 (S6K1; also known as p70S6 kinase), and eukaryotic initiation factor 4E binding protein (4E-BP1) to promote protein synthesis (Laplante and Sabatini, 2012). 4E-BP1 is a translational repressor, the un-phosphorylated form binds eukaryotic translation initiation factor- 4E (eIF4E) leading to its inhibition (Laplante and Sabatini, 2012). Crucially, the eIF4E complex is required for the initiation of cap-dependent translation; therefore, 4E-BP1 inhibits translation from occurring (Kim, 2009). After mTOR phosphorylates 4E-BP1, 4E-BP1 dissociates with eIF4E, allowing the latter to recruit other components to form eukaryotic initiation factor-4F complex (eIf-4F) and initiate translation (Redpath *et al.,* 1996; Yang and Guan, 2007). mTOR phosphorylates pyruvate dehydrogenase kinase 1 (PDK1) and works in conjunction with it to activate p70S6K. Activation of p70S6K phosphorylates a number of its substrates, such as ribosomal protein S6, which in turn regulates initiation of the 5′ TOP mRNAs (5’ terminal oligopyrimidine tract) translation

protein (Pópulo, Lopes and Soares, 2012).

To summarize, mTOR regulates proteins downstream that are crucial in the control of protein translation and cell growth.

1.4.2.2. Upstream signalling pathways of mTORC1

mTOR is involved in multiple signalling pathways in cell growth. Stimulation by growth factors and a change in nutritional status or energy requirements are transmitted to mTOR through a variety of signalling pathways, thereby affecting the downstream targets of mTOR to achieve the regulation of protein synthesis (energy dependent process) and cell growth.

mTOR regulated cell growth is controlled through three upstream signalling pathways. First is the PI3K/Akt/mTOR pathway. As highlighted in section 1.2.3, both PI3K and Akt are important upstream proteins for mTOR. Akt directly phosphorylates mTOR at Ser2448, thereby activating mTOR and its downstream pathways (Gao *et al.,* 2004). In ovarian cancer cells, PI3k transmits a mitogenic signal through Akt and mTOR to p70S6K (Kurebayashi *et al.,* 2012).

The second pathway is the Akt/TSC1-TSC2/mTOR pathway. The Tuberous Sclerosis Complex (TSC) is comprised of two subunits, TSC1 (also known as hamartin) and TSC2 (also known as tuberin). TSC1/TSC2 integrates many upstream signals that affect mTOR, including insulin and insulin-like growth factor 1 (IGF1). These growth factors through stimulating PI3K and Akt,

phosphorylate the TSC1/TSC2 complex to inactivate it and thus activate mTORC1 (Laplante and Sabatini, 2012). TSC1/TSC2 complex negatively regulates mTORC1 signalling by functioning as a GTPase-activating protein (GAP) for the small GTPase Rheb and converts Rheb to GDP-bound inactive form (Kim, 2009).

Rheb (Ras-homolog enriched in brain) small GTPase is an indispensable and essential regulator of mTORC1 and it can modulate kinase activity by directly binding to the carboxyl-terminal lobe of the mTOR catalytic domain (Long *et al.,* 2005; Sancak *et al.,* 2007). It has been proved *in vitro*, where Rheb was knocked down, that p70S6K and 4E-BP1 cannot be phosphorylated, however, overexpression of Rheb stimulates p70S6K and 4EBP1 phosphorylation (Zhang *et al.,* 2003; Tee *et al.,* 2003). Recently, it has been found that GTP-bound active Rheb sequesters FKBP38 to activate mTOR (Kim, 2009). The structure of FKBP38 is similar to FKBP12 and has an endogenous inhibitory effect on mTOR. Therefore, Akt phosphorylates (inactivates) TSC1/TSC2 and the mutational inactivation of TSC1/TSC2 leads to active mTORC1.

The last pathway is the LKB1/AMPK/TSC/mTOR pathway. Many stresses, such as low energy and oxygen levels, can influence mTORC1 via TSC1/2 (Laplante and Sabatini, 2012). Adenosine monophosphate-activated protein kinase (AMPK) is a cellular energy sensor that through combining of subunit (AMPKα) with its two regulatory subunits (AMKPβ and AMPKγ) forms a functional enzyme (Inoki, Zhu and Guan, 2003). Liver kinase B1 (LKB1) is an upstream kinase of AMPK that can phosphorylate the AMPKα activation loop under conditions of energy stress (ATP declines and AMP increases) (Shackelford and Shaw,

2009). When the intracellular AMP/ATP ratio increases, AMP combines with the gamma regulatory subunit and induces phosphorylation of AMPK on Thr172. Activated AMPK phosphorylates TSC2 and increases its GAP activity towards Rheb (Inoki, Zhu and Guan, 2003). Furthermore, activated AMPK also can directly phosphorylate mTOR on Thr2446, leading to inhibition of the kinase (Cheng *et al*., 2004).

Besides AMPK, another protein Sestrin 2 is also in the regulation of mTOR. Sestrin 2 is a leucine sensor for the mTORC1 pathway; it inhibits mTOR through activation of AMPK. A detailed description of Sestrin 2 is included in introduction will be shown in chapter 6.

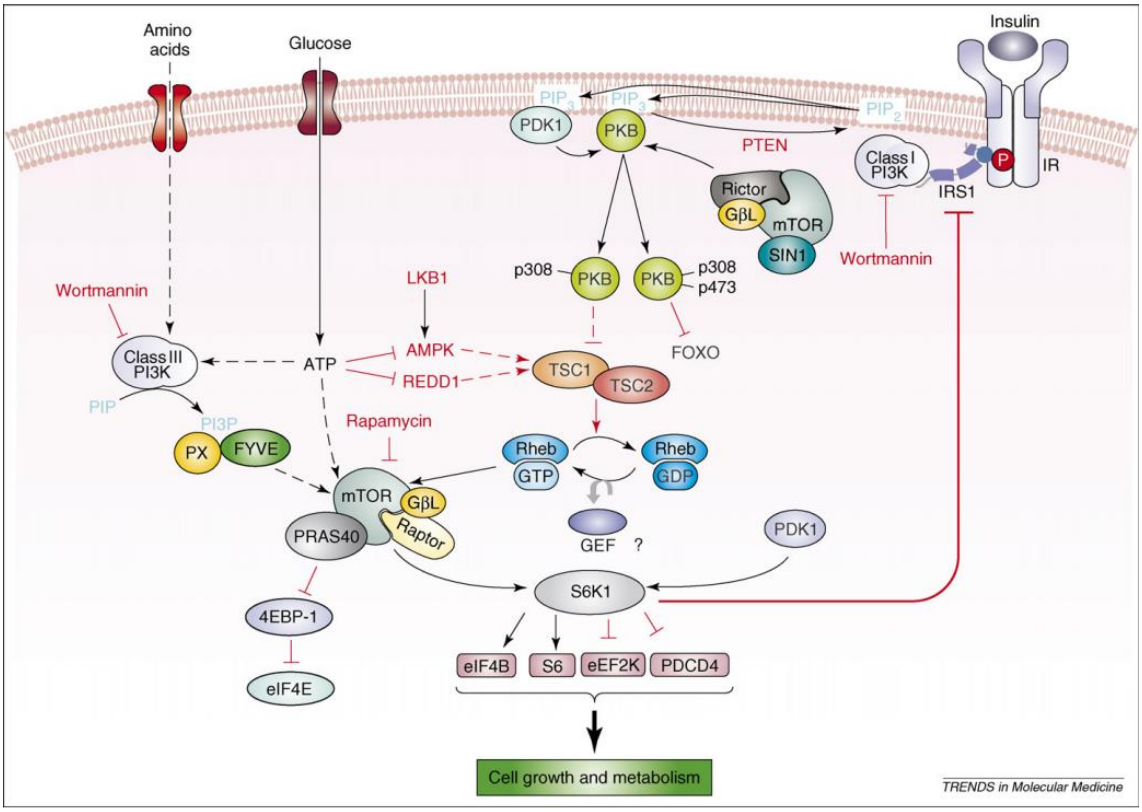


Figure 0.10 The Akt/mTOR signalling pathway. Reproduced from Dann, Selvaraj and Thomas, 2007

Insulin stimulates several proteins, leading to the activation of Akt. Activated Akt regulates cell proliferation and survival through mTORC1 and other intermediate proteins, including TSC1/2 and Rheb. mTORC1 phosphorylates its downstream protein 4E-BP1 and P70S6K to initiate protein translation. mTOR is inhibited by AMPK/TSC1/2 through cellular energy status (ATP declining and AMP increasing). Inhibitory phosphorylation events on IRS1 and the mTORC2 component Rictor by mTORC1 and/or p70S6K suppress the ability of insulin to stimulate Akt. **FYVE:** Fab1/YOTB/2K632.12/Vac1/EEA1 domain; **GEF:** guanosine nucleotide exchange factor; **PDCD4:** programmed cell death protein 4; **PX:** Phox homology domain. Wortmannin inhibits Akt whilst rapamycin inhibits mTOR.

1.4.2.3. mTORC2

Compared with mTORC1, there is limited information on the regulation of mTORC2. Some research has shown that mTORC2 activity is not inhibited by short term exposure to rapamycin, meaning mTORC2 is a rapamycin-insensitive protein (Jacinto *et al.,* 2004; Sarbassov *et al.,* 2004). However, with long time treatment, rapamycin reduces mTORC2 signalling by suppressing mTORC2 assembly in some cell types (Phung *et al.,* 2006; Sarbassov *et al.,* 2006). There is still a lot of unresolved questions regarding mTORC2 function, however, like mTORC1, the kinase responds to growth factors like insulin but is not sensitive to nutrients. It is known that mTORC2 directly phosphorylates Akt at Ser473, which is a site required for its maximal activation (Sarbassov *et al*., 2005). The phosphorylation of some Akt targets are impaired by Akt-Ser473, like forkhead box O1/3a (FoxO1/3a) but not TSC2 and GSK3-β (Guertin *et al*., 2006; Jacinto *et al*., 2006). Furthermore, mTORC2 directly activates SGK1, a kinase controlling ion transport and growth (Garcia-Martinez and Alessi, 2008). To conclude, in functional tissues like liver, muscle, and white and brown adipose tissue, the mTOR signalling pathway is a central regulator of mammalian metabolism and physiology. Dysregulation of mTOR signalling pathway in humans is a central player in many serious diseases including cancer and diabetes,

1.4.3. mTOR and glucose homeostasis

The potential relationship between mTOR and glucose homeostasis appears complex, with the topic still in its infancy. It has been argued that increased mTOR activity possibly impairs glucose homeostasis. Research has shown that in adipose tissue, mTORC1 promotes insulin resistance through the activation of p70S6K, leading to the inhibition of insulin signalling, principally through phosphorylation of a serine residue of IRS-1(Um, D'Alessio and Thomas, 2006; Werner *et al*., 2004). As a result, the recruitment and activation of PI3K in response to insulin-stimulated conditions is impaired. Similarly, in the liver, mTORC1/p70S6K activation caused the same serine phosphorylation of IRS-1, impairment of PI3K-Akt signalling, and in this tissue, the promotion of gluconeogenesis (Vergès and Cariou, 2015). Furthermore, other studies performed in rodents also confirmed that not only in the liver, but also in other insulin-target tissues (adipose tissue and skeletal muscle), increased mTOR and p70S6K activity contributes to elevated serine phosphorylation of IRS-1, leading to impaired insulin signalling to Akt (Um *et al.,* 2004, Khamzina *et al.,* 2005, Tremblay *et al.,* 2007b). Collectively, these experiments illustrated that continual activation of the mTOR pathway leads to harmful effects on insulin sensitivity. Furthermore, chronic mTOR activation enhances IRS-2 serine phosphorylation, which could offer a basis for how chronic mTOR could lead to insulin resistance (Briaud *et al.,* 2005).

As mentioned earlier, the pancreatic β-cell is a very critical component in the pathogenesis of type 2 diabetes mellitus, and mTORC1 is also involved in the regulation of β-cell mass and function. Rachdi *et al.,* (2008) demonstrated that

both β-cell size and count are increased by sustained activation of mTORC1, which led to increased insulin secretion and blood glucose concentrations decreasing. This infers that mTOR is a positive regulator of β-cell function. However, insulin secreting capacity reduces and glucose homeostasis deteriorates in mice with sustained activation of mTORC1 in β-cells (Shigeyama *et al.,* 2008). To conclude, it is very important to balance mTOR activity to control energy homeostasis under physiological conditions.

1.4.4. mTOR, BCAAs and glucose uptake

In mammalian cells, the BCAAs, particularly leucine, regulate cellular protein synthesis through activating the mammalian target of the rapamycin (mTOR) signalling pathway. Therefore, a possible link between BCAAs (via mTOR) and the regulation of glucose uptake, and by virtue, glucose homeostasis, exists.

In further support of the existence of an mTOR/p70S6K and IRS-1 feedback mechanism, regulated via BCAA stimulation, Newgard *et al.,* (2009) designed an experiment. His team reported that male Wistar rats who had a standard chow, high fat, or high fat+BCAAs for 13 weeks, then fasted for 48 hours, refed original diet for 4 hours showed increased phosphorylation of mTOR and p70S6K, in conjunction with increased phosphorylation of IRS-1 Ser307 in skeletal muscle (Newgard *et al.,* 2009). Similar results were observed by Tremblay *et al.,* (2005b) where in skeletal muscle of humans infused amino acids, mTOR/p70S6K signalling was enhanced in conjunction with phosphorylation of IRS-1 at Ser636/639, concomitant with decreased PI3K

activity. Further, experiments in L6 myotubes confirmed that amino acid–induced phosphorylation of IRS-1 Ser636/639 was prevented by blocking the mTOR/p70S6K pathway with rapamycin, whilst PI3K activity and glucose transport were also improved (Tremblay *et al.,* 2005a). By using L6 myotubes and 3T3-L1 adipocytes, Tzatsos and Kandror (2006) demonstrated that leucine regulated PI3K/Akt signalling through stimulation phosphorylation of IRS-1 on Ser636/639 in a rapamycin-sensitive, but AMPK-independent manner. This phosphorylation with other mTOR/p70S6K-mediated phosphorylation events together suppressed insulin-stimulated PI3K activity and the interaction of IRS-1 with the insulin receptor. This may cause impairing of adaptor abilities of IRS-1 and, finally, lead to degradation of IRS-1. Furthermore, they demonstrated that treating HepG2 cells and to a lesser effect L6 myotubes, with metformin, causes AMPK to become activated and the phosphorylation of IRS-1 on Ser636/639 and p70S6K on Thr389 suppressed. This caused an improvement to insulin-stimulated phosphorylation of Akt and activation of phosphorylated glycogen synthetase kinase 3β. It has been demonstrated in another experiment, performed in mice, leucine deprivation improves insulin sensitivity in peripheral tissues, including liver, white adipose tissue, and muscle (Xiao *et al.,* 2011). Xiao *et al.,* (2011) confirmed this result in an *in vitro* experiment performed in HepG2 cells, illustrating an improvement of insulin sensitivity with leucine deprivation, concomitant to decreased mTOR/p70S6K signalling and increased activation of AMPK.

All of the above experiments show that increased circulating BCAA concentrations impair glucose uptake, potentially as a consequence of increase

in mTOR activity which phosphorylates (inhibits) IRS-1, leading to a reduction in insulin signaling. However, controversy remains in the scientific community. p70S6K promotes IRS-1 degradation, therefore, with sirolimus (rapamycin, mTOR inhibitor) treatment, intracellular IRS-1 protein content should increase. However, in male Wistar rats, Deblon *et al.,* (2012) showed that after sirolimus treatment, phosphorylation of IRS-1 and IRS-2 either decreased or displayed no change in soleus and gastrocnemius muscle, without any difference in their mRNA levels. Furthermore, phosphorylation of Akt at Ser473 significantly decreased (vs control, $p<0.001$). However, this experiment did not investigate the impact of leucine or BCAAs in this process.

Other studies showed that BCAAs influenced glucose uptake via an unknown mechanism independent of negative feedback between mTOR/p70S6K and IRS-1, potentially because leucine affects other proteins, such as Akt and GLUT4. Insulin-induced glucose uptake was promoted by leucine in cultured primary rat muscle cells, but leucine alone did not increase phosphorylation of Akt and drive glucose uptake (Liu *et al.,* 2014). This may be because leucine alone cannot activate Akt. Liu *et al.,* (2014) indicated that leucine is involved in increasing glucose uptake via a pathway that is independent of the insulin signalling pathway, because a PI3K inhibitor can only partially blocked this effect. Another experiment from Nishitani *et al*., (2002) showed that soleus muscles isolated from normal rats incubated in 2mM leucine for 30 minutes, stimulated glucose uptake via PI3K and Protein kinase C (PKC) pathways, but independent of mTOR. Furthermore, they proved that 2mM alpha-KIC, a

metabolite of leucine, also improved glucose uptake when incubated for 30 minutes. However, the effect of this metabolite is not as profound as leucine. They suggested that leucine promotes glucose uptake through an insulin-independent mechanism. C2C12 skeletal muscle cells treated for 24 hours with 2mM leucine exhibited increase total GLUT4 protein content (Schnuck *et al*., 2016) and both GLUT4 and glucose uptake are increased in skeletal muscle of Sprague Dawley rats with liver cirrhosis when treated with 180 min leucine oral gavage (Nishitani *et al*., 2005).

Increasing evidence suggests that leucine treatment increases the tyrosine kinase phosphorylation of the insulin receptor, and stimulates glucose uptake in skeletal muscle both *in vivo* and *ex vitro* (Li *et al*., 2013; Macotela *et al*., 2011; Peyrollier *et al*., 2000; Morato *et al*., 2013; Liu *et al*., 2017). However, this is at odds with studies demonstrating a relationship between leucine and/or BCAA plasma concentrations, mTOR/p70S6K signalling pathway activity, and impaired glucose uptake. Thus, the role of BCAA in the control of muscle glucose uptake remains controversial with many questions unsolved. Therefore, this topic formed the focus of the Ph.D. studies described in this thesis.

1.5. Aim and Objectives

1.5.1. Hypothesis and Aim

Previous literatures have indicated that increased intracellular BCAA in muscle cells impairs glucose uptake, purportedly through the activity of mTOR. However, this conclusion is still controversial and the mechanisms are unclear.

Besides, no study has focused on whether intracellular BCAA concentrations are changed by chemical reagents that affected mTOR activity (e.g. rapamycin). Therefore, the overall aim of this thesis is to investigate the relationship between changes in intracellular BCAAs, mTOR activity and glucose uptake in muscle cells and the mechanisms responsible. The hypothesis was that increased intracellular branched chain amino acids would impair insulin-stimulated glucose uptake in muscle cells via the mTOR/p70S6K pathway.

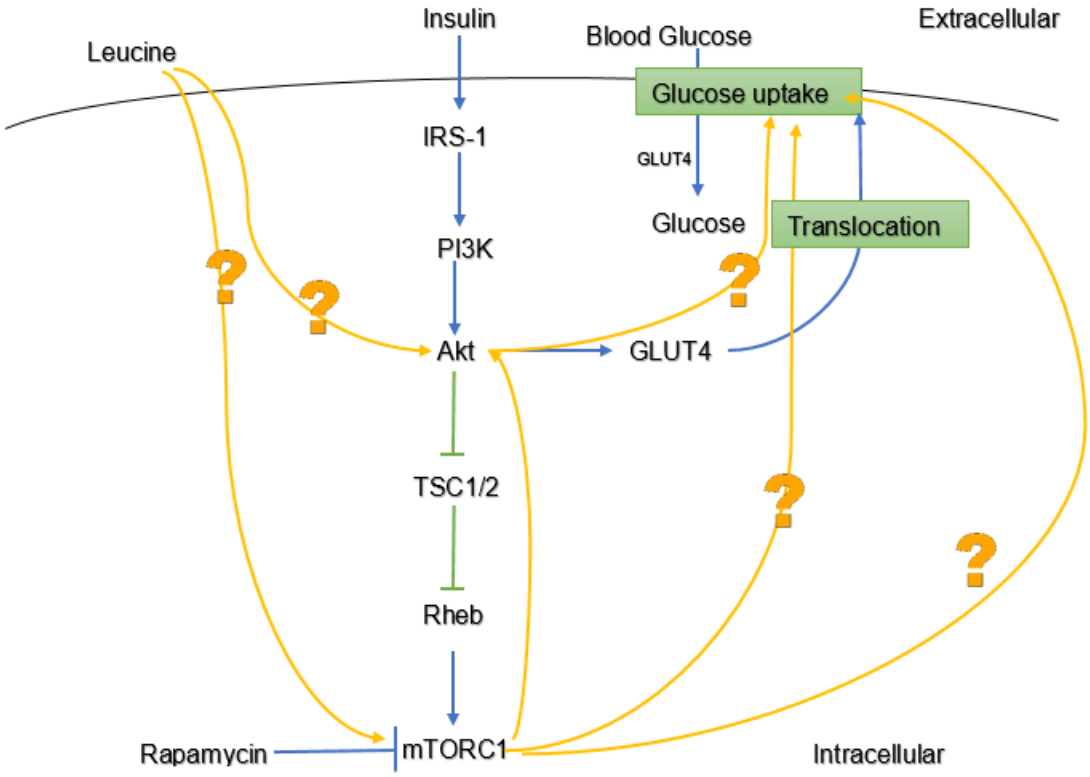


Figure 0.11 The hypothesis of this research

Insulin through PI3K/Akt/TSC1-2 signalling pathway stimulate mTORC1 promote protein synthesis. By stimulating with insulin and PI3K, Akt recruits GLUT4 to the cells membrane (translocation), which allow glucose into cells. This process is called

glucose uptake. The figured showed some questions: whether mTOR directly affects glucose uptake or via Akt? Whether leucine will affect glucose uptake and via mTOR signaling pathway or Akt? **Blue and green full line:** the mechanisms has been proved by others. **Yellow full line:** possible mechanism. **IRS-1:** Insulin receptor substrate 1, **PI3K:** Phosphoinositide 3-kinases, **Akt/PKB:** Protein kinase B, **TSC1/2:** Tuberous sclerosis 1/2, **mTOR:** mammalian target of rapamycin, **GLUT4:** Glucose transporter type 4

1.5.2. Objectives

1. Under conditions of cycloheximide-induced increases in intracellular BCAA concentrations, examine the impact on mTOR and its downstream proteins (4E-BP1, p70S6K) in muscle cells.
2. Investigate how pharmacological modulation of mTOR phosphorylation by rapamycin, 3BDO (an activator of mTOR) and BCH (inhibitor of leucine transporter) affects glucose uptake in muscle cells.
3. Investigate the impact of manipulating extracellular leucine concentrations on glucose uptake and mTOR, 4E-BP1, p70S6K, Akt phosphorylation in muscle cells.
4. Utilize Adeno-Associated Viruses to induce overexpression of the mTOR inhibitor, Sestrin 2, to examine the impact on mTOR signalling and glucose uptake.

CHAPTER 2: GENERAL MATERIALS AND METHODS

2.1. General materials

All laboratory reagents that were described in this thesis were purchased from various suppliers. The detailed information and product codes were showed in this methods chapter or within specific results chapters. Water used for buffer preparation was purified by MilliQ Elix® water purification system.

2.2. Mammalian Cell Culture

2.2.1. Techniques for cell culture

All cell culture work was performed in a Class II microbiological safety cabinet. The media and reagents purchased were suitable for cell culture work (sterile-filtered). Non-sterile reagents were filtered through a 0.2μm filter (Sarstedt) before being added to the media and filtered through a 250 or 500ml Filtration Systems (431096 or 431097, Corning) prior to cell culture work. Non-sterile equipment was autoclaved at 121°C for 15min (MP24 Control System, Rodwell Scientific Instruments) before use.

2.2.2. L6 Cell line

2.2.2.1. Passaging of L6 cells

L6 cells were transferred to a new flask at 50%-60 confluence to continue growth (passaged) in order to maintain the cells in an optimal proliferative state. For all the experiments, L6 cells were kept between passages 10 and 20. In brief, passaging was performed by the removal of growth media (Minimum Essential Media Eagle (M4526, Sigma-Aldrich) supplemented with 10% (v/v)

Heat inactivated Foetal bovine serum (FBS; 11550356, Gibco by Life technologies) and 1% (v/v) Penicillin/Streptomycin (p/S; 10,000units/ml penicillin and 10,000µg/ml streptomycin; 15140122, Gibco by Life technologies), cells washed by sterile phosphate buffer saline (10 ml; PBS, phosphate buffer saline tablets, P4417, Sigma-Aldrich) and 2ml of warm trypsin-EDTA solution (0.25% trypsin-EDTA, Gibco by Life technologies) added to dislodge cells. After 5 minutes in 37 ºC incubator, 8 ml of growth media was added to the flask and the resultant cell suspension was centrifuged at 1000rpm for 5 minutes (Eppendorf Centrifuge 5702R) and the supernatant was discarded. The cell pellet was re-suspended in 10 ml of fresh growth media. The resultant cell suspension (1ml) was transferred to a new T75 flask (430641U, Corning) containing 13ml growth media

2.2.2.2. Culturing L6 cells

L6 cells stored in liquid nitrogen were thawed at 37°C until 90% thawed, and then transferred to a T75 cell culture flask with 13ml growth media. The flask was kept in a 37°C humidified incubator with 5% CO_2 overnight.

After cells reached 80%-90% confluence, L6 myoblasts were differentiated by replacing the media with a low serum differentiation media (alpha-MEM (M4526, Sigma-Aldrich), supplemented with 2% (v/v) Horse Serum (Thermo Fisher Scientific; 26050070) and 1% (v/v) p/S. As L6 cells were switched to differentiation media, this day was labelled as ‘day 0’. Differentiation media was replaced every 2 days. Myoblasts would fuse to form multinuclear myotubes

within 4-8 days of differentiation.

.

2.2.2.3. Freezing and thawing L6 cells

In order to maintain a cell population for subsequent experiments, at first passage, one flask of cells would be frozen down and stored in liquid nitrogen. To accomplish this, cells were dislodged via the use of trypsin-EDTA solution as described above, the cell suspension pelleted (see 2.2.2.2 Passaging of L6 cells), and the cells frozen in freezing media containing 90% FBS and 10% dimethyl sulfoxide (DMSO; D/4120/PB08, Fisher Chemicals). The vials were placed in a Mr Frosty^{TM} Freezing Container (within 100% isopropanol (p/7500, Fisher Scientific) 5100-0001, Thermo ScientificTM) and stored in the -80°C freezer overnight before being transferred to liquid nitrogen for long-term storage.

2.2.2.4. Counting L6 cells

Ensuring the same number of cells are used between treatment groups is important in reducing experimental variability, so it is important to transfer the same number of cells in to each well. To count the number of cells in a cell suspension, a drop (~10µl) of the suspension is placed in the space between the counting chamber and the glass cover of a haemocytometer, before being examined under a microscope. Counting three of four squares in the counting chamber and average this number, by using the following formula to calculate total cell number in the suspension.

$\boldsymbol{Total\ cell\ number}$=$Average\ cell\ number\ x\ 10^4\ x\ Total\ volume\ of\ cell$

$suspension\ (\mu l)$

Different cell culture plates required different cell numbers to be seeded at the start of the experiment; table 2.1 shows the particular seeding densities used throughout the studies described in this thesis.

Table 0.1 The seeding density of different plates in Cell Culture

	Surface area (cm2)	**Seeding density**	**Growth media (mL)**
6-well	9	0.3 x 10^6	2
12-well	4	0.1 x 10^6	1
24-well	2	0.05 x 10^6	0.5

(Source from: Thermo fisher scientific)

Using this formula to determine the volume of cell suspension required for the needful cell number.

***Volume Required* (*µl*)=** $Cell\ number\ required/Total\ cell\ number\ x\ Total\ volume\ of\ cell\ suspension\ (\mu l)$

2.2.3. C2C12 cell line

The cell culture procedures for C2C12 cells were identical to those described for the L6 cell line, with the exception that the growth media used to culture C2C12 cells differed (high-glucose Dulbecco's Modified Eagle's Media (D5796, Sigma-Aldrich)) and supplemented with 10% (v/v) FBS and 1% (v/v)

Penicillin/Streptomycin. Likewise, for the differentiation media, DMEM supplemented with 2% (v/v) Horse Serum and 1% (v/v) Penicillin/Streptomycin was used.

2.3 Adeno-Associated Viruses (AAV)

Adreno-Associated Virus (AAV) is a small, non-coating virus with an icosahedral structure. It contains a linear single-stranded DNA genome that is between 4.7 and 6kb in size. Furthermore, it can infect dividing and non-dividing cells. Therefore, AAV is an ideal viral vector for genetic manipulation.

So far, there are 11 serotypes of AAV from 1 to 11, and they all have different tropism that can infect cells from multiple diverse tissue types, with tissue specificity determined by the capsid serotype. Therefore, selection of the right serotype is critical in delivery of a target gene to cells or tissues (Vigene Biosciences, 2016). In our lab, we utilise AAV1, which is known to be compatible with gene delivery to muscle tissue and muscle cells (Ellis *et al*., 2013).

2.3.1 Preparing of samples and reagents

AAV1 (Table 2.2) stocks were supplied in liquid form, and aliquoted before storage to prevent titer reduction from multiple freeze-thaw cycles. To induce Sestrin 2 over-expression, the gene was inserted in to the AAV1 vector under a cytomegalovirus promoter and containing a green fluorescent protein (GFP) reporter, the latter allowing transduction efficiency into the target cell to be assessed via fluorescence microscopy.

Table 0.2 The information of AAV1-Sestrin2 and GFP.

GFP

Vector ID	VB170330-1063sby
Vector Name	pAAV[Exp]-CMV>EmGFP:WPRE
Size	5118 bp
Vector Type	Adeno-associated virus gene expression vector
Inserted Promoter	CMV
Inserted ORF	EmGFP
Plasmid Copy Number	High
Antibiotic Resistance	Ampicillin
Cloning Host	Stbl3 (or alternative strain)

Sestrin2

Vector ID	VB170330-1051zkn
Vector Name	pAAV[Exp]-CMV>mSesn2[NM_144907.1](ns):T2A:EmGFP:WPRE
Size	6621 bp
Vector Type	Mammalian Gene Expression AAV Vector
Inserted Promoter	CMV
Inserted ORF	mSesn2[NM_144907.1](ns), EmGFP
Inserted Linker	T2A
Plasmid Copy Number	High
Antibiotic Resistance	Ampicillin
Cloning Host	Stbl3 (or alternative strain)

The original stock of GFP was $4.12X10^{12}$ in 1ml, after divided stock into aliquots (5), each vial was $8.24X10^{11}$ GC (200 µl). One of the vials was used to make

the 1:100 solution with cold media (500 µl, $4.12X10^9$ GC) and 1:10 solution with cold media (50 µl, $4.12X10^{10}$ GC). For the Sestrin 2 was $8.61X10^{11}$ in 1ml, each vial was $1.722X10^{11}$GC (200 µl). Again, these were diluted to make the 1:10 solution with cold media (50 µl, $8.61X10^9$ GC). Both GFP and Sestrin 2 (200 µl) vials were further aliquoted to 5 µl in 0.5 ml microcentrifuge tubes and frozen in a -80°C freezer. On each use, cold PBS was added to make new stock.

For AAV1 experiments, the day before transduction, L6 cells were seeded in to 24-well plates at a density of $1x10^4$ cells per well and maintained in growth media. After 24 hours, the cells became adhered to the surface of the plate and the transduction experiment was performed as described below.

2.3.2 Determination of the MOI (multiplicity of infections)

Multiplicity of Infection (MOI) equals the number of viral particles (vp) per cell. In other words, 'a MOI of 1 means infecting with 1 viral genome (vg) per cell' (Vigene Biosciences, 2016). AAV genome copies (GC) per ml was measured by real-time qPCR in comparison with a standard reference plasmid with known genome copy number (Vigene Biosciences, 2016). In order to determine this optimal concentration of virus to be used in the current study, a viral vector containing GFP under a CMV promoter was first used. For an unknown infection rate, a wide MOI range is important to set up. The following formula was used to calculate the amount of AAV needed:

AAV GC particles needed= *MOI* Number of cells to be infected*

For the first AAV experiment, a wide MOI range was selected prior to optimization. Therefore, selected MOI were $1X10^4$, $5X10^4$,$1X10^5$, $2X10^5$, $5X10^5$,

with each performed in duplicate. The dilution required to reach the desired multiplicity of infection are detailed in tables 2.3 and 2.4.

Table 0.3 The media needed for each GC (250 µl/well) of GFP

GC	Media required for 2 wells	GFP required from stock
$1X10^8$	475 µl	24 µl
$5X10^8$	379 µl	121 µl
$1X10^9$	257 µl	243 µl
$2X10^9$	15 µl	485 µl
$5X10^9$	493.9 µl	6.1 µl (1:10 stock)

Table 0.4 The media needed for each GC (250 µl/well) of Sestrin 2 (Stock 1:10)

GC	Media required for 3 wells	Sestrin 2 required from stock
$1X10^9$	733 µl	17µl
$2X10^9$	715 µl	35 µl

2.3.3 Protocol for *in vitro* cell transduction

At the start of the experiment, tips, pipettes and microcentrifuge tube were

cooled to 4 ºC before use and the thawed AAV virus kept on ice throughout. Growth media was removed from the wells and directly replaced with differentiation media containing the AAV1-GFP plasmid. Afterwards, the L6 cells in the virus containing media were incubated at 37°C with 5% CO_2. Transduction efficiency was confirmed by fluorescent microscopy with Lumen 200 Fluorescence Illumination System (Prior Scientific) at 24h, 48h, 72h and 96h. On inspection, a GC of $1X10^9$ and $2X10^9$ for AAV1-GFP showed very good transduction (results showed in chapter 6); for the Sestrin 2 containing vector, only these two GC were considered.

2.4 Glucose uptake Assay

2.4.1 Principle

Glucose uptake was determined using a commercial kit from Promega (Glucose Uptake-Glo™ Assay J1343 50ml, Promega). The assay uses a non-radioactive, plate-based, homogeneous bioluminescent method for measuring glucose uptake in mammalian cells based on the detection of 2-deoxyglucose-6-phosphate (2DG6P) (Glucose Uptake-Glo™ Assay Instructions for Use of Products, 2017).

In short, 2-Deoxy-D-glucose (2-DG) is a compound closely related in structure to glucose and can be taken up in to cells in response to insulin (Wick *et al.,* 1957). When 2DG is added to cells, it is transported across the membrane and rapidly phosphorylated to form 2-deoxyglucose-6-phosphate (2DG6P). The enzymes within the cells that can metabolise glucose-6-phosphate (G6P) cannot metabolise 2DG6P, and therefore 2DG6P accumulates in cells in a

manner that is proportional to its uptake (Glucose Uptake-Glo™ Assay Instructions for Use of Products, 2017).

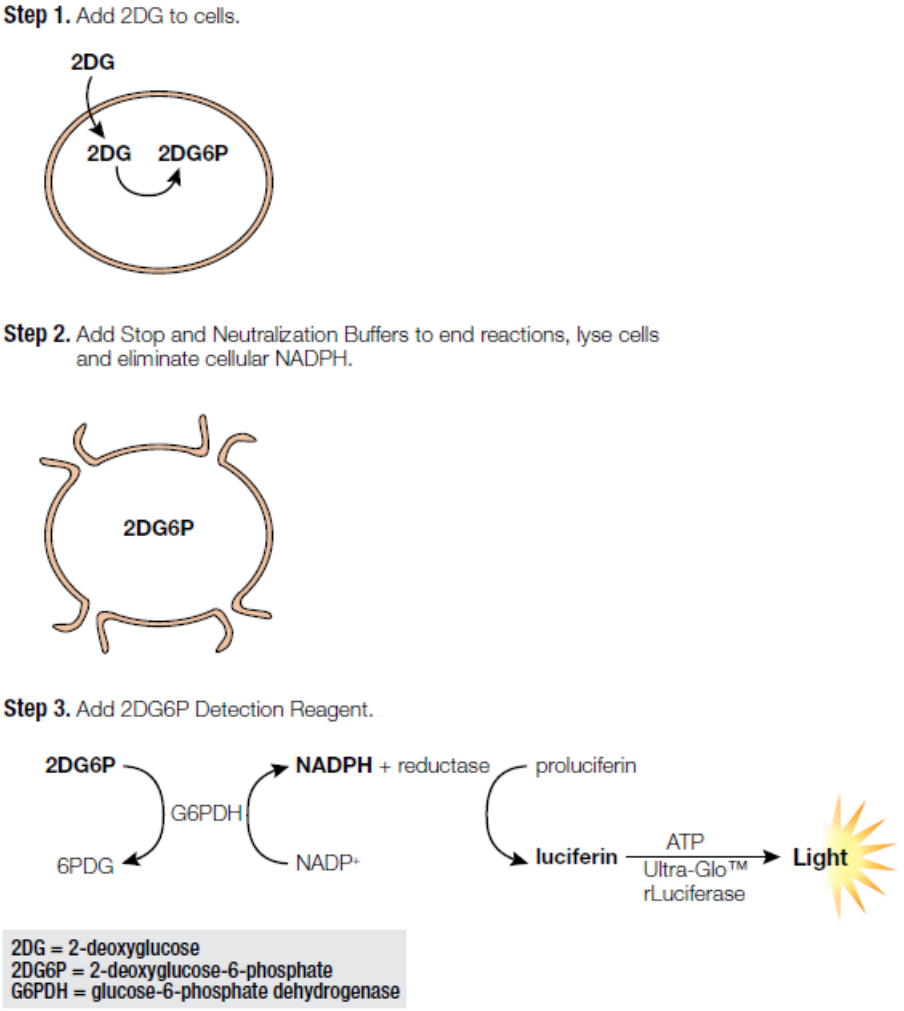


Figure 0.1 The step of Glucose Uptake-Glo™ Assay technology. Reproduced from Glucose Uptake-Glo™ Assay Instructions for Use of Products, 2017

Following addition of 2DG to cells and its conversion to 2DG6P, it begins to accumulate in the cells. 2DG6P is detected by a solution containing glucose-6-phosphate dehydrogenase (G6PDH), NADP+, Reductase, Ultra-Glo™ Recombinant Luciferase and proluciferin substrate. Under these conditions, 2DG6P is oxidized to 6-phosphodeoxygluconate by G6PDH, simultaneously reducing NADP+ to NADPH. In parallel, reductase causes the conversion of proluciferin to luciferin, which in combination with the Ultra-Glo™ Recombinant Luciferase reagent, produces a luminescent signal that is proportional to the concentration of 2DG6P.

2.4.2 Sample preparation

Myoblast C2C12 cells and L6 cells were cultured in 24-well plates (Costar®, 3524) with $2x10^4$ cells per well and grown for about 1-2 days in growth media (DMEM, 10% FBS, 1% Penicillin/Streptomycin). After cells reached ~65% confluence they were switched to differentiation media (DMEM, 2% HS, 1% Penicillin/Streptomycin) for 5-7 days, with the first application of differentiation media termed day '0'. Only after cells were fully differentiated, did the cells receive the desired treatments.

2.4.3 Reagent preparation

All of the components were thawed to room temperature in a water bath, after which the Luciferase Reagent, Stop Buffer, and Neutralization Buffer were kept at room temperature; all other components were stored on ice.

2.4.4 Procedure

The day before the assay, the differentiation media was replaced with no serum DMEM media (containing 1% (v/v) Penicillin/Streptomycin). On the day of the assay, investigatory reagents associated with the stimulation or inhibition of anabolic signalling were added as described in subsequent chapters. After the allotted time, cells were incubated in 1mM insulin for 1 hour at 37°C in 5% CO_2. After 1h, the media was removed and the cells washed once in PBS, 0.1mM 2DG (250µl) in PBS was added to each well. Cells were incubated for 30

minutes at 25°C. The 2DG6P detection reagent was reconstituted 1h before use and kept at room temperature to minimize assay background.

After 30 minutes, 125µl stop buffer was added to each well and after about 15 minutes, samples were mixed and 75 µl of each sample transferred to a 96-well plate (Costar®, 3904), followed by addition of 25 µl of neutralization buffer. Afterwards, 100µl of detection reagent (Table 2.5) was added and the samples incubated for 1 hour at 25°C before being read on a luminometer (Fluostar, Omega).

Table 0.5 Relative volumes of different components for detection reagent

Component	Per Reaction
Luciferase Reagent	100µl
NADP+	1µl
G6PDH	2.5µl
Reductase	0.5µl
Reductase Substrate	0.0625µl

2.5 Intracellular BCAAs Assay

Intracellular BCAA concentrations were determined using two different methods, however they both relied upon the same fundamental principle. Because three BCAAs shared the first enzymatic steps in their metabolic pathways, therefore, leucine dehydrogenase can catalyzes all of them to produce NADH, which as a colored product, can be detected spectrophotometrically.

Leucine dehydrogenase (NAD^+, EC 1.4.1.9) catalyzes the following reactions:

Leucine + NAD^+ ⇋ a-ketoisocaproate + NADH+ H^+

Isoleucine + NAD^+ ⇋ a-ketomethylvalerate + NADH+ H^+

Valine + NAD^+ ⇋ a-ketovalerate + NADH+ H^+

The rate of appearance of NADH was determined spectrophotometrically by assessing the samples absorbance at 340 nm.

2.5.1 Spectrophotometric Assay for Measuring Branched-Chain Amino Acids

2.5.1.1 Preparation of reagents

The following solutions are prepared fresh each day, including Glycine–KCL–KOH buffer (0.2 M, pH 10.5), 2 mM EDTA and NAD (120 mM, pH 10.7), diluted in 0.1 M sodium carbonate buffer. The glycine-KCL-KOH buffer consist of 0.2M glycine and 0.2M KCL, with 2M KOH used to adjust the pH to 10.5, followed by the addition of 2mM EDTA. Leucine dehydrogenase (1027 units/ml, 79846-1ML, Sigma-Aldrich) was diluted to 200 units/ml in 25 mM sodium phosphate buffer, pH 7.2, and divided into aliquots of 10 U, and stored at -20 °C. Leucine dehydrogenase and NAD were maintained at 5°C; the buffers were maintained at room temperature. All reagents were sourced from Sigma Aldrich.

2.5.1.2 Standard Curve and sample preparation

The production of NADH (nmol/min) was determined in response to

concentrations of 50, 100, 200, 400, 600, 800 and 1000μM leucine to produce a standard curve.

The C2C12 cells were cultured in 6 well plates with 3 x 10^5 cells per well (Costar®, 3516). After being subjected to various treatments described in subsequent chapters, cells were washed in PBS three times and extracted using a glycine-KCL-KOH buffer (0.1M, pH 10.5) containing 2mM EDTA with cells gently lysed using a glass Potter-Elvehjem homogeniser attached to an overhead stirrer (Heidolph).

2.5.1.3 Procedure for the spectrophotometric assessment of Branched-Chain Amino Acids concentrations

After centrifugation (14,000rpm for 5 minutes) to remove insoluble material, the BCAA concentrations in the supernatant was assessed using the following procedure: to 10 μl of sample in a 96-well clear bottom plate, 270 μl of a glycine-KCL-KOH buffer was added, along with 10 μl of 120 mM NAD (diluted in 0.1M sodium carbonate buffer, pH 10.7) and 10 μl of leucine dehydrogenase (2 units). The reaction was initiated by addition of the leucine dehydrogenase and the optical density measured after 1 min at 340 nm using a spectrophotometer. The concentration was calculated from a standard curve performed in parallel using standards of known leucine concentrations.

2.5.2 BCAAs Assay kit (K564-100)

This Assay kit included BCAA Assay Buffer (25ml), BCAA Enzyme Mix (lyophilized), WST Substrate Mix (lyophilized) and Leucine Standard (1 μmol;

100µl). Before use, components were allowed to warm to room temperature and vials were briefly centrifuged prior to opening. The BCAA Enzyme Mix and WST Substrate Mix were added with 220 µl BCAA Assay Buffer and 220 µl of dH2O, separately. The WST Substrate Mix was shielded from light during use.

2.5.2.1 Standard curve and Samples preparation

The 10µl leucine standard was diluted with 90µl dH_2O to generate 1 mM leucine standard. Next, 0, 2, 4, 6, 8, 10 µl of the diluted 1 mM leucine Standard was added into a clear 96 well plates (Greiner Bio-One, 655101) to produce a 0 to 10 nmol/well standard curve. To each well Assay Buffer was added to make up the volume to 50µl.

The L6 cells were cultured in 6 well plate with 3×10^5 per well (Costar®, 3516). After being subjected to various treatments described in subsequent result chapters, the cells were collected in BCAA Assay Buffer (50µl each well). A sonicator was used to lyse the cells (10-15 second for each sample). Afterwards, samples were centrifuged at 14,000rpm for 10 minutes to remove cell debris and other insoluble materials. Afterwards, samples of different volumes (10 µl, 15 µl, 20 µl) were added to separate wells to make sure the readings were within the standard curve range, with Assay Buffer added to make the final volume 50µl.

2.5.2.2 Process of testing intracellular BCAA concentrations

After samples and standard wells, a Reaction Mix reagent that included 46µl Assay Buffer, 2µl Enzyme Mix and 2µl WST Substrate Mix were added to each well. A background correction consisting of 48µl Assay Buffer, 2µl WST Substrate Mix and 50 µl of sample or leucine standard were also included. The 96-well plate for was incubated for 30 minutes at room temperature while being protected from light. After 30 minutes, the plate was read at 450 nm in a microplate reader (Fluostar, Omega).

2.5.2.3 Calculations

Intracellular BCAA concentrations were determined from a standard curve run in parallel, with background reading subtracted from the BCAA test sample readings.

2.6. Western Blot

2.6.1. Preparing of reagents

To quantify the abundance and phosphorylation state of various proteins of interest, western blot analysis (also called protein immunoblot) was performed. A stock of 2X Sodium Dodecyl Sulfate (2XSDS) buffer was prepared as described in Table 2.6. The lysis buffer (1xSDS) consisted of 5ml of Elix water (dH_20) and 5ml of 2XSDS stock solution, to which two tablets of a protease inhibitor cocktail was added (cOmplete,11697498001, Sigma-Aldrich, Poole, Dorset, UK) and phosphatase inhibitor cocktail (PhosSTOP, 04906845001, Sigma-Aldrich, Poole, Dorset).

Normally, antibodies recognize a small portion of the protein of interest, and this

domain may be masked by the 3D conformation of the protein. Therefore, proteins need to be unfolded or “denatured”, to make sure that antibody binds the intended site. SDS is used to denature secondary and tertiary protein structures and change the conformation of the protein, while DL-Dithiothreitol (DTT) is used to reduce the disulphide bonds of proteins. The inclusion of protease and phosphatase inhibitors prevents protein degradation or dephosphorylation. Glycerol is added to increase the density of the sample and aid loading of the sample on to the gel.

Table 0.6 The components in 10ml 2XSDS

Reagents	**Volume (ml)**
Glycerol (>=99%)	2
1M Tris-HCl (pH 6.8)	1.25
SDS Solution (10% w/v)	4
1M DTT (0.154g/ml)	1ml or 0.154g
Bromophenol Blue	Few grains
Elix water	1.75
Total volume	10

(UltraPure™ Glycerol, ThermoFisher 15514011; DTT, D9779 Sigma-Aldrich; SDS, L4390 Sigma-Aldrich; Tris, Fishersci BP1521; Bromophenol Blue, B/P620/44 Fishersci)

2.6.2. Collecting cell samples for western blot analysis

After being subjected to various treatments described in subsequent result chapters, media was completely removed from each well, and cells were washed gently in 1ml iced-cold PBS. Afterwards, lysis buffer (1xSDS) was added and the sample incubated at room temperature for about 5 minutes, using a cell scraper to scrape (83.1830, SARSTEDT) the surface of the well to help assist with the cell lysing process before samples were collected. 6 well plates were used (Costar®, 3516), with 150-200 µl of lysis buffer added to each well. The samples were kept on ice during the collection process, and then stored at -20°C or below prior to subsequent analysis.

2.6.3. Quantification of protein concentration by 2D Quant kit method

All of the aforementioned samples underwent protein quantification prior to western blot analysis to allow for even loading of samples on to the polyacrylamide gels. In short, samples were heated to between 95-100°C for 5 minutes and then centrifuged at a minimum of 14,000rpm for 10 minutes (Microfuge® 22R microcentrifuge, Beckman Coulter UK Ltd.) and placed on ice. Afterwards, protein concentrations were determined using the 2D-Quant kit (80-0483-56, GE Healthcare Life Sciences).

A standard curve (from 0-25 µl) was created using 2mg/ml bovine serum albumin (BSA) in 2ml clean microcentrifuge tubes (S1620-2700, TubeOne® Microcentrifuge Tubes), in which the final protein concentration was 0, 10, 20, 30, 40 and 50µg.

10-20µl of samples were pipetted into 2ml clean microcentrifuge tubes, then

500µl of Precipitant reagent added to both samples and standard curve. Samples were vortexed briefly and incubated at room temperature for 2-3 minutes. After that, 500µl of Co-precipitant reagent was added to each tube and mixed briefly. The Precipitant reagent and Co-precipitant reagent can help protein to quantitatively precipitate while leaving interfering contaminants in solution. Afterwards, all the tubes were centrifuged at 14,000rpm for 10min to pellet the protein, followed by careful and complete removal of the supernatant, and the pellet retained.

After centrifugation, 100µl copper solution and 400µl Elix water was added to each tube and vortexed until the pellet was dissolved. The working colour reagent was mixed by combining colour reagent A and B in 100:1. 1ml of working reagent was added to each tube, mixed well and incubated at room temperature for 15-20 minutes.

Before the results were read, samples and standards were transferred to cuvettes (10x4x45mm, 67.742, Sarstedt), and read at an absorbance of 480nm on a UV/Vis Spectrophotometer (Ultrospec III, Pharmacia LKB). Elix water was used as a reference, and the absorbance read within 40 minutes of the addition of working colour reagent. The liner standard curve was generated by plotting the absorbance of the standards against the quantity of protein, and used to quantify unknown sample protein concentration. All samples were then normalised to 1 or 2µg/µl with 1x SDS loading buffer.

2.6.4. Polyacrylamide gel electrophoresis (PAGE)

In short, samples were thawed on ice, then equal amounts of protein in a final volume of 15µl were loaded into the wells of a SDS-PAGE gel (4–15% Criterion™ TGX™ Precast Midi Protein Gel, 26 well), which included in separate wells 10 µl of a stained molecular weight marker (Color-coded Prestained Protein Marker, Broad Range (11-250 kDa) #14208). All samples were run on the same gel, and separated through sodium dodecyl sulfate polyacrylamide gel electrophoresis (SDS-PAGE) at 200V for 30-45 minutes. The running buffer was diluted fresh before use from a 10X Tris glycine SDS stock solution (final concentration is 1x).

As the protein is negatively charged, it migrates to the positive electrode located at the bottom of the gel. Small molecular weight proteins easily pass through the gel with low resistance and fast migration speed, while the migration of large molecular weight proteins is impeded by greater resistance, allowing proteins to be separated by molecular weight.

2.6.5. Transfer gels to polyvinylidene difluoride membrane

The transfer buffer was prepared (Table 2.7) before the gel was removed from the plastic cassette, and kept gel in transfer buffer to prevent it from drying out. Simultaneously, the materials for the ‘transfer sandwich’, which including sponges, filter papers and membrane were prepared. Specifically, the big filter paper was cut to an appropriate size and then soaked with the sponges in transfer buffer for a minimum of 20min. The polyvinylidene difluoride (PVDF) (Amersham Hybond p 0.45 PVDF 300mmx4m, 10600023 GE Healthcare)

membrane was soaked in methanol for 2-3 minutes and then incubate in cold transfer buffer for 10 minutes before use.

Table 0.7 The components of transfer buffer

Products	**Quantity**
Glycine	60g
Tris	6g
Isopropanol	100ml
Elix water	Fill up to 2L

(Glycine, G8898, Sigma; Tris, BP152-1, Fisher Scientific; Isopropanol, P7500, Fisher Scientific)

In wet transfer, the gel and membrane were sandwiched between sponges and paper, with all materials clamped tightly together to discharge air bubbles. The sandwich was submerged with the transfer buffer in the transfer tank (Trans-blot cell No.36S/3076, Bio-Rad), with the transfer direction from negative to positive, the membrane would bind the protein during its migration out of the (Figure 2.2). Two cooling coils were used to keep transfer buffer cool.

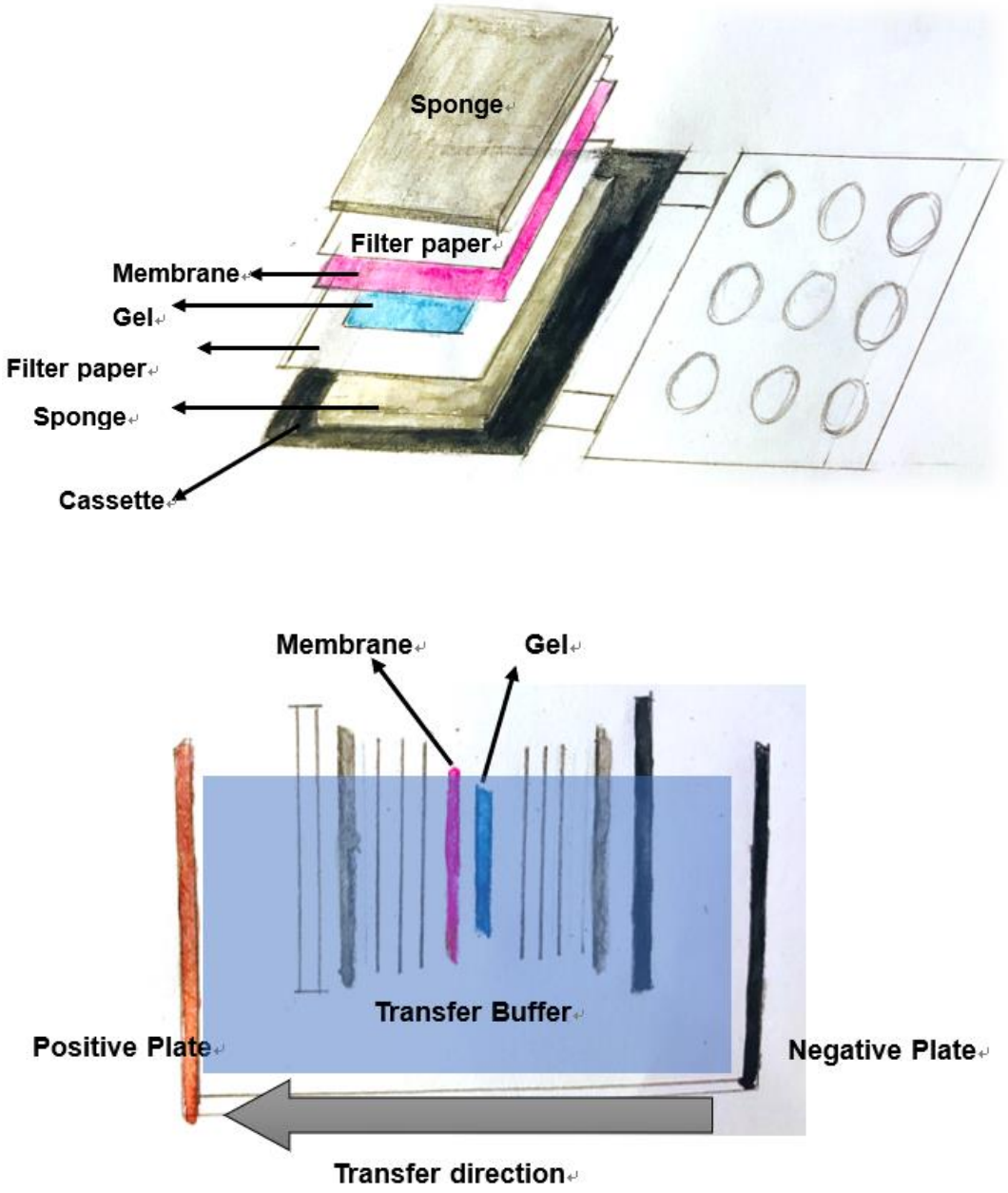


Figure 0.2 The Organisation of the transfer cassette.

The transfer sandwich is sponge/paper/gel/membrane/paper/sponge, after the cassette is clamped tightly and air bubbles discharged, the cassette is placed in to a transfer tank with transfer buffer. The transfer tank connected to a PowerPac (PowerPac™ Basic Power Supply, Bio-Rad) with 1 Ampere of current applied for 2 hours to aid transfer.

2.5.8 Ponceau-S stain and Blocking

After transfer finished, the membrane was removed from the cassette and cut to an appropriate size. Ponceau S was used to check for success of transfer. If the transfer was successful, the protein band could be seen (Figure 2.3). Afterwards the membrane was washed extensively and carefully for several times with Elix water to remove the stain; if red colouration was still seen, TBST was used to completely destain the membrane while on a rocker (SSL4, Stuart; washing speed: 25 oscillations/min). The TBST was made by 10XTBS (concentrated Tris-buffered saline, Table 2.8), Elix water and Tween 20. After being washed with TBST, the PVDF membrane was reactivated by methanol again.

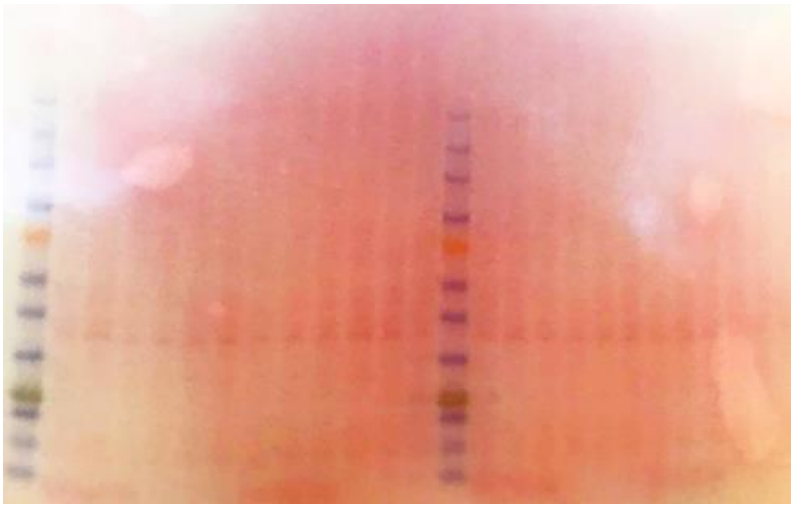


Figure 0.3 The example of Ponceau-S red stain.

Table 0.8 Volume of components for 10X TBS.

Product	Quantity
Sodium chloride	90g
Tris (1M, pH 7.5)	200ml
Elix water	Top up to 1L
For TBST 1L: 100ml of 10XTBS+900ml Elix water+1ml Tween20	

(Sodium chloride, S9626 Sigma-Aldrich; Tris, BP152-1, Fisher Scientific; Tween 20, P1379 Sigma-Aldrich)

To prevent the primary and secondary antibodies binding the non-specific background on the membrane, blocking is necessary. Because phosphorylated proteins were required to be tested, milk cannot be used as it contains casein which is a phospho-protein. Therefore, Bovine Serum Albumin (BSA, A7906 Sigma-Aldrich) was used as a blocking agent instead. The membrane was soaked with 5% BSA solution (5g BSA+100ml TBST) for 1 hour while being agitated and at room temperature.

2.6.7. Primary and secondary antibody

The primary antibody was diluted in 5%BSA at the protocol suggested dilution. After 1h blocking, the membrane was incubated with primary antibody in 5%BSA and left on a rocker at 4°C overnight. The next day primary antibody was removed, and the membrane washed with 1XTBST a minimum of three times. The secondary antibody was diluted in 5%BSA at the protocol suggested dilution. Afterwards, the membrane was incubated in secondary antibody for 1.5

hours on a rocker at room temperature. Antibody concentration was important as too much antibody will result in non-specific bands.

After the allotted time, the secondary antibody was removed and the membrane washed several times in TBST as descried above.

2.6.8. Detection

The protein bands were detected using ECL (RPN2109, GE Healthcare) or ECL Select detection reagents (RPN2235, GE Healthcare), with the reagents used according to manufacturer's instructions. Protein bands were visualized using x-ray films and the resultant bands quantified by using Quantity One 4.6.8 Software to normalize. On occasion, a ChemiDoc MP Imaging System (Bio-Rad) was used in combination with the ECL reagent to detect and quantify protein bands. The included software (Image Lab 6.0.1 Software for Windows) was used to analyze the data.

2.6.9. Stripping

When measuring the phosphorylation levels of specific proteins, membranes were washed afterwards by stripping buffer (Restore™ PLUS Western Blot Stripping Buffer, 46430; Thermo Fisher), and the membranes reprobed with total protein primary antibody as described above. In short, membranes were stripped by using 20ml of the stripping buffer per membrane and with the membrane and reagent incubated at room temperature on a rocker for 15

minutes. Afterwards the membrane was washed for 30 minutes with TBST and blocked with 5%BSA for 30 minutes. To confirm successful stripping of the original primary antibody before reuse, the membrane was incubated with secondary antibody for 1h and protein bands visualized using ECL as described above. If successful, the membrane was washed in TBST, blocked with 5%BSA for 30 minutes, and then incubated with primary antibody on the rocker at 4°C overnight, before proceeding with subsequent steps of the western blotting protocol as described above.

2.7. Real Time Quantitative Polymerase Chain Reaction (RTqPCR)

2.7.1. Collecting cell samples

Samples used for RTqPCR were collected with RNase-free PBS. In short, after completely removing the media, 200µl of ice-cold RNase-free PBS was added to each well of a 6 well plate and a cell scraper used to dislodge the attached cells. For 24 well plates, 45µl of ice-cold RNase-free PBS was added and a sterile pipette tip used to remove the cells. Afterwards samples were stored at -80 ºC before subsequent processing.

2.7.2. RNA extraction methods

Due to time issues, the RNA extractions, cDNA synthesis and subsequent RTqPCR analyses were all performed by Dr Zoe Daniel on the samples I generated. The methods she used are described briefly here.

Total RNA from cultured cells was extracted using the High Pure RNA Isolation Kit (Roche, Burgess Hill, UK) following the manufacturers guidelines. The

eluted, purified RNA was stored at –80°C for later analysis.

2.7.3. RevertAid RT First Strand cDNA Synthesis kit

After quantity and quality of RNA was confirmed, first strand cDNA synthesis was performed on 500ng RNA using the RevertAid First Strand cDNA Synthesis Kit (#K1622, Thermo Fisher Scientific) according to manufacturer's instructions.

2.7.4. Real time quantitative PCR (RTqPCR)

RTqPCR was used to measure the relative mRNA transcript abundance of genes of interest, performed on a Lightcycler® 480 instrument, using SYBR Green I Master (04707516001, Roche). The reaction was performed in a 384 well optical plate, with each reaction consisting of 5 µl of cDNA, 7.5 µl of SYBR green master mix (Roche), 0.45 µl each of a forward and reverse primer targeting the gene of interest (10 µM stock; final concentration 0.3 µM of each, see 2.7.5) and 1.6 µl RNase-free H_2O, giving a final volume of 15 µl per well. Samples were pre-incubated at 95°C for 5 min followed by 45 PCR amplification cycles consisting of: de-naturation: 95°C for 10 s; annealing: 60°C for 15 s; elongation: 72°C for 15 s.

2.7.5. Primer designs and synthesis

Primers were designed using Primer Express© Software Version 3.0.1 (11983, Applied Biosystems). Table 2.9 shows the primer information of studied genes.

Table 0.9 RTqPCR primers for mouse genes measured.

Gene	Forward (F) and reverse (R) primer sequences (5' to 3')
GLUT1	F: AGAGTGTGCTGAAGAAGCTTCGA
	R: GCCGACCCTCTTCTTTCATCT
GLUT2	F: TGGCTGCCTTCAGCAACTG
	R: CAAGGAAGTCCGCAATGTACTG
GLUT3	F: CCCTCAGCTGCAGCCTACTTA
	R: CTCCGGGACTTTGAAGAAGGT
GLUT4	F: CAGTATGTTGCGGATGCTATGG
	R: GGCACTTTTAGGAAGGTGAAGATG
Sestrin2	F:CGCCACTCAGAGAAGGTTCAC
	R:CATAGAGCAAAGCTGCTTGCA

2.8. Statistics

All experiments were performed in triplicate unless specified otherwise. Description of the statistical tests performed are described in each of the experimental chapters. Chapter 3 results (one-way ANOVA) was performed by IBM SPSS Statistics (24th edition). Chapter 4 and 5 results, one-way and two-way ANOVA tests were performed by Genstat (19th edition) followed by post-hoc Bonferroni test when appropriate (ANOVA $p<0.05$). A value of $p < 0.05$ was considered statistically significant. Data are presented as Means ± standard error of the mean (SEM).

CHAPTER 3: EXAMINATION OF WHETHER ACUTELY INCREASED INTRACELLULAR BCAA CONCENTRATIONS INFLUENCE GLUCOSE UPTAKE IN CULTURED MUSCLE CELLS

3.1. Introduction

Peripheral insulin resistance is common in the obese and strongly linked to the development of diabetes. Therefore, it is important to identify the causative features of insulin resistance to develop effective treatments that can prevent or reverse this condition. Recent studies revealed strong evidence that elevated circulating BCAA concentrations are commonly observed in the obese, even under fasting conditions, and have been implicated as a causative feature of insulin resistance (Chen *et al.,* 2016; Shah *et al.,* 2012; Wang *et al.,* 2011; Newgard, *et al.*, 2009; Huffman *et al.,* 2009). The data from previous studies described in the introduction chapter clearly displayed the relationship between IR and BCAAs. When compared with some IR risk factors, like obesity, blood lipids and inflammatory cytokines, BCAAs seem better as a predictor of the future development of diabetes for humans.

Although the relationship between IR and BCAAs is still not fully understood, there exists several possible mechanisms to explain this relationship. One of them is the mTOR pathway. The mTOR pathway, which is a nutrient-sensing pathway, can combine both nutrient sensing and insulin signalling to coordinate cell growth and metabolism (Rietman, 2015). mTOR plays a crucial role in the association between BCAAs and insulin action.

As highlighted in the introduction, some reports have demonstrated that mTORC1 promotes IRS-1 serine-phosphorylation, thereby impairing PI3K-Akt signalling, a pivotal process in driving the cellular uptake of glucose in response to insulin. This negative feedback loop may lead to decreased insulin sensitivity.

Therefore, activated mTOR via increased intracellular BCAA concentrations may cause insulin resistance.

Cycloheximide (CHX) is a eukaryotic protein synthesis inhibitor produced by the bacterium, *Streptomyces griseus.* The main biological activity of CHX is to inhibit translational elongation of protein, resulting in inhibition of cell growth or induction of cell death. It has been shown in other studies that CHX activates mTORC1 through increases in intracellular amino acid concentrations, due to its ability to inhibit protein synthesis in the face of persistent protein breakdown (Beugnet *et al.,* 2003; Watanabe-Asano, Kuma and Mizushima, 2014).

Therefore, the aim of this chapter was to determine the effects of acutely increased intracellular BCAA concentrations on glucose uptake via the mTOR pathway in muscle cells. C2C12 myotubes were used as the muscle cell line and CHX used as a method to increase intracellular BCAA concentrations, due to the inhibition of protein synthesis. Therefore, the first step was to check if CHX would increase intracellular BCAA concentrations and thereby stimulate the mTOR signalling pathway.

The next step was to then investigate the effects of increased intracellular BCAA concentrations on insulin-stimulated glucose uptake. However, it has been suggested that C2C12 cells do not always show insulin-stimulated glucose uptake (Dr. John Brameld, personal communication). To date, a number of *ex vitro* model systems have been utilised for in-depth studies on the glucose uptake in muscle cells and several cell lines derived from skeletal muscle (e.g. rat L6 and mouse C2C12) have been used to investigate glucose metabolism

(Yap *et al.,* 2007). Both L6 myoblasts and myotubes have been suggested to have GLUT4 translocation machinery that can be activated by insulin stimulation. Therefore, rat L6 skeletal muscle cell line is the most frequently used to study the insulin-stimulated glucose transport system. On the other hand, C2C12 cells, which are derived from mouse skeletal muscle, are mostly used to investigate muscle cell differentiation and development, such as myofibrillogenesis, sarcomere development, and myotube contractions (Cooper *et al.,* 2004; Moran *et al.,* 2002; Kislinger *et al.,* 2005). This cell line has had limited use in research investigating insulin-dependent glucose transport (Nedachi and Kanzaki, 2006). Although, these two cell lines have been used to investigate insulin-stimulated glucose transporters, some reports have suggested that when stimulated with insulin, L6 myotubes appeared to exhibit glucose uptake to a larger extent than C2C12 cells, and the latter's insulin responsiveness is reported to be minimal even after differentiation (Yap *et al.,* 2007), possibly due to C2C12 cells not expressing sufficient GLUT4 protein (Kotliar and Pilch, 1992; Tortorella and Pilch, 2002). Yap *et al*., (2007) found that L6 cells were the best choice to research glucose uptake in muscle cells. Therefore, the second part of this chapter was to test whether C2C12 or L6 cells have stronger insulin sensitivity and to compare the mRNA expression of the glucose transporter genes, GLUT1, GLUT2, GLUT3 and GLUT4.

3.2. Materials and Methods

C2C12 and L6 cells are used in this experiment, for the detailed methods please see section 2.2. The specific treatments will be introduced in this part.

3.2.1. The treatment of C2C12 cells

The C2C12 cell culture (6 well plates) was described in section 2.2.2 and 2.2.3. After cells were fully differentiated, cells were divided into six groups: control group which were incubated in fresh differentiation media for 4 hours; an amino acid starved group incubated in PBS for 4 hours, a time period known to result in dephosphorylation of mTOR in C2C12 cells (Atherton *et al.,* 2010); or treatment with CHX (C7698, Sigma) in differentiation media at a final concentration of either 5, 10, 25 or 50 µg/ml (n=3 per group). According to previous studies, the effective CHX concentration and treatment time were 10 µg/ml or 50 µg/ml (Beugnet *et al*., 2003; Watanabe-Asano, Kuma and Mizushima, 2014), therefore, we set up a dose-dependent experiment. A diagrammatic representation of the study protocol can be seen in Figure 3.1. The control and PBS groups were treated for four hours, whereas the CHX treatment groups were kept in differentiation media for 3.5h, with CHX added for the last 30 min.

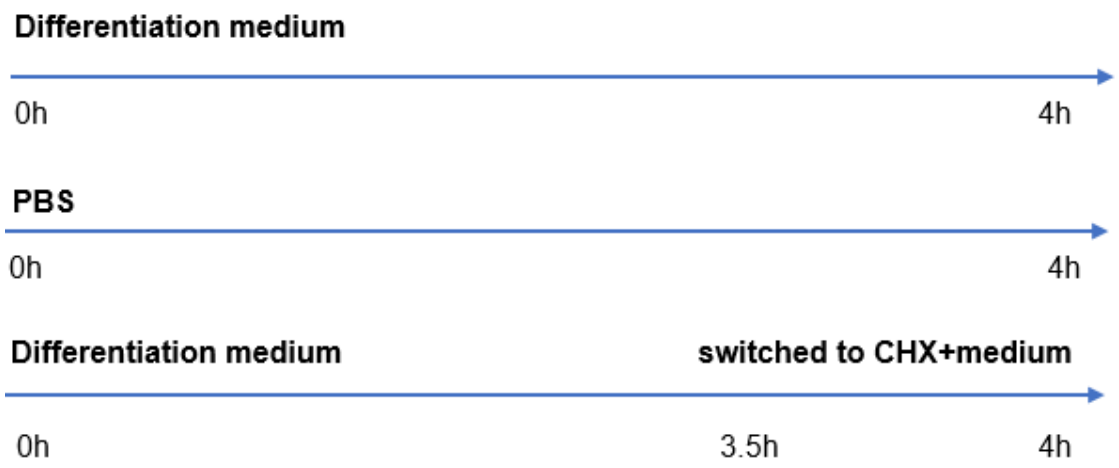


Figure 3. 1 Timeline of different treatment groups

For the control and PBS groups were 4 hours differentiation media treatment; for CHX group, treated with 3.5 hours differentiation media, then switched to different concentration CHX differentiation media for 0.5 hours.

3.2.2. Determination of intracellular BCAA concentrations

After removing the media, samples were washed once by PBS, then samples were collected into glycine-KCL-KOH buffer (0.1M, pH 10.5) containing 2mM EDTA (see 2.4.2.2).

Intracellular BCAA concentrations were determined using a modified enzymatic fluorimetric assay (as describe in chapter 2.5.1).

3.2.3. Western blot antibodies

After removing the media, samples were washed once with PBS and then collected into lysis buffer, the rest of steps were described in chapter 2.6.

Antibodies : rabbit anti mTOR antibody (#2972), rabbit anti-phospho-mTOR (Ser2448; #2971), rabbit anti-phospho-4E-BP1 (Thr37/46; #9459), rabbit anti-phospho-p70 S6 Kinase (Thr389; #9205), rabbit anti-β-Actin Antibody (#4967),

anti-rabbit IgG, and HRP-linked Antibody (#7074) were all purchased from Cell Signalling Technologies. All the primary antibodies were diluted 1:1000 with 5%BSA and the secondary antibody diluted 1:5000 with 5%BSA.

3.2.4. L6 and C2C12 cells treated for glucose uptake and RTqPCR

To assess glucose uptake, L6 and C2C12 cells were cultured in 24 well plates, and for RTqPCR experiment, 6 well plates were used. The associated experimental steps were described in detail in section 2.4 and 2.7.

3.2.5. Statistical Analyses

All statistics were performed by IBM SPSS Statistics 24 software. CHX treatment experiment, one-way ANOVA was performed. For L6 and C2C12 comparison experiment (glucose uptake and qPCR), Student's t test was performed. The western blot data was quantified by Image Lab (V 5.2.1 Bio-Rad). Significant differences were considered as $p<0.05$.

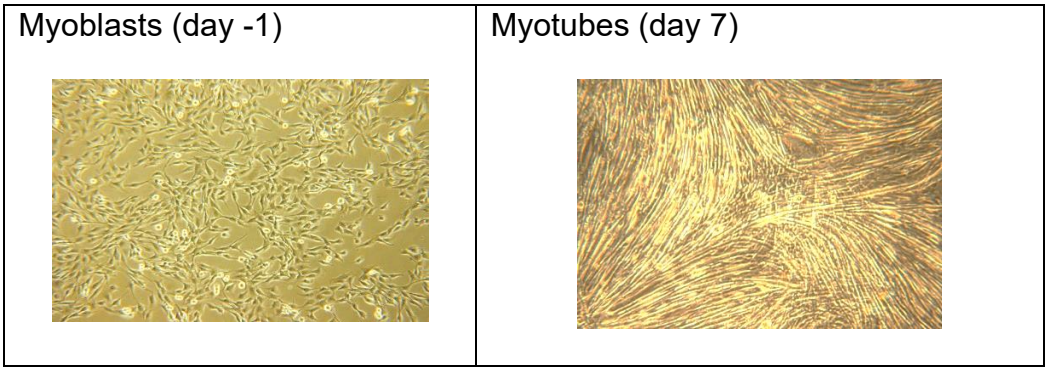
3.3. Results

3.3.1. Effects of 30 minutes CHX treatment on C2C12 cells

As indicated, the aim of this chapter was to increase intracellular BCAA concentrations and activate mTOR by treating cells with CHX. Due to the known toxic side effects (like DNA damage) of CHX, long-time and high doses of CHX may cause cell death. Hence, a dose range of 5μg/ml to 50 μg/ml CHX was

used, with the treatment time being 30 minutes. All the cells were treated at day 7 and observed under the microscope (Leica DFC420 C, 5x/0.12). After 4 hours treatment with differentiation media, PBS or media +30mins CHX, no cell death was observed. Moreover, there were no obvious morphological differences (Figure 3.2), although there appeared to be less myotubes with PBS treatment.

A.



B.

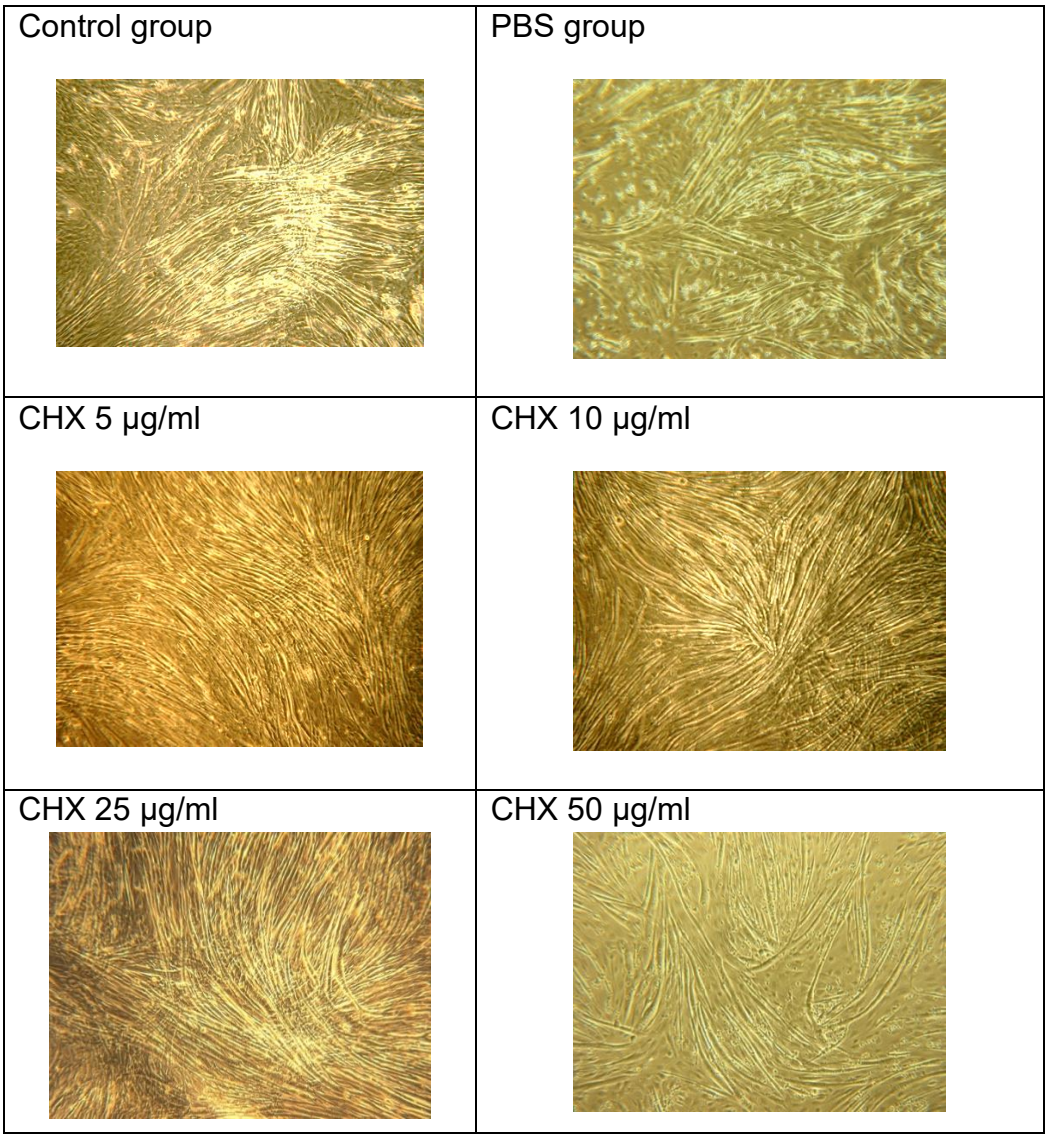


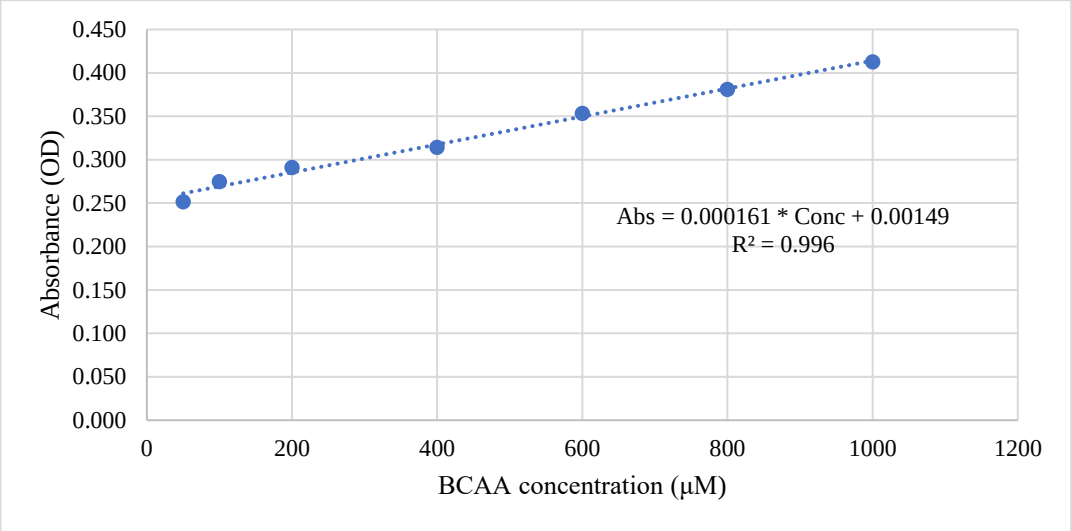
Figure 3. 2 Effects of 30 minutes CHX treatment on differentiated C2C12 cells

Images (captured at 5X/0.12 magnification) of C2C12 muscles cells the day before being switched to differentiation media (myoblasts, day -1) and before treatment (myotubes, day 7). B) Images of C2C12 myotubes after 4 hours treatment with media, PBS or media plus different concentrations of CHX.

3.3.2. Intracellular BCAA concentrations in C2C12 myotubes after 30 minutes CHX treatment

After 30 minutes treatment with different concentrations of CHX, there were no significant differences in intracellular BCAA concentrations in C2C12 myotubes between groups ($p=0.39$). Contrary to expectations, the intracellular BCAA concentrations did not differ between the six treatment groups.

A.



B.

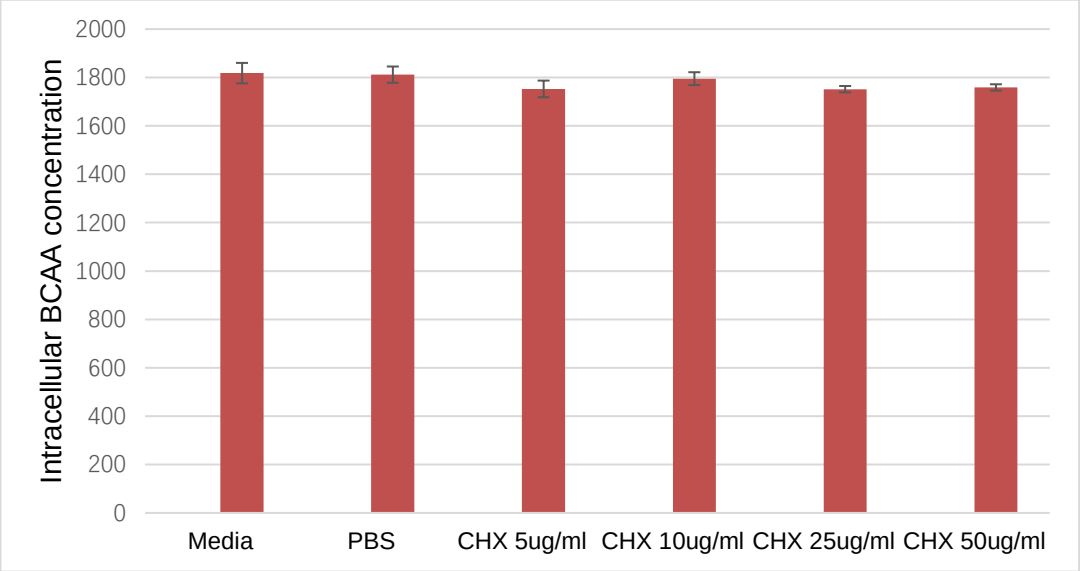


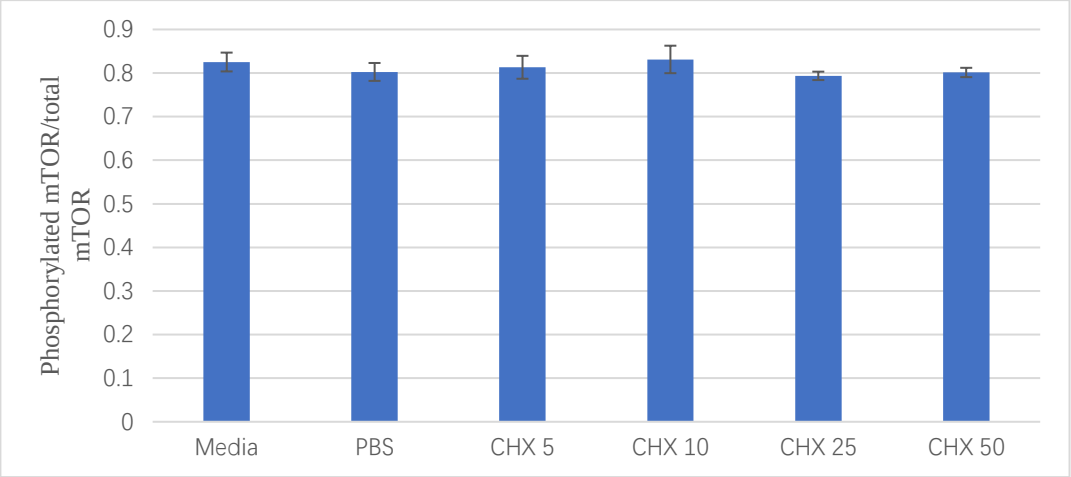
Figure 3. 3 Intracellular BCAA concentrations in C2C12 myotubes after 30 minutes CHX treatment

After one minute incubated at room temperature, with a reaction mixture containing 0.2 M glycine-KCl-KH2PO4-KOH buffer (pH 10.5), 4mM NAD, 5 nmol of leucine A) Standard curve of the Spectrophotometric Assay. B) Intracellular BCAAs concentration among six groups, no sig difference (p=0.39). Data are presented as means ± SEM for n=6 wells for each treatment group.

3.3.3. Effects of 30 minutes CHX treatment on mTOR and downstream target proteins in C2C12 myotubes

While were no significant differences in the intracellular BCAA concentrations, how phosphorylation of mTOR and downstream target proteins were tested. As with intracellular BCAA concentrations, there were no differences in mTOR ratio (phos/total, p=0.792, Figure 3.4A). Similarly, there were no effects on either 4E-BP1 ratio (p=0.616, Figure 3.5A) or p70S6K ratio (p=0.527, Figure 3.5B).

A.

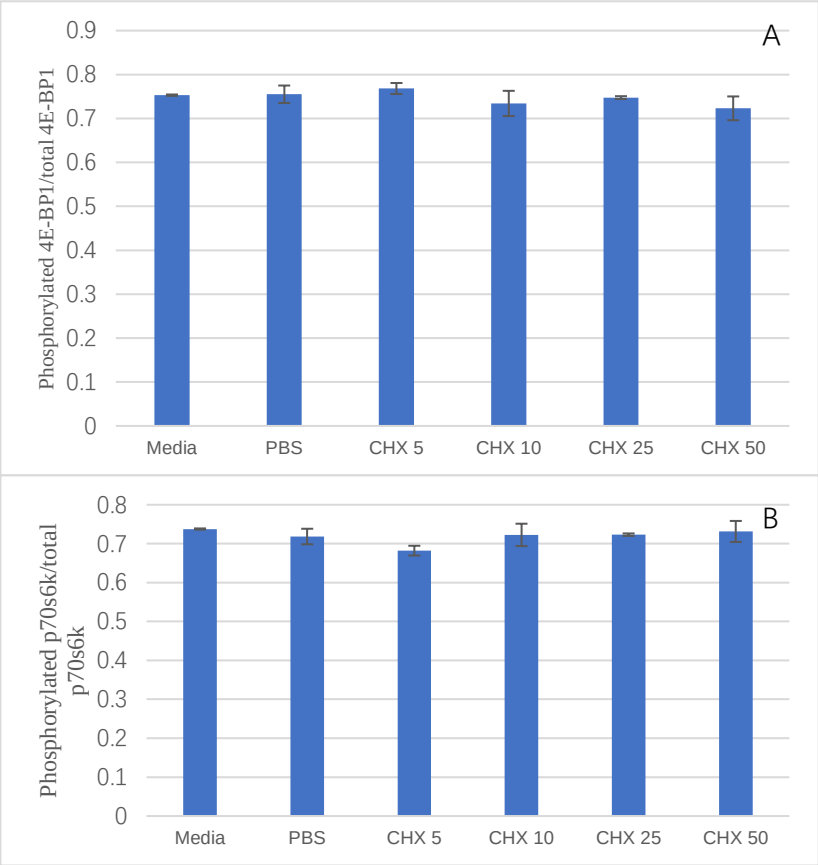


B.

	Control	PBS	CHX 5 µg/ml	CHX 10 µg/ml	CHX 25 µg/ml	CHX 50 µg/ml
Phosphorylation mTOR (Ser2448); 289kDa						
Total mTOR						

Figure 3. 4 Effects of CHX on the phosphorylation of mTOR

Western blot analysis of phosphorylated and total mTOR protein levels in C2C12 myotubes treated with media, PBS for 4 hours, or 3.5h media plus different concentrations of CHX for 30 minutes. CHX concentrations were 5µg/ml, 10µg/ml, 25µg/ml or 50µg/ml. A) Relative amounts of phospho-mTOR. B) Images of western blots for phosphorylated and total mTOR. p=0.792. Data are presented as means ± SEM for n=3 wells for each treatment group.



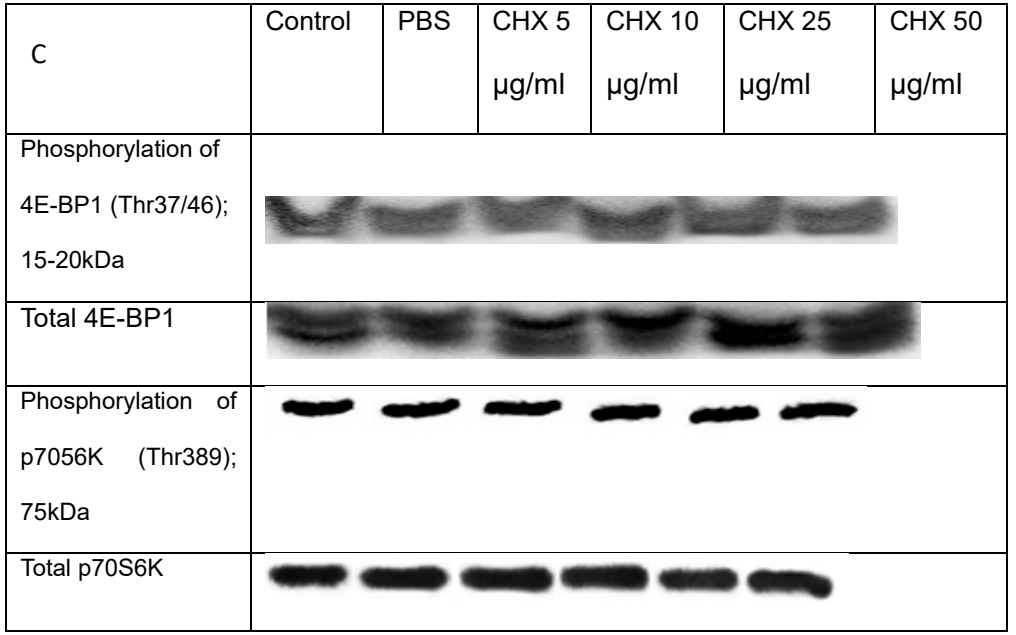


Figure 3. 5 Effects of CHX on the phosphorylation of 4E-BP1 and p70S6K

Western blot analyses of mTOR downstream targets, 4E-BP1 and p70S6K, protein levels in C2C12 myotubes treated with media, PBS for 4 hours, or 3.5h media plus different concentration of CHX for 30 minutes. CHX concentrations were 5µg/ml, 10µg/ml, 25µg/ml or 50µg/ml. A) Relative amounts of phospho-4E-BP1. B) Relative amounts of phospho-p70S6K. C) Images of western blots for phosphorylated and total 4E-BP1, phosphorylated and total p70S6K. p=0.616 for 4E-BP1, p=0.527 for p70S6K. Data are presented as means ± SEM for n=3 wells for each treatment group

3.3.4. Effects of 30 minutes CHX on Beta-actin in C2C12 myotubes

There was no difference of beta-actin (loading control) in 30 minutes CHX treatment groups, suggesting the quantity of each sample that was loaded in the gels was the same.

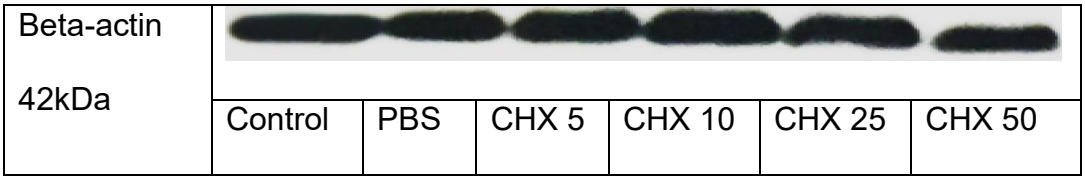


Figure 3. 6 Effects of 30 minutes CHX on Beta-actin in C2C12 myotubes

Differentiated C2C12 myotubes treated with media, PBS for 4 hours, or 3.5h media plus different concentration of CHX for 30 minutes. Western blot of Beta-actin protein in control (media only), PBS, and CHX 5μg/ml, 10μg/ml, 25μg/ml or 50μg/ml treatment groups, n=3 wells for each treatment group.

3.3.5. A comparison of insulin-stimulated glucose uptake between L6 and C2C12 Myotubes

While numerous groups have described that glucose-uptake is enhanced in C2C12 myotubes following insulin administration, this is not a universally consistent finding. There is heterogeneity in the responsiveness of C2C12 cells to insulin, especially whether this stimulates rapid glucose uptake. Given that this cellular response is fundamental to the planned experiments, the objective of the next experiment was to determine the ability of insulin to stimulate glucose uptake in both L6 (Aston) and C2C12 myotubes, assessed using the glucose analogue, 2-DG. The cell line found to be most responsive to the effects of insulin (as assessed by glucose uptake) would then be used exclusively for all subsequent experiments. To investigate the insulin sensitivity of L6 and C2C12 myotubes, both were stimulated with insulin for 1h. The results showed that L6 myotubes had slightly higher basal (control) levels of glucose uptake and that a response to insulin was only seen in L6 myotubes ($p<0.001$, insulin treatment); with no significant difference between control and insulin treatment in C2C12 myotubes. This suggests that the L6 myotubes should be used as an *in vitro* model system to investigate glucose uptake in muscle cells.

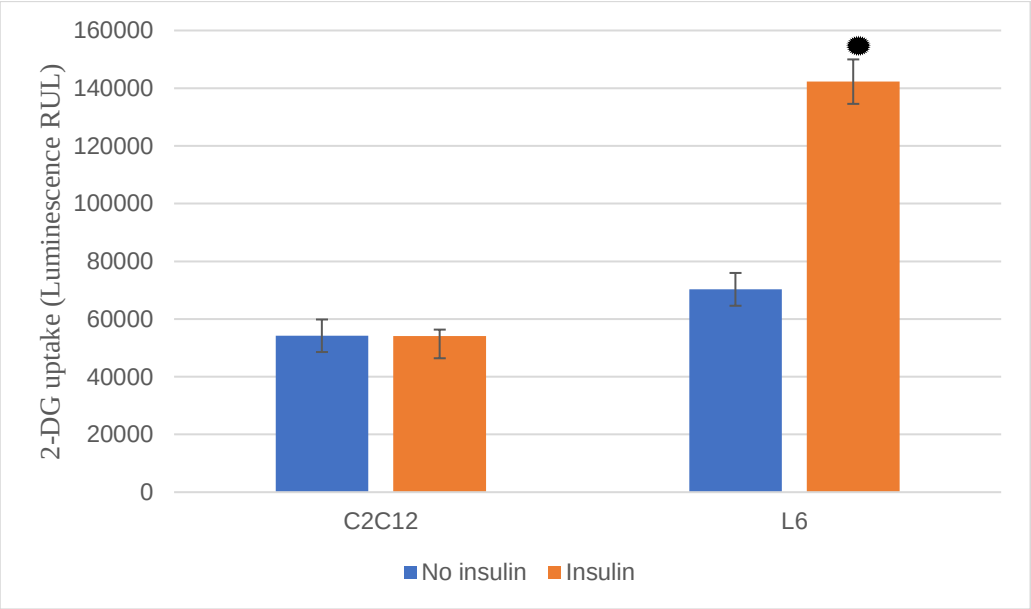


Figure 3. 7 Effects of insulin on glucose uptake in C2C12 and L6 skeletal muscle cell lines.

L6 and C2C12 myotubes were exposed for 24h to no serum media before the day of analyses. On the day of analyses, the control groups were treated with no serum and no glucose differentiation media, while the insulin groups were treated with 1mM insulin for 1 hour (in no serum and no glucose differentiation media). $p<0.001$ compared with control L6 cells. Data are presented as means ± SEM (n = 6 for each treatment)

3.3.6. The gene expressions of glucose transporters in L6 and C2C12 myotubes

It should be noted that the RNA extractions, cDNA synthesis and RT-qPCR analyses were done by Dr. Zoe Daniel, while I performed the cell culture experiments and analysed the data. The Cp (crossing point-PCR-cycle) value is the cycle at which fluorescence achieves a defined threshold (Rodriguez-Lazaro and Hernandez, 2013). The level of GLUT1-4 mRNA was very low in C2C12 and L6 myotubes, therefore, the standard curve cannot be calculated and only Cp value can be reported. A higher Cp value means lower mRNA level or even no mRNA (and vice versa). There were significant differences between L6 and C2C12 cells for GLUT1 ($p=0.008$, Figure 3.8) and GLUT2 ($p=0.032$, Figure 3.8) mRNA, with L6 cells expressing higher GLUT1 mRNA (lower Cp value), but lower GLUT2 mRNA (higher Cp value). However, there were no differences between the two cells line in expression of GLUT3 ($p=0.414$, Figure 3.8) or GLUT 4 mRNA ($p=0.636$, Figure 3.8). Hence the lack of insulin stimulated glucose uptake in C2C12 cells was not due to a lack of GLUT4 mRNA expression.

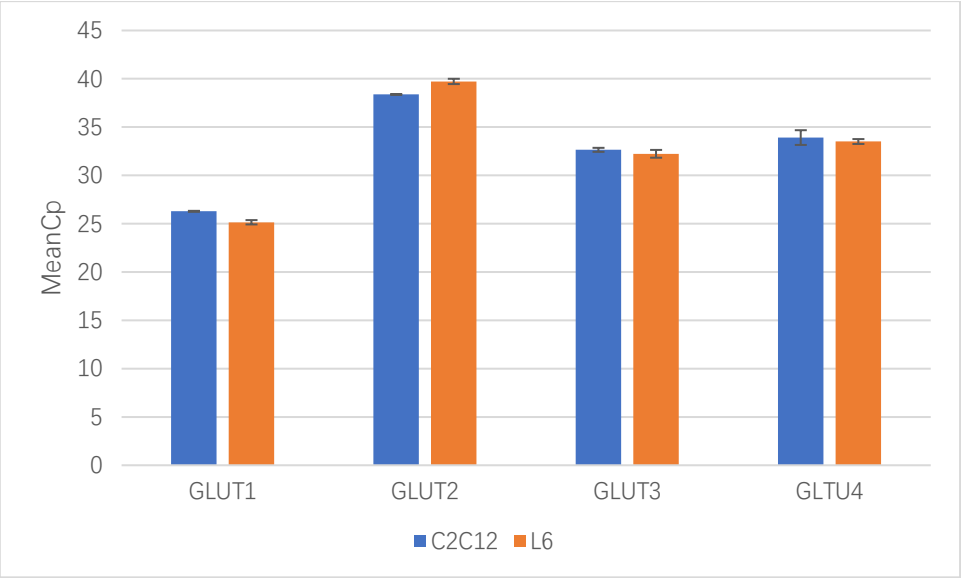


Figure 3. 8 mRNA expression of the different Glucose transporters in differentiated C2C12 and L6 muscle cells

The mean Cp values of GLUT1, GLUT2, GLUT3, GLUT4 following normal differentiation of C2C12 and L6 muscle cells. Data are presented as means ± SEM (n = 3). p=0.008 for GLUT1, p=0.032 for GLUT2, p=0.414 for GLUT3, p=0.636 for GLUT4.

3.4. Discussion and Conclusion

In this study, CHX had no effect on intracellular BCAA concentrations in C2C12 myotubes, nor influenced mTOR and downstream target proteins. L6 myotubes exhibited insulin-stimulated glucose uptake, whereas C2C12 myotubes did not.

Intracellular amino acids concentrations are decided by the balance between supply (extracellular sources or protein degradation in cells) and consumption (protein synthesis). It is possible that depriving cells of external amino acids might significantly decrease intracellular amino acid levels and that inhibition of protein synthesis might further increase their concentrations (Beugnet *et al.,* 2003). The hypothesis for the CHX experiments was that protein synthesis would be blocked, but the breakdown of protein to produce intracellular amino acids would continue (Figure 3.7)

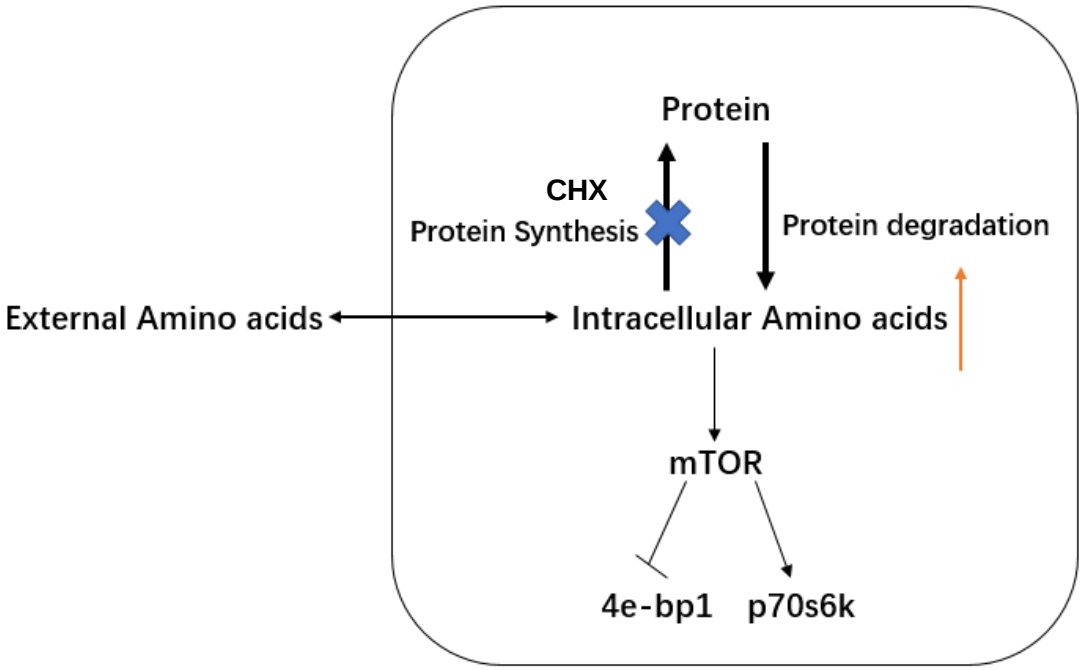


Figure 3. 9 Balance of intracellular amino acids

There is a balance between protein synthesis and protein degradation. When protein synthesis was blocked, the protein breakdown still happens and would be expected to cause increased intracellular amino acids. BCAAs can stimulate mTOR and downstream target proteins. **mTOR:** mammalian target of rapamycin, **P70S6K (S6K):** Ribosomal protein S6 kinase beta-1, **4E-BP1:** Eukaryotic translation initiation factor 4E-binding protein 1

BCAAs, especially leucine, are the main regulators of the mTOR pathway in most cells (Kimball, 2001). Therefore, altering intracellular amino acids could also influence phosphorylation of mTOR. CHX was used to block protein synthesis in the current experiment, and after 4 hours treatment with normal media, PBS (amino acids starvation) or CHX (3.5 hours media + 30 minutes treatment), the

intracellular amino acids, phosphorylation of mTOR and its downstream target proteins were examined. However, the results demonstrated that acute CHX treatment did not modulate intracellular amino acids concentrations in C2C12 myotubes, nor the phosphorylation of mTOR and downstream target proteins. This suggests that CHX may be not inhibit protein synthesis and other alternatives will need to be investigated.

Our findings are in contrast to the reports from other laboratories using CHX. Indeed, some studies have found CHX to activate mTORC1 through increases in intracellular amino acid concentrations, due to its ability to inhibit protein synthesis in the face of persistent protein breakdown (Beugnet *et al.,* 2003; Watanabe-Asano, Kuma and Mizushima, 2014). Beugnet *et al.,* (2003) showed that treatment of amino-acid deprived Chinese-hamster ovary (CHO) cells for 30 min with CHX (10 μg/ml) resulted in a marked rise in intracellular BCAAs levels, almost to the levels seen in the control cells. They also confirmed that CHX promoted phosphorylation of p70S6K and 4E-BP1, the latter of which was further enhanced via the administration of insulin. Likewise, Watanabe-Asano, Kuma and Mizushima (2014) confirmed that the phosphorylation of p70S6K and 4E-BP1 were elevated by CHX administration in HEK293 cells even under conditions of amino acid starvation.

It is worth noting that the concentration and duration of CHX treatment used in the current study is comparable to previous reports. Beugnet *et al.,* (2003) used 10 μg/ml CHX for 30 minutes, and Watanabe-Asano, Kuma and Mizushima (2014) used 50 μg/ml CHX for 5 minutes. It has been demonstrated that CHX only affected the mTOR signalling pathway at concentrations that substantially inhibit protein synthesis (Beugnet *et al.,* 2003). However, even when we used a dose of 50 μg/ml

for 30 minutes we still can not observed effect of CHX on intracellular BCAA concentrations or mTOR signalling in C2C12 cells. May *et al.,* (1987) mentioned that 0.5mM (140.675 μg/ml) CHX had been shown to inhibit more than 95% muscle protein synthesis, so the concentrations of CHX that used in our experiment may not high enough.

There are a number of potential reasons for the observed differences. Firstly, all of the previous studies used non-muscle cell lines. Beugnet *et al.,* (2003) used CHO K1 cells, while Watanabe-Asano, Kuma and Mizushima (2014) used mouse embryonic fibroblasts and HEK293T cells. Thus, our results suggest that the effectiveness of CHX to elicit increases in BCAA concentrations is not as great in C2C12 cells as in these other cell lines.

An additional subtle difference between our study design and that of others is the media used. In the previous studies, amino acid starvation was induced using either amino acid-free DMEM with 10% dialyzed FBS (Watanabe-Asano, Kuma and Mizushima, 2014) or PBS containing 10mM D-glucose (Beugnet *et al.,* 2003). However, in the current study only PBS was used to treat cells, although it is unlikely that this would be responsible for the results observed.

An alternative approach to investigate the effects of intracellular BCAA concentrations and mTOR activity on insulin-stimulated glucose uptake is to modulate BCAA concentrations by impairing BCAAs metabolism. The first step in the metabolism of the BCAAs is a reversible transamination reaction producing BCKAs and glutamate. The enzyme BCAT catalyses this step and therefore it

could represent a potential target for inhibition strategies. Reducing BCAAs metabolism would be expected to lead to profound increases in intracellular BCAA concentrations, however it may have other untoward effects, which would need to be considered.

Skeletal muscle is a major target for insulin-stimulated glucose disposal and suppression of fatty acid oxidation after a meal (Sipula *et al.*, 2006;). However, the response of skeletal muscles cells in culture is not consistent. The two *in vitro* model systems, C2C12 and L6 cell lines, used to research the glucose uptake in skeletal muscle exhibited different results. In the present study, L6 myotubes displayed a 2-fold increase in glucose uptake in response to insulin, but C2C12 cells did not, suggesting that L6 myotubes are more sensitive to insulin. This finding also matches with previous studies (*Yap et al.,* 2007; Nedachi and Kanzaki, 2006). The qPCR results showed that there is no difference in GLUT4 mRNA expression between L6 and C2C12 cells. This means at the basal level, L6 cells have same GLUT4 mRNA level as C2C12 cells, but after insulin treatment, the GLUT4 in L6 cells must have translocated to the cells' membrane, whereas GLUT4 in C2C12 cells do not. However, the GLUT4 translocation was not measured in this study, so this is a hypothesis. Ueyama *et al.,* (1999) used L6-GLUT4myc to show that both L6 myoblasts and myotubes appear to have GLUT4 translocation machinery that can be activated by insulin stimulation. This insulin-induced GLUT4 translocation accounts for a significant portion of insulin stimulated glucose uptake (Nedachi and Kanzaki, 2006). However, Nedachi and Kanzaki (2006) also showed that GLUT4 translocation was activated by insulin stimulation in C2C12 cells.

To summarize, this study demonstrates that CHX does not affect intracellular

BCAA concentrations in C2C12 myotubes, nor influence mTOR and downstream target proteins. It is possible that 30minus CHX treatment is not enough to influence intracellular amino acid concentrations or that the muscle cell line is not sensitive to CHX. Also, L6 myotubes exhibited insulin-stimulated glucose uptake, whereas C2C12 myotubes did not. Therefore, the next step is to investigate whether manipulation of mTOR affects glucose uptake in L6 myotubes.

CHAPTER 4: EXAMINATION OF WHETHER mTOR IS INVOLVED IN GLUCOSE UPTAKE

4.1. Introduction

As described in the previous chapter, CHX did not increase intracellular BCAA concentrations or affect phosphorylated mTOR and its downstream target proteins. However, compared with C2C12 cells, L6 cells displayed an increase in glucose uptake after insulin treatment, but this difference was not because of differences in GLUT4 mRNA levels. Therefore, the L6 myotubes were used to further investigate the relationship between mTOR signalling pathway and glucose uptake. The purpose of this chapter is to investigate whether changes in mTOR signalling by chemical reagents will influence glucose uptake.

Although mTOR has a central role in insulin signalling, the function of mTOR is still not fully understood. Rapamycin (sirolimus), which was produced by the bacterium *Streptomyces hygroscopicus*, is a macrolide immunosuppressant and was first found by Surendra Nath Sehgal and colleagues in 1972 (Sehgal *et al.,* 1975). Rapamycin was researched as an antifungal agent, but later studies showed that it had immunosuppressant activity, inhibiting T-cell proliferation (Martel *et al.,* 1977; Dumont *et al.,* 1990). Furthermore, it was found that rapamycin suppressed incorporation of amino acids into cellular proteins by inhibiting protein translation (Sehgal *et al.,* 1975). After nearly 20 years, the mechanism for rapamycin effects on mTOR signalling is still evolving. It is clear now that rapamycin inhibits mTOR activity through binding the immunophilin FK506-binding protein (FKBP12) to form a complex (Laplante and Sabatini, 2012; Arriola Apelo and Lamming; 2016). This FKBP12-rapamycin complex binds to FRB domain in mTOR and inhibits the

physiological functions of mTOR.

3-Benzyl-5-((2-nitrophenoxy)methyl)-dihydrofuran-2(3H)-one (3BDO) is a new activator for mTOR which can inhibit autophagy in Human Umbilical Vein Endothelial Cells (HUVECs) (Peng *et al.,* 2014 and Ge *et al.,* 2014). Therefore, they deduced that 3BDO might activate the mTOR pathway as an antagonist of rapamycin. Molecular docking studies illustrated that 3BDO could bind with FKBP12, which is the direct target of rapamycin, and then activate the mTOR signalling pathway (Ge *et al.,* 2014). Ge *et al.,* (2014) overexpressed FKBP12 cDNA in HUVECs and treated them with or without 3BDO and showed that phosphorylation of p70S6K 1 and 4E-BP1 was significantly increased by 3BDO, but suppressed with FKBP12 overexpression. Therefore, indicating that 3BDO could target FKBP12 and activate the mTOR signalling pathway (Figure 4.1).

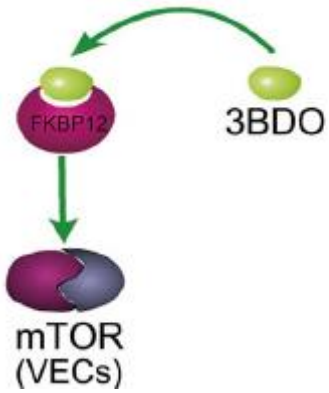


Figure 4. 1 Conceptual schematic of 3BDO and mTOR action mechanism. Reproduced from Peng *et al.,* 2014

3BDO will bind to FKBP1A and then activate the mTOR signalling pathway. **FKB12:** FK506-binding protein, **mTOR:** mammalian target of rapamycin, **3BDO:** 3-Benzyl-5-((2-nitrophenoxy)methyl)-dihydrofuran-2(3H)-one

The L-type amino acid transporters (LATs) are Na^+-dependent neutral amino acid transporters, including four members (LAT1, LAT2, LAT3, LAT4) in two sub-families (Wang and Holst, 2015). L-type amino acid transporter 1 (LAT1), which belongs to solute carrier (SLC) family 7, is overexpressed in many tumours (Dann *et al.,* 2007). It transports amino acids like leucine, isoleucine and valine into cells and increases mTOR complex 1 to promote ribosome biogenesis and cell growth (Dann *et al.,* 2007). 2-amino-3-norbane carboxylic acid (BCH) is an inhibitor of LAT1, which blocks the uptake of L-leucine with an IC_{50} value of 131.5 μM (Fraga *et al.,* 2002; Kim *et al.,* 2002). The researchers showed that BCH inhibited all LAT family members at 10 mM concentration, and that BCH also suppressed mTORC1 signalling (Wang and Holst, 2015; Dann *et al.,* 2007). Therefore, BCH can be considered as an inhibitor of mTOR by blocking amino acid transport into cells.

To summarize, the purposes of this chapter are to verify the relationship between mTOR activity and glucose uptake, and further characterise how mTOR influences glucose uptake.

4.2. Methods

The detail of L6 cell culture was described in section 2.2.2.

4.2.1. Effects of Rapamycin treatment on insulin-stimulated glucose uptake and mTOR signalling in L6 myotubes

10nmol (9.1µg) Rapamycin (CST, #9904) was dissolved in 100µl DMSO to make 100 µM stock, then split into 0.5ml tubes and stored at -20°C. After 7 days in differentiation medium (the day before experiment), L6 cells were changed to serum free DMEM for 24h for serum starvation. The following day, L6 cells were treated with DMEM (serum free) containing 100nM rapamycin or equivalent volume of vehicle control (DMSO) for 1h or 4h, followed by 1h with or without insulin (1mM). Both 4h and 1h treatment groups were tested for glucose uptake. However, only the 4h group were used for western blot analyses. Figure 4.2 shows a diagrammatic representation of the study protocol.

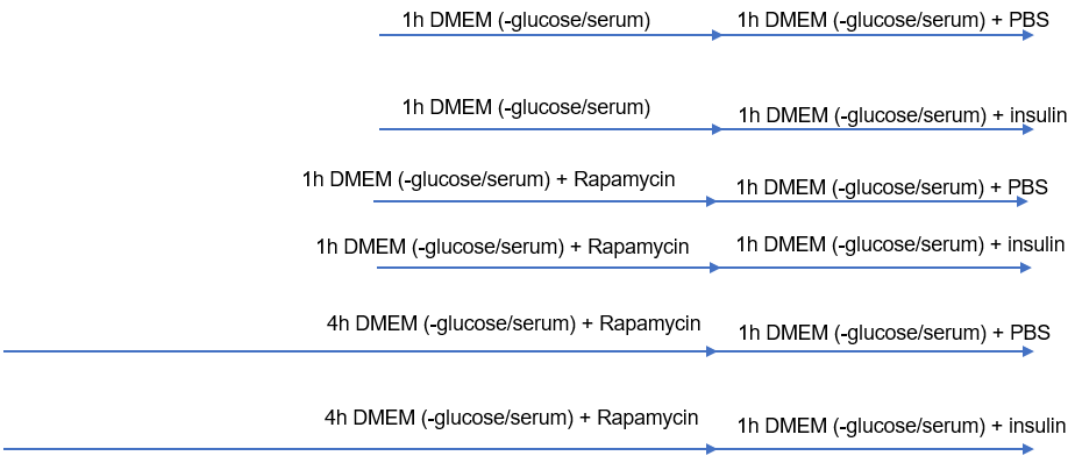


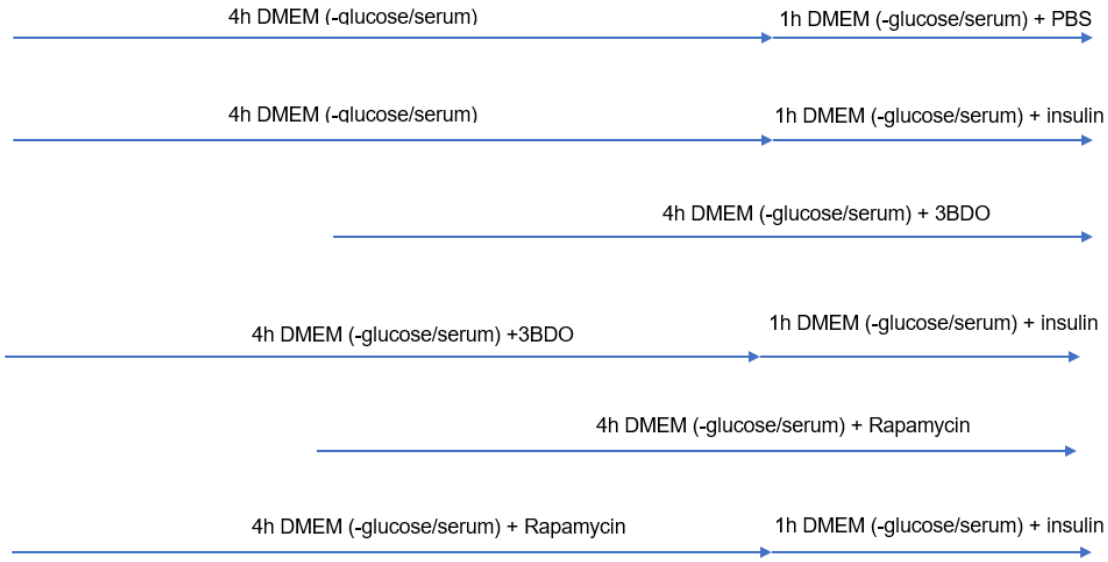
Figure 4. 2 Timeline of treatment groups.

L6 cells were treated with or without rapamycin (100nM) for different times (1h or 4h), followed by 1h treatment with or without insulin (1mM), prior to measurement of glucose uptake or mTOR signalling (via western blot).

4.2.2. Effects of Rapamycin and 3BDO treatments on insulin-stimulated glucose uptake and mTOR signalling in L6 myotubes

To make 5mM 3BDO (SML1687, Sigma) stock, 3.1ml DMSO was added to 5mg 3BDO then split into 1.5ml tubes and stored at -20°C. After 7 days in differentiation medium (the day before experiment), L6 cells were changed to serum free DMEM for 24h for serum starvation. On the day of experiment, L6 cells were treated with DMEM (serum free) containing 100nM rapamycin, 60μM 3BDO or equivalent volumes of vehicle control (DMSO) for 4h, then treated with or without insulin (1mM) for 1h. Figure 4.3 shows a diagrammatic representation of the study protocol.

Figure 4. 3 Timeline of treatment groups.



L6 cells were treated with 3BDO (60μM), rapamycin (100nM) or vehicle (DMSO) for 4h, with some cells also undergoing 1h treatment with insulin (1mM), prior to measurement of glucose uptake or mTOR signalling (via western blot).

4.2.3. Effects of Rapamycin and BCH treatment on insulin-stimulated glucose uptake and mTOR signalling in L6 myotubes

BCH (A7902, Sigma) was prepared fresh each time. After 7 days in differentiation medium (the day before experiment), L6 cells were changed to serum free DMEM for 24h for serum starvation. On the day of experiment, L6 cells were treated with DMEM (serum free) containing 100nM rapamycin, 25mM BCH or equivalent volume of vehicle control (DMSO) for 4h, then treated with or without insulin (1mM) for 1h. Figure 4.4 shows a diagrammatic representation of the study protocol.

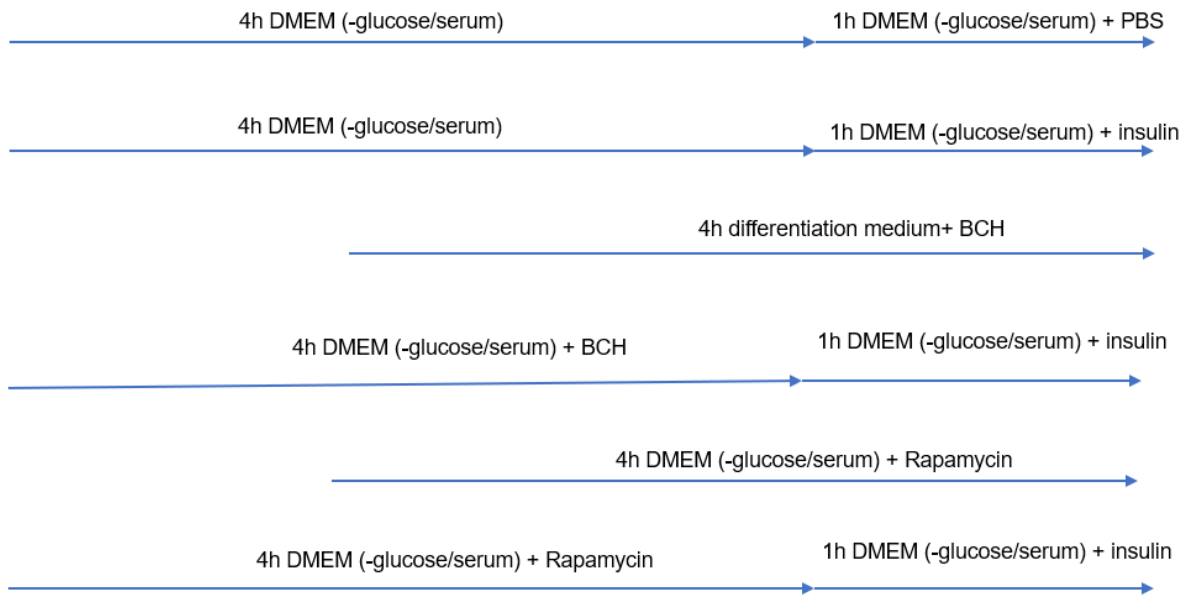


Figure 4. 4 Timeline of treatment groups.

L6 cells were treated with BCH (25mM), rapamycin (100nM) or vehicle (DMSO) for 4h, with some cells also undergoing 1h treatment with insulin (1mM), prior to measurement of glucose uptake or mTOR signalling (via western blot)

4.2.4. Determination of Glucose uptake

For glucose uptake, L6 cells were cultured in 24 well plates and treated as described above (section 4.2.1). The subsequent experimental steps were as described in section 2.4.

4.2.5. Western blot analyses of mTOR signalling

After removing the medium (6 well plates), samples were washed once with PBS and then collected into 150µl lysis buffer, the rest of steps were described in chapter 2.6.

Antibodies : rabbit anti mTOR antibody (#2972), rabbit anti-phospho-mTOR (Ser2448; #2971), rabbit anti-phospho-4E-BP1 (Thr37/46; #9459), rabbit anti-4E-BP1 (#9452), rabbit anti-phospho-p70 S6 Kinase (Thr389; #9205), rabbit anti-p70 S6 Kinase (#9202), rabbit anti-phospho-Akt (Ser473, #9271), rabbit anti-Akt (#9272), rabbit anti-β-Actin Antibody (#4967), anti-rabbit IgG, and HRP-linked Antibody (#7074) were all purchased from Cell Signalling Technologies. All the primary antibodies were diluted 1:1000 with 5%BSA and the secondary antibody diluted 1:5000 with 5%BSA.

4.2.6. Determination of intracellular BCAA concentrations

After removing the medium (6 well plates), samples were washed once with PBS, then collected into 50µl BCAA Assay Buffer. Intracellular BCAA concentrations were determined by Assay kit (as described in section 2.5.2).

4.2.7. Statistical Analyses

One-way ANOVA was performed using Genstat (19th edition) software, followed by Bonferroni test when appropriate (ANOVA $p<0.05$). The western blot data was quantified by Image Lab (V 5.2.1 Bio-Rad). Significant differences were considered as $p<0.05$.

4.3. Results

4.3.1. Effects of rapamycin treatment for different times on glucose uptake in L6 myotubes

To further delineate whether mTOR is involved in regulating glucose uptake, the effects of rapamycin on glucose uptake in cultured L6 myotubes exposed to 100nM rapamycin for 1h or 4h were determined (Figure 4.5). As expected, compared with control group, glucose uptake was increased 67% following incubation with insulin ($p<0.05$). In contrast, in the absence of insulin, 100nM rapamycin treatment for 4h decreased glucose uptake of L6 myotubes by 17%. However, there was no effect of 1h rapamycin treatment ($p>0.05$) and no difference between 1h and 4h rapamycin treatment on glucose uptake. Both 1h and 4h rapamycin significantly decreased the insulin-stimulated glucose uptake ($p<0.05$), but there was no difference between 1h and 4h treatments ($p>0.05$).

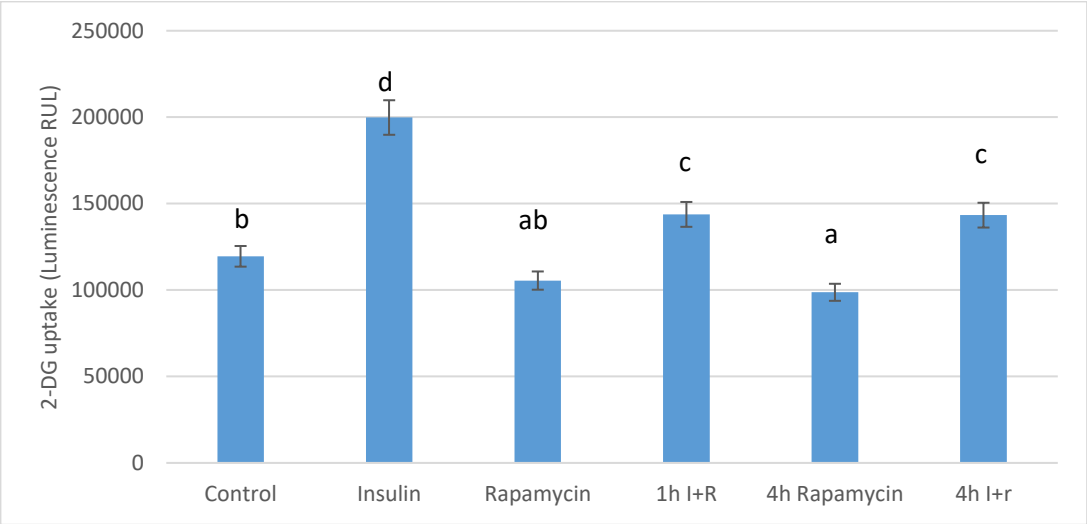


Figure 4. 5 Effects of rapamycin (1h or 4h) +/- insulin on glucose uptake in L6 myotubes.

Differentiated L6 myotubes were pre-treated with or without rapamycin (100nM) for 1h or 4h and then incubated with insulin as noted for 1h before measurement of 2-DG uptake. Results are mean± SEM for n=6 wells for each treatment group. $p<0.001$ for one-way ANOVA. Means with the same letter are not different ($p>0.05$ for Bonferroni), whereas those with different letters are significantly different ($p<0.05$ for Bonferroni)

4.3.2. Effects of 4 hours rapamycin treatment on mTOR and downstream target proteins in L6 myotubes

L6 myotubes were treated for 4h with rapamycin, followed by 1h insulin stimulation. The activation of mTOR, p70S6K and 4E-BP1 were then assessed by western blot analyses.

As expected, insulin significantly increased the mTOR ratio (phos/total) by 77% ($p<0.05$ vs control, Figure 4.6A) and for downstream target proteins, 4E-BP1 and p70S6K, insulin increased protein ratios by 96% and 70% respectively ($p<0.05$ vs control, Figures 4.7A and 4.8A). On the other hand, rapamycin, as an mTOR inhibitor, down regulated both the mTOR ratio (40%, $p<0.05$ vs control, Figure 4.6A,) and downstream target proteins (39% for 4E-BP1 ratio, 50% for p70S6K ratio, $p<0.05$ vs control, Figures 4.7A and 4.8A) in L6 myotubes. When insulin was added as well as rapamycin, the mTOR ratio in L6 myotubes was reduced by 32% compared with the insulin alone group ($p<0.05$ vs insulin, Figure 4.6A), which meant rapamycin inhibited the stimulatory effect of insulin. Ratios of 4E-BP1 and p70S6K showed similar results, as rapamycin blocked the insulin effect by about 37% and 24% ($p<0.05$ vs insulin, Figures 4.7A and 4.8A).

The phosphorylated mTOR, 4E-BP1 and p70S6K displayed the same effects as the ratios ($p<0.001$ for mTOR, 4E-BP1 and p70S6K; Figures 4.6C, 4.7C, 4.8C), but there were no effects of rapamycin or insulin treatment on the total (phosphorylated plus unphosphorylated) protein levels (mTOR, $p=0.769$; 4E-BP1, $p=0.213$; p70S6K, $p=0.12$; Figures 4.6D, 4.7D, 4.8D). This result showed that the effects of both insulin and rapamycin were on the levels of

phosphorylated proteins, and not due to a change in total protein levels.

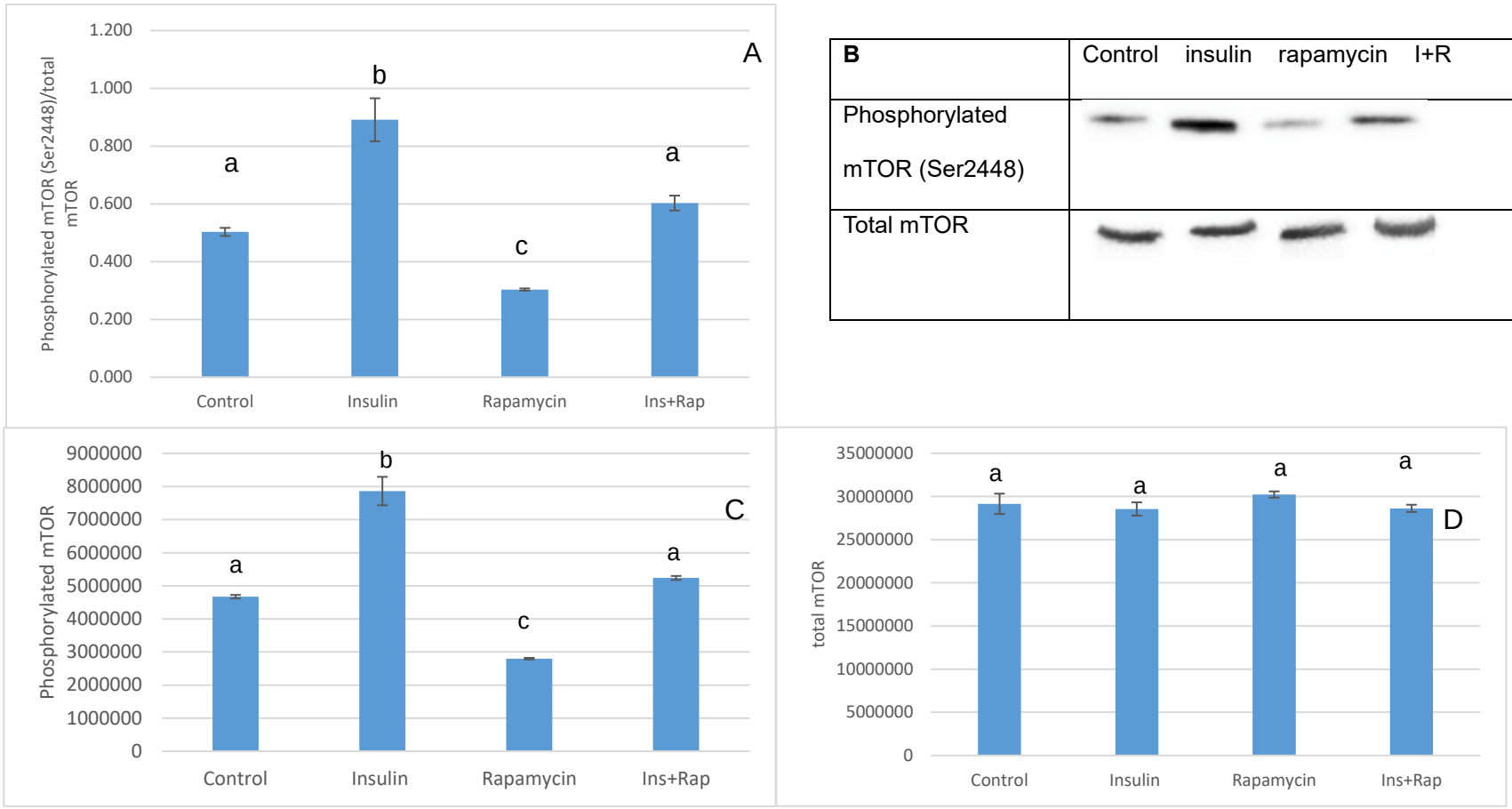


Figure 4. 6 Effects of rapamycin (4h) +/- insulin on mTOR activity in L6 myotubes.

Differentiated L6 myotubes were pre-treated with or without rapamycin (100nM) for 4h and then incubated with insulin as noted for 1h before western blot analysis. Representative western blots and quantification of A) phospho/ total mTOR ratio, B) example western blots, C) phosphorylated mTOR and D) total mTOR. Results are mean± SEM for n=3 wells for each treatment group, I+R: Ins+Rap. one-way ANOVA: $p<0.001$ for A and C. $p=0.769$ (D). Means with the same letter are not different ($p>0.05$ for Bonferroni), whereas those with different letters are significantly different ($p<0.05$ for Bonferroni)

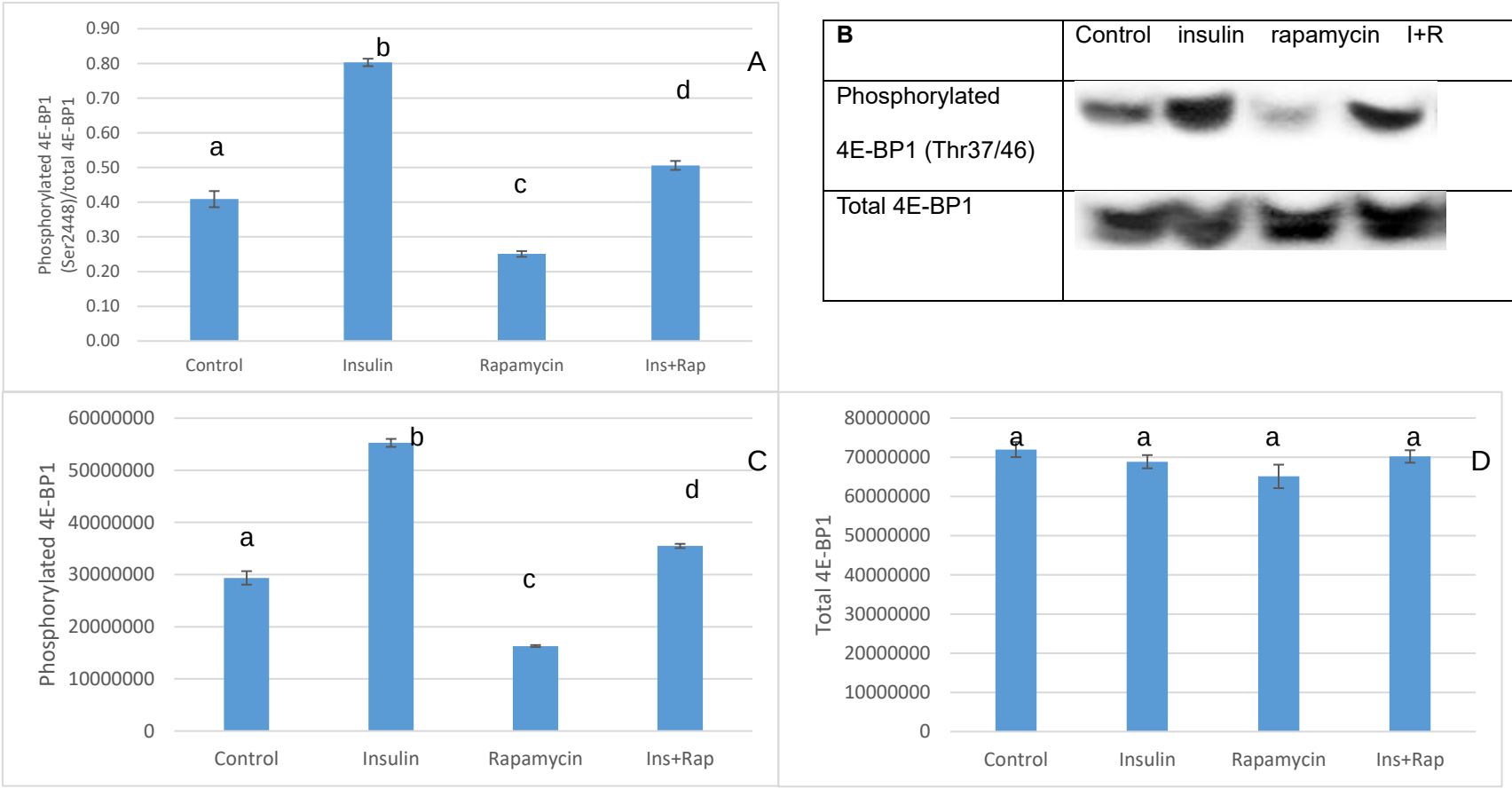


Figure 4. 7 Effects of rapamycin (4h) +/- insulin on 4E-BP1 activity in L6 myotubes.

Differentiated L6 myotubes were pre-treated with or without rapamycin (100nM) for 4h and then incubated with insulin as noted for 1h before western blot analysis. Representative western blots and quantification of A) phospho/ total 4E-BP1 ratio, B) example western blots, C) phosphorylated 4E-BP1 and D) total 4E-BP1. Results are mean± SEM for n=3 wells for each treatment group. I+R: Ins+Rap. one-way ANOVA: $p<0.001$ for A and C. $p=0.213$ (D) Means with the same letter are not different ($p>0.05$ for Bonferroni), whereas those with different letters are significantly different ($p<0.05$ for Bonferroni)

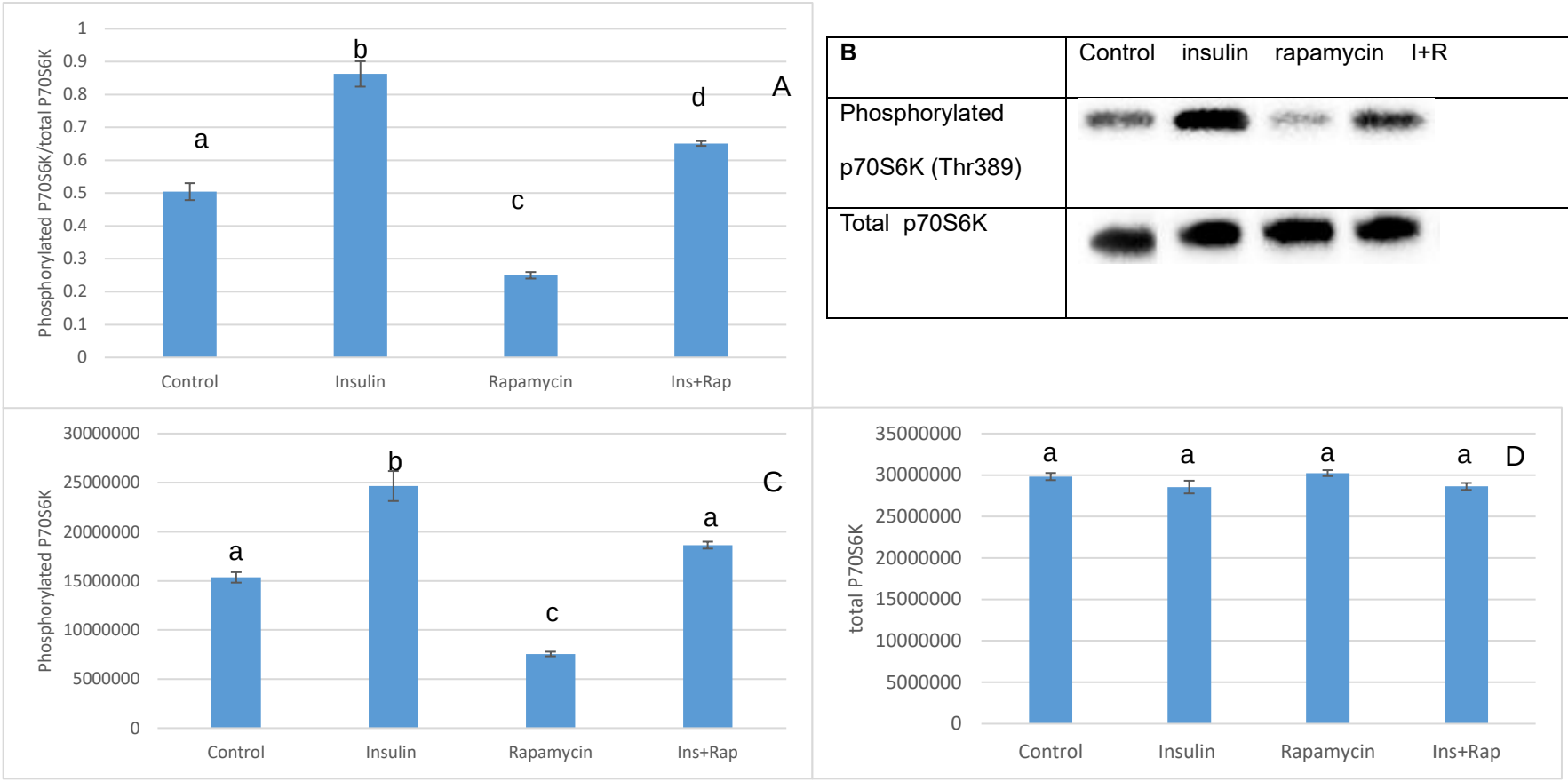


Figure 4. 8 Effects of rapamycin (4h) +/- insulin on p70S6K activity in L6 myotubes.

Differentiated L6 myotubes were pre-treated with or without rapamycin (100nM) for 4h and then incubated with insulin as noted for 1h before western blot analysis. Representative western blots and quantification of A) phospho/ total p70S6K ratio, B) example western blots, C) phosphorylated p70S6K and D) total p70S6K. Results are mean± SEM for n=3 wells for each treatment group. I+R: Ins+Rap. one-way ANOVA: $p<0.001$ for A and C. $p=0.12$ (D) Means with the same letter are not different ($p>0.05$ for Bonferroni), whereas those with different letters are significantly different ($p<0.05$ for Bonferroni)

4.3.3. Effects of 4 hours rapamycin treatment on beta-actin in L6 myotubes

There was no difference of beta-actin (loading control) in 4 hours rapamycin treatment groups, suggesting the quantity of each sample that loaded in the gels is same.



Figure 4. 9 Effects of rapamycin (4h) +/- insulin on Beta-actin in L6 myotubes.

Differentiated L6 myotubes were pre-treated with or without rapamycin (100nM) for 4h and then incubated with insulin as noted for 1h before western blot analysis. Example blots are shown for Beta-actin for control (C), insulin (I), rapamycin (R) and ins+rap (I+R) treatment groups, n=3.

4.3.4. Effects of 4 hours 3BDO treatment on mTOR and downstream target proteins in L6 myotubes

The previous study suggested that mTOR might be involved in regulating glucose uptake. To further test the effects of mTOR activity on glucose uptake, L6 myotubes were exposed for 4h to either 100nM rapamycin or 60μM 3BDO (mTOR activator) prior to treatment with or without insulin. Phosphorylation of mTOR and downstream target proteins were tested first to verify that the 3BDO did activate mTOR.

As expected, rapamycin treatment resulted in significant decreases in mTOR ratio (phos/total, 77%) as shown in both the immunoblot and quantification ($p<0.05$, Figures 4.10A and B). In the absence of rapamycin, insulin increased the mTOR ratio approximately 34% compared with control ($p<0.05$, Figure 4.10A). In the presence of rapamycin, the mTOR ratio response to insulin decreased 55% (vs. insulin alone, $p<0.05$, Figure 4.10A), meaning rapamycin blocked the effect of insulin. Unexpectedly, 3BDO did not increase mTOR ratio, but actually reduced it compared to the control group ($p<0.05$, Figure 4.10A). There was also no statistically significant difference between insulin alone and insulin+3BDO groups ($p>0.05$, Figure 4.10A). These results demonstrate an effective inhibition of mTOR activity by rapamycin, but 3BDO alone failed to increase mTOR activity, it acted more like an inhibitor rather than an activator.

The results for the phosphorylated (Ser2448) mTOR showed the same trend as the mTOR ratio ($p<0.001$, Figure 4.10C). Furthermore, insulin, rapamycin and 3BDO did not influence total mTOR protein ($p>0.05$, Figure 4.10D).

Figures 4.11 and 4.12 show immunoblots and quantification for 4E-BP1 and p70S6K in L6 cells. As for mTOR, rapamycin reduced 4E-BP1 ratio by 22% and p70S6K ratio by 65% ($p<0.05$, Figure 4.11A and Figure 4.12A). Insulin treatment increased 4E-BP1 ratio by 62% and p70S6K ratio approximately 2-fold compared with control group ($p<0.05$, Figure 4.11A and Figure 4.12A) and rapamycin reduced the insulin-stimulated 4E-BP1 (23%) and p70S6K ratios (50%; $p<0.05$, Figure 4.11A and Figure 4.12A).

In contrast to the effects on mTOR, 3BDO alone increased 4E-BP1 ratio about 10% compared with control ($p<0.05$, Figure 4.11A), but with insulin, it did not increase further (compared to insulin alone). The results for p70S6K ratio were similar to mTOR, 3BDO alone reduced the ratio, and 3BDO in the presence of insulin decreased 4E-BP1 and p70S6K ratios by 26% and 24% compared with insulin alone ($p<0.05$, Figure 4.11A and Figure 4.12A).

The phosphorylated 4E-BP1 and p70S6K showed similar trend with their ratios ($p<0.001$, Figure 4.11C and Figure 4.12C). There were no significant differences for both total 4E-BP1 and total p70S6K, the total proteins were not influenced by either 3BDO or rapamycin ($p=0.487$ mTOR; $p=0.215$ 4E-BP1; $p=0.983$ p70S6K. Figure 4.11D and Figure 4.12D).

These data showed that rapamycin decreased phosphorylation of mTOR and downstream proteins, but 3BDO did not activate mTOR, even with insulin present.

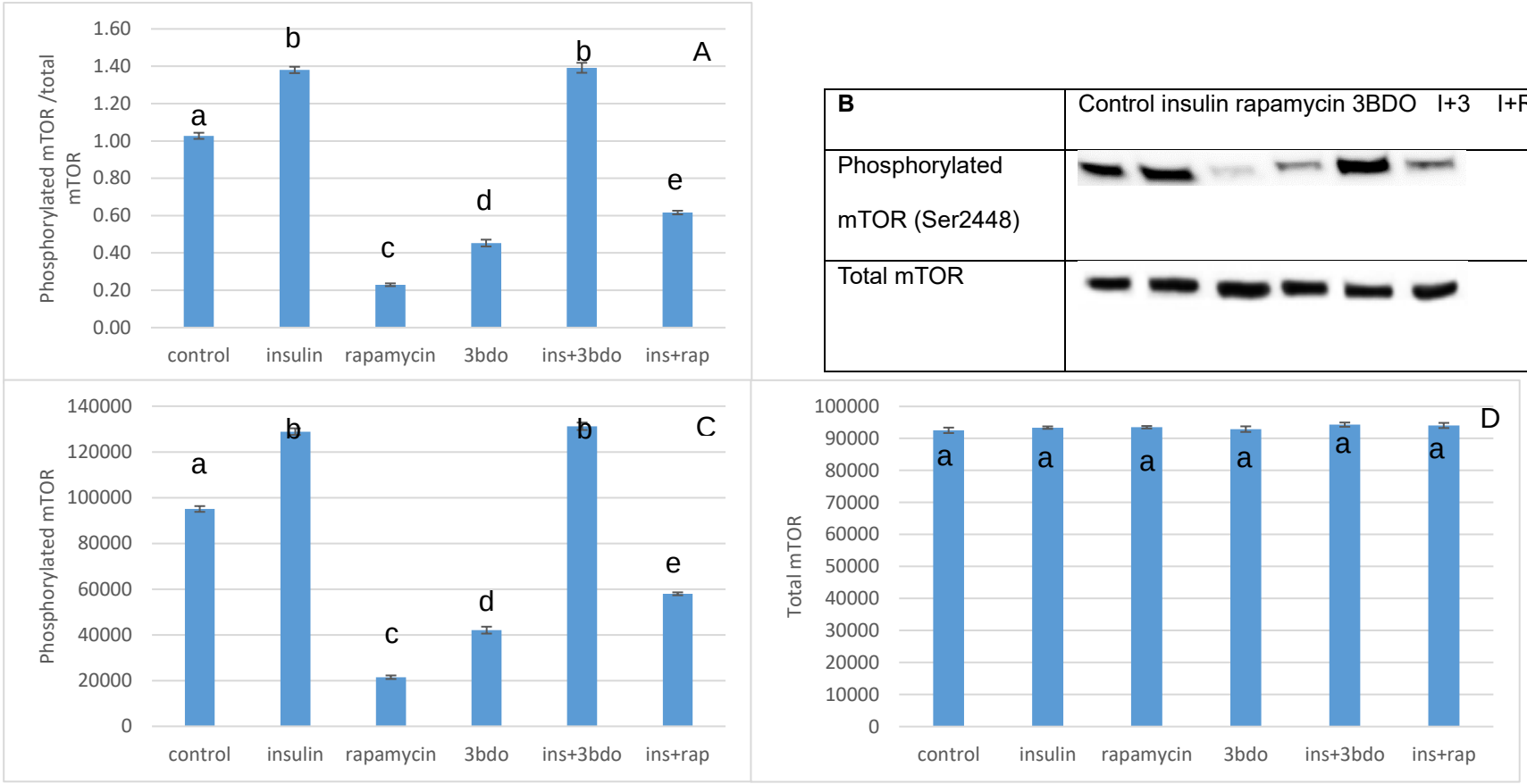


Figure 4. 10 Effects of 4h rapamycin or 3BDO +/- 1h insulin on mTOR activity in L6 myotubes.

Differentiated L6 myotubes were pre-treated with or without rapamycin (100nM) or 3BDO (60μM) for 4h and then incubated with insulin as noted for 1h. Representative western blots and quantification of A) phospho/ total mTOR ratio, B) example western blots, C) phosphorylated mTOR and D) total mTOR. Results are mean± SEM for n=3 wells for each treatment group. I+R: Ins+Rap. I+3: Ins+3BDO. One-way ANOVA : $p<0.001$ for A and C; $p=0.487$ (D). Means with the same letter are not different ($p>0.05$ for Bonferroni), whereas those with different letters are significantly different ($p<0.05$ for Bonferroni)

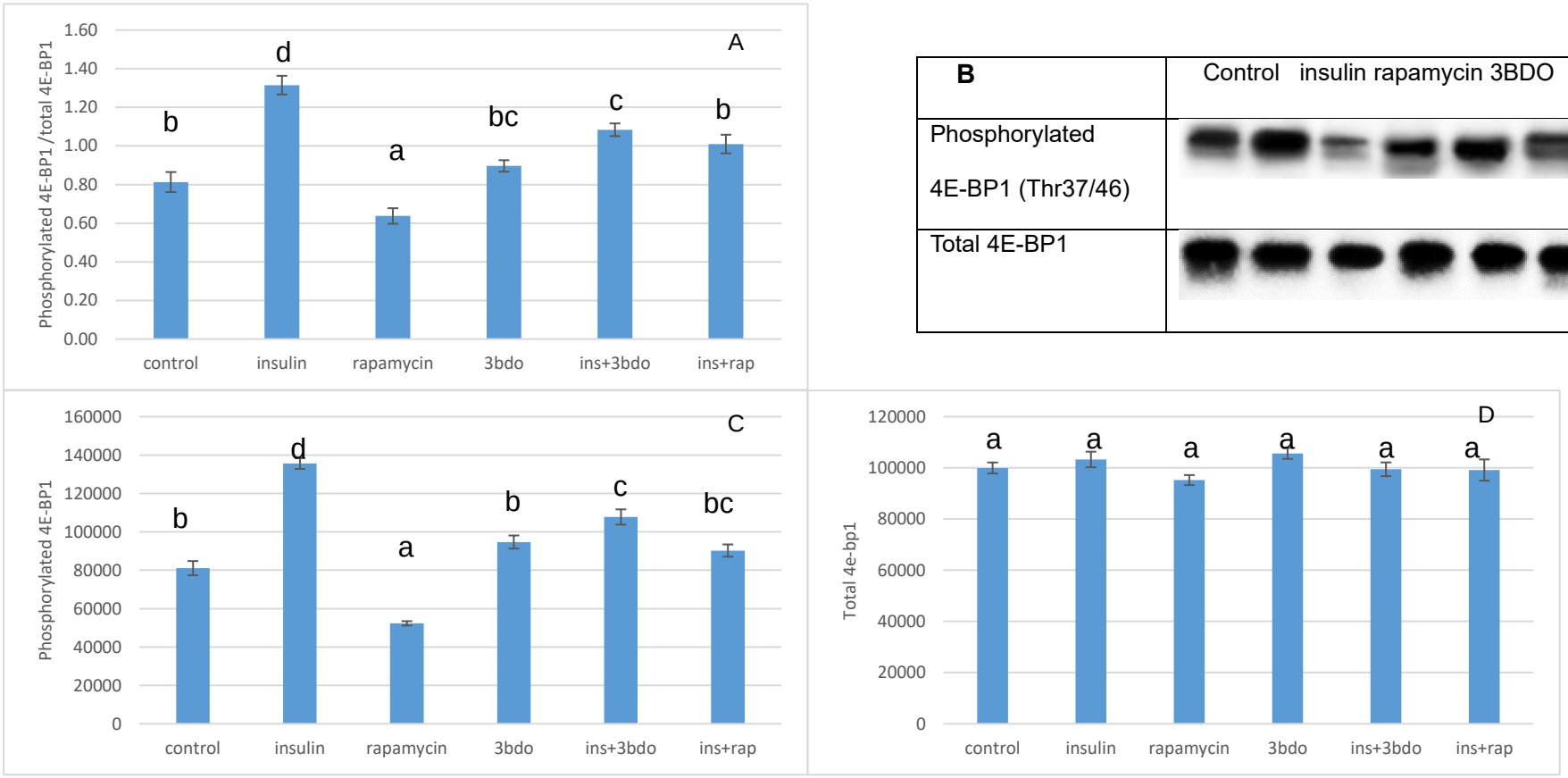


Figure 4. 11 Effects of 4h rapamycin or 3BDO +/- 1h insulin on 4E-BP1 activity in L6 myotubes.

Differentiated L6 myotubes were pre-treated with or without rapamycin (100nM) or 3BDO (60μM) for 4h and then incubated with insulin as noted for 1h. Representative western blots and quantification of A) phospho/ total 4E-BP1 ratio, B) example western blots, C) phosphorylated 4E-BP1 and D) total 4E-BP1 Results are mean± SEM for n=3 wells for each treatment group. I+R: Ins+Rap. I+3: Ins+3BDO. One-way ANOVA: $p<0.001$ for A and C, $p=0.215$ (D). Means with the same letter are not different ($p>0.05$ for Bonferroni), whereas those with different letters are significantly different ($p<0.05$ for Bonferroni)

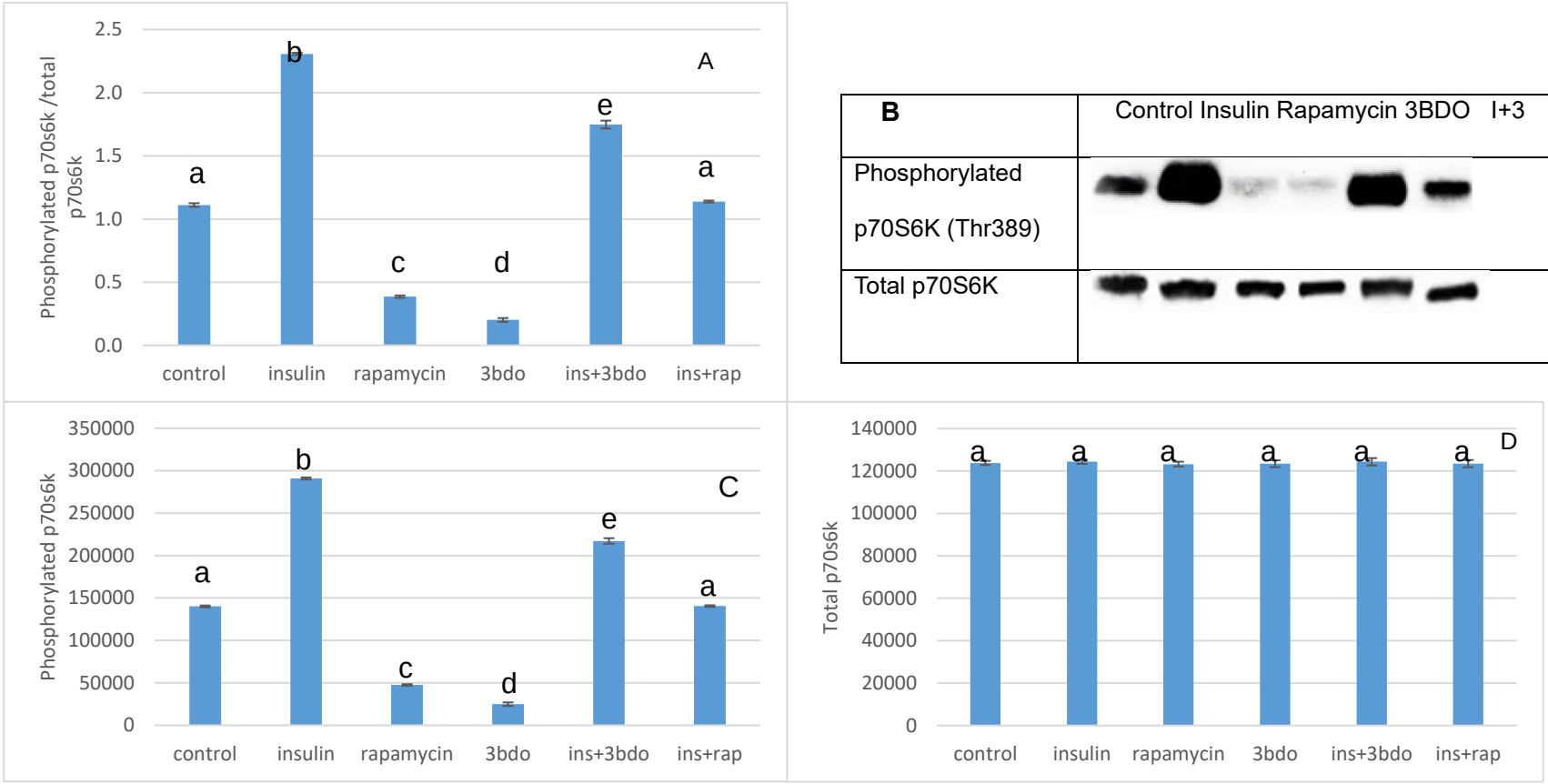


Figure 4. 12 Effects of 4h rapamycin or 3BDO +/- 1h insulin on p70S6K activity in L6 myotubes.

Differentiated L6 myotubes were pre-treated with or without rapamycin (100nM) or 3BDO (60μM) for 4h and then incubated with insulin as noted for 1h. Representative western blots and quantification of A) phospho/ total p70S6K ratio, B) example western blots, C) phosphorylated p70S6K and D) total p70S6K. Results are mean± SEM for n=3 wells for each treatment group. I+R: Ins+Rap. I+3: Ins+3BDO. One-way ANOVA: $p<0.001$ for A and; $p=0.983$ (D). Means with the same letter are not different ($p>0.05$ for Bonferroni), whereas those with different letters are significantly different ($p<0.05$ for Bonferroni)

4.3.5. Effects of 4 hours 3BDO treatment on beta-actin in L6 myotubes

There was no difference of beta-actin (loading control) in 4 hours 3BDO treatment groups, suggesting the quantity of each sample that was loaded in the gels was the same.

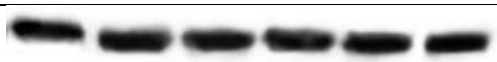
	Control insulin rapamycin 3BDO I+3 I+R
Beta-actin	

Figure 4. 13 Effects of 4h rapamycin or 3BDO +/- 1h insulin on Beta-actin in L6 myotubes

Differentiated L6 myotubes were pre-treated with or without rapamycin (100nM) or 3BDO (60μM) for 4h and then incubated with insulin as noted for 1h. Western blot of Beta-actin protein in control, insulin, rapamycin, 3BDO, ins+3BDO (I+3) and ins+rap (I+R) treatment groups, n=3.

4.3.6. Effects of 4 hours 3BDO treatment on glucose uptake in L6 myotubes

Previous experiment indicated that 3BDO appeared to inhibit rather than activate mTOR, but whether it influenced glucose uptake in L6 myotubes still needed to be verified. After 24h serum starvation, L6 myotubes were exposed for 4h to either 100nM rapamycin or 60μM 3BDO prior to 1h treatment with or without insulin.1h insulin significantly stimulated glucose uptake by 119% compared with control group ($p<0.05$, Figure 4.14). As observed previously, rapamycin decreased basal glucose uptake ~45% ($p<0.05$, Figure 4.14) and reduced the insulin-stimulated glucose uptake by 54% compared with insulin alone group ($p<0.05$, Figure 4.14). These results were consistent with the results of previous rapamycin experiments. In contrast, treatment with 3BDO increased glucose uptake by 70% in the absence of insulin and surprisingly, there was no further increase when insulin was added. Indeed, 3BDO appeared to decrease the insulin-stimulated glucose uptake by 15% (vs insulin alone, $p<0.05$, Figure 4.14).

These data confirmed that rapamycin blocked insulin-induced glucose uptake in L6 cells, and this maybe by inhibiting mTOR. 3BDO alone increased glucose uptake, but addition of insulin did not increase the glucose uptake further, and this maybe because it failed to activate mTOR.

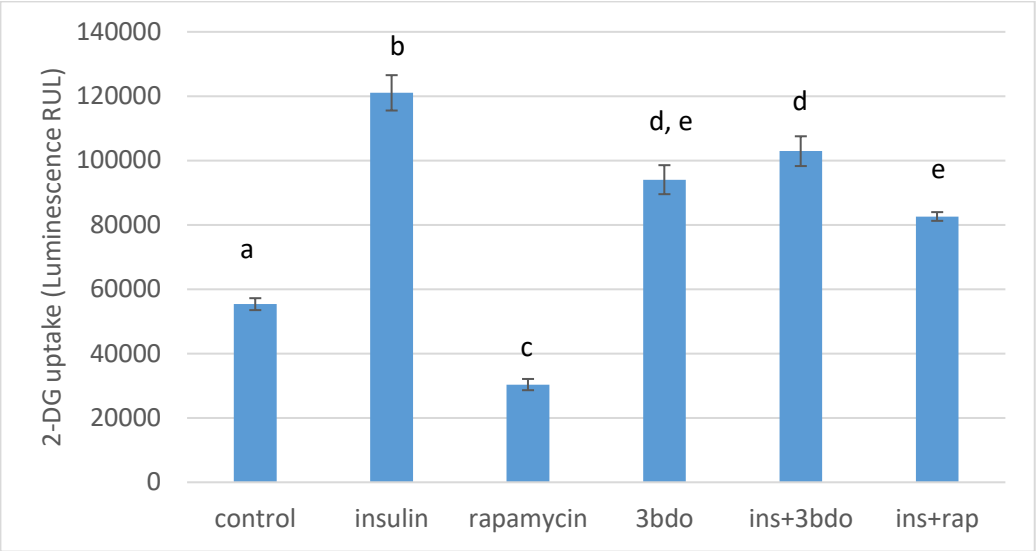


Figure 4. 14 Effects of 4h rapamycin or 3BDO +/- insulin on glucose uptake in L6 myotubes.

Differentiated L6 myotubes were pre-treated with or without rapamycin (100nM) or 3BDO (60μM) for 4h and then incubated with insulin as noted for 1h before measurement of 2-DG uptake. Results are mean± SEM for n=6 wells for each treatment group. $p<0.001$ for one-way ANOVA. Means with the same letter are not different ($p>0.05$ for Bonferroni), whereas those with different letters are significantly different ($p<0.05$ for Bonferroni)

4.3.7. Effects of 4 hours 3BDO treatment on Akt in L6 myotubes

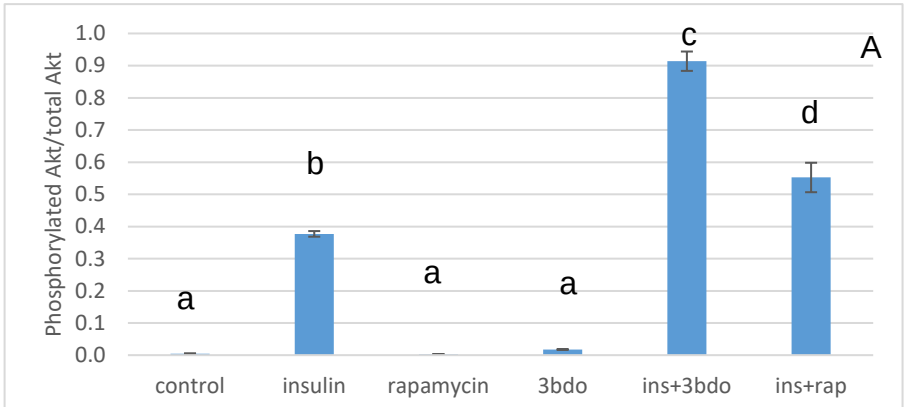
Akt is an upstream protein of mTOR and plays an important role in insulin

metabolism, therefore, phosphorylated and total Akt were also measured.

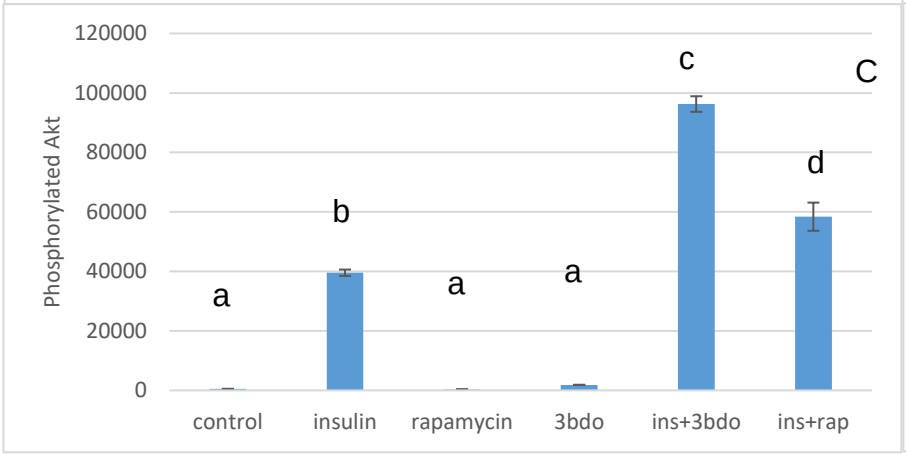
In the absence of insulin, there were no differences between control, rapamycin and 3BDO groups ($p>0.05$, Figure 4.15A). As expected, insulin significantly increased the Akt ratio ($p<0.05$, Figure 4.15A), but unexpectedly rapamycin increased the insulin-induced Akt ratio by 50% (compared with insulin alone; $p<0.05$, Figure 4.15A) and 3BDO also increased the Akt ratio 73% (compared with insulin alone). Hence, the insulin effect on Akt was enhanced, particularly by 3BDO.

Once again, the phosphorylated (Ser473) Akt results showed the same effects as the Akt ratio ($p<0.001$, Figure 5.15C) and there were no differences in total Akt ($p=0.618$, Figure 5.15D).

These results indicated that both 3BDO and rapamycin increased the insulin-induced phosphorylation of Akt at site Ser473, with 3BDO having a greater effect.



B	Control	Insulin	Rapamycin	3BDO	I+3	I+R
Phosphorylated Akt Ser473						
Total Akt						



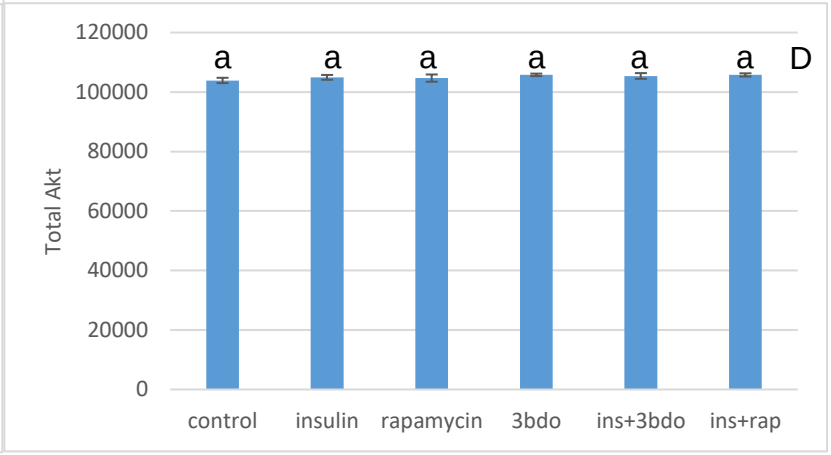


Figure 4. 15 Effects of 4h rapamycin or 3BDO +/- 1h insulin on Akt activity in L6 myotubes.

Differentiated L6 myotubes were pre-treated with or without rapamycin (100nM) or 3BDO (60μM) for 4h and then incubated with insulin as noted for 1h. Representative western blots and quantification of A) phospho/total Akt ratio, B) example western blots, C) phosphorylated Akt and D) total Akt. Results are mean± SEM for n=3 wells for each treatment group. I+R: Ins+Rap. I+3: Ins+3BDO. One-way ANOVA: $p<0.001$ for A and C; $p=0.618$ (D). Means with the same letter are not different ($p>0.05$ for Bonferroni), whereas those with different letters are significantly different ($p<0.05$ for Bonferroni)

4.3.8. Effects of 4 hours BCH treatment on mTOR and downstream target proteins in L6 myotubes

Representative experiments are presented here and data from repeat experiments on L6 myotubes treated with BCH are shown in the appendix (chapter 9).

Leucine regulates multiple cellular activities through activation of mTOR and BCH is an inhibitor of the system L transporter and therefore inhibits leucine uptake by the cells. To test whether BCH inhibits the mTOR signalling pathway by blocking leucine entering cells, L6 myotubes were pre-incubated for 4h with either 100nM rapamycin or 25mM BCH prior to 1h treatment with or without insulin. Phosphorylation of mTOR, 4E-BP1, and p70S6K were tested first to verify that the BCH did inhibit with the mTOR signalling pathway.

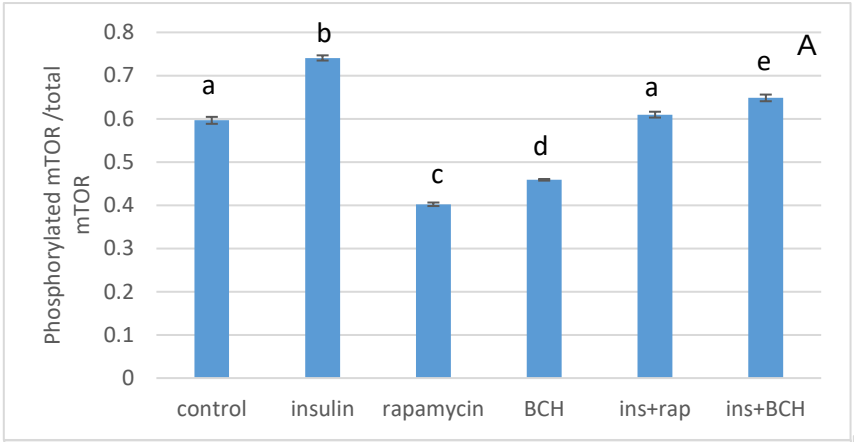
Figure 4.16A showed that both rapamycin and BCH alone inhibited mTOR ratio (phos/total) in L6 myotubes (32% for rapamycin, 23% for BCH; $p<0.05$). 1h insulin treatment increased mTOR ratio by 24% (vs. control) and rapamycin diminished this effect by 18% (vs. insulin alone, $p<0.05$, Figure 4.16A). As expected, BCH also reduced (about 12%) insulin-stimulated mTOR ratio (vs. insulin alone, $p<0.05$, Figure 4.16A).

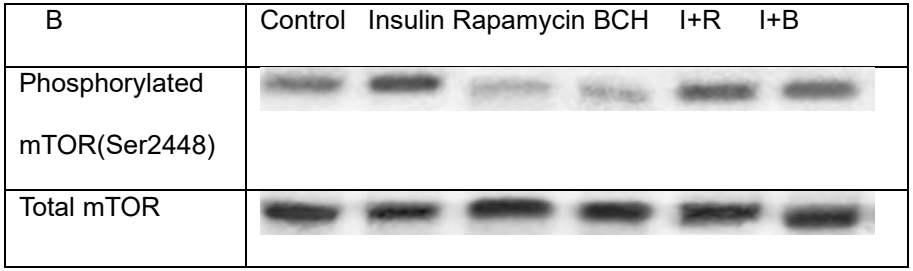
Once again, as downstream target proteins of mTOR, 4E-BP1 and p70S6K displayed same results as mTOR. Insulin increased 4E-BP1 and p70S6K ratios ($p<0.05$, Figures 4.17A and 4.18A). Rapamycin alone reduced 4E-BP1 ratio by 37% and p70S6K ratio by 86%. BCH alone also decreased 4E-BP1 ratio by 33% and p70S6K ratio by 52% ($p<0.05$, Figures 4.17A and 4.18A). Insulin-induced

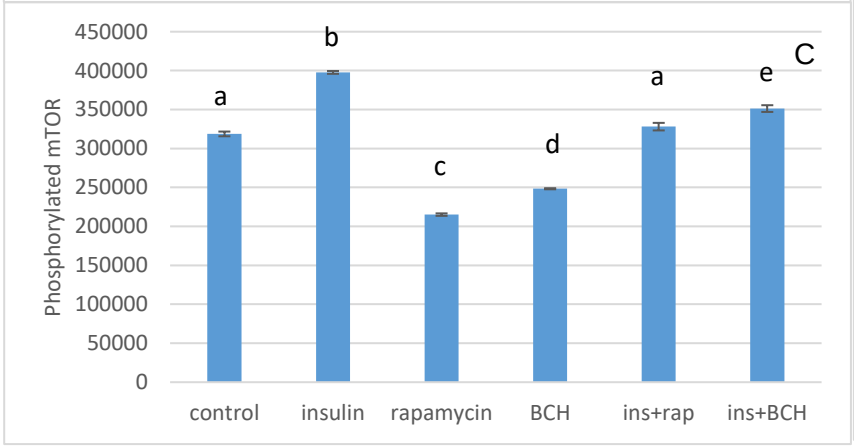
4E-BP1 (rapamycin: 20%; BCH: 35%) and p70S6K (rapamycin: 77%; BCH 34%) were inhibited by rapamycin and BCH, respectively ($p<0.05$, Figures 4.17A and 4.18A).

For the phosphorylated mTOR, 4E-BP1 and p70S6K, they showed same pattern with ratios of mTOR, 4E-BP1 and p70S6K ($p<0.001$, Figures 4.16C, 4.17C, 4.18C). There was no difference among all treatment groups for total mTOR, 4E-BP1 and p70S6K ($p= 0.677$, mTOR. $p= 0.964$, 4E-BP1. $p=0.972$, p70S6K. Figures 4.16D, 4.17D, 4.18D).

These results suggested that rapamycin reduced mTOR phosphorylation and its downstream target proteins, even with insulin, supporting previous results. BCH worked like rapamycin, it also inhibited insulin-stimulated phosphorylation of mTOR and its downstream target proteins.







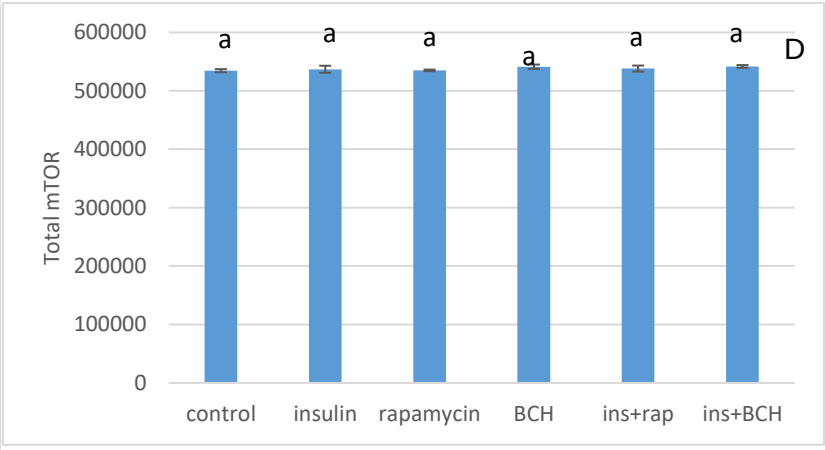
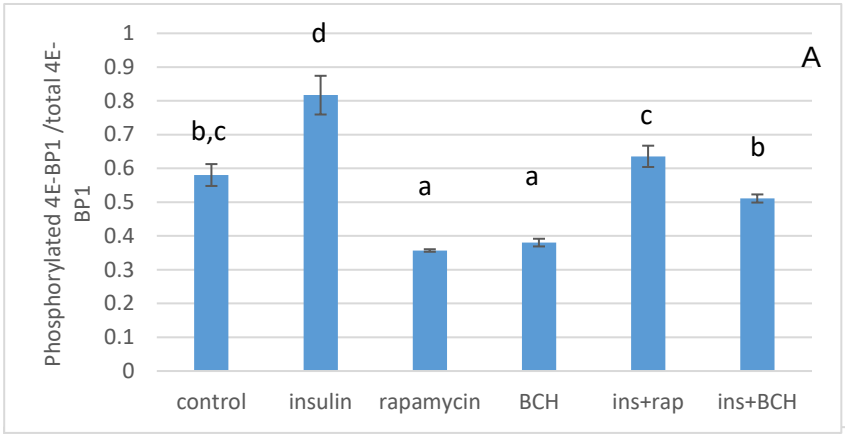
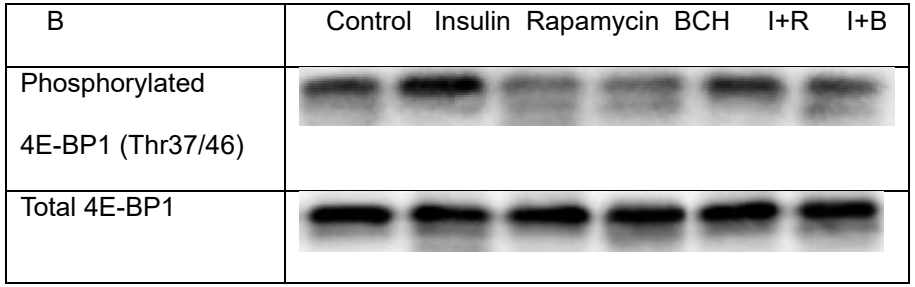
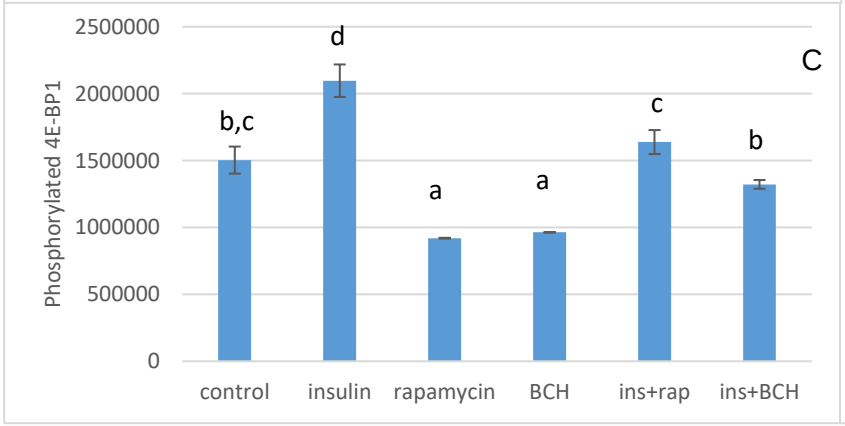


Figure 4. 16 Effects of 4h rapamycin or BCH +/- 1h insulin on mTOR western blot in L6 myotubes.

Differentiated L6 myotubes were pre-treated with or without rapamycin (100nM) or BCH (25mM) for 4h and then incubated with insulin as noted for 1h. Representative western blot analysis and quantifications of A) ratio mTOR, B) western blot C) phosphorylated mTOR and D) total mTOR. Results are mean± SEM for n=3 wells for each treatment group. I+R: Ins+Rap I+B: Ins+BCH. One-way ANOVA: $p<0.001$ for A and C; $p=0.677$ (D). Means with the same letter are not different ($p>0.05$ for Bonferroni), whereas those with different letters are significantly different ($p<0.05$ for Bonferroni)







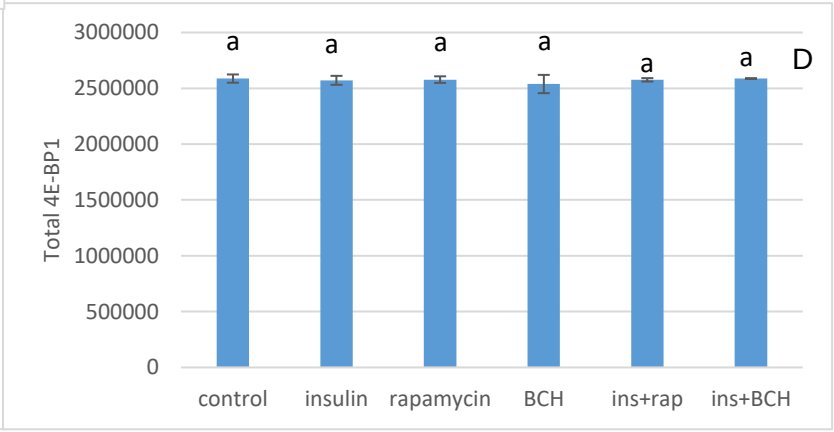
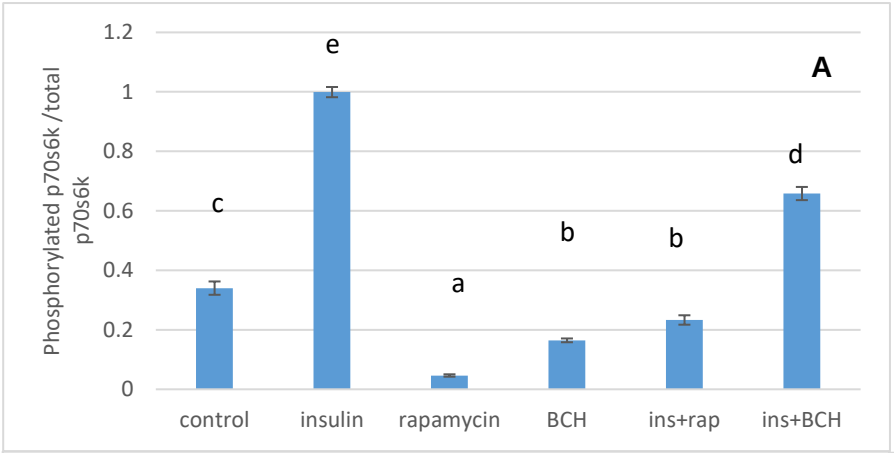
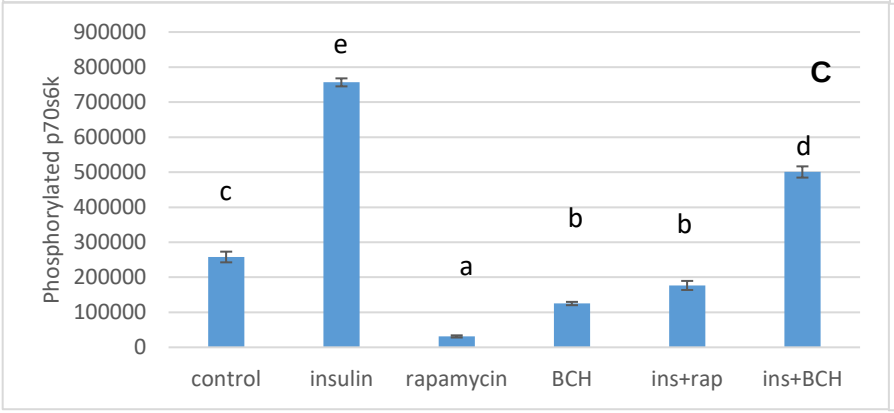


Figure 4. 17 Effects of 4h rapamycin or BCH +/- 1h insulin on 4E-BP1 western blot in L6 myotubes.

Differentiated L6 myotubes were pre-treated with or without rapamycin (100nM) or BCH (25mM) for 4h and then incubated with insulin as noted for 1h. Representative western blot analysis and quantifications of A) ratio 4E-BP1, B) western blot C) phosphorylated 4E-BP1 and D) total 4E-BP1 Results are mean± SEM for n=3 wells for each treatment group. I+R: Ins+Rap I+B: Ins+BCH. One-way ANOVA: $p<0.001$ for A and C; $p=0.964$ (D). Means with the same letter are not different ($p>0.05$ for Bonferroni), whereas those with different letters are significantly different ($p<0.05$ for Bonferroni)



B	Control Insulin Rapamycin BCH I+R I+B
Phosphorylated p70S6K(Thr 389)	
Total p70S6K	



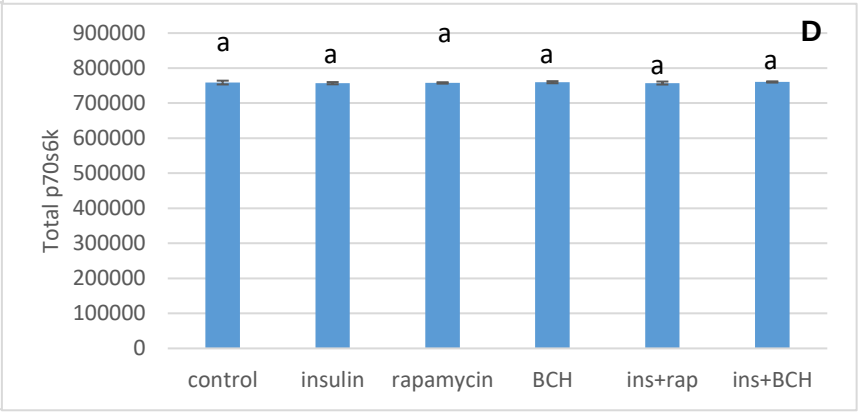


Figure 4. 18 Effects of 4h rapamycin or BCH +/- 1h insulin on p70S6K western blot in L6 myotubes.

Differentiated L6 myotubes were pre-treated with or without rapamycin (100nM) or BCH (25nM) for 4h and then incubated with insulin as noted for 1h. Representative western blot analysis and quantifications of A) ratio p70S6K, B) western blot C) phosphorylated p70S6K and D) total p70S6K. Results are mean± SEM for n=3 wells for each treatment group. I+R: Ins+Rap I+B: Ins+BCH. One-way ANOVA: $p<0.001$ for A and C; $p=0.972$ (D). Means with the same letter are not different ($p>0.05$ for Bonferroni), whereas those with different letters are significantly different ($p<0.05$ for Bonferroni).

4.3.9. Effects of 4 hours BCH treatment on beta-actin in L6 myotubes

There was no difference of beta-actin (loading control) in 4 hours BCH treatment groups, suggesting the quantity of each sample that was loaded in the gels was the same.

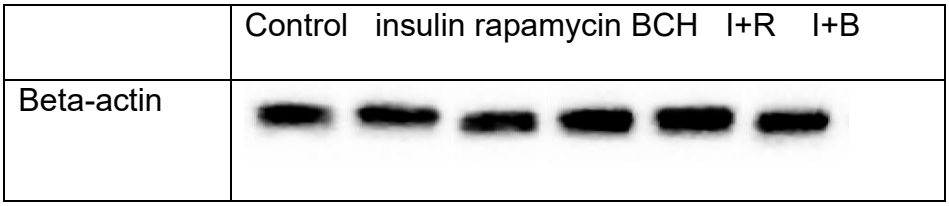


Figure 4. 19 Effects of 4h rapamycin or BCH +/- 1h insulin on Beta-actin in L6 muscle cells

Differentiated L6 myotubes were pre-treated with or without rapamycin (100nM) or 3BDO (60μM) for 4h and then incubated with insulin as noted for 1h. Western blot of Beta-actin protein in control, insulin, rapamycin, BCH, ins+rapamycin (I+R) and ins+BCH (I+B) treatment groups, n=3.

4.3.10. Effects of 4 hours BCH treatment on glucose uptake in L6 myotubes

Although BCH alone reduced the phosphorylated mTOR and its downstream target proteins, it was unknown whether BCH influenced glucose uptake in L6 myotubes. Hence, the effect of BCH on glucose uptake would be investigated next.

After 24h serum starvation, L6 myotubes were exposed for 4h to either 100nM rapamycin or 25mM BCH prior to 1h treatment with or without insulin. Compared with control group, glucose uptake was doubly increased by insulin and rapamycin alone still reduced it by 19% ($p<0.05$, Figure 4.20). Furthermore, rapamycin reduced insulin-stimulated glucose uptake by 23% (vs. insulin, $p<0.05$, Figure 4.20). These results were still consistent with the first two experiments (rapamycin alone and 3BDO treatment). Like rapamycin, BCH also decreased glucose uptake by 50% and in the presence of insulin, it decreased glucose uptake by 72% (vs. insulin, $p<0.05$, Figure 4.20). As expected, both BCH and rapamycin reduced glucose uptake, but BCH reduced insulin-stimulated glucose uptake more than rapamycin, where it apparently blocked the insulin effect (BCH vs. BCH+ins, $p>0.05$).

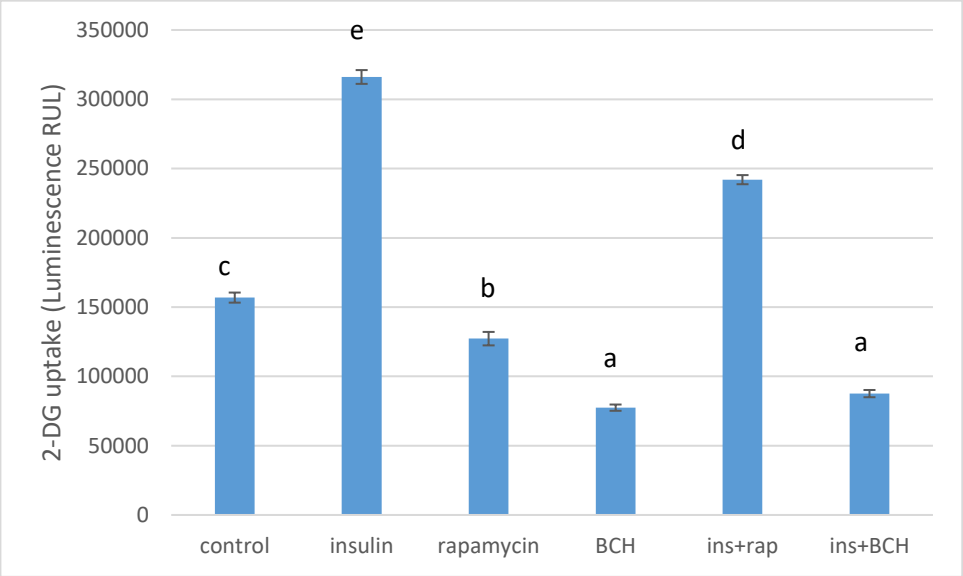
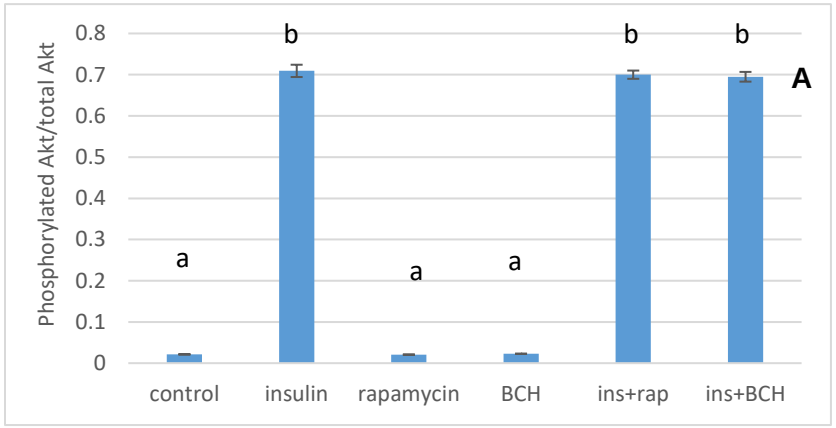


Figure 4. 20 Effects of 4h rapamycin or BCH +/- insulin on glucose uptake in L6 myotubes.

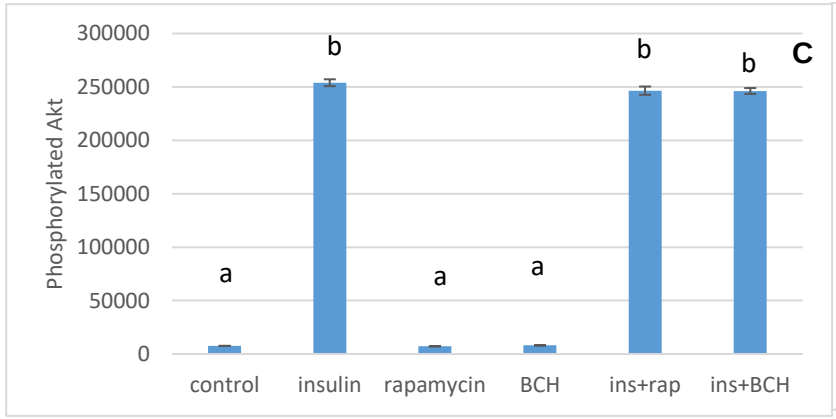
Differentiated L6 myotubes were pre-treated with or without rapamycin (100nM) or BCH (25nM) for 4h and then incubated with insulin as noted for 1h before measurement of 2-DG uptake. Results are mean± SEM for n=6 wells for each treatment group. $p<0.001$ for one-way ANOVA. Means with the same letter are not different ($p>0.05$ for Bonferroni), whereas those with different letters are significantly different ($p<0.05$ for Bonferroni)

4.3.11. Effects of 4 hours BCH treatment on Akt in L6 myotubes

Akt is an upstream protein of mTOR and since both rapamycin and BCH worked on mTOR, they should not influence Akt. Indeed, only insulin increased Akt ratio ($p<0.05$, Figure 4.21A). Compared with control, rapamycin and BCH did not affect Akt ratio ($p>0.05$, Figure 4.21A). Furthermore, rapamycin and BCH also did not decrease insulin-stimulated Akt ratio ($p>0.05$ vs. insulin, Figure 4.21A). For phosphorylated Akt, it showed the same trend with Akt ratio (Figure 4.21C, $p<0.001$). There was no difference among all treatment groups for total Akt ($p= 0.667$, Figure 4.20D).



B	Control Insulin Rapamycin BCH I+R I+B
Phosphorylated Akt Ser473	
Total Akt	



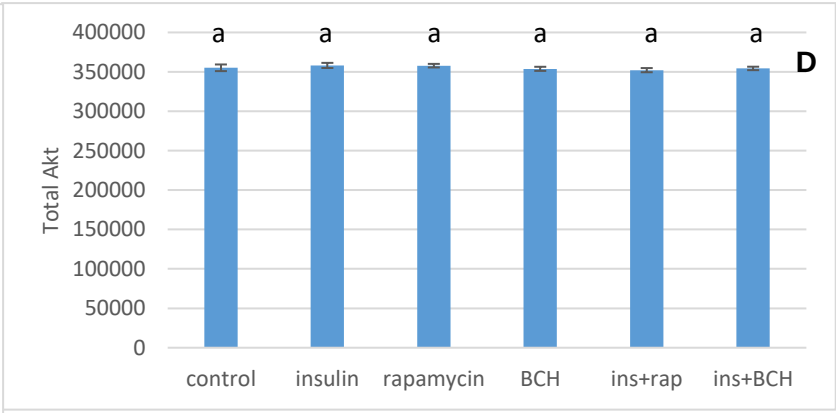


Figure 4. 21 Effects of 4h rapamycin or BCH +/- 1h insulin on Akt western blot in L6 myotubes.

Differentiated L6 myotubes were pre-treated with or without rapamycin (100nM) or BCH (25nM) for 4h and then incubated with insulin as noted for 1h. Representative western blot analysis and quantifications of A) ratio Akt, B) western blot C) phosphorylated Akt and D) total Akt. Results are mean± SEM for n=3 wells for each treatment group. I+R: Ins+Rap I+B: Ins+BCH. One-way ANOVA: $p<0.001$ for A and C; $p=0.677$ (D) Means with the same letter are not different ($p>0.05$ for Bonferroni), whereas those with different letters are significantly different ($p<0.05$ for Bonferroni).

4.3.12. Effects of 4 hours BCH treatment on intracellular BCAA concentrations in L6 myotubes

BCH should inhibit leucine uptake in L6 cells through inhibiting the system L transporters. Therefore, the intracellular BCAA concentrations were determined to confirm that BCH reduced mTOR phosphorylation and glucose uptake by decreasing leucine uptake.

As figure 4.22 shows, insulin reduced (23%) intracellular BCAA concentrations ($p<0.05$ vs. control), presumably because insulin stimulated both amino acid uptake into the cells and protein synthesis. The function of rapamycin was to inhibit mTOR phosphorylation, which should lead to reduced protein synthesis. Hence intracellular BCAA concentrations were significantly higher in the rapamycin than control group (78% $p<0.05$ vs. control, Figure 4.22). There was no difference between control group and ins+rap, possibly because the effects of rapamycin and insulin cancelled out each other ($p>0.05$ vs. control).

However, there was also no significant difference between control and BCH group ($p>0.05$), suggesting that BCH did not inhibit leucine uptake into cells. However, the BCAA assay measures concentration of all three intracellular BCAAs together (leucine, isoleucine and valine), so maybe the other two BCAAs influenced this result. Interestingly, ins+BCH group was higher than both insulin and BCH alone group ($p<0.05$ vs. insulin; $p<0.05$ vs. BCH), which was unexpected. In theory, insulin stimulates protein synthesis and BCH inhibits uptake of leucine, both of which should reduce intracellular BCAA

concentrations.

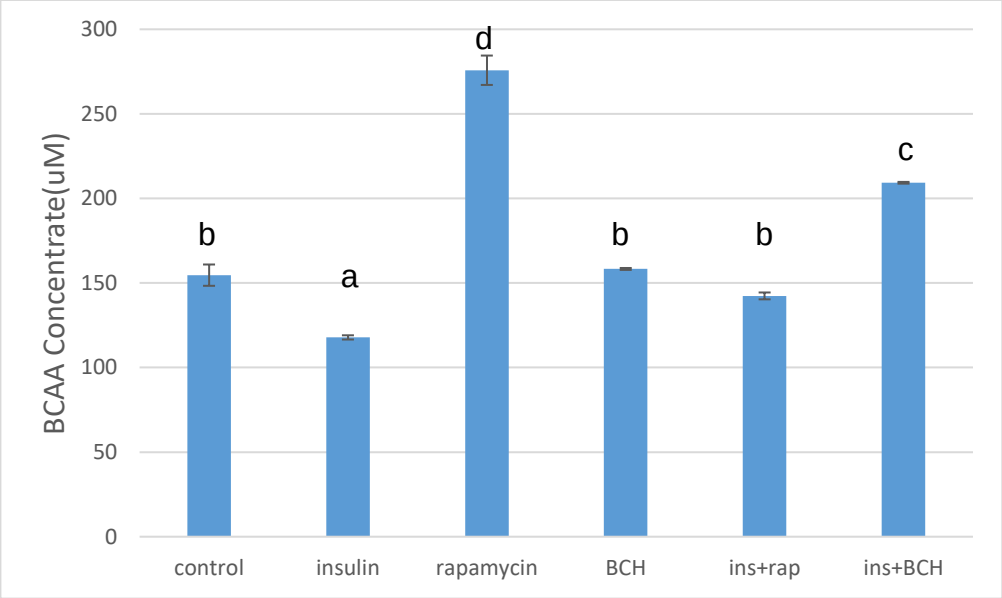


Figure 4. 22 Effects of 4h rapamycin or BCH +/- insulin on intracellular BCAAs in L6 myotubes.

Differentiated L6 myotubes were pre-treated with or without rapamycin (100nM) or BCH (25nM) for 4h and then incubated with insulin as noted for 1h before measurement of intracellular BCAAs concentration. Results are mean± SEM for n=6 wells for each treatment group. $p<0.001$ for one-way ANOVA. Means with the same letter are not different ($p>0.05$ for Bonferroni), whereas those with different letters are significantly different ($p<0.05$ for Bonferroni).

4.4. Discussion and Conclusion

The present study demonstrated for the first time that 4h rapamycin and BCH (an inhibitor of L-type amino acid transporters) decreased both basal and insulin-stimulated glucose uptake in L6 muscle cells. Furthermore, the data revealed that 3BDO (an mTOR activator) increase basal glucose uptake, but not insulin-induced glucose uptake. Previous studies have suggested that treatment of human subcutaneous and omental adipocytes (Pereira *et al.*, (2012) and L6 myotubes (Sipula *et al.*, 2006; Deblon *et al.*, (2012) with rapamycin reduces the basal and insulin-induced glucose uptake. Interestingly, all of these three experiments treated adipocytes or L6 myotubes with rapamycin for a long time (more than 20h). Sipula *et al.,* (2006) treated L6 cells for 24h to 48h with 15nM rapamycin before measurement of glucose uptake, as well as Deblon *et al.* (2012) exposed L6 myotubes to 10-100nM rapamycin for 48h before analyses. In order to verify this outcome, a long-time treatment experiment was designed, L6 myotubes were treated with 100nM rapamycin for 24h before testing glucose uptake. However, the result showed that long-time treatment of rapamycin (did not change the media during 24h) did not affect glucose uptake in L6 myotubes (Figure 9.1, Appendix). The reason seems to be that rapamycin has a short half-life. Both Sadiq *et al.*, (2007) and Leontieva *et al.*, (2013) mentioned that the half-life of rapamycin is less than 6 hours. If it is used for long-time treatment, the media should be refreshed or supplemented with rapamycin after the first 4-6 hours of incubation (Comas *et al.*, 2012). Indeed,

the 4h rapamycin treatment experiment showed a reduced insulin-induced glucose uptake ($p<0.001$, Figure 4.5), which confirms this theory. Deblon *et al.* (2012) and Sipula *et al.* (2006) did not mention whether they changed the media during the experiment, they maybe change it every 4-6 hours. Although, there are some slight differences in experimental design, this study still showed the same results as most studies. A conflicting study showed that short-term (1h) treatment of 3T3-L1 cells with 25nM rapamycin increased insulin stimulated glucose uptake (Tremblay *et al.*, 2005a). The reason could be the different cell type and the concentration of insulin, as they used 100nM insulin, whereas we used a higher concentration of insulin (1mM).

This is the first study to show that 3BDO and BCH influence glucose uptake in L6 myotubes. In the current studies, 3BDO (without insulin) seems to increase glucose uptake. However, when added with insulin, the glucose uptake does not increase further. 3BDO is a new activator of mTOR, so there are few studies on 3BDO in muscle cells nor research on glucose uptake. 3BDO was found to compete with rapamycin in HUVECs cells where bound with FKBP12, a direct target of rapamycin, resulting in activation of mTOR (Ge *et al.*, 2014). Therefore, 3BDO could increase glucose uptake by increasing phosphorylation of mTOR even in the presence of rapamycin.

In the current studies, BCH decreased the glucose uptake in L6 myotubes, with or without insulin. However, there are no previous studies examining BCH's effects on glucose uptake in muscle cells, it effects on the mTOR-signalling pathway have been described.

Recently, mTOR has been described as a very important regulator of glucose uptake (Groenewoud and Zwartkruis, 2013), this relationship has been demonstrated not only in muscle cell lines, but also in 3T3-L1, hematopoietic myeloid/lymphoid cell line and Human HepG2 hepatoma cells (Wieman *et al.*, 2007; Deblon *et al.*, 2012; Khamzina *et al*, 2005; Tremblay *et al.*, 2005a; Pereira *et al.*, 2012). The results of the current study showed that rapamycin decreased the basal and insulin-induced phosphorylation of mTOR (Ser2448) and downstream target proteins (4E-BP1 and p70S6K) confirmed in three experiments. These results were confirmed by Deblon *et al.*, (2012) and Sipula *et al.*, (2006), both of who indicated that rapamycin reduced the insulin-induced mTOR downstream protein, p70S6K. Two phosphorylation sites of p70S6K (T389 and T421/S424) were tested by Sipula *et al.*, (2006), in both cases insulin-stimulated levels were decreased by rapamycin, which is consistent with current results (for three separate experiments). In contrast, Sipula *et al.*, (2006) showed that rapamycin reduced insulin-stimulated phosphorylation of mTOR on Ser2481, but not on Ser2448. However, in the current studies, insulin-induced phosphorylation of mTOR on Ser2448 was inhibited by rapamycin (three experiments) and mTOR Ser2481 was not tested. Ouwens *et al.*, (1999) showed that insulin stimulated an increase in phosphorylation on Ser2448 of mTOR, while Ser2481 is an auto-phosphorylated site that is insensitive to rapamycin and amino acid withdrawal (Foster and Fingar, 2010; Peterson *et al.*, 2000). Copp and Hunter (2009) illustrated that mTORC2 contains mTOR

phosphorylated predominantly on Ser2481, therefore mTOR phosphorylated on Ser2481 is more like a biomarker for intact mTORC2.

From immunoblotting analysis of the current study, 3BDO did not increase basal or insulin-induced phosphorylation of mTOR and p70S6K. It only increased basal phosphorylation of 4E-BP1. In contrast, Ge *et al.*, (2014) showed that in 3BDO+rapamycin treatment groups, phosphorylated p70S6K and mTOR still increased (vs. rapamycin alone group $p < 0.05$) and almost the same as 3BDO alone. Furthermore, Wu *et al.*, (2018) showed that metformin significantly suppressed the upregulation of phosphorylation of p70S6K1 and 3BDO (100 mg/kg) could reverse this in lung tissue. Besides these two studies, Peng *et al.*, (2014), Sheng *et al.*, (2017) and Wang *et al.*, (2016) showed that 3BDO increased mTORC1 activity. It is noticeable that these four papers (except Wu *et al.*, 2018) used 60μM of 3BDO which was the same as used in the current study. However, examination of the concentration of 3BDO had the greatest effect on competition with rapamycin in muscle cells was not performed. Therefore, the observed effects in the current studies may be because the concentration of 3BDO is not sufficient. Moreover, both Peng *et al.*, (2014) and Ge *et al.*, (2014) used HUVECs, which is different from muscle cells, so this could be another reason for the differing results. Although other researches showed 3BDO is an mTOR activator, in this study, the results showed that 3BDO more acted like an mTOR inhibitor.

In the current studies, BCH significantly reduced basal and insulin-stimulated phosphorylation of mTOR and downstream target proteins. BCH is a well-

documented inhibitor of system L amino acid transporters, some researchers showed that BCH inhibited phosphorylation of mTOR and downstream target proteins (Cheng *et al.*, 2016; Yamauchi *et al.*, 2009; Imai *et al.*, 2010). In Hep-2 cells (human head and neck Cancer cell line) or H1395 (lung cancer cell line) cells treated with 20mM BCH for 4 (Yamauchi *et al.*, 2009) or 6 (Imai *et al.*, 2010) days, the phosphorylation of mTOR, 4E-BP1 and p70S6K1 was reduced when compared with control group. In Cheng *et al.*, (2016) experiment, INS1E cells depleted of leucine were incubated with 0.8 mM or 0.4 mM l-leucine in the presence or absence of 10 mM BCH and BCH inhibited phosphorylation of p70S6K1 on T389. These data are consistent with current results, even with different cell types. Two controversial studies illustrated that 8mM BCH did not influence phosphorylation of 4E-BP1 by leucine in adipocytes and 4x BCH (4x the concentration of leucine) itself even slightly increased phosphorylation of p70S6k in rat hepatocytes (Lynch *et al.*, 2000; Kanazawa *et al.*, 2004). However, 4x BCH had no effect on leucine-induced phosphorylation of p70S6k (Kanazawa *et al.*, 2004). All of these studies used different cells type, but none of them used muscle cells, therefore, it is hard to say whether any differences in results are due to the different cell types used. Since BCH inhibits system L leucine transporter competitively (Kanazawa *et al.*, 2004), the concentration ratio of BCH to leucine is likely to be critical. In the current study, 25mM of BCH was used, whereas both Yamauchi *et al.*, (2009) and Imai *et al.*, (2010) used 20mM BCH, but the Lynch *et al.*, (2000) study used 8mM BCH for only 10mins.

This concentration is much lower than we used, so it may not inhibit leucine uptake into cells.

The eariler literature review showed that Akt was an important kinase involved in regulating glucose uptake, but rapamycin did not affect or reduce phosphorylated Akt Ser473 in the current experiments (BCH and 3BDO). This result is similar to a previous study (Houde *et al.*, 2010), where Akt phosphorylation on Ser473 as well as Akt kinase activity were not affected by rapamycin in liver lysates of Sprague-Dawley rats. However, Pereira *et al.*, (2012), Tremblay *et al.*, (2005a) and Deblon *et al.*, (2012) all showed that short-term (15min and 1h) and long-term (20h and 48h) treatment with rapamycin inhibited insulin-stimulated phosphorylation of Akt on Ser473 in human subcutaneous adipocytes, 3T3-L1 cells and L6 myotubes. The discrepancies with the current study are still unclear. For the Deblon *et al.*, (2012) experiment, it could be the treatment time, and with others, it could be the different cell type. BCH also did not display any effect on basal or insulin-induced phosphorylation of Akt on Ser473, whereas 3BDO increased insulin-induced, but not basal, phosphorylation of Akt. 3BDO seems to enhance the effect of insulin on phosphorylation of Akt on Ser473. Interestingly, this increase did not result in an increase in glucose uptake.

Lastly, for the first time we showed whether rapamycin and BCH influence intracellular BCAA concentrations. Rapamycin significantly increased the intracellular BCAA concentrations, presumably because it inhibits protein synthesis. On the contrary, BCH did not influence intracellular BCAA

concentrations. Yamauchi *et al.*, (2009) and Imai *et al.*, (2010) both showed that BCH (0.1–20 mM)) inhibited [14C] L-leucine (3μM) uptake in Hep-2 cells or H1395 cells, and this inhibitory effect was concentration-dependent. However, they only tested if BCH inhibited leucine uptake by cells, they did not analyse the intracellular BCAAs concentrations. Although cells may not uptake leucine, the other two BCAAs (valine and isoleucine) could influence the results obtained. In summary, the studies presented here suggest that there is a relationship between the mTOR activity and glucose uptake in L6 myotubes, which is independent of phosphorylation of Akt (Figure 4.23, below). Future studies should focus on identifying the mechanisms involved, possibly by determining how intracellular BCAAs affect glucose uptake, and whether this is through effects on mTOR signalling pathway or not.

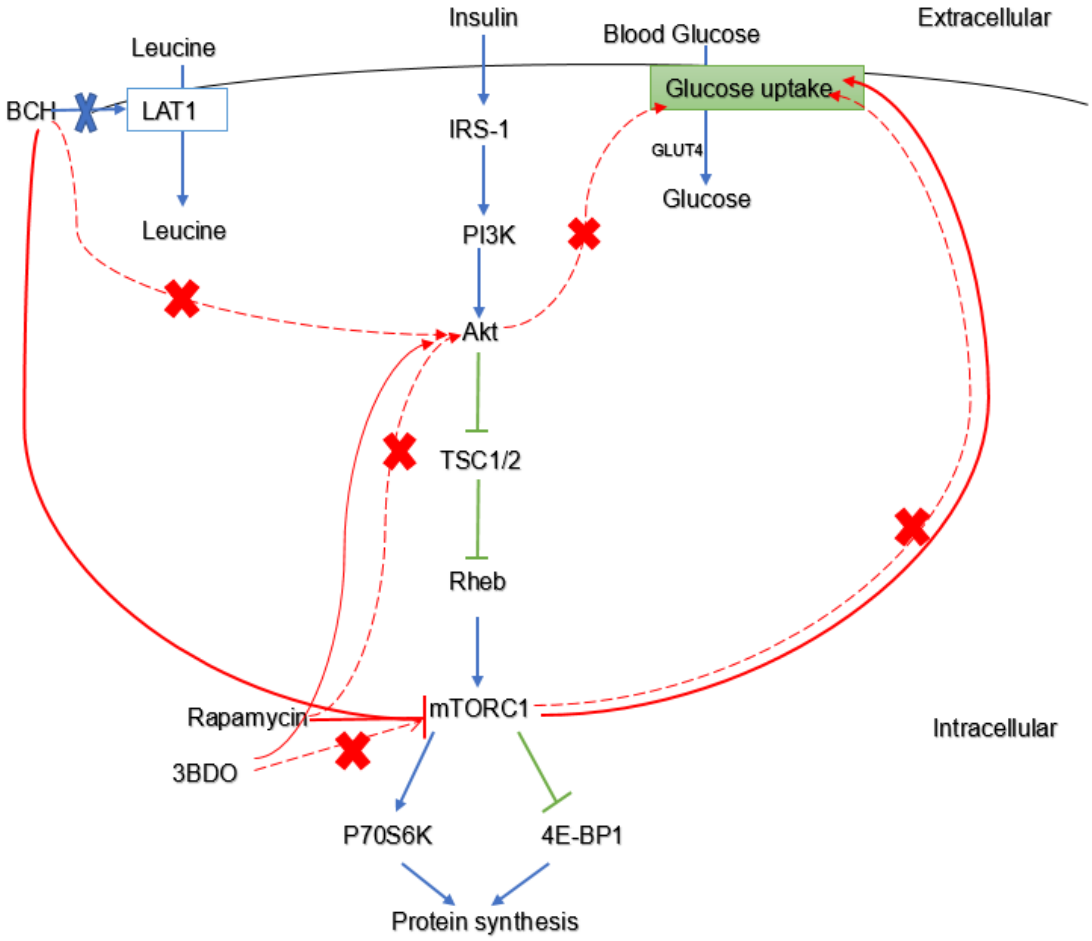


Figure 4. 23 Schematic of the relationship between mTORC1 and glucose uptake

Insulin through PI3K/Akt/TSC1-2 signalling pathway stimulate mTORC1 promote protein synthesis. By stimulating with insulin and PI3K, Akt recruits GLUT4 to the cells membrane (translocation), which allow glucose into cells. This process is called glucose uptake. Reducing glucose uptake. However, this regulation is independent with Akt. **Red full line:** the mechanisms that we tested and found the relationship. **Red full line:** the mechanisms that was tested in the current study and found a relationship. **Red dashed line:** the mechanisms that was tested in the current study and no relationship can be found. **LAT1:** large neutral amino acid transporter, **IRS-1:** Insulin receptor substrate 1, **PI3K:** Phosphoinositide 3-kinases, **Akt/PKB:** Protein kinase B, **TSC1/2:** Tuberous sclerosis 1/2, **mTOR:** mammalian target of rapamycin, **P70S6K:** Ribosomal protein S6 kinase beta-1, **4E-BP1:** Eukaryotic translation initiation factor 4E-binding protein 1, **GLUT4:** Glucose transporter type 4, **BCH:** 2-aminobicyclo-(2,2,1)-heptane-2-carboxylic acid, **3BDO:** 3-Benzyl-5-((2-nitrophenoxy)methyl)-dihydrofuran-2(3H)-one

CHAPTER 5: HOW DIFFERENT LEUCINE CONCENTRATIONS INFLUENCE GLUCOSE UPTAKE IN L6 MYOTUBES

5.1. Introduction

The results of chapter 4 illustrated that mTOR was involved in glucose uptake by using rapamycin, a well-known mTOR inhibitor. Reduced phosphorylation of mTOR and its downstream target proteins could be one of the reasons for a reduction of glucose uptake. Furthermore, BCH an amino acid transporter inhibitor, also confirmed that decreased glucose uptake was related to decreased phosphorylation of mTOR and downstream target proteins. Both of these two inhibitors did not show any effect on the phosphorylation of Akt.

The main effect of BCAAs is to enhance protein synthesis via stimulation of mTOR and its downstream target proteins, 4E-BP1 and p70S6K. Recently, observations from previous studies indicated that BCAAs, as important nutrient-signalling molecules, have been shown to influence glucose uptake and glucose homeostasis *in vivo* and *ex vitro* (Schnuck *et al.*, 2016; Baum *et al.*, 2005; Jaiswal *et al.*, 2012; Doi *et al.*, 2003). The reason could be because protein synthesis as a process is energetically costly (transcription stage), and as such is always accompanied by increased glucose uptake in energetically-demanding tissues, like skeletal muscle, possibly contributing to enhance insulin signalling, GLUT4 content, and glucose uptake (Gannon and Vaughan, 2016; Depaoli *et al.,* 2019).

Another mechanism for leucine enhancing glucose uptake is through peroxisome proliferator-activated receptor gamma coactivator 1-alpha (PGC-1α). Leucine enhances mTORC1 activity, followed by increasing

phosphorylation of p70S6K, result in increased S6 ribosomal protein synthesis. This synthesis could be expected to result in a reduction of ATP content (or increased ATP consumption). The change of ATP relative to AMP would activate AMPK, enhancing the activity of transcriptional co-activators, such as PGC-1α. In turn, an increase of PGC-1α content could lead to increased GLUT4 expression and translocation, which may also contribute to increase glucose uptake (Gannon and Vaughan, 2016). This theory is supported by Vaughan *et al.,*(2013), they showed that showed that leucine (100-500μM. 24-48h) significantly decreased ATP content and increased PGC-1α expression in C2C12 myocytes.

mTOR is an important intersection for amino acid-mediated signalling and insulin signalling pathways (ref). BCAAs include leucine, isoleucine and valine, (Wolfe, 2017) but previous literature review suggested that leucine increased glucose uptake compared to valine or isolecucine (ref). It has been suggested that leucine alters glucose uptake through regulating proteins involved in insulin signalling, such as PI3K and Akt (Nishitani *et al.,* 2002; Liu *et al.,* 2014; Nishitani *et al.,* 2005; Peyrollier *et al.*, 2000). However, this influence is independent of mTOR/p70S6K. On the contrary, leucine has been shown to inhibit glucose uptake by degrading IRS-1 via activation of mTOR/p70S6K signalling pathway (Xiao *et al.,* 2011; Tremblay *et al.,* 2005a; Tremblay *et al.,* 2005b). Alongside mTORC1, a recent study suggested that mTORC2 might also participate in the leucine promoted glucose uptake (Liu *et al.,* 2014).

To conclude, leucine may influence glucose uptake through mTOR signalling pathway or independent of the mTOR pathway, therefore, the aim of this chapter was to investigate whether leucine influences glucose uptake and whether this effect is due to altered phosphorylation of mTOR and downstream target proteins?

5.2. Materials and Methods

5.2.1. Effects of different leucine concentrations on insulin-stimulated glucose uptake and mTOR signalling in L6 and C2C12 myotubes

The L6 cell culture was described in section 2.2.2. After day 4 of differentiation, L6 cells were treated with different leucine concentrations in differentiation medium for 24h (changed on day 6) or 48h (changed on day 5). Three different concentrations of leucine were used, 0x (no leucine), 0.5x (half of leucine concentrations in DMEM medium, 0.0525g/L), or 1x (same concentrations as DMEM medium, 0.105g/L). DMEM without glucose and L-leucine and L-leucine free medium (DMEM-LM, 30030) were ordered from Cell Culture Technologies (private Swiss biotech company) and Thermo Fisher respectively. Concentrations of all the other components' in the medium were the same as DMEM 5796. There was no L-methionine in DMEM-LM (30030), so L-methionine (M9625, Sigma) was added at the same concentration (0.03g/L) as in DMEM 5796. C2C12 cells were treated the same as L6 cells. Figure 5.1 shows the diagrammatic representation of the study protocol.

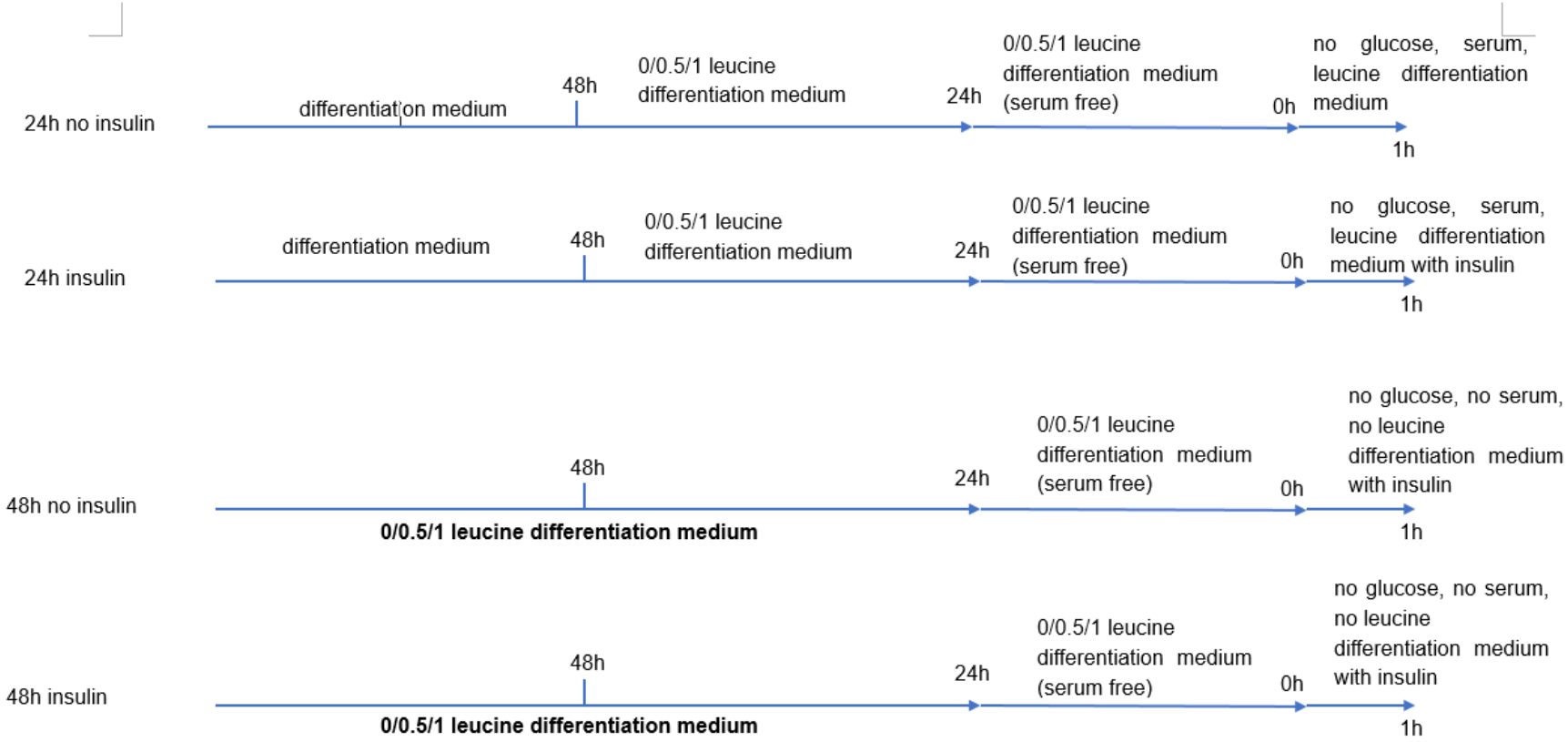


Figure 5. 1 Timeline of treatment groups.

L6 or C2C12 cells were treated with or without different concentrations of leucine (0x, 0.5x, 1x) for different times (24h or 48h), followed by 1h treatment with or without insulin (1mM), prior to measurement of glucose uptake or mTOR signalling (via western blot).

5.2.2. Glucose uptake testing for L6 and C2C12 myotubes

For the glucose uptake, L6 or C2C12 cells were cultured in 24 well plates and treated as described above (section 4.2.1). The subsequent experimental steps were as described in section 2.4.

5.2.3. Western blot antibodies

After removing the medium (6 well plates), samples were washed once with PBS and then collected into 150µl lysis buffer, the antibodies and dilutions were described in section 2.6. All the antibodies used are same as described in chapter 4.

5.2.4. Determination of intracellular BCAA concentrations

After removing the medium (6 well plates), samples were washed once with PBS, then collected into 50µl BCAAs Assay Buffer. Intracellular BCAA concentrations were determined by Assay kit (as described in section 2.5.2).

5.2.5. Statistical Analyses

Two-way (insulin x leucine) ANOVA were performed by Genstat (19th edition) software followed by Bonferroni post-hoc test. The western blot data was quantified by Image Lab (V 5.2.1 Bio-Rad). Significant differences were considered as $p<0.05$.

5.3. Results

Representative experiments are presented here and data from repeat experiments on L6 and C2C12 myotubes treated with different concentrations of leucine are shown in the appendix (chapter 9).

5.3.1. Effects of 24 hours treatment with different concentrations of leucine on mTOR and downstream target proteins in L6 myotubes

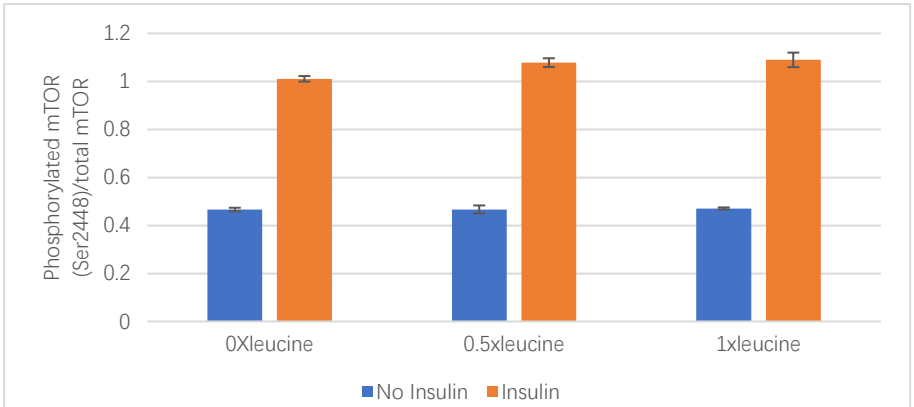
To investigate how different leucine concentrations influence the mTOR signalling pathway in L6 myotubes, the effects of different leucine concentrations (0x, 0.5x, 1x) for 24h on mTOR and downstream target proteins were determined in cultured L6 myotubes exposed to 1mM insulin (Figure 5.2).

There was neither an interaction nor leucine influence on the mTOR ratio (phos/total, $p=0.092$, insulin x leucine; $p= 0.069$, leucine; Figure 5.2A). Whereas, compared to non-insulin groups, insulin significantly increased mTOR ratio (121% in 0x leucine, 130% in 0.5x leucine; 131% in 1x leucine, $p<0.001$).

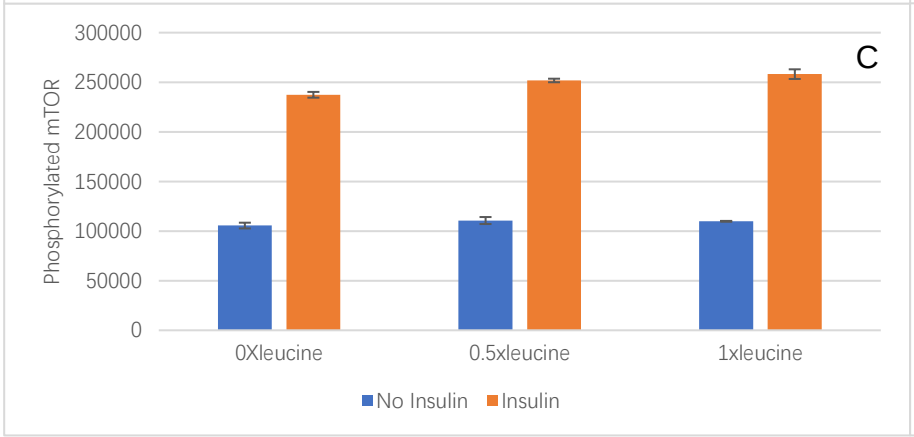
Phosphorylated mTOR (Ser2448) exhibited similar results to the mTOR ratio, where insulin significantly increased phosphorylated mTOR ($p<0.001$, Figure 5.2C). There was neither an interaction nor insulin or leucine effects on total mTOR ($p=0.397$, insulin x leucine; $p=0.638$, insulin; $p=0.692$, leucine; Figure 5.2D).

There was neither an interaction nor leucine influence on the downstream target proteins (4E-BP1 ratio: $p=0.238$, insulin x leucine; $p=0.407$, leucine. p70S6K

ratio: p=0.991, insulin x leucine; p=0.295, leucine. Figure 5.3A and 5.4A.). Only insulin increased 4E-BP1 ratio (p<0.001 insulin) and p70S6K ratio (p<0.001 insulin). Similarly, phosphorylated 4E-BP1 (p=0.181, insulin leucine; p=0.607, leucine; p<0.001, insulin) and p70S6K (p=0.493, insulin x leucine; p=0.825, leucine; p<0.001, insulin) were only increased in response to insulin (Figure 5.3C and 5.4C). There was no interaction nor any effect of insulin or leucine for total 4E-BP1 (p=0.128, insulin x leucine; p=0.759, leucine; p=0.606, insulin. Figure 5.3D) and total p70S6K (p=0.317, insulin x leucine; p=0.519, leucine; p=0.314, insulin. Figure 5.4D).



24h B	0leu 0.5leu 1leu 0 insx leu 0.5 insx leu 1 insx leu
Phosphorylated mTOR (Ser2448)	
Total mTOR	



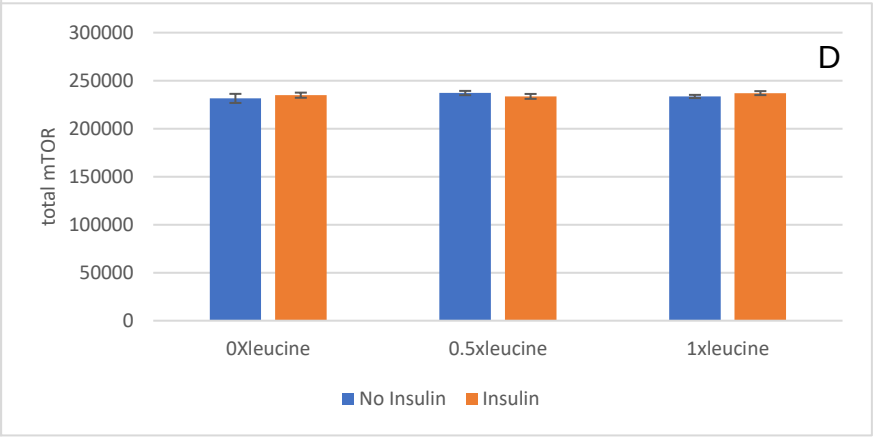
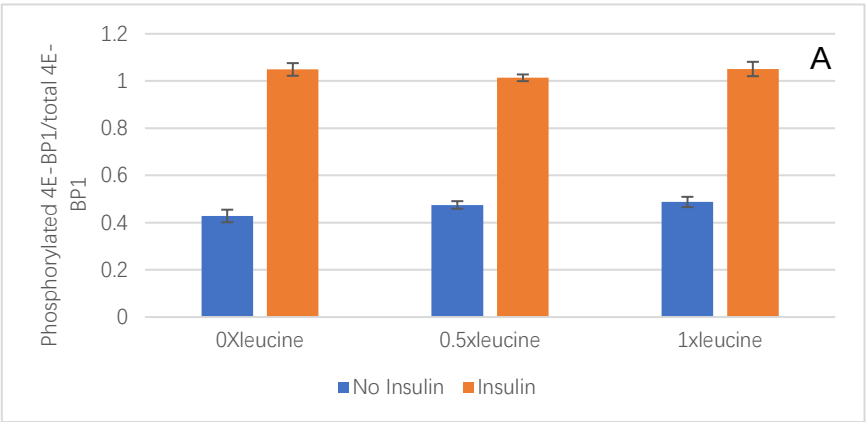
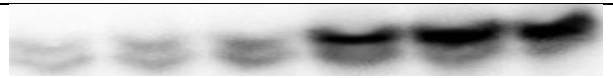
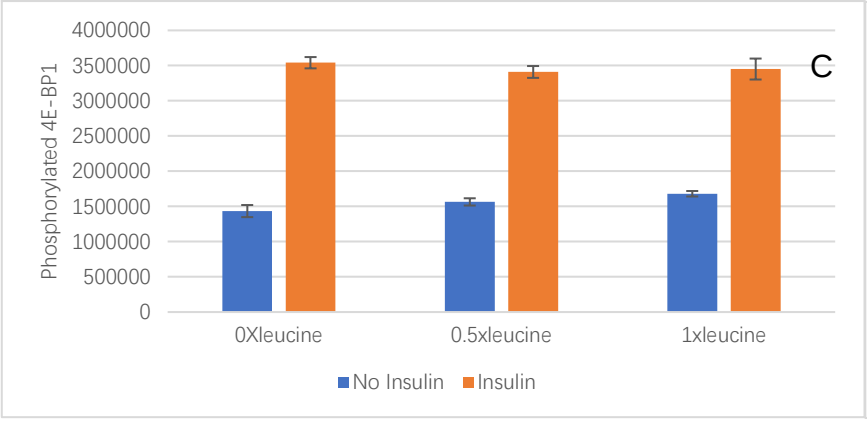


Figure 5. 2 Effects of 24 hours treatment with different concentrations of leucine +/- 1 hour insulin on mTOR activity in L6 myotubes

Differentiated L6 myotubes were pre-treated with or without different leucine concentrations (0x, 0.5x,1x) for 24h, and then incubated with insulin as noted for 1h or equivalent volume of vehicle control. A) phospho/ total mTOR ratio, B) example western blots, C) phosphorylated mTOR and D) total mTOR. Results are mean± SEM for n=3 wells for each treatment group. A: $p<0.001$ for insulin only C: $p<0.001$ for insulin only, $p=0.004$ leucine; D: $p=0.397$, insulin x leucine; $p=0.638$, insulin; $p=0.692$, leucine.



24h B	0leu 0.5leu 1leu 0 insx leu 0.5 insx leu 1 insx leu
Phosphorylated 4E-BP1	
Total 4E-BP1	



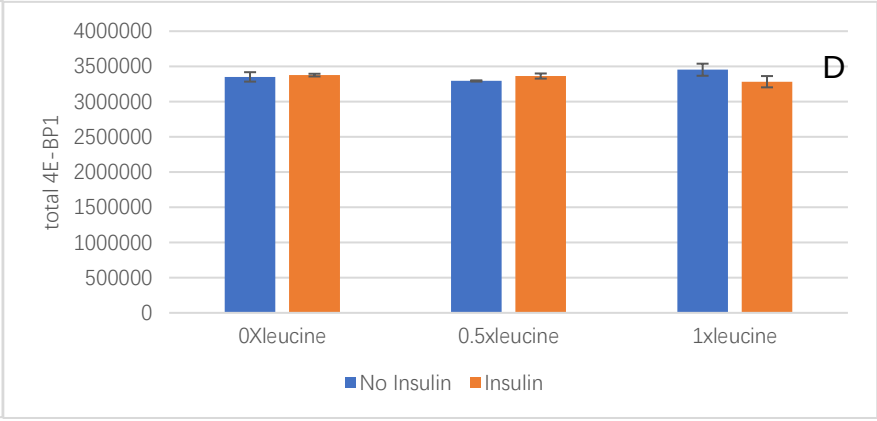
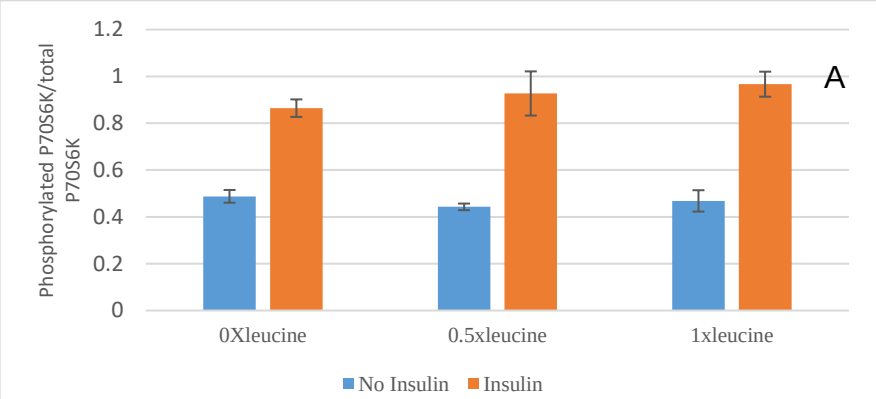
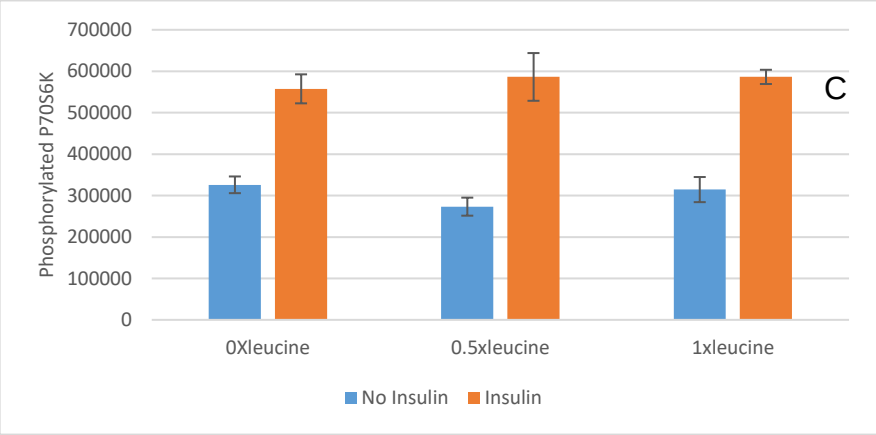


Figure 5. 3 Effects of 24 hours treatment with different concentrations of leucine +/- 1 hour insulin on 4E-BP1 activity in L6 myotubes

Differentiated L6 myotubes were pre-treated with or without different leucine concentrations (0x, 0.5x,1x) for 24h and then incubated with insulin as noted for 1h or equivalent volume of vehicle control. A) phospho/ total 4E-BP1 ratio, B) example western blots C) phosphorylated 4E-BP1 and D) total 4E-BP1. Results are mean± SEM for n=3 wells for each treatment group. A: $p<0.001$ for insulin only, C: $p<0.001$ for insulin only; D: $p=0.128$, insulin x leucine; $p=0.759$, leucine; $p=0.606$, insulin



24h B	0leu 0.5leu 1leu 0 insx leu 0.5 insx leu 1 insx leu
Phosphorylated P70s6k	
Total P70s6k	



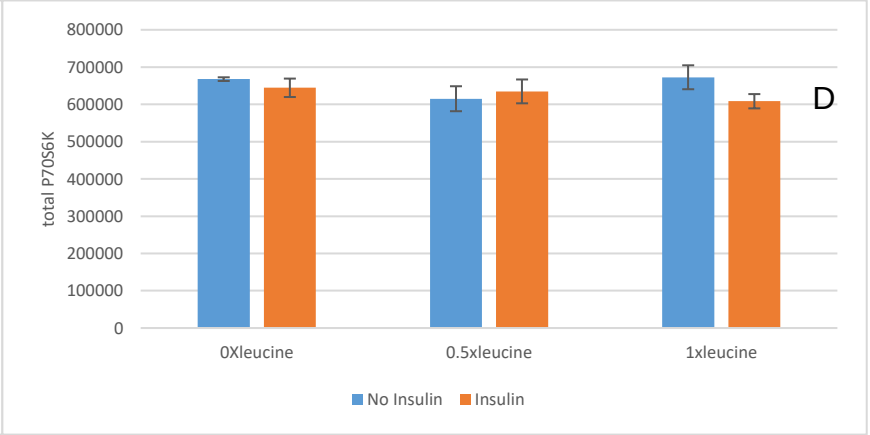


Figure 5. 4 Effects of 24 hours treatment with different concentrations of leucine +/- 1 hour insulin on p70S6K activity in L6 myotubes

Differentiated L6 myotubes were pre-treated with or without different leucine concentrations (0x, 0.5x,1x) for 24h and then incubated with insulin as noted for 1h or equivalent volume of vehicle control. A) phospho/ total p70S6K ratio, B) example western blots C) phosphorylated p70S6K and D) total p70S6K. Results are mean± SEM for n=3 wells for each treatment group. A: $p<0.001$ for insulin only, C: $p<0.001$ for insulin only, D: $p=0.317$, insulin x leucine; $p=0.519$, leucine; $p=0.314$, insulin

0

5.3.2. Effects of 48 hours treatment with different concentrations of leucine on mTOR and downstream target proteins in L6 myotubes

Figures 5.5, 5.6, 5.7 demonstrated that mTOR and downstream target proteins in L6 myotubes treated for 48h with different leucine concentrations, followed by 1h insulin stimulation.

With 48h treatment, there was a significant insulin x leucine interaction on mTOR ratio (phos/total, p=0.003, Figure 5.5A), which differed from that seen with only 24h of leucine treatment. Insulin increased mTOR ratio (p=0.003, Figure 5.5A), but there was no difference between leucine treatment groups. In the absence of insulin, mTOR ratio was increased with 1x leucine compared to 0x and 0.5x leucine.

Phosphorylation of mTOR displayed a significant insulin x leucine interaction (p<0.001, Figure 5.5C). Insulin increased phosphorylation of mTOR at 0.5x and 1x leucine compared with 0x leucine. In the absence of insulin, 1x leucine increased phosphorylation of mTOR by 56% compared with 0x leucine and 0.5x leucine groups. Total mTOR was not affected by either leucine or insulin treatment (p=0.924, insulin x leucine. p=0.547, leucine. p=0.774, insulin. Figure 5.5D).

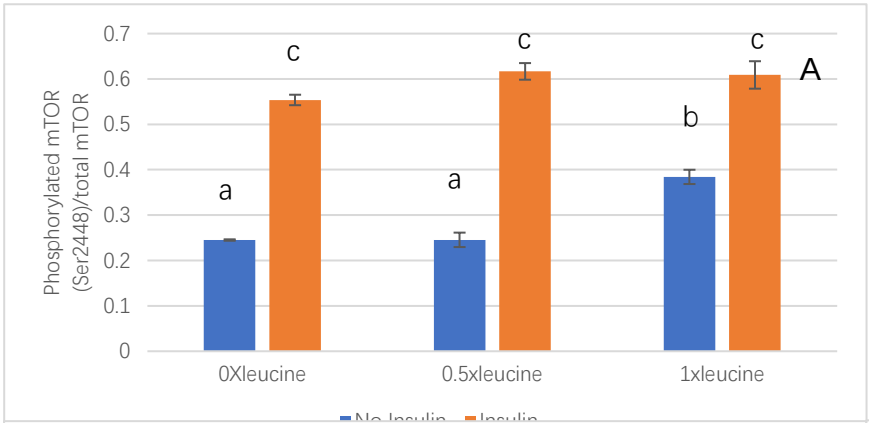
There was no significant interaction for 4E-BP1 ratio (p=0.143, insulin x leucine, Figure 5.6A), but there were significant effects for insulin (p<0.001) and leucine concentration (p=0.009). Insulin increased 4E-BP1 ratio and 0.5x leucine

increased 4E-BP1 ratio compared to 0x and 1x leucine.

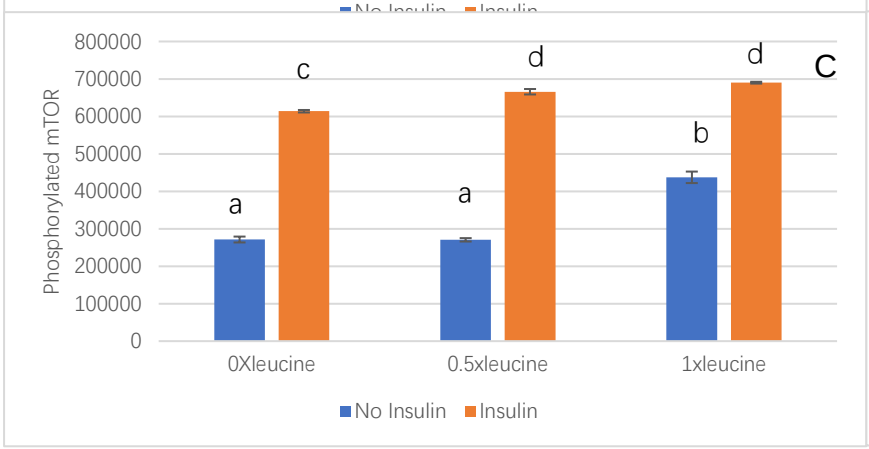
In contrast, phosphorylated 4E-BP1 showed an insulin x leucine interaction ($p<0.001$, Figure 5.6C). Without insulin, 0.5x leucine increased phosphorylation of 4E-BP1 compared to 0x leucine, but then reduced again at 1x leucine, although 1x was still higher than 0x. In contrast, insulin increased phosphorylation of 4E-BP1, but there was no difference between leucine treatment groups. There was no significant difference in total 4E-BP1 between each treatment group ($p=0.129$, insulin x leucine; $p=0.125$, leucine; $p=0.308$, insulin. Figure 5.6D).

Another downstream protein p70S6K showed a significant interaction for insulin x leucine ($p<0.001$, Figure 5.7A). Insulin induced the phosphorylation of p70S6K and this was further increased with 1x leucine compared to 0x leucine. Whereas, in the absence of insulin, 0.5x leucine and 1x leucine unexpectedly reduced p70S6K ratio (21% and 41% respectively) compared to 0x leucine.

The phosphorylation of p70S6K showed similar responses to insulin and leucine treatment as that observed for p70S6K ratio ($p<0.001$, insulin x leucine, Figure 5.7C). As expected, total p70S6K was not affected by insulin or leucine concentrations ($p=0.51$, insulin x leucine; $p=0.132$, leucine; $p=0.83$, insulin. Figure 5.7D).



48h B)	0leu	0.5leu	1leu	0 insx leu	0.5 insx leu	1 insx leu
Phosphorylated mTOR (Ser2448)						
Total mTOR						



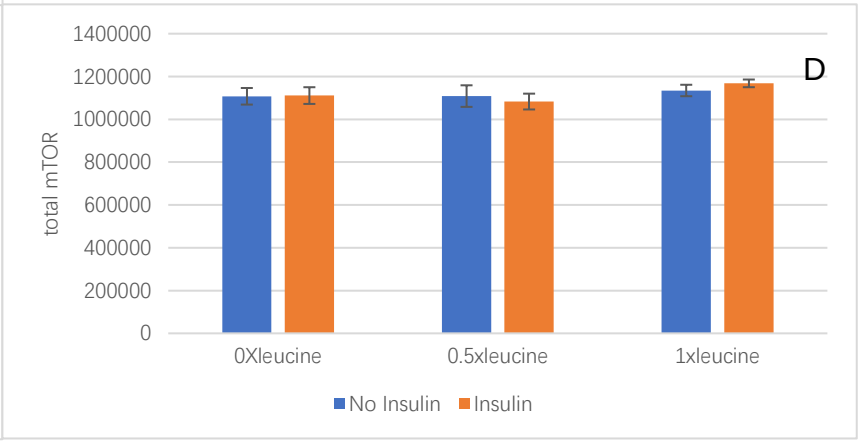


Figure 5. 5 Effects of 48 hours treatment with different concentrations of leucine +/- 1 hour insulin on mTOR activity in L6 myotubes

Differentiated L6 myotubes were pre-treated with or without different leucine concentrations (0x, 0.5x,1x) for 48h and then incubated with insulin as noted for 1h or equivalent volume of vehicle control. A) phospho/ total mTOR ratio, B) example western blots C) phosphorylated mTOR and D) total mTOR. Results are mean± SEM for n=3 wells for each treatment group. A: p=0.003, insulin x leucine; C: p<0.001 insulin x leucine; D: p=0.924 insulin x leucine. Means with the same letter are not different (p>0.05 for Bonferroni), whereas those with different letters are significantly different (p<0.05 for Bonferroni)

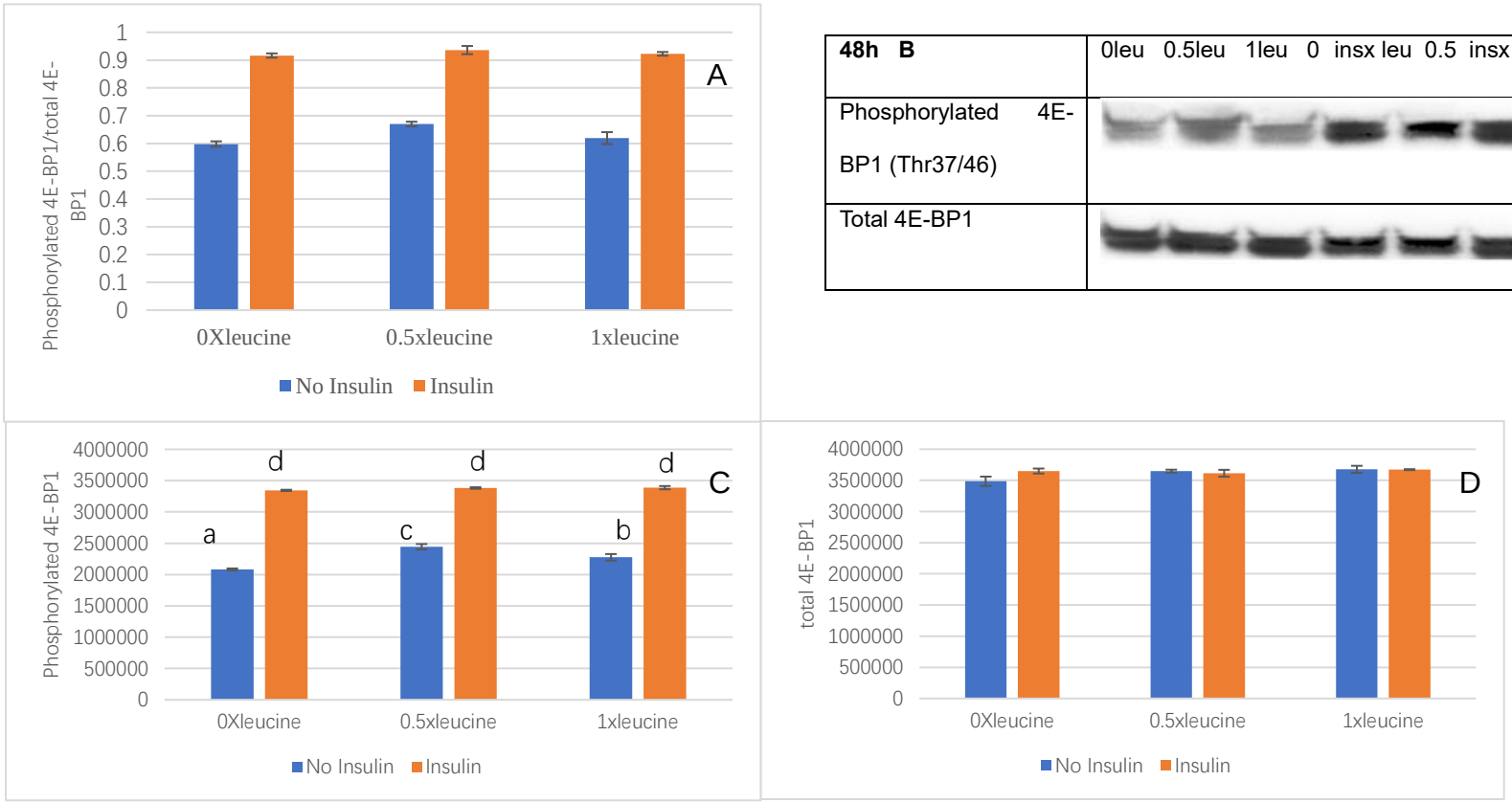
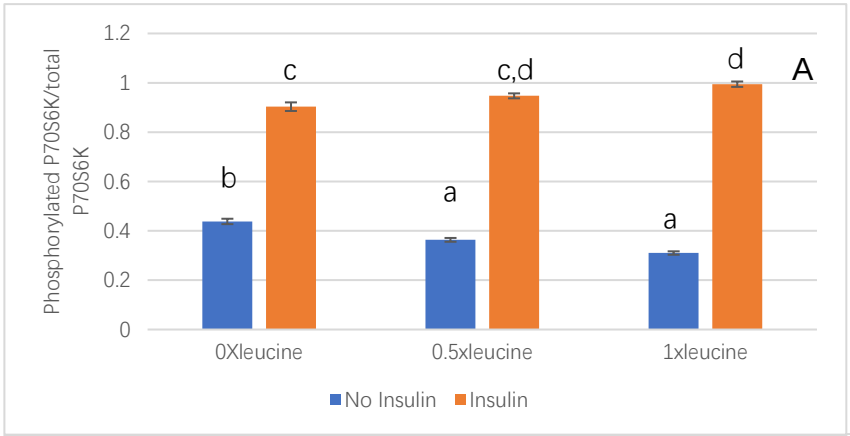
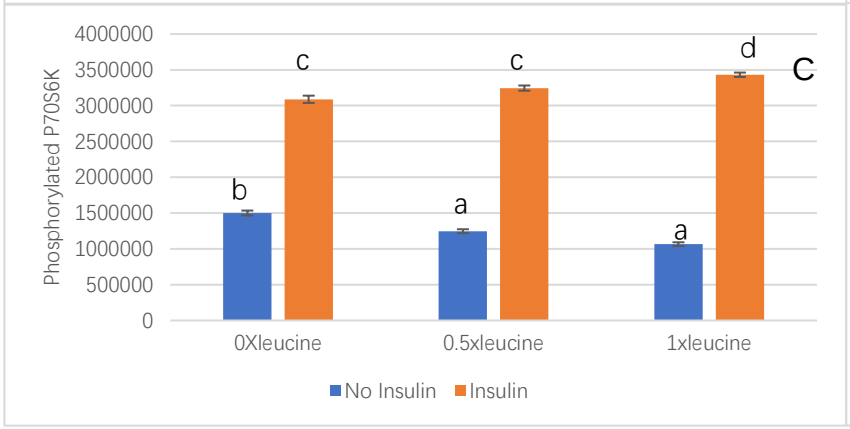


Figure 5. 6 Effects of 48 hours treatment with different concentrations of leucine +/- 1 hour insulin on 4E-BP1 activity in L6 myotubes

Differentiated L6 myotubes were pre-treated with or without different leucine concentrations (0x, 0.5x,1x) for 48h and then incubated with insulin as noted for 1h or equivalent volume of vehicle control. A) phospho/ total 4E-BP1 ratio, B) example western blots C) phosphorylated 4E-BP1 and D) total 4E-BP1. Results are mean± SEM for n=3 wells for each treatment group. A: $p<0.001$ for insulin only, $p=0.009$ for leucine only C: $p<0.001$ insulin x leucine; D: $p=0.129$, insulin x leucine; $p=0.125$, leucine; $p=0.308$, insulin.



48h B	0leu 0.5leu 1leu 0 insx leu 0.5 insx leu 1 insx leu
Phosphorylated P70s6k (Thr389)	
Total P70s6k	



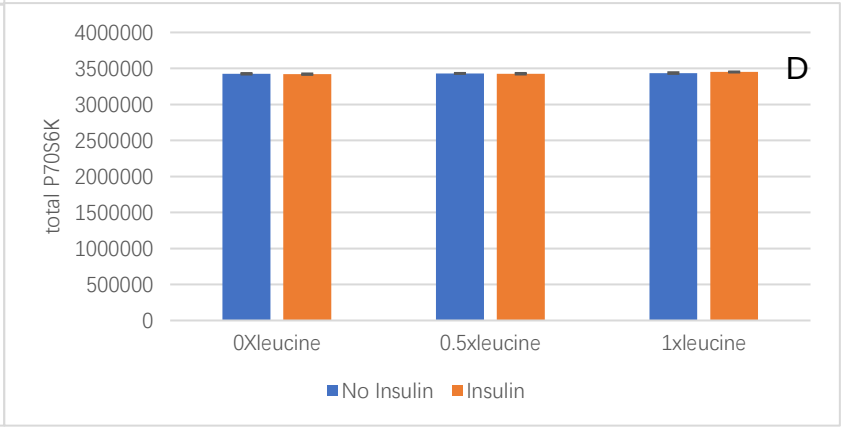


Figure 5. 7 Effects of 48 hours treatment with different concentrations of leucine +/- 1 hour insulin on p70S6K activity in L6 myotubes

Differentiated L6 myotubes were pre-treated with or without different leucine concentrations (0x, 0.5x,1x) medium for 48h and then incubated with insulin as noted for 1h or equivalent volume of vehicle control. A) phospho/ total p70S6K ratio, B) example western blots C) phosphorylated p70S6K and D) total p70S6K. Results are mean± SEM for n=3 wells for each treatment group. A: $p<0.001$ insulin x leucine C: $p<0.001$ insulin x leucine; D: $p=0.51$, insulin x leucine; $p=0.132$, leucine; $p=0.83$, insulin

5.3.3. Effects of 24 hours treatment with different concentrations of leucine on glucose uptake in L6 myotubes

To further confirm whether different concentrations of leucine influence glucose uptake in cultured L6 myotubes. After overnight serum starvation, L6 myotubes were treated with 0x, 0.5x or 1x leucine for 24h, followed by 1h insulin stimulation, with glucose uptake then measured.

As figure 5.8 shows, there was a significant insulin x leucine interaction ($p<0.001$) on glucose uptake after 24 hours treatment. Insulin increased glucose uptake with a further increase with 0.5x leucine compared to 0x leucine, but there was no effect of further increasing the leucine concentration (to 1x). In the absence of insulin, there was a dose-dependent increase in glucose uptake with increasing leucine concentration.

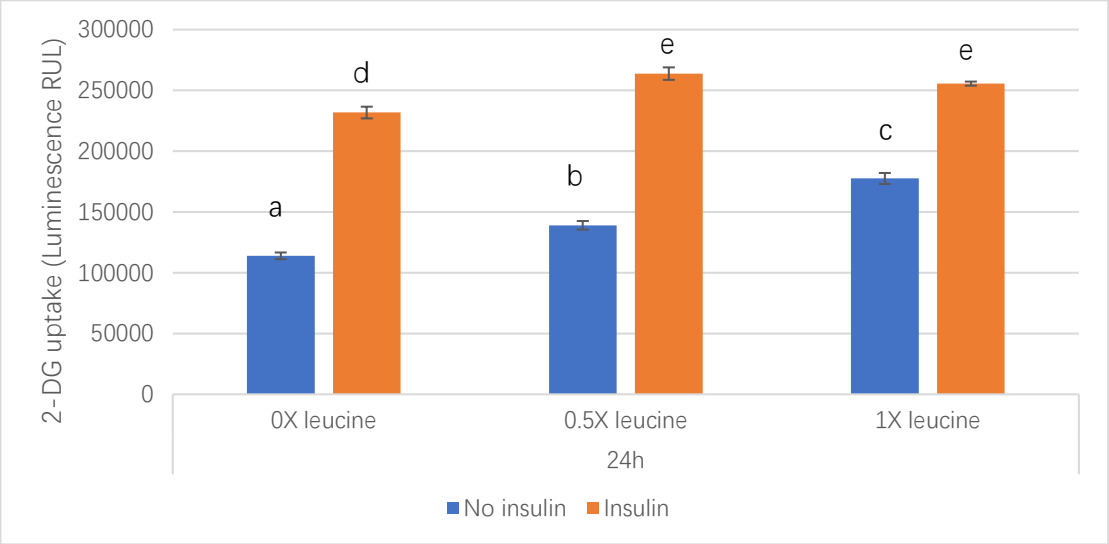


Figure 5. 8 Effects of 24 hours treatment with different concentrations of leucine +/- 1 hour insulin on glucose uptake in L6 myotubes

Differentiated L6 myotubes were pre-treated with or without different leucine concentrations (0x, 0.5x,1x) for 24h and then incubated with insulin as noted or equivalent volume of vehicle control for 1h before measurement of 2-DG uptake. Results are mean± SEM for n=6 wells for each treatment group. $p<0.001$ (insulin x leucine). Means with the same letter are not different ($p>0.05$ for Bonferroni), whereas those with different letters are significantly different ($p<0.05$ for Bonferroni)

5.3.4. Effects of 48 hours treatment with different concentrations of leucine on glucose uptake in L6 myotubes

The results of 48h of leucine treatment showed very similar results as when the amino acid was supplied for 24h. A strong interaction effect between insulin and leucine on glucose uptake was observed ($p<0.001$ insulin x leucine, Figure 5.9). In the absence of insulin, 1x leucine increased glucose uptake compared to 0x and 0.5x leucine. Insulin increased glucose uptake with no further effect of leucine.

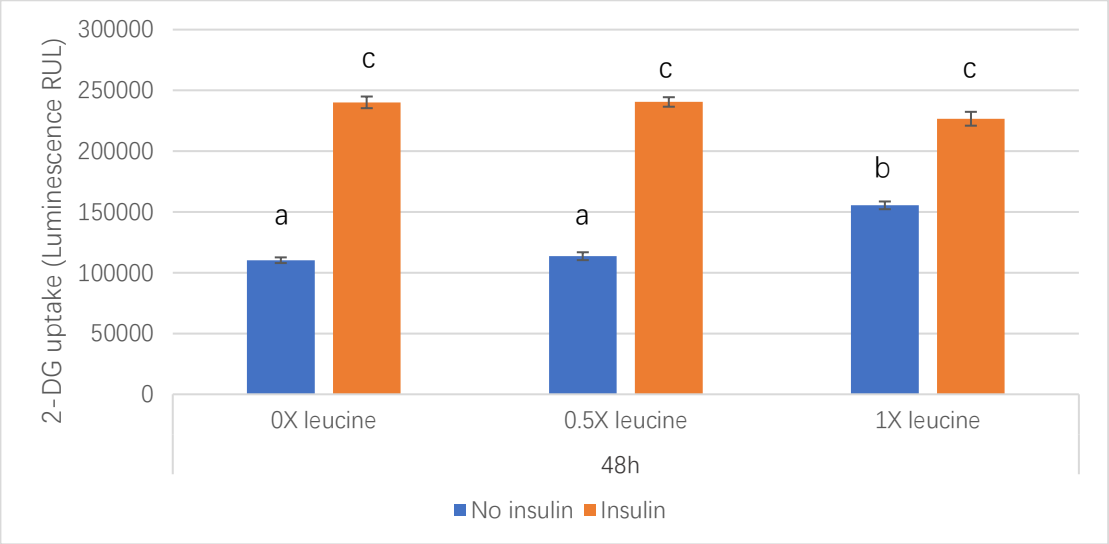
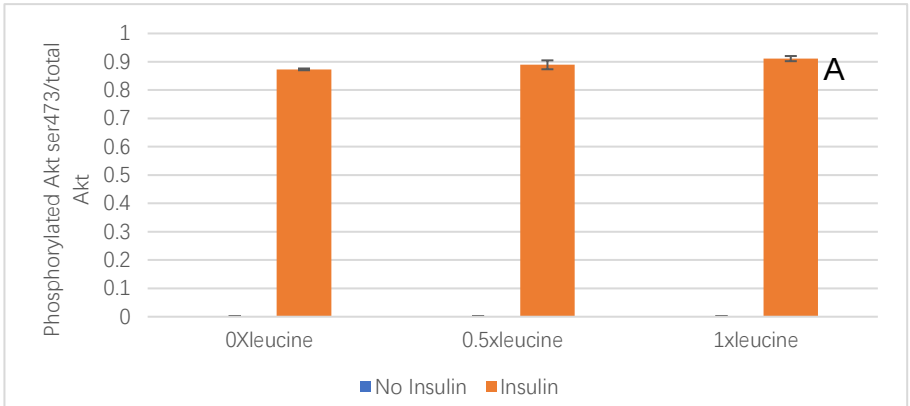


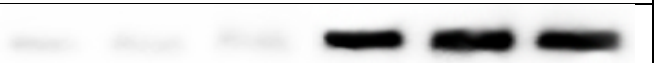
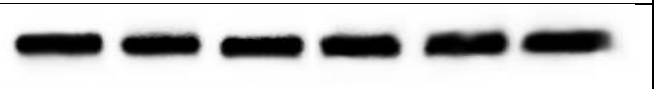
Figure 5. 9 Effects of 48 hours treatment with different concentrations of leucine +/- 1 hour insulin on glucose uptake in L6 myotubes

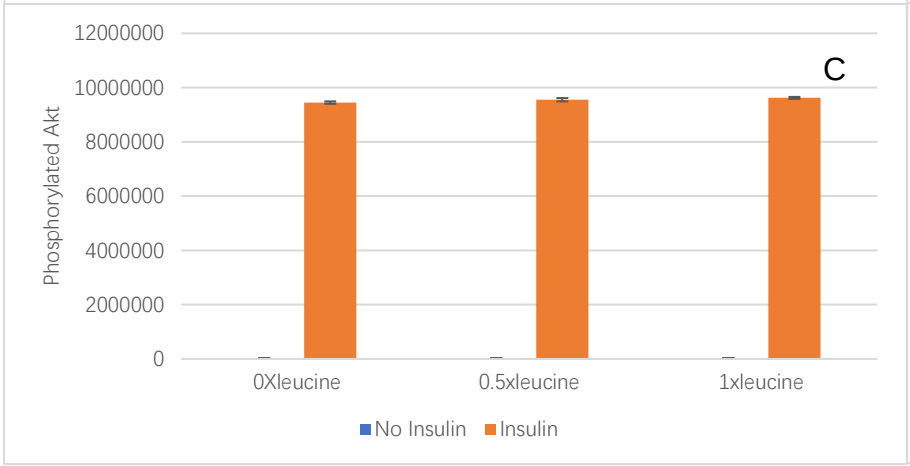
Differentiated L6 myotubes were pre-treated with or without different leucine concentrations (0x, 0.5x,1x) for 48h and then incubated with insulin as noted or equivalent volume of vehicle control for 1h before measurement of 2-DG uptake. Results are mean± SEM for n=6 wells for each treatment group. $p<0.001$ insulin x leucine. Means with the same letter are not different ($p>0.05$ for Bonferroni), whereas those with different letters are significantly different ($p<0.05$ for Bonferroni)

5.3.5. Effects of 24 hours treatment with different concentrations of leucine on Akt in L6 myotubes

There was no significant insulin x leucine interaction (p=0.074, Figure 5.10A) for Akt ratio, nor an effect of leucine (p=0.076, Figure 5.10A). As expected, Akt ratio was only increased by insulin (p<0.001, insulin; Figure 5.10A). Phosphorylated Akt Ser473 displayed same results as Akt ratio, only insulin increased it (p<0.001, insulin; Figure 5.10C). There was no effect of leucine or insulin on total Akt (p=0.566, insulin x leucine; p=0.8, leucine; p=0.507, insulin. Figure 5.10D).



24h B)	0leu 0.5leu 1leu 0 insx leu 0.5 insx leu 1 insx leu
Phosphorylated Akt Ser473	
Total Akt	



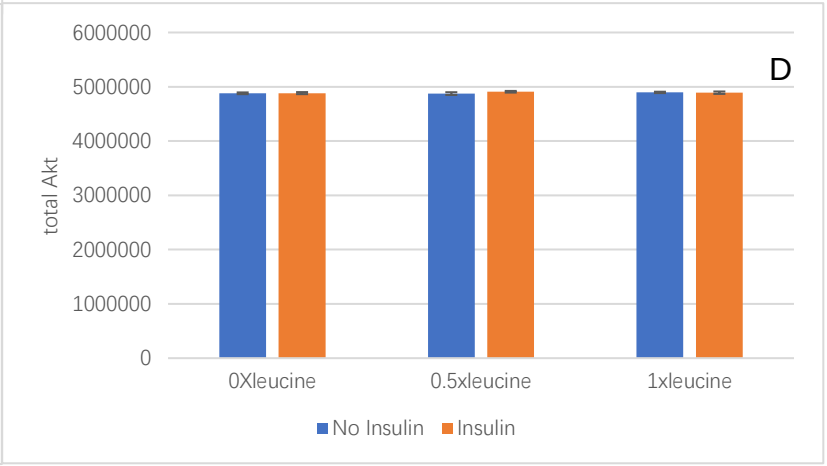


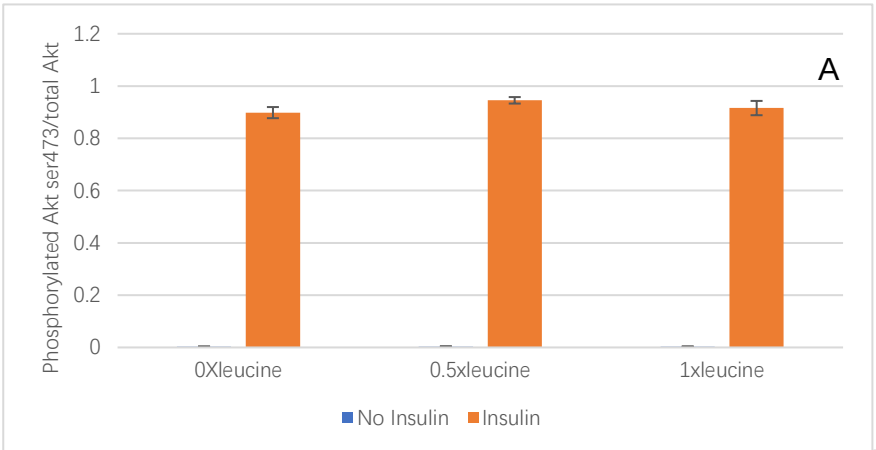
Figure 5. 10 Effects of 24 hours treatment with different concentrations of leucine +/- 1 hour insulin on Akt in L6 myotubes

Differentiated L6 myotubes were pre-treated with or without different leucine concentrations (0x, 0.5x,1x) for 24h and then incubated with insulin as noted for 1h or equivalent volume of vehicle control. A) phospho/ total Akt ratio, B) example western blots C) phosphorylated Akt and D) total Akt. Results are mean± SEM for n=3 wells for each treatment group. A: $p<0.001$ for insulin only C: $p<0.001$ for insulin only; D: $p=0.566$, insulin x leucine; $p=0.8$, leucine; $p=0.507$, insulin

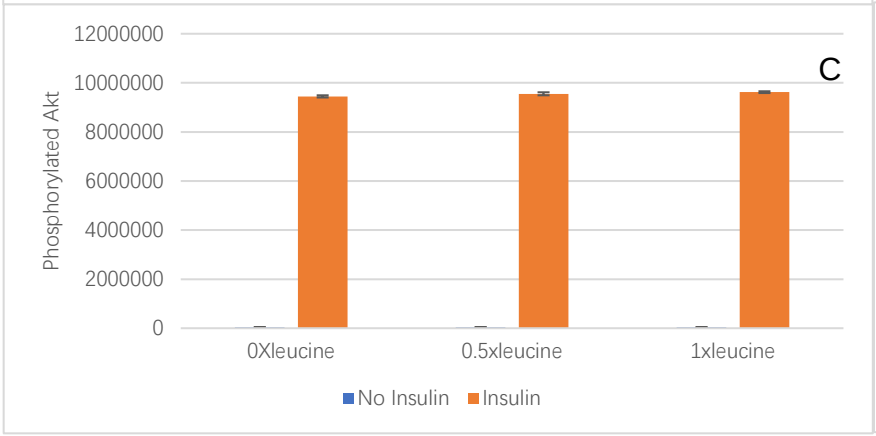
5.3.6. Effects of 48 hours treatment with different concentrations of leucine on Akt in L6 myotubes

Long-term (48h) treatment with leucine did not alter Akt ratio ($p=0.324$, insulin x leucine; $p=0.316$, leucine). Whereas, Akt ratio was increased by insulin ($p<0.001$, insulin; Figure 5.11A).

Similarly, there was no interaction for phosphorylated Akt Ser473 ($p=0.079$, Figure5.11C) and no significant effect of leucine ($p=0.077$), but phosphorylation was significantly increased by insulin ($p<0.001$, insulin; Figure5.11C). Neither insulin nor leucine influenced total Akt ($p=0.898$, insulin x leucine; $p=0.084$, leucine; $p=0.51$, insulin. Figure5.11D).



48h B)	0leu 0.5leu 1leu 0 insx leu 0.5 insx leu 1 insx leu
Phosphorylated Akt Ser473	
Total Akt	



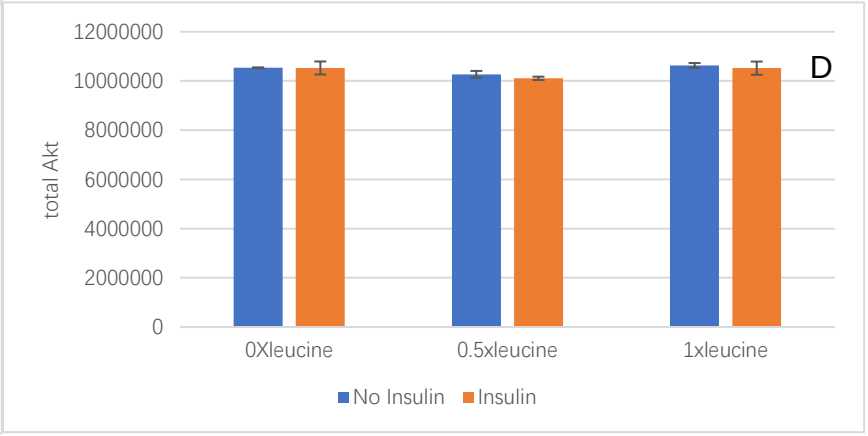


Figure 5. 11 Effects of 48 hours treatment with different concentrations of leucine +/- 1 hour insulin on Akt in L6 myotubes

Differentiated L6 myotubes were pre-treated with or without different leucine concentrations (0x, 0.5x,1x) for 48h and then incubated with insulin as noted for 1h or equivalent volume of vehicle control. A) phospho/ total Akt ratio, B) example western blots C) phosphorylated Akt and D) total Akt. Results are mean± SEM for n=3 wells for each treatment group. A: $p<0.001$ for insulin only C: $p<0.001$ for insulin only; D: $p=0.898$, insulin x leucine; $p=0.084$, leucine; $p=0.51$, insulin

5.3.7. Effects of the 24 and 48 hours treatment with different concentrations of leucine on Beta-actin in L6 myotubes

There was no difference of beta-actin (loading control) between leucine treatment groups in both 24h and 48h treatment groups, suggesting the quantity of each sample that was loaded in the gels was the same.

Beta-actin	0leu 0.5leu 1leu 0 ins x leu 0.5 ins x leu 1 ins x leu
24h	
48h	

Figure 5. 12 Effects of the 24 and 48 hours treatment with different concentrations of leucine +/- 1 hour insulin on Beta-actin in L6 myotubes

Differentiated L6 myotubes were pre-treated with or without different leucine concentrations (0x, 0.5x,1x) for 24h and 48h and then incubated with insulin as noted for 1h or equivalent volume of vehicle control. Western blot of Beta-actin protein in 0x leucine, 0.5x leucine, 1x leucine, 0 leucine x insulin, 0.5 leucine x insulin, 1 leucine x insulin. Results are mean± SEM for n=3 wells for each treatment group.

5.3.8. Effects of 24 hours treatment with different concentrations of leucine on intracellular BCAA concentrations in L6 myotubes

The leucine concentration in medium was changed, but whether the intracellular BCAA concentrations were altered was unknown.

Figure 5.13 displayed the intracellular BCAA concentrations in L6 myotubes after 24h treatment with different leucine concentrations, followed by 1h insulin stimulation. There was a significant insulin x leucine interaction ($p<0.001$). The effect of insulin on intracellular BCAA concentrations was different between the leucine concentrations, with insulin increasing the concentration of BCAAs by 22% at 0.5x leucine but then decreasing by 28% at 1x leucine. In the absence of insulin, intracellular BCAA concentrations were reduced with 0.5x leucine compared to 0x (-18%) and 1x leucine (-28%).

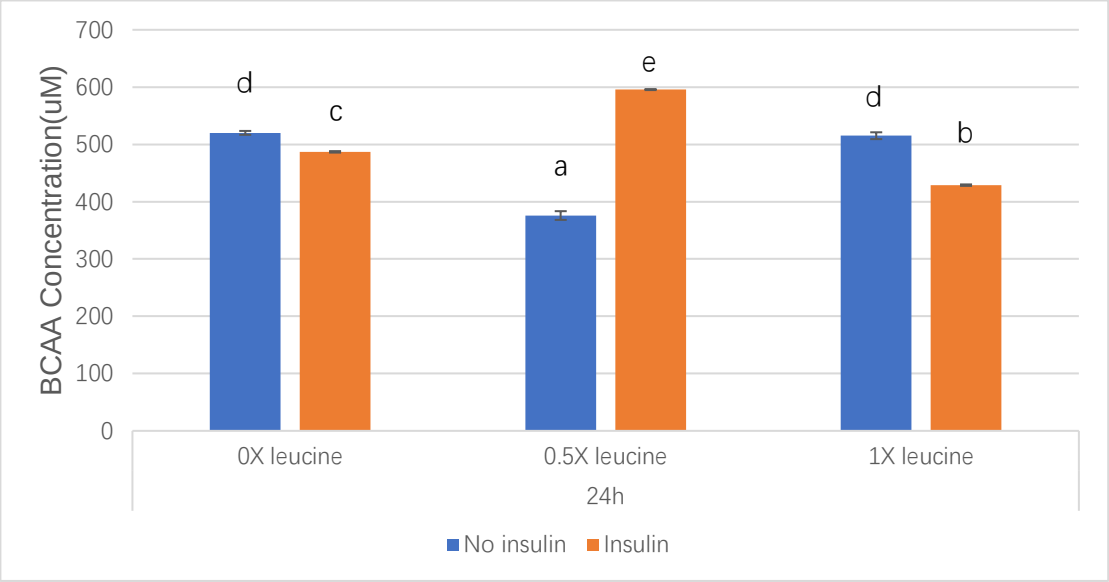


Figure 5. 13 Effects of 24 hours treatment with different concentrations of leucine +/- 1 hour insulin on intracellular BCAA concentrations in L6 myotubes

Differentiated L6 myotubes were pre-treated with or without different leucine concentrations (0x, 0.5x,1x) for 24h and then incubated with insulin as noted or equivalent volume of vehicle control for 1h before measurement of intracellular BCAA concentrations. Results are mean± SEM for n=3 wells for each treatment group. $p<0.001$ insulin x leucine. Means with the same letter are not different ($p>0.05$ for Bonferroni), whereas those with different letters are significantly different ($p<0.05$ for Bonferroni)

5.3.9. Effects of 48 hours treatment with different concentrations of leucine on intracellular BCAA concentrations in L6 myotubes

There was a significant insulin x leucine interaction effect on intracellular BCAA concentrations in 48h treated L6 myotubes ($p<0.001$, Figure 5.14). In the presence of insulin, intracellular BCAA concentrations were increased with 0.5x leucine but reduced with 1x leucine. Whereas, in the absence of insulin, intracellular BCAA concentrations increased by 24% at 0.5x leucine and 27% at 1x leucine compared to 0x leucine.

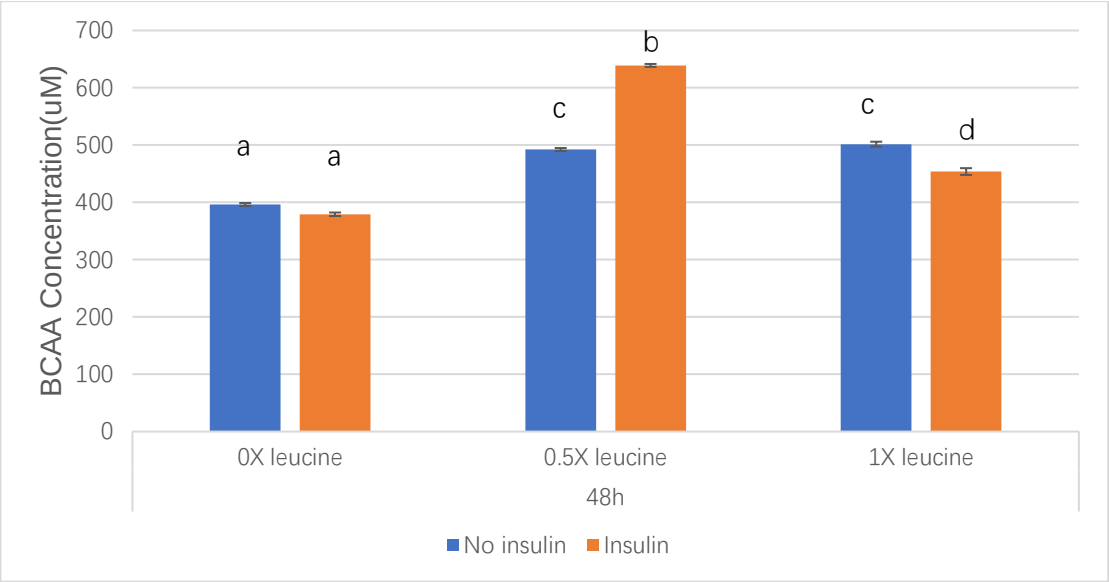


Figure 5. 14 Effects of 48 hours treatment with different concentrations of leucine +/- 1 hour insulin on intracellular BCAA concentrations in L6 myotubes

Differentiated L6 myotubes were pre-treated with or without different leucine concentrations (0x, 0.5x,1x) for 48h and then incubated with insulin as noted or equivalent volume of vehicle control for 1h before measurement of intracellular BCAA concentrations. Results are mean± SEM for n=3 wells for each treatment group. $p<0.001$ insulin x leucine. Means with the same letter are not different ($p>0.05$ for Bonferroni), whereas those with different letters are significantly different ($p<0.05$ for Bonferroni)

5.3.10. Effects of 24 hours treatment with different concentrations of leucine on glucose uptake in C2C12 myotubes

Previous experiments (chapter 3) showed that there was no difference in GLUT4 expression between L6 and C2C12 myotubes. But after insulin stimulation, glucose uptake of L6 myotubes was higher than C2C12 myotubes (Chapter 3). A possible explanation for this is that with insulin stimulation, GLUT4 would be translocated to the cell membrane in L6 myotubes but not in C2C12 myotubes. The influence of leucine on glucose uptake could also be due to its effect on GLUT4 translocation or on other glucose transporters in L6 myotubes. Therefore, the glucose uptake of C2C12 myotubes treated with different leucine concentrations for 24h and 48h was tested.

Figure 5.15 showed there was a significant two-way interaction between insulin and leucine on glucose uptake ($p<0.001$, insulin x leucine). In the absence of insulin, there was no difference between 0x and 1x of glucose uptake, but an increase at 0.5x treatment group. Unexpectedly, insulin appeared to decrease glucose uptake with 0.5x leucine treatment.

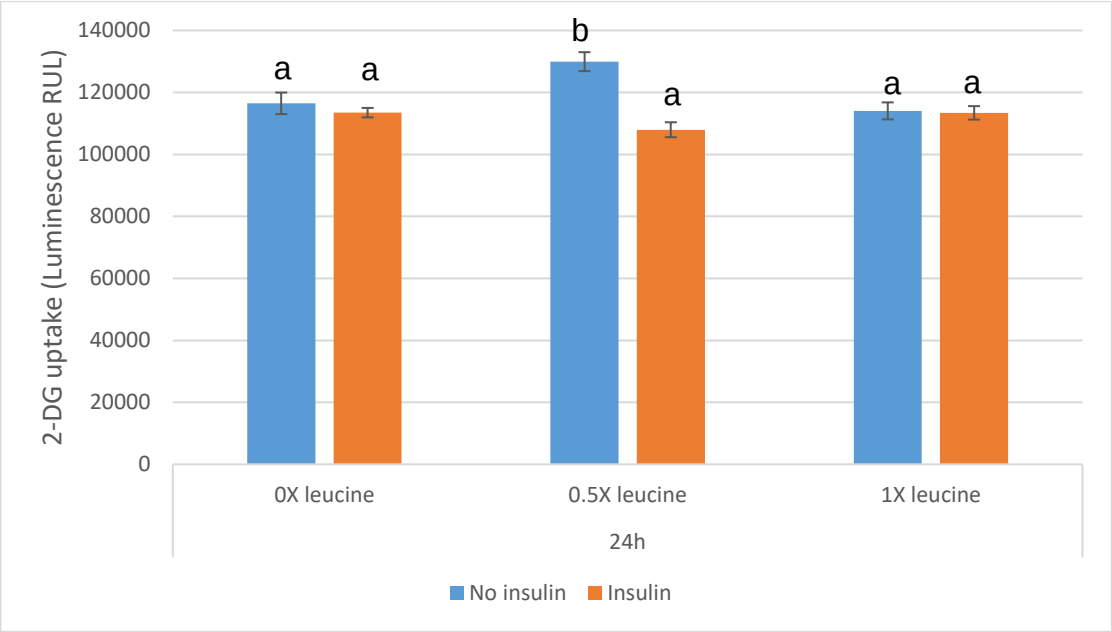


Figure 5. 15 Effects of 24 hours treatment with different concentrations of leucine +/- 1 hour insulin on glucose uptake in C2C12 myotubes

Differentiated C2C12 myotubes were pre-treated with or without different leucine concentrations (0x, 0.5x,1x) for 24h and then incubated with insulin as noted or equivalent volume of vehicle control for 1h before measurement of 2-DG uptake. Results are mean± SEM for n=6 wells for each treatment group. $p<0.001$ insulin x leucine. Means with the same letter are not different ($p>0.05$ for Bonferroni), whereas those with different letters are significantly different ($p<0.05$ for Bonferroni)

5.3.11. Effects of 48 hours treatment with different concentrations of leucine on glucose uptake in C2C12 myotubes

There was an insulin x leucine interaction for glucose uptake after 48h treatment ($p<0.001$, Figure 5.16). It was more obvious at 48h that leucine increased glucose uptake without insulin. In the absence of insulin, 1x leucine increased glucose uptake by 37% compared to 0x and 0.5x leucine. In the presence of insulin, there was no difference between leucine treatment groups, but insulin reduced glucose uptake at 1x leucine (vs. non-insulin 1x leucine).

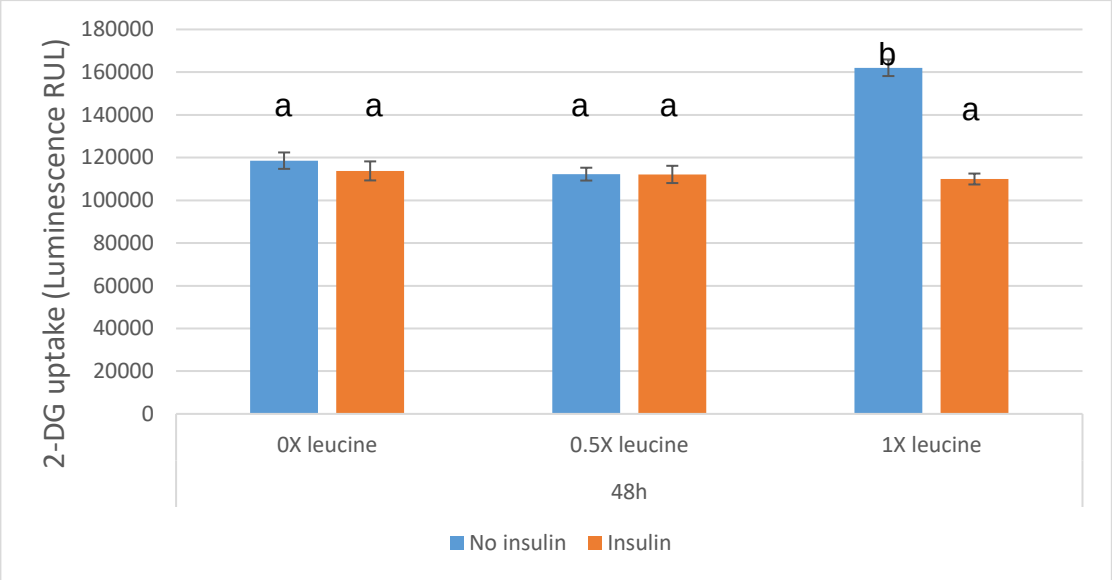


Figure 5. 16 Effects of 48 hours treatment with different concentrations of leucine +/- 1 hour insulin on glucose uptake in C2C12 myotubes

Differentiated C2C12 myotubes were pre-treated with or without different leucine concentrations (0x, 0.5x, 1x) for 48hand then incubated with insulin as noted or equivalent volume of vehicle control for 1h before measurement of 2-DG uptake. Results are mean± SEM for n=6 wells for each treatment group. $p<0.001$ insulin x leucine. Means with the same letter are not different ($p>0.05$ for Bonferroni), whereas those with different letters are significantly different ($p<0.05$ for Bonferroni)

5.4. Discussion and Conclusion

This is the first study to demonstrate that increased leucine concentrations result in increases in glucose uptake in both L6 and C2C12 myotubes after treatment for 24h and 48h. However, it was not a dose-dependent increase in glucose uptake (increased at 0.5x leucine vs 0x and 1x leucine) in C2C12 myotubes treated for 24h. Furthermore, as before, insulin increased glucose uptake in L6 myotubes, but not C2C12 myotubes after both 24h and 48h of leucine treatment, which was consistent with the results in chapter 3. Leucine did not alter insulin-induced glucose uptake in either C2C12 myotubes (24h and 48h) or L6 myotubes (48h). This effect appeared to be independent of phosphorylation of mTOR and Akt.

Leucine, which is the most studied BCAA, has been shown to promote insulin stimulated anabolic processes, such as protein synthesis in skeletal muscle (Yoshizawa 2012). Furthermore, it also can facilitate glucose metabolism that is mediated by insulin, such as glucose uptake in skeletal muscle (Kleinert *et al.* 2011). In the current study, increased leucine concentrations resulted in increases in glucose uptake in both L6 and C2C12 myotubes after treatment for 24h and 48h. Whereas, leucine only increased insulin-induced glucose uptake in L6 myotubes after treatment for 24h. Previous results (chapter 3) displayed that unlike L6 muscle cells, the glucose uptake of C2C12 myotubes did not respond to insulin stimulation, but there was no difference between L6 and C2C12 cells on GLUT4 mRNA expression. Therefore, we thought that in L6

myotubes, GLUT4 response to insulin is via translocation to the cell membrane to allow glucose into cells, but this was not observed in C2C12 myotubes. If leucine increases glucose uptake in C2C12 myotubes, the reasons could be leucine increases GLUT4 translocation and/or increases expression of other glucose transporters. In the current studies, in the absence of insulin, either 0.5x and/or 1x leucine increased glucose uptake in comparison to 0x leucine in C2C12 myotubes. This result suggested that leucine increased glucose uptake might be because leucine increased GLUT4 translocation or expression of other glucose transporters. This conclusion still needs further work by testing GLUT4 translocation. Nishitani *et al.* (2005) showed that leucine promoted GLUT4 translocation without activation of phosphorylation of Akt in isolated soleus muscle from CCI_4 rats, a model of CCl_4-induced cirrhosis.

These glucose uptake results agree with previous studies (Doi *et al.,* 2003, Nishitani *et al.,* 2005). For example, 2-DG uptake by C2C12 myotubes was significantly increased upon exposure (preincubation for 3 hours without insulin) to 5-10mM leucine (Doi *et al*., 2003) and 2mM leucine (without insulin) stimulated glucose uptake in isolated soleus muscle from CCI_4 rats (Nishitani *et al.,* 2005). In contrast, 2mM leucine did not alter glucose uptake (without insulin) in primary rat skeletal muscle cells (Liu *et al.*, 2014), and Renguet *et al.,* (2017) showed that 20h preincubation with 10nM leucine significantly reduced glucose uptake in primary cultured cardiomyocytes.

In the current studies, there was a consistent insulin-stimulated increase in

glucose uptake in L6 myotubes, but no effect in C2C12 myotubes. This response to insulin in L6 myotubes was further increased by 0.5x and 1.0x leucine after 24h treatment, but not after 48h treatment. The 48h leucine seemingly less potent with respect to stimulating glucose uptake, while this may be due to the half-life of leucine which has been shown to be between 24h and 48h. However, I haven't found any research to support this conclusion, so it's just the speculation. Previous studies showed leucine increased or decreased insulin-induced glucose uptake in different cell types. Liu *et al.*, (2014) showed leucine increased insulin-stimulated glucose uptake and reached a peak at 2mM in primary rat skeletal muscle cells. Another study (Tremblay and Marette, 2001) showed that 1h preincubation with 0.8mM leucine significantly reduced insulin-stimulated (100nM) glucose uptake in L6 mytoubes. Similarly, preincubation for 20h with 10nM leucine significantly reduced insulin-stimulated (3nM) glucose uptake in primary cultured cardiomyocytes (Renguet *et al.,* 2017).

The possible reasons for the different results between these experiments could be a combination of the cell or tissue used, the actual leucine concentration or the time of exposure. In the current studies, insulin-stimulated (1mM) glucose uptake reached a peak at 0.5x leucine (0.4mM) concentrations after 24h of treatment and did not increase further at 1x leucine (0.8mM) concentration. In contrast, insulin-stimulated (1mM) glucose uptake was unaffected by leucine after 48h treatment. Most of the published studies used higher concentrations of leucine (e.g. 2mM), but lower concentrations of insulin. Secondly, all three BCAAs could influence glucose uptake, but only leucine concentration was

manipulated in current study. Rawat *et al.,* (2014) and Doi *et al.*, (2003) displayed that isoleucine increased glucose uptake in L6 and C2C12 myotubes respectively, whereas Nishitani *et al.,* (2005) showed that valine had no effect on glucose uptake in isolated soleus muscle from the CCl4 rats. Therefore, isoleucine (and valine) could also affect glucose uptake in L6 and C2C12 myotubes. Nishitani *et al.,* (2002) showed that 2mM leucine initially (0-15mins) increased glucose uptake in the soleus muscle, then maintained the glucose uptake rate from 15-45mins, but then reduced it after 60mins. The treatment times for my studies were 24h or 48h, much longer than 1h. Therefore, differences between short and long-time treatments could be a reason.

The main function of leucine, which also applies to insulin, is to promote protein synthesis through activation of mTOR/p70S6k signalling pathway in muscle. In this study, there was no difference on phosphorylation of mTOR and downstream target proteins in L6 myotubes treated with different concentrations of leucine (0x, 0.5x, 1x) for 24h. These findings are in agreement with the work of Kleinert *et al.*, (2011) and Jeganathan *et al.*, (2014), who were also unable to detect any leucine induced phosphorylation of mTOR and p70S6K. Kleinert *et al.,* (2011) showed that 1h amino acid mixture (2 mM isoleucine, 0.0016 mM valine, and 0.014 mM leucine) did not affect phosphorylation of mTOR on Ser2448 in isolated rat epitrochlearis muscle. Similarly, in L6 myotubes, leucine-enriched α-MEM (final concentration of leucine was 0.8mM) did not affect phosphorylation of p70S6K in short-time (up to 2hours) (Jeganathan *et al.*,

2014),

However, there are some conflicting studies (Liu *et al.*, 2014; Atherton *et al.,* 2010). Leucine (2mM for 30 minutes) significantly increased phosphorylation of mTOR (Ser2448), 4EBP1 (Thr37/46) and p70S6K (Thr389) in C2C12 myotubes after 4h serum free and 1h amino acid starvation (Atherton *et al.,* 2010). Similarly, Liu *et al.,* (2014) confirmed that 2mM leucine (45mins) caused a small but significant increase in phosphorylation of mTOR Ser2448, using primary rat skeletal muscle cells. In these two experiments, the leucine treatment time was much shorter (30 mins and 45mins) than in the current studies (24h and 48h), so time could be a reason for this difference. Indeed, short-time (1h) 10mM leucine significantly increased phosphorylation of p70S6K in rat cardiomyocytes (Renguet *et al.*, 2017), but this effect tended to disappear after 20h incubation. In the current studies, 24h leucine treatment did not increase the phosphorylation of mTOR, p70S6K or 4E-BP1e, while 48h leucine treatment only increased phosphorylation of mTOR, and not downstream target proteins. These results seem to support the idea that long-time leucine treatment does not affect the mTOR/p70S6K signalling pathway. Since only leucine concentration was manipulated in the current studies, the other BCAAs might be more effective than leucine. However, Atherton *et al.,* (2010) indicated that only leucine had an effect on phosphorylation of mTOR/p70S6K, with other EAAs (valine, isoleucine, lysine, methionine, phenylalanine, tryptophan, and threonine) having no effect. In the current studies, the concentration of valine (0.094g/L=0.8mM) plus isoleucine (0.105g/L=0.8mM) was higher than that of

leucine (0.105g/L=0.8mM for 1x), so could be responsible for some of the results described.

As expected, insulin stimulated phosphorylation of mTOR and downstream target proteins in L6 myotubes in both 24h and 48h experiments. Leucine had no effect on insulin-induced phosphorylation of mTOR and downstream target proteins, except 48h treatment where 1x leucine increased insulin-stimulated phosphorylation of p70S6K. These results are consistent with those from Peyrollier *et al.*, (2000), who showed that leucine had no effect on insulin-stimulation of p70S6K activity (vs. insulin alone) in L6 myotubes, but insulin alone increased p70S6K activity. Furthermore, Jeganathan *et al.,* (2014) showed that 100nM insulin stimulated phosphorylation of p70S6K (between 5mins and 2h) in L6 myotubes and Liu *et al.*, (2014) also showed that insulin (100nM) stimulated phosphorylation of mTOR (45mins) in primary rat skeletal muscle cells. However, incubation with AA plus insulin increased p70S6K abundance at the 1h time point (Jeganathan *et al.,* 2014) and insulin increased phosphorylation of mTOR was enhanced by addition of 2mM leucine treatment (45mins) (Liu *et al.*, 2014). These results indicate that leucine does promote insulin-stimulated phosphorylation of mTOR/p70S6K signalling pathway. The differences may be due to the time again, since 1h leucine increased insulin-induced phosphorylation of p70S6K, whereas 20h leucine decreased it (Renguet *et al.,* 2017). Furthermore, insulin concentrations may also influence the results. The submaximal insulin (sINS, 75μU/ml) treatment of isolated rat

epitrochlearis muscle failed to increase phosphorylation of mTOR Ser2448 compared with control (Kleinert *et al.,* 2011), but maximal insulin concentrations (mINS, 2mU/ml) significantly increased phosphorylation of mTOR Ser2448 (vs submaximal and basal). In addition, AA mixture had no effect on basal or sINS-stimulated phosphorylation of mTOR Ser2448, but significantly increased mINS-induced phosphorylation of mTOR Ser2448 (Kleinert *et al.,* 2011).

Since the leucine-induced increase in glucose uptake was not associated with increased phosphorylation of mTOR and downstream target proteins, it may be because leucine affects phosphorylation of Akt Ser473. However, without insulin, phosphorylation of Akt was not detectable in any leucine concentration after both 24h and 48h treatments. Only insulin increased phosphorylation of Akt. All other studies showed that insulin significantly increased phosphorylation of Akt (Renguet *et al.,* 2017; Tremblay and Marette, 2001; Liu *et al.*, 2014; Peyrollier *et al.*, 2000). When leucine was added, there were some conflicting results. Tremblay and Marette (2001) showed that insulin-stimulated phosphorylation of Akt Ser473 in L6 myotubes was unaffected by 2xAA (leucine concentration: 0.8mM), the same as the current study. Liu *et al.*, (2014) showed that leucine increased insulin-stimulated phosphorylation of Akt, but Renguet *et al.,* (2017) showed that leucine reduced insulin-stimulated phosphorylation of Akt after treatment for both 1h and 20h. The differences between experiments are unclear, but it should be noted that the concentrations of leucine used in the current studies and Tremblay and Marette (2001) were 0.8mM, whereas Liu *et al.*, (2014) used 2mM leucine and Renguet *et al.,* (2017) used 10mM.

In summary, Table 5.1 shows the differences between the current and other studies. All the other studies showed a shorter treatment time compared with the current study, which means that time could be the first factor to influence the results. Secondly, most of the other studies used 2mM leucine, which may be more effective than the 0.8mM leucine used here. Finally, insulin concentration in the current study exceeded the physiological concentration (10nM), and most other studies showed that 100nM insulin is enough. However, the choice of 1mM insulin was required for the glucose uptake Assay Kit. Nishitani *et al.,* (2002) showed that with 2mM leucine, 2-DG uptake was increased by insulin at physiological concentrations (1-10nM) and reached a peak at 100nM insulin. Therefore, use of different concentrations of insulin might have been judicious.

Table 5. 1 Summary of effect of leucine on glucose uptake, mTOR/P70S6K and Akt signalling pathways

Experiment model	Treatment	Findings	Reference
L6 myotubes	0x, 0.5x(0.4mM), 1x (0.8mM) leucine for 24/48 hours; 1mM insulin for 1hour	↑ Glucose uptake (- insulin+ leucine) ↔ mTOR, 4E-BP1, p70S6K, Akt (-insulin+ leucine)	This thesis
L6 myotubes	2mM leucine up to 10min;100nM insulin up to 10min	↔ Akt activity (-insulin+ leucine)	Peyrollier *et al.*, (2000)
Primary rat skeletal muscle cells	2mM leucine, 45 min 100nM insulin, 45 min	↑ Glucose uptake (+insulin+ leucine), mTOR, Akt (+insulin+ leucine)	Liu *et al.*, (2014)
L6 myotubes	2x Mix AA (leucine 0.8mM) 1 hour 100nM insulin 45 min	↓ Glucose uptake (+insulin, +leucine) ↔ p-Akt and Akt activity (+insulin+ leucine)	Tremblay and Marette (2001)
Soleus muscles isolated from normal rats	Leucine 0-4mM; 2mM 0-60 min; 2mM leucine+ insulin (0-100nM)	↑ Glucose uptake (15-45min, -insulin+ leucine) or (0-100nM insulin+ leucine) ↓ Glucose uptake (45-60min, -insulin+ leucine)	Nishitani *et al.*, (2002)
Primary cultured cardiomyocytes	10mM leucine for 1 or 20 hours 3nM insulin	↓ glucose uptake (20h +/-insulin + leucine); Akt (1/20h, +insulin), p70S6K (20h; +/-insulin+ leucine); ↑ p70S6K (1 hour; +/- insulin+ leucine)	Renguet *et al.,* (2017)

The effects of manipulating leucine concentrations in the media on the intracellular BCAA concentrations were highly variable. Pre-incubation for 48h with increasing leucine concentrations only increased intracellular BCAA concentrations in the absence of insulin. However, this trend was not observed after 24h. The effect of insulin on intracellular BCAA concentrations was highly variable and dependent upon both the leucine concentration and pre-incubation time, with insulin having either no effect, increasing or decreasing BCAA concentrations. In the absence of insulin, increasing leucine concentrations would be expected to increase intracellular BCAA concentrations, unless there was an increase in protein synthesis, which would then reduce intracellular BCAA concentrations. Insulin would be expected to stimulate uptake of BCAAs by cells, but also promote protein synthesis and inhibit protein degradation. Hence, the variability in the intracellular BCAA concentrations is likely to be dependent upon the balance between BCAA uptake and rates of protein synthesis vs. degradation. Since only leucine concentration in the media was manipulated, but BCAA concentrations include leucine, valine and isoleucine together, then the other two BCAAs (isoleucine and valine) may also influence the results.

In conclusion, increased leucine concentrations were associated with increased glucose uptake by L6 myotubes after long-time treatment, but there was little (24h) or no effect (48h) on insulin-induced glucose uptake. This appeared to be independent of phosphorylation of mTOR, downstream target proteins and Akt, and it is unclear whether this relates to increased GLUT4 translocation or expression of other glucose transporters (Figure 5.17, below).

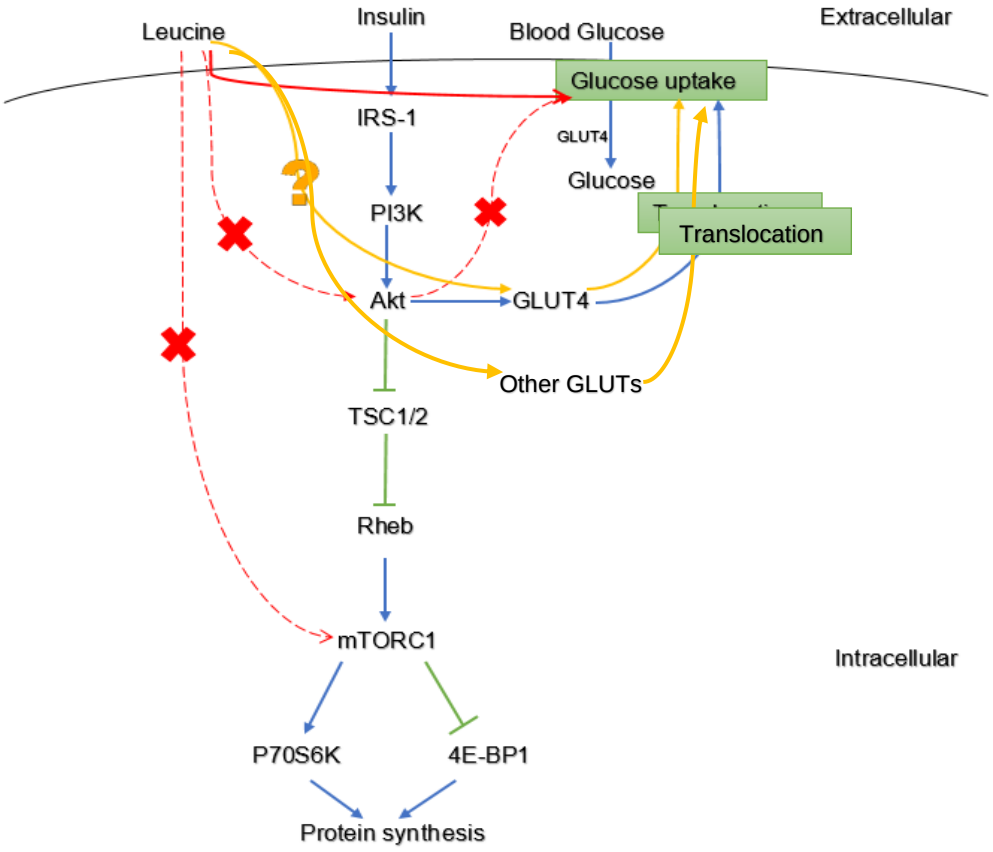


Figure 5. 17 Schematic of the relationship between mTORC1, leucine and glucose uptake in L6 myotubes

Insulin through PI3K/Akt/TSC1-2 signalling pathway stimulate mTORC1 promote protein synthesis. By stimulating with insulin and PI3K, Akt recruits GLUT4 to the cells membrane (translocation), which allow glucose into cells. This process is called glucose uptake. Leucine increase glucose uptake, but this process is independent with mTOR, downstream target proteins and Akt. It is possibly because leucine influence GLUT4 translocation or other GLUTs expression. **Red full line:** the mechanisms that was tested in the current study and found a relationship. **Red dashed line:** the mechanisms that was tested in the current study and no relationship can be found. **Blue and green full line:** the mechanisms has been proved by others. **Yellow full line:** possible mechanism. **LAT1:** large neutral amino acid transporter, **IRS-1**: Insulin receptor substrate 1, **PI3K:** Phosphoinositide 3-kinases, **Akt/PKB:** Protein kinase B, **TSC1/2:** Tuberous sclerosis 1/2, **mTOR:** mammalian target of rapamycin, **P70S6K:** Ribosomal protein S6 kinase beta-1, **4E-BP1:** Eukaryotic translation initiation factor 4E-binding protein 1, **GLUT4:** Glucose transporter type 4

CHAPTER 6: EVALUATION OF SESTRIN 2 OVEREXPRESSION AS A STRATEGY TO INHIBIT mTOR FUNCTION AND ASCERTAIN ITS IMPACT ON GLUCOSE UPTAKE

6.1. Introduction

Sestrins are encoded by an evolutionarily conserved, stress-inducible gene family that can protect cells from various stressful conditions such as oxidative or genotoxic stress (Lee, Budanov, and Karin, 2013; Johnson *et al.,* 2015; Hu *et al.,* 2015). There are three members of the Sestrin family expressed in mammals—Sestrin 1, Sestrin 2, and Sestrin 3. Sestrin 1 and Sestrin 2 regulate cell growth and viability under different cellular stressors (Budanov *et al*., 2012). Under normal conditions, the expression of the Sestrins is very low. In contrast, during cellular stress, such as seen following DNA damage, low oxygen, endoplasmic reticulum stress, energy deprivation or amino acid starvation, the expression of Sestrins are increased through activation of the tumor suppressor p53, FOXO (the forkhead transcription factor) and CCAAT-enhancer-binding proteins (or C/EBPs) (Nogueira *et al*., 2008; Budanov *et al*., 2012; Lee, Budanov, and Karin, 2013). Specifically, Sestrin 1 and 2 are target genes of p53 and the FOXO family of transcription factors stimulate Sestrin 3 expression.

As mentioned in the introduction chapter, AMPK and mTOR are two important proteins in regulating energy balance. Braunstein *et al.,* (2009) indicated that in breast epithelial MCF10A cells, Sestrin 1 and 2, through activation of AMPK, inhibit mTOR function and blunt protein synthesis in response to ionizing radiation. Furthermore, Budanov, and Karin, (2008) showed that Sestrin 2 activated AMPK and inhibited mTOR in breast carcinoma MCF7 cells. All of these results suggest that Sestrin 2 plays an important role in regulating the activity of the AMPK/mTOR signaling pathway and may represent a useful target for investigating the role of mTOR in the control of cellular glucose uptake.

There are two enzymes, Rag A/B and Rheb, required for mTORC1 activation. Sestrin 2 increases AMPK phosphorylation at Thr172, which in turn activates AMPK and promotes TSC2 activation. TSC1/2 converts the GTP form of Rheb (Rheb-GTP) to the GDP form (Rheb-GDP), thereby negatively regulating the mTORC1 signaling pathway (Figure 6.1) (Budanov, and Karin, 2008). In parallel, AMPK can directly phosphorylate Raptor, an important subunit of mTORC1, thereby inhibiting the activity of mTORC1 in the case of low energy status (Inoki, Kim and Guan, 2012).

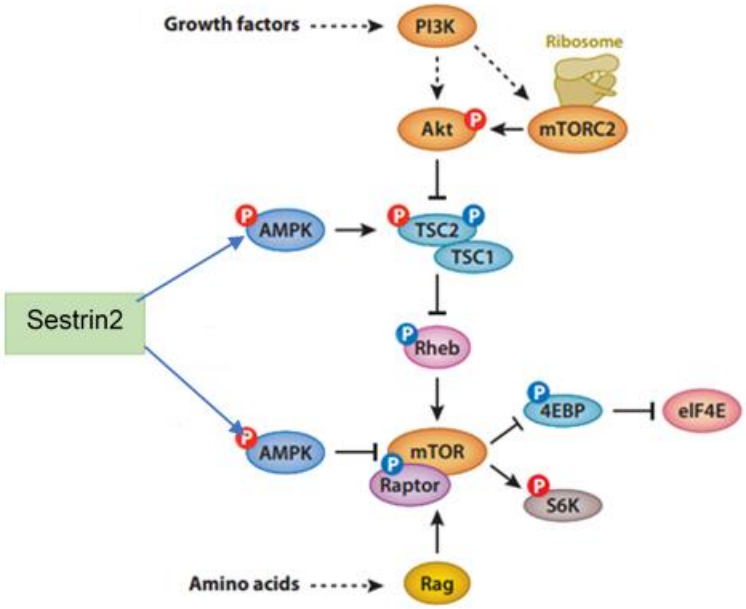


Figure 6. 1 The diagram of how Sestrin 2 regulate AMPK/mTORC1 signalling pathway. Reproduced from Inoki, Kim and Guan, 2012**.**

Under energetic stress conditions, Sestrin activate AMPK, which in turn phosphorylates TSC2 and Raptor to inhibit the mTORC1 pathway. **AMPK:** 5' AMP-activated protein kinase, **PI3K**: Phosphoinositide 3-kinases, **Akt/PKB**: Protein kinase B, **TSC1/2:** Tuberous sclerosis 1/2, **Rheb:** Ras homolog enriched in brain, **mTOR:** mammalian target of rapamycin, **P70S6K (S6K):** Ribosomal protein S6 kinase beta-1, **4E-BP1:** Eukaryotic translation initiation factor 4E-binding protein 1, **eIF4E:** Eukaryotic translation initiation factor 4E

Sestrin 2 has also been shown to inhibit mTORC1 by reducing Rag. The mammalian Rag subfamily consists of four members—Rag A, Rag B, Rag C, and Rag D (Sekiguchi *et al*., 2001). In the Rag complex, Rag A/B form a stable dimer with Rag C/D. Under normal conditions, Rag A/B and Rag C/D are bound with GTP and GDP respectively, resulting in an active Rag dimer state. The Rag A/B-GTP and Rag C/D- GDP initiation complex interacts with Raptor of the

mTORC1 complex to produce a docking site allowing mTORC1 to become located on the lysosomal membrane, an essential step for mTORC1 activation. Sestrin 2 can be considered as a GDP dissociation inhibitor (GDI), inhibiting mTORC1 function by reducing the GTP activity form of Rag A/B (Peng, Yin, and Li, 2014). Alternatively, Sestrin 2 can also impact the GATOR complex, which consists of 2 sub complexes—GATOR 1 and GATOR 2. GATOR 2 (Rag A/B-regulating hetero-pentameric protein complex 2) can bind and inhibit GATOR1 in the presence of amino acids, therefore, GATOR2 is a negative regulator of GATOR1 and subsequent mTORC1 inactivator (Bar-Peled *et al*., 2013). Under stress conditions (e.g. AA starvation), Sestrin 2 expression (mRNA) increases and combine with GATOR2, thereby releasing GATOR1 from the GATOR complex. Free GATOR1 inhibits the activity of Rag A/B, thereby further inhibiting the membrane localization function of the Rag A/B-GTP and Rag C/D-GDP initiation complex for mTORC1 (Parmigiani *et al*., 2014; Kim *et al*., 2015; Chantranupong *et al*., 2014). As a consequence, mTORC1 is released to the cytoplasm, rendering mTORC1 inactive.

Furthermore, Sestrin 2 is a leucine sensor for mTORC1 pathway. Wolfson *et al.,* (2016) showed that for leucine to activate mTORC1, it requires leucine to bind to Sestrin 2, and the mTORC1 pathway is insensitive to the absence of leucine when there is a loss of Sestrin 2.

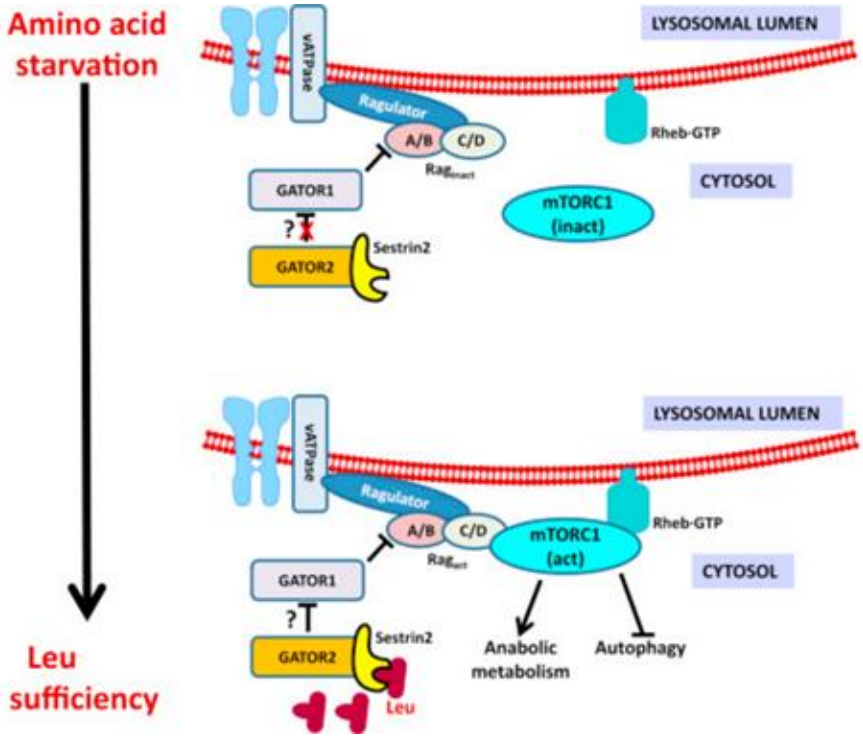


Figure 6. 2 Diagram of how Sestrin 2 regulate mTORC1 via the GATOR complex. Reproduced from Abraham, 2016.

Under AA starvation, Sestrin 2 binds to and inhibits GATOR2, thereby releasing GATOR1 to inhibit the activity of Rag A/B. This prevents the localization of mTORC1 to the lysosome and the interaction of mTORC1 with activated Rheb (Rheb-GTP). In AA sufficiency conditions, Sestrin 2 binds to leucine, blocking Sestrin 2-GATOR2 interaction. This allows GATOR2 to overcome the GAP activity of GATOR1 and then helps to activate the RAG heterodimer (RAGact). The Rag A/B-GTP and Rag C/D- GDP initiation complex interacts with Raptor of the mTORC1 complex to produce a docking site allowing mTORC1 to become located on the lysosomal membrane. mTORC1 is recruited to the lysosomal membrane, together with Rheb·GTP, and becomes activated, driving its downstream cellular effects. **mTOR:** mammalian target of rapamycin.

To conclude, Sestrin 2 inhibits phosphorylation of mTOR and is also regulated by leucine. Therefore, the aim of this chapter is to overexpress AAV1-Sestrin 2 in L6 myotubes to investigate the effects on glucose uptake and phosphorylation of mTOR in L6 myotubes.

6.2 Methods

In order to overexpress Sestrin 2, an AAV1 overexpression vector was designed by Dr. David Brown along with a similar control vector overexpressing GFP. The control vector (pAAV-CMV>EmGFP:WPRE, called AAV1-GFP from now, see Figure 6.3A) has a CMV promoter driving the transcription of Emerald GFP (EmGFP). The Sestrin 2 vector (pAAV-CMV>mSesn2:T2A:EmGFP:WPRE, called AAV1-Sestrin 2 from now, see Figure 6.3B) has a CMV promoter driving transcription of both Sestrin 2 (Accession number NM_144907.1) and EmGFP, with the T2A linker ensuring co-translational cleavage of both proteins. Both vectors were synthesized and packaged into AAV1 by Cyagen Biosciences (USA).

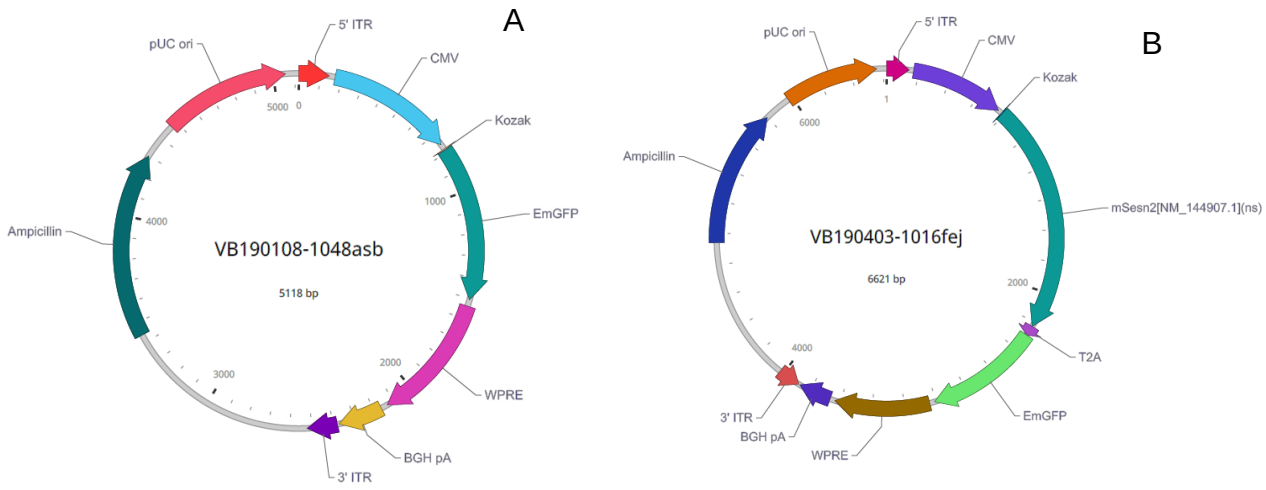


Figure 6. 3 GFP and Sestrin 2 vector map

6.2.1 Cell culture and infections

L6 cells were seeded at a density of $1x10^4$ cells per well in 24-well plates and allowed to adhere overnight (see section 2.2.2). The following day, with L6 cells ~ 50-60% confluent, the cells were infected with either AAV1-GFP (control) or

AAV1-Sestrin 2 in DMEM media at a GC (genome copies/ml) of $1x10^8$ to $5x10^9$ as described previously in section 2.3.2 and 2.3.3. After 24 hours, the media of the L6 myoblasts was replaced with differentiation media (day 0) and refreshed every 48h, until L6 cells differentiated to myotubes. Cell images were taken at day 7 by fluorescence microscopy (LEICA DFC420) using the LEICA Application Suite, to determine transduction efficiency.

6.2.2 Real Time Quantitative PCR analysis

L6 cells were cultured in 24-well plates and infected with AAV1-GFP or AAV1-Sestrin 2 as described above (section 6.2.1). At day 7, infected L6 myotubes were treated with insulin for 1 hour or equivalent volume of vehicle control before harvesting into ice cold RNase-free PBS for RTqPCR analysis (section 2.7.1). Cells from three wells were pooled (45 µl RNase-free PBS added to the first well and transferred along with the cells to next well and repeated), allowing sufficient volume for RNA analysis. Sestrin2 mRNA expression was determined by Dr. Zoe Daniel (sections 2.7.2-2.7.5).

6.3 Results

6.3.1 Fluorescence images at 7 days following AAV1-GFP infection in L6 cells.

An approximate efficiency of infection was estimated by monitoring the level of GFP fluorescence. There were no previous reports describing the expected efficiency seen with AAV1-GFP infection in L6 myotubes, therefore, five different GC levels of AAV1-GFP were used. On investigation, the infection efficiency was greatest when $1x10^9$ GC or $2x10^9$GC were used (Figure. 6.4). In subsequent experiments investigating Sestrin 2 infection, these two GC were used.

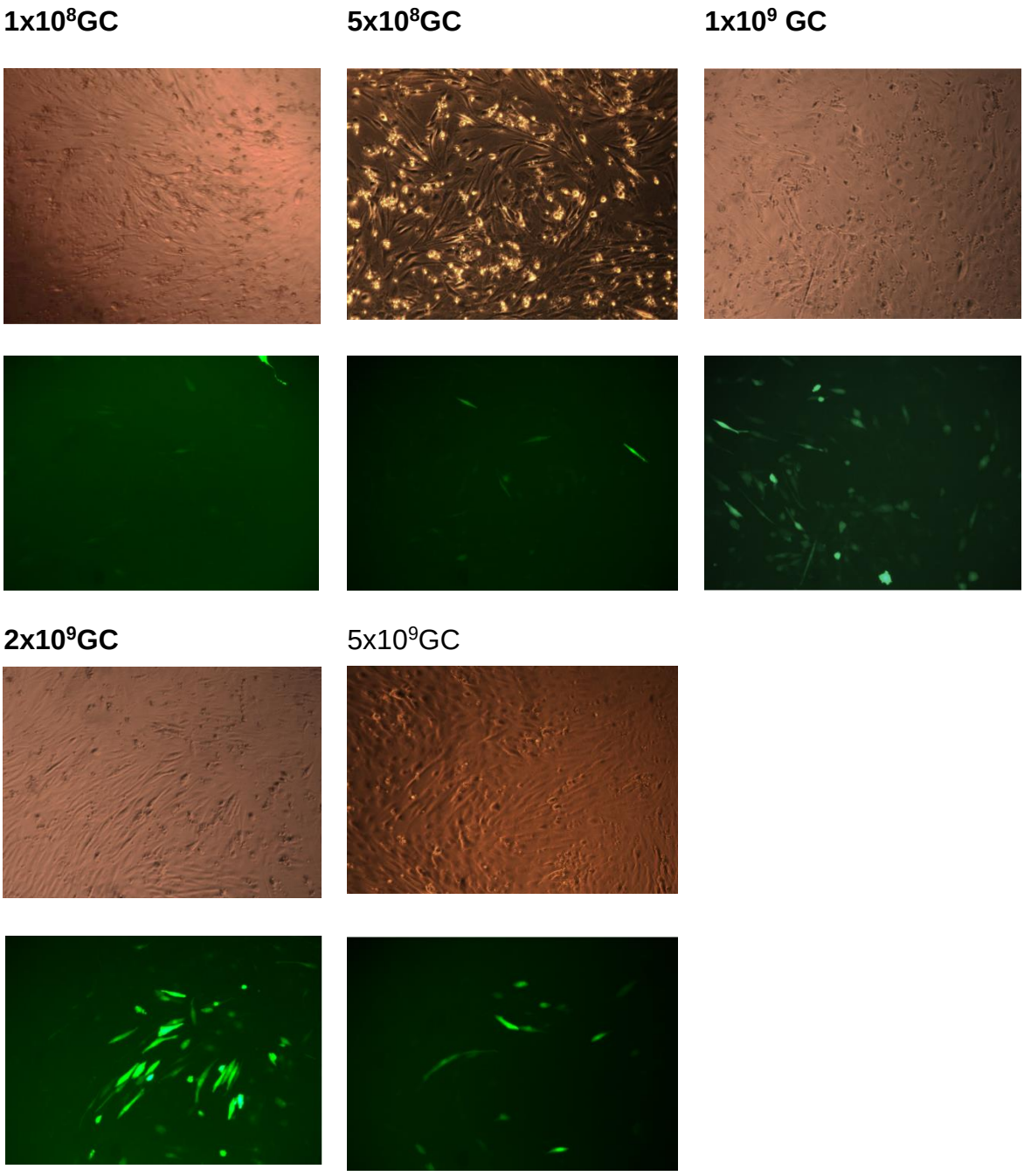


Figure 6. 4 Bright-field and fluorescence photographs following 7 days infected with AAV1-GFP in L6 cells.

L6 cells were infected with AAV1-GFP at different GC and images captured at day 7. Images were captured at 5X/0.12 magnification for both bright-field and fluorescence.

6.3.2 Sestrin 2 mRNA level in L6 myotubes after infection with AAV1-mSESN2

In order to examine whether overexpression of Sestrin 2 was successful, L6 myoblasts were infected with AAV1-Sestrin 2 at day -1. At day 7, there was no fluorescence observed in L6 myotubes (Figures are not shown). This may indicate that the infection failed, but Sestrin 2 mRNA expression was still measured.

The level of Sestrin 2 mRNA in L6 cells was very low, therefore, a standard curve could not be generated and only mean Cp values are shown in Figure 6.5. As mentioned in Chapter 3, higher Cp values indicate lower mRNA expression, and 40 Cp was the highest reported value. There was no significant difference between the different GC ($p=0.175$, Figure 6.5), although there did appear to be some expression in the $2x10^9$ GC groups. In order to demonstrate that the high Cp values were due to infection failure, not because of inadequate cDNA, cyclophilin mRNA was determined in the same samples. As can be seen in figure 6.6, the mean Cp values for cyclophilin were less than 27, which meant there was enough cDNA in the samples.

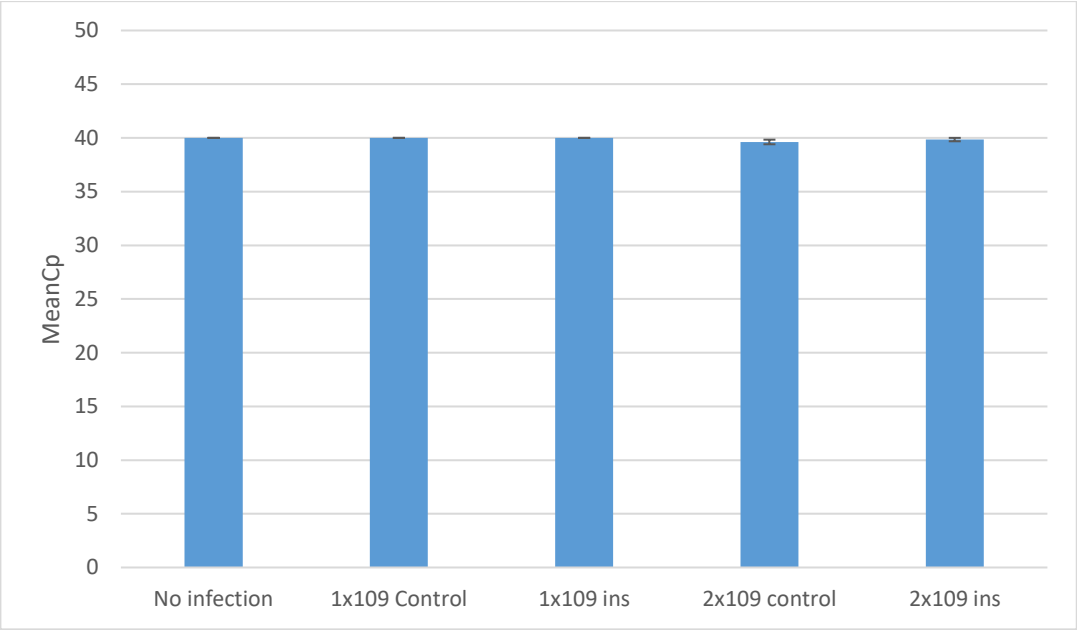


Figure 6. 5 Mean Cp values for Sestrin 2 mRNA in L6 myotubes.

L6 myoblasts were infected with $1x10^{9}$GC or $2x10^{9}$ GC AAV1-Sestrin 2, at day 7. Only the infection groups incubated with or without insulin as noted for 1h. Results are mean± SEM for n=3 wells for each treatment group. p=0.117.

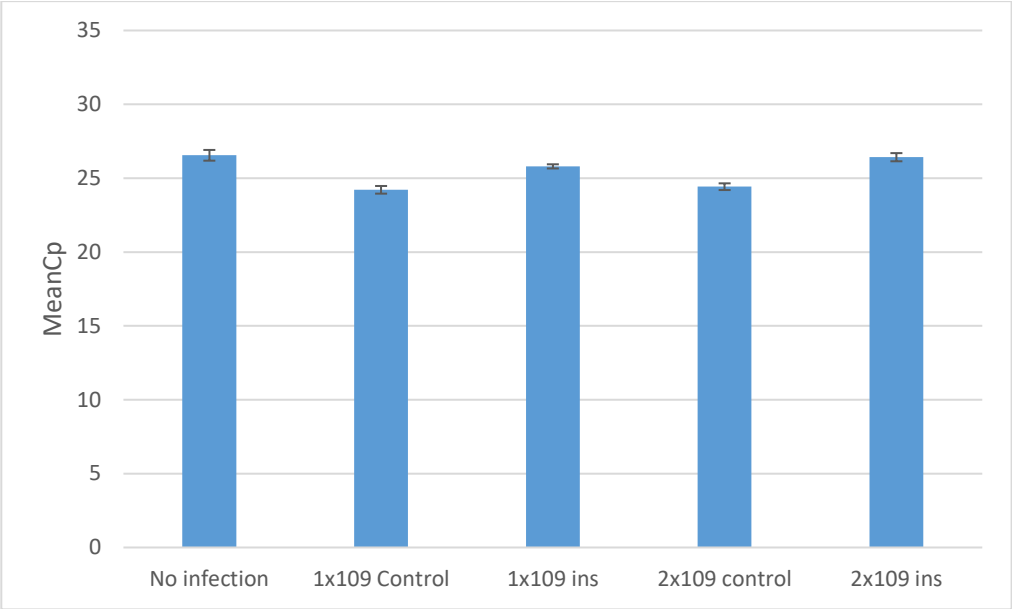


Figure 6. 6 Mean Cp values of cyclophilin mRNA in L6 myotubes.

L6 myoblasts were infected with $1x10^9$GC and $2x10^9$ AAV1-Sestrin 2, at the day 7. Only the infection groups incubated with or without insulin as noted for 1h. Results are mean± SEM for n=3 wells for each treatment group

6.4 Discussion and Conclusion

Due to time constraints, no further AAV1 infection experiments were possible. Therefore, the existing results and others results are only discussed very briefly

The data showed that AAV1-GFP successfully infected L6 muscle cells with fluorescence observed at day 7 of differentiation (8 days after infection). There are few studies showing that AAV1 can infect L6 muscle cells, but a number of studies indicate that AAV1 can infect both skeletal and cardiac muscles *in vivo*, in either localized or widespread manner (Lorain *et al*., 2008; Palomeque *et al*., 2007; Karakikes *et al*., 2012; Brantly, *et al*., 2009). All of these experiments used mice, rats, pigs or humans, but there appear to be no published *ex vitro* studies. After entering host cells, the rAAV genome mainly exists in the form of episomal, and episomal rAAV genome is connected with others to form a stable circular structure (Duan *et al*., 1998), which allow gene expressed for a long time in terminally differentiated tissues such as muscle (Wang *et al*., 2014). Ellis *et al*., (2013) designed an experiment to show the transduction efficiency of mammalian primary cells and cell lines with nine natural adeno-associated viruses (AAV1-9). They did not try L6 muscle cells, but they used C2C12 muscle cells. In C2C12 cells, AAV1 transduction efficiency was 60% and other serotypes were very low. Therefore, AAV1-Sestrin 2 should be able to infect L6 muscle cells, but more experiments are required to verify this.

Interestingly, endogenous Sestrin 2 expression was very low in non-infected L6 cells, whereas, endogenous expression of Sestrin 2 in pig muscles was much higher (the mean Cp value was 28-33) and was induced with beta-adrenergic agonist treatment (Brown *et al,* 2018). This may be because the L6 cells are

proliferating and differentiating rapidly and therefore require high rates of protein synthesis, whereas mature pig muscle is already differentiated and therefore requires lower rates of protein synthesis.

Although the Sestrin 2 infection of L6 muscle cells was not successful, this method could be an effective way to inhibit mTOR activity. Budanov, and Karin, (2008) illustrated that AMPK (activated by Sestrin 2) phosphorylated TSC2 and stimulated its GAP activity, thereby inhibiting mTOR in breast carcinoma MCF7 cells. When Sestrin 2 was knocked down (by shRNA) in H1299 cells, phosphorylation of both p70S6K and S6 were increased (Budanov, and Karin, 2008). Furthermore, Sanli *et al.,* (2012) also showed in MCF7 breast cancer cells, overexpression Sestrin 2 by using a Flag-tagged SESN2 expression vector or a stably-integrated tetracycline-inducible system increased phosphorylation of AMPKα1 and AMPKβ1 subunits and co-localized with phosphorylated AMPKα-Thr127 in the cytoplasm. The protein and mRNA levels of LKB1 and AMPKα1 β 1 were increased by overexpression of Sestrin 2.

The mechanism of Sestrin 2 inhibiting mTOR is through suppression of mTOR lysosomal localization by regulation of Rag and GATOR. This mechanism is potentially involved in mTORC1 regulation by amino acids. Indeed, leucine binds Sestrin 2 with a dissociation constant of 20 μM (this is the half-maximal concentration of leucine to activate mTOR) to break the interaction of Sestrin 2-GATOR2 in HEK-293T cells (Wolfson *et al*., 2016). Besides, leucine binding to Sestrin 2 is necessary for leucine to activate mTORC1. All these results indicate that Sestrin 2 is a leucine sensor for the mTORC1 pathway (Wolfson *et al*.,

2016).

Sestrin 2 not only influences mTOR, but also affects Akt, which is a critical protein in insulin-induced glucose uptake. In MCF7 cells, increased Sestrin 2 expression inhibited phosphorylation of Akt on both Ser473 and Thr308 residues, as well as phosphorylation of mTOR and its downstream protein p70S6K (Sanli *et al*., 2012). However, another experiment (Lee *et al*., 2012) showed that phosphorylation of Akt (Ser473 and Thr308) was significantly reduced in Sesn2−/− mice compared with control mice. Sestrin 2 induced Akt activation was dependent on AMPK, TSC2, and Rictor, suggesting that Sestrin 2 upregulated Akt signaling through AMPK and mTORC2 (Lee *et al*., 2012).

In conclusion, previous chapters showed a relationship between mTOR activity and glucose uptake, therefore overexpression of Sestrin 2 was hypothesized to reduce phosphorylation of Akt and mTOR and therefore reduce glucose uptake in L6 muscle cells. Since Sestrin 2 is a leucine sensor, therefore Sestrin 2 may connect leucine, mTOR and glucose uptake together. Further experiments should focus on overexpression of Sestrin 2 in L6 muscle cells and then test the effects on both glucose uptake and Akt/ mTOR signalling.

CHAPTER 7: GENERAL DISCUSSION AND CONCLUSIONS

7.1. General Discussion and Conclusions

Branched-chain amino acids (BCAAs), in particular the leucine, are widely known to improve protein synthesis within skeletal muscle that is a major site of glucose disposal in the body (Gannon, Schnuck and Vaughan, 2018). Recently, multiple human studies have reported that serum concentrations of BCAAs, (especially leucine) correlate closely with the degree of insulin resistance observed in pre-diabetic, diabetic and healthy individuals. (Newgard *et al.*, 2009, Tai *et al.,* 2010; Chen *et al.*, 2016; Huffman *et al.,*2009; Shaham *et al.,*2008; Floegel *et al.,* 2013; Würtz *et al.,* 2012). The mechanism could be due to negative feedback of mTOR/p70S6K and IRS-1. The increased circulating BCAA concentrations increased mTOR activity and phosphorylation of IRS-1, leading to an impairment in insulin signalling. Contrary to original hypothesis and also the studies conducting in human participants, my results suggested that there is a relationship between mTOR activity and glucose uptake in L6 myotubes, but this occurs independent of the phosphorylation of Akt. Furthermore, leucine promotes basal glucose uptake but there was little (24h) or no effect (48h) on insulin-induced glucose uptake. This appeared to be independent of phosphorylation of mTOR and Akt.

A potential explanation for the discord between findings to date, is the challenge associated with studying the impact of amino acids on tissue metabolism *in vivo*. As noted by others (White and Newgard 2019), supplementing with individual amino acids or manipulating systemic mTOR function also impacts metabolism in distal tissues, potentially underpinning the inconsistent observations seen between studies. Besides, our experiments as *in vitro* study focused on the

intracellular BCAA concentrations and *in vivo* studies tested the circulating BCAA concentrations. It's worth nothing that intracellular BCAA concentrations may not be equal to circulating BCAA concentrations. Indeed Bergström *et al.,* (1974) showed intracellular free amino acids concentrations are higher in human muscle tissue than the concentrations in plasma (overnight fasting samples). After the plasma EAAs uptake by muscle cells, most part of EAAs synthesize to proteins, small part of EAAs are oxidized in muscle and unavailable for protein synthesis (Wolfe, 2017). Comparing the difference between intracellular and extracellular concentrations was beyond the scope of this study. Tom and Nair (2006) showed that the function of BCAAs might be more determined by intracellular concentrations than by plasma concentrations, while Beugnet *et al.,* (2003) mentioned that the intracellular and not extracellular amino acid levels regulated mTOR signalling. Our study based on the cell culture, so we can only measure the intracellular BCAA concentrations, the extracellular (circulating) BCAA concentrations mean the BCAA concentrations in the medium. Thus, to circumvent these issues, the aim of the current study was to investigate whether increased intracellular BCAA concentrations (especially for leucine) will influence insulin-stimulated glucose uptake in muscle cells.

Some studies displayed that CHX increased in intracellular amino acid concentrations and activated mTORC1, due to its ability to inhibit protein synthesis in the face of persistent protein breakdown (Beugnet *et al.,* 2003; Watanabe-Asano, Kuma and Mizushima, 2014). Therefore, we tried to use CHX

to increase the intracellular amino acids concentration in C2C12 muscle cells. However, different concentrations of CHX (for 30 minutes) did not increase intracellular BCAA concentrations or phosphorylation of mTOR and downstream target proteins in C2C12 muscle cells. One thing to note is that CHX inhibits protein synthesis, and impaired protein synthesis is associated with decreased mTOR levels. You *et al.,* (2015) showed that blocking mTOR signalling by rapamycin inhibit the increase in eIF4F complex formation and reduced protein synthesis. Therefore, CHX did not increase phosphorylation of mTOR in C2C12 muscle cells possibly due to impaired protein synthesis.

In recent years, it has been suggested that mTOR is able to phosphorylate upstream targets of the insulin signalling pathway in muscle, leading to inhibition of the pathway, and in turn impaired translocation of the GLUT4 glucose transporter to the plasma membrane (Yoneyama *et al.,* 2018). mTOR has been considered as the central signalling molecule mediating the crosstalk between amino acids and insulin. Thus, it has been proposed that a potential mechanism by which obesity-induced increases in blood BCAA concentrations could lead to the development of insulin resistance is through the chronic activation of mTOR suppressing insulin signalling in skeletal muscle. Our results showed that both basal and insulin-stimulated glucose uptake was reduced by rapamycin and BCH in L6 myotubes. These reductions appear to relate with mTOR signalling status, but normally independent of phosphorylation of Akt, which is another protein related with insulin-induced glucose uptake. mTOR was not only proven to be related to protein synthesis (Laplante and Sabatini, 2012), but also was proven to be involved in glucose uptake in this experiment.

In the most human studies, they did not research the possible mechanisms, except the study of Newgard *et al.,* (2009) who explained how BCAA caused insulin resistance. His team showed that BCAA supplementation increased the activation of mTOR and coupled with IRS-1 phosphorylation in the skeletal muscle of rats. Our work did not test the IRS-1 activity, which is another important protein involving in insulin-stimulated glucose uptake (detail in 'future works'). While, our results still demonstrated that mTOR was involved in glucose uptake. Furthermore, our results failed to show that increase the activity of mTOR can improve the glucose uptake in muscle cells, as 3BDO was more like an inhibitor of mTOR than an activator.

mTOR is the sensor of nutrients and cellular energy, insulin signalling required the appropriate mTOR activity to activate, but too much activation of mTOR may cause insulin resistance (Liu *et al*., 2014). Therefore, the different outcomes of BCAA regulate mTOR may cause by many reasons, such as the concentration or composition of BCAA (Nishitani *et al.,* 2002; Kleinert *et al*., 2011; Atherton *et al.,* 2010, Doi *et al*., 2003), and the concentration of insulin (Kleinert *et al*., 2011).

A definitive role for obesity-induced hyperleucinaemia in the induction of type-2 diabetes has remained controversial, due in part to inconsistent reports on the impact of leucine on insulin-stimulated glucose uptake in skeletal muscle. To provide much needed clarity on the role of leucine in regulating glucose uptake in muscle cells, we have examined the impact of modifying leucine availability and mTOR function on insulin-stimulated glucose uptake in myotubes. Our results demonstrate that leucine increased the basal and insulin-induced

glucose uptake in 24h treatment group. Moreover, the leucine's ability to modulate glucose uptake is independent with Akt/mTOR and downstream signalling pathway. Numerous studies have demonstrated that leucine administration impairs the ability of insulin to stimulate glucose uptake and worsens glucose tolerance in animals (Balage *et al*. 2011; Moghei *et al*. 2016; Saha *et al*. 2010), this is far from universally observed. Rats administered a diet for 5 weeks containing 15% protein supplemented with 4.5% leucine, have been shown to experience a significant increase in insulin-stimulated glucose transport in epitrochlearis muscle when assessed ex vivo (Balage *et al*. 2011). Similarly, administration of high doses of leucine (5-10 mM) have been shown to result in significant increases in 2-deoxyglucose uptake in C2C12 myotubes, even in the absence of insulin (Doi *et al*. 2003). While our findings are unable to definitely address these contradictory reports, they provide further support for leucine playing an important role in glucose uptake in muscle cells, under both insulin and non-insulin stimulated conditions.

Previous results (chapter 3) displayed that unlike L6 muscle cells, the glucose uptake of C2C12 myotubes did not respond to insulin stimulation, but there was no difference between L6 and C2C12 cells in GLUT4 mRNA expression. The results from chapter 5 suggested that leucine increased basal glucose uptake may be because it increased the translocation of GLUT4 or expression of other glucose transporters. Furthermore, this improvement may be independent of insulin. C2C12 skeletal muscle cells treated for 24 hours with 2mM leucine exhibited increase total GLUT4 protein content (Schnuck *et al.,* 2016) and both GLUT4 and glucose uptake are increased in skeletal muscle of Sprague Dawley

rats with liver cirrhosis when treated with 180 min leucine oral gavage (Nishitani *et al.,* 2005). They confirmed that leucine promoted the translocation of GLUT4 and GLUT1 to the blood membrane in the absence of additional insulin release and without activation of Akt phosphorylation (Nishitani *et al.,* 2005). Taken together, my results suggested that leucine could be a useful method to improve insulin sensitivity in muscle cells by improvement the translocation of glucose transporters and without insulin stimulation.

In the current study, the inhibitory action of rapamycin on glucose uptake was consistently observed and occurred independent of insulin administration. Others displayed that the promotion of glucose uptake by leucine (2mM) did not inhibit by rapamycin (1μM) In isolated rodent muscle, suggesting that this stimulatory effect was independent of mTOR activity (Nishitani *et al.* 2002). However, they failed to demonstrate that mTOR was inhibited by rapamycin at the dose used, questioning the validity of their findings. In contrast, and in full agreement with the data we present, others have shown that rapamycin blocks the beneficial effect of leucine on insulin stimulated glucose uptake in rat primary skeletal muscle cells (Liu *et al*., 2014). Moreover, after they inhibited PI3K, a kinase upstream of mTOR in canonical pathways, insulin-stimulated glucose uptake in cultured muscle cells was impaired. This inhibitory effect was partially rescued by leucine administration, but blocked by rapamycin, demonstrating that insulin and leucine's beneficial impact on glucose uptake occur via different but overlapping mechanisms, with the latter likely involving the activation of mTOR in a PI3K/Akt independent manner. Our results also

support this view, Akt phosphorylation was significantly increased in response to insulin administration, and this was not blunted by declining leucine media concentrations or the administration of either rapamycin or BCH.

Insulin resistance is always companied with obesity and obesity caused a reduction of GLUT4 (Friedman *et al.,* 1992). In morbidly obese patients, GLUT4 protein reduced about 20% in rectus abdominis and vastus lateralis muscles (Dohm *et al.,* 1991). Besides, *King et al.,* (1992) showed that in obese Zucker rats, the levels of GLUT4 protein in muscle was normal, but they were not translocated after maximal insulin stimulation. Our research did not show if leucine can improve GLUT4 translocation or content in obese models. While, other study (Macotela *et al*., 2011) showed that GLUT4 expression increased to normal level (control) in HFD+ dietary leucine mice (vs. HFD). Besides GLUT4, obesity also cause dysregulation of mTOR/S6K1. Overactivation of this pathway could led to the increase of serine phosphorylation of IRS-1 and then caused insulin resistance (Khamzina *et al.,* 2005). Interestingly, Macotela *et al*., (2011) showed that despite compare to HFD group, the activation of p70S6K in HFD+leucine group increased, increased serine phosphorylation of IRS-1 is associated with improved insulin signalling. This result also supports our result from the side that leucine can improve insulin resistance. Furthermore, in obesity, there is a chronic and low-grade inflammation that is involved in the pathogenesis of insulin resistance (Ye, 2013). TNF-α is a pro-inflammatory cytokine, after adding leucine to HF diet, the levels of TNF-α reduced 40% in perigonadal adipose tissues (Macotela *et al*., 2011). Leucine supplementation prevent the HFD induced insulin resistance through increased glucose

transporter and reduced inflammation in adipose tissue. These conclusions still need further experiments to prove as we did not test yet.

In summary, results from this study demonstrate that there is a relationship between mTOR activity and glucose uptake in L6 myotubes, but this occurs independent of the phosphorylation of Akt. Furthermore, leucine promotes basal glucose uptake but there was little (24h) or no effect (48h) on insulin-induced glucose uptake. This appeared to be independent of phosphorylation of mTOR and Akt. For the diabetics, after meals, the insulin in their body cannot be fully used by muscle or other insulin sensitive organs, so the blood glucose will increase and finally cause peripheral insulin resistance. Leucine may improve improvement the translocation of glucose transporters to reduce blood glucose levels. Collectively, our findings reinforce the direct role that leucine plays in the regulation of muscle carbohydrate metabolism and suggests that strategies aimed at reducing obesity-induced hyperleucinaemia to improve peripheral insulin sensitivity could be counterproductive. Manipulation of leucine may represent an effective nutritional strategy to relieve peripheral insulin resistance and eventually to improve type 2 diabetes.

My work has shown for the first time, the following:

1. Different concentrations of CHX (for 30 minutes) had no effect on intracellular BCAA concentrations, mTOR and downstream target proteins activity in C2C12 muscle cells. In addition, L6 cells showed 2-fold increase in glucose uptake in response to insulin, but not C2C12 cells, suggesting that L6 myotubes are a better in vitro model system to investigate glucose uptake in muscle cells. This result provides useful information for future research conducted using L6 muscle cells.

2. There is a relationship between mTOR activity and glucose uptake in L6 myotubes, but independent of phosphorylation of Akt. The mTOR activator (3BDO) reduced phosphorylation of mTOR and p70S6K, suggesting that it was acting as an mTOR inhibitor rather than activator. Besides, 3BDO only increased glucose uptake in the absence of insulin. However, the inhibitors, rapamycin and BCH, both reduced mTOR activity, downstream target proteins, as well as glucose uptake in L6 myotubes.

3. Both 24h and 48h incubation with increased leucine concentrations increased non insulin-stimulated glucose uptake in L6 myotubes, but this was independent of phosphorylation of mTOR, p70S6K, 4E-BP1 and Akt. Leucine may influence GLUT4 translocation or regulate other glucose transporters to increase glucose uptake in L6 myotubes.

4. Attempts to overexpress Sestrin2 in L6 myotubes using an AAV1 virus were not successful. Only the control, AAV1-GFP virus successfully infected L6 myotubes, resulting in green fluorescence. The diagram below attempts to

summarize all my findings.

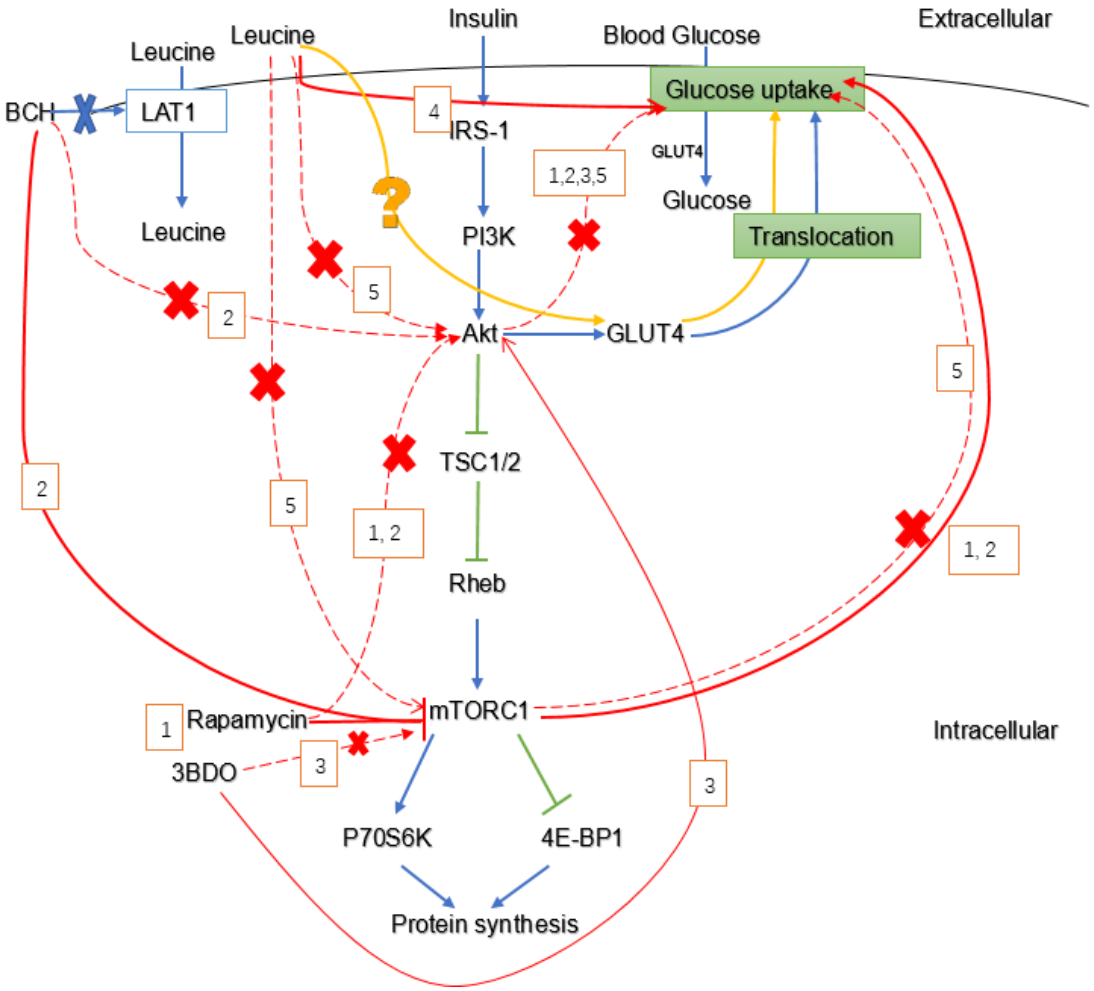


Figure 7. 1 Schematic of the relationship between mTORC1, leucine and glucose uptake

Insulin through PI3K/Akt/TSC1-2 signalling pathway stimulate mTORC1 promote protein synthesis. By stimulating with insulin and PI3K, Akt recruits GLUT4 to the cells membrane (translocation), which allow glucose into cells. This process is called glucose uptake. **1-2:** Reducing mTOR by rapamycin or BCH reduces glucose uptake, suggesting that mTOR is involved in glucose uptake. However, this regulation is independent of Akt. **3**: 3BDO did not activate phosphorylation of mTOR, but it activated phosphorylation of Akt. **4-5:** Leucine increased glucose uptake, but this process is independent of mTOR, downstream target proteins and Akt. It is possibly because leucine influence GLUT4 translocation. **Red full line:** the mechanisms that was tested in the current study and found a relationship. **Red dashed line:** the mechanisms that was tested in the current study and no relationship can be found. **Blue and green full line**: the mechanisms has been proved by others. **Yellow full line**: possible mechanism. **LAT1:** large neutral amino acid transporter, **IRS-1:** Insulin receptor substrate 1, **PI3K:** Phosphoinositide 3-kinases, **Akt/PKB:** Protein kinase B, **TSC1/2:** Tuberous sclerosis 1/2, **mTOR:** mammalian target of rapamycin, **P70S6K:** Ribosomal protein S6 kinase beta-1, **4E-BP1:** Eukaryotic translation initiation factor 4E-binding protein 1, **GLUT4:** Glucose transporter type 4, **BCH:** 2-aminobicyclo-(2,2,1)-heptane-2-carboxylic acid; **3BDO:**3-Benzyl-5-((2-nitrophenoxy)methyl)-dihydrofuran-2(3H)-o

7.2. Limitations

Firstly, the insulin concentration used (1mM) in the 3BDO, BCH and leucine experiments was higher than physiological concentrations (~10nM) or the concentration used in other studies (100nM). This is because a high concentration of insulin (1mM) was required for the glucose uptake Assay Kit to make sure this assay works. Therefore, in any future work, it would be better to reduce the insulin concentration to a physiological concentration, and repeat this experiment to confirm the results are the same. Secondly, this experiment only uses cultured muscle cells. As we mentioned the different results between human studies and animals or cell culture, if there is a chance in the future, an animal or human (blood) experiments should be included.

7.3. Future works

As mentioned in chapter 6, the future work should focus on the AAV1 transfection experiment; this biological method is more precise than chemical method. If Sestrin2 is overexpressed successfully in L6 myotubes, then leucine concentrations in the medium can be manipulated to further investigate regulation of glucose uptake, mTOR activity and downstream target proteins.

There are also some other important proteins that link glucose uptake and mTOR signalling pathway, such as PI3K, AMPK and GLUT4. The translocation of GLUT 4 and protein levels of PI3K and AMPK should be tested in future experiments. However, it is not easy to test the GLUT4 translocation, so another method that knocks out the GLUT4 gene could be tried, then manipulate leucine

concentrations and test the effects on glucose uptake again. If it shows same results as current studies, it would confirm that mTOR activity truly influences glucose uptake, via non-GLUT4 transport mechanisms. Otherwise, leucine might partially influence GLUT4 or other glucose transporters to affect glucose uptake.

Kurth-Kraczek *et al.,* (1999) showed that 5-Aminoimidazole-4-carboxamide-1-beta-D-ribofuranoside (AICA-riboside, AICAR) added into media could significantly increase AMPK activity, GLUT4 translocation and glucose uptake in rat hind limb skeletal muscle. AICAR is an analog of AMP that can stimulate AMPK activity. Increased content of Sestrin2 can also stimulate AMPK (Lee *et al.,* 2013), and long-term activation of AMPK with AICAR increased the expression of GLUT4 in gastrocnemius/plantaris muscles of rats (Holmes *et al.,* 1999). Therefore, overexpression of Sestrin 2 might lead to increased AMPK, as a mechanism to impact glucose uptake and GLUT4. Importantly, sestrin 2 is a leucine sensor, so next; we could manipulate leucine concentrations, to determine the impact on glucose uptake and phosphorylation of mTOR/ Akt. In conclusion, the sestrin2-AMPK-mTOR pathway could be an interesting research topic of future work.

PI3K is a key protein involved in GLUT4 translocation regulated by insulin (Kanai *et al.,* 1993). Wortmannin is a cell-permeable, fungal metabolite that acts as a potent, selective and irreversible inhibitor of PI3K (Arcaro and Wymann, 1993). Same as the mTOR inhibitor rapamycin, wortmannin can be added in

the medium of L6 myotubes, then test the glucose uptake and protein levels by western blotting. Peyrollier *et al.,* (2000) showed that leucine activated PI3K, which is a key enzyme related to the translocation of GLUT4 to the membrane in L6 myotubes. Nishitani *et al.,* (2002) displayed that leucine increased glucose uptake in skeletal muscle via PI3K-Protein kinase C pathway and independently of mTOR. Therefore, PI3K might be involved in the relationship between leucine and glucose uptake. Figure 7.2 showes the possible mechanisms that should be the focus of future works.

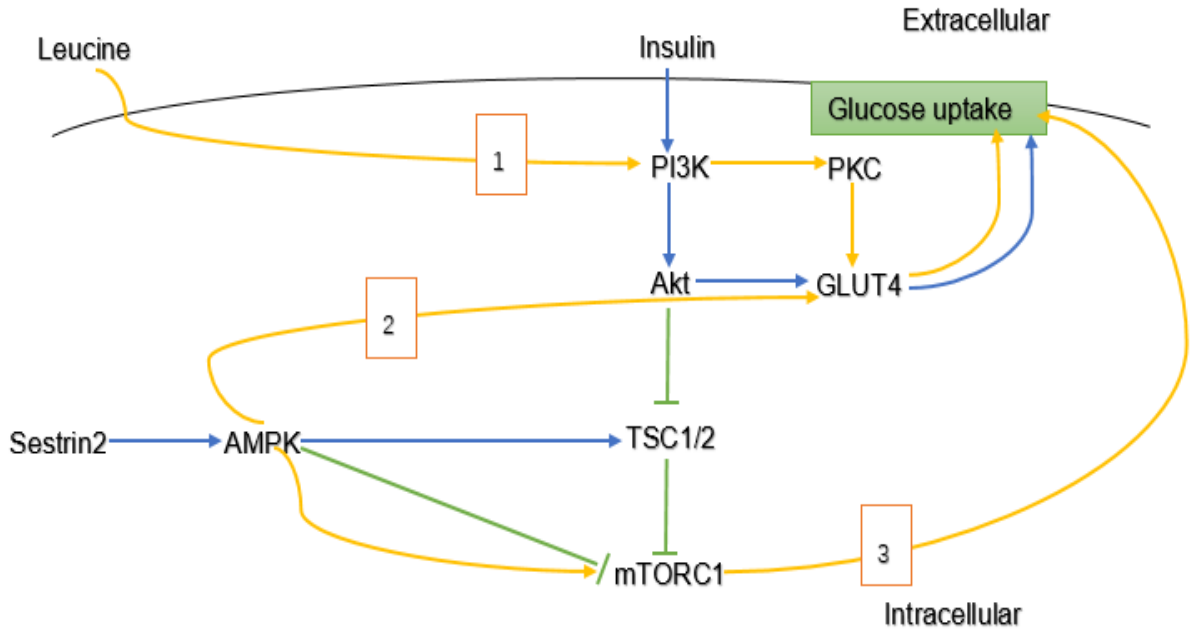


Figure 7. 2 Schematic of the mechanisms in the future works

1: Leucine increases glucose uptake because it increases GLUT4 content or translocation. Furthermore, leucine may influence PI3K and PKC to increase GLUT4. **2:** Long-term activation of AMPK with AICAR increases the expression of GLUT4 in skeletal muscle. Whether increases phosphorylation of AMPK by overexpression Setrin2 will increases GLUT4 and further increases glucose uptake. **3:** Sestrin2 increases phosphorylation of AMPK, which activates AMPK and further promotes TSC2 activation and inhibits mTORC1. We already show that decreased mTOR activity reduced glucose uptake. Therefore, whether phosphorylation of AMPK by overexpression of Setrin2 will influences (reduces?) mTOR and glucose uptake? **Blue and green full line**: the mechanisms has been proved by others. **Yellow full line**: possible mechanism. **PI3K:** Phosphoinositide 3-kinases, **Akt/PKB:** Protein kinase B, **TSC1/2:** Tuberous sclerosis 1/2, **mTOR:** mammalian target of rapamycin, **GLUT4:** Glucose transporter type 4, **AMPK：** 5' AMP-activated protein kinase, **PKC:** Protein kinase C

CHAPTER 8: REFERENCES

Abdul-Ghani, M.A. and DeFronzo, R.A., 2010. Pathogenesis of insulin resistance in skeletal muscle. *BioMed Research International*, *2010*.

Abraham, R.T., 2016. Toward a Molecular Definition of Leucine-Dependent mTORC1 Activation. *Cell metabolism*,*23*(3), pp.397-398.

Adams, S.H., 2011. Emerging perspectives on essential amino acid metabolism in obesity and the insulin-resistant state. Advances in nutrition, 2(6), pp.445-456.

Adeva, M.M., Calviño, J., Souto, G. and Donapetry, C., 2012. Insulin resistance and the metabolism of branched-chain amino acids in humans. Amino acids, 43(1), pp.171-181.

Arcaro, A. and Wymann, M.p., 1993. Wortmannin is a potent phosphatidylinositol 3-kinase inhibitor: the role of phosphatidylinositol 3, 4, 5-trisphosphate in neutrophil responses. *Biochemical Journal*, *296*(2), pp.297-301.

Aronoff, S.L., Berkowitz, K., Shreiner, B. and Want, L., 2004. Glucose metabolism and regulation: beyond insulin and glucagon. Diabetes spectrum, 17(3), pp.183-190.

Arriola Apelo, S.I. and Lamming, D.W., 2016. Rapamycin: an InhibiTOR of aging emerges from the soil of Easter Island.*Journals of Gerontology Series A: Biomedical Sciences and Medical Sciences*, *71*(7), pp.841-849.

Atherton, p.J., Smith, K., Etheridge, T., Rankin, D. and Rennie, M.J., 2010. Distinct anabolic signalling responses to amino acids in C2C12 skeletal muscle cells. *Amino acids*,*38*(5), pp.1533-1539.

Bar-Peled, L., Chantranupong, L., Cherniack, A.D., Chen, W.W., Ottina, K.A., Grabiner, B.C., Spear, E.D., Carter, S.L., Meyerson, M. and Sabatini, D.M., 2013. A Tumor suppressor complex with GAP activity for the Rag GTPases that signal amino acid sufficiency to mTORC1. *Science*, *340*(6136), pp.1100-1106.

Baum, J.I., O'Connor, J.C., Seyler, J.E., Anthony, T.G., Freund, G.G. and Layman, D.K., 2005. Leucine reduces the duration of insulin-induced PI 3-kinase activity in rat skeletal muscle. *American Journal of Physiology-Endocrinology and Metabolism*, *288*(1), pp.E86-E91.

Balage, M., Dupont, J., Mothe-Satney, I., Tesseraud, S., Mosoni, L. and Dardevet, D., 2011. Leucine supplementation in rats induced a delay in muscle IR/PI3K signaling pathway associated with overall impaired glucose tolerance. The Journal of nutritional biochemistry, 22(3), pp.219-226.

Bajotto G, Murakami T, Nagasaki M, Sato Y, Shimomura Y. 2009. Decreased

enzyme activity and contents of hepatic branched-chain alpha-keto acid dehydrogenase complex subunits in a rat model for type 2 diabetes mellitus. Metabolism, 58:1489–95

Bergström, J., Fürst, P., Noree, L.O. and Vinnars, E., 1974. Intracellular free amino acid concentration in human muscle tissue. Journal of applied physiology, 36(6), pp.693-697.

Beugnet, A., Tee, A.R., Taylor, p.M. and Proud, C.G., 2003. Regulation of targets of mTOR (mammalian target of rapamycin) signalling by intracellular amino acid availability. Biochemical Journal, 372(Pt 2), p.555.

Boulet, M.M., Chevrier, G., Grenier-Larouche, T., Pelletier, M., Nadeau, M., Scarpa, J., Prehn, C., Marette, A., Adamski, J. and Tchernof, A., 2015. Alterations of plasma metabolite profiles related to adipose tissue distribution and cardiometabolic risk. American Journal of Physiology-Endocrinology and Metabolism, 309(8), pp.E736-E746.

Brantly, M.L., Chulay, J.D., Wang, L., Mueller, C., Humphries, M., Spencer, L.T., Rouhani, F., Conlon, T.J., Calcedo, R., Betts, M.R. and Spencer, C., 2009. Sustained transgene expression despite T lymphocyte responses in a clinical trial of rAAV1-AAT gene therapy. *Proceedings of the National Academy of Sciences*, *106*(38), pp.16363-16368.

Braunstein, S., Badura, M.L., Xi, Q., Formenti, S.C. and Schneider, R.J., 2009. Regulation of protein synthesis by ionizing radiation. *Molecular and cellular biology*, *29*(21), pp.5645-5656.

Briaud, I., Dickson, L.M., Lingohr, M.K., McCuaig, J.F., Lawrence, J.C. and Rhodes, C.J., 2005. Insulin receptor substrate-2 proteasomal degradation mediated by a mammalian target of rapamycin (mTOR)-induced negative feedback down-regulates protein kinase B-mediated signaling pathway in β-cells. *Journal of Biological Chemistry*, *280*(3), pp.2282-2293.

Brosnan, J.T. and Brosnan, M.E., 2006. Branched-chain amino acids: enzyme and substrate regulation. The Journal of nutrition, 136(1), pp.207S-211S.

Brown, D., Ryan, K., Daniel, Z., Mareko, M., Talbot, R., Moreton, J., Giles, T.C., Emes, R., Hodgman, C., Parr, T. and Brameld, J.M., 2018. The Beta-adrenergic agonist, Ractopamine, increases skeletal muscle expression of Asparagine Synthetase as part of an integrated stress response gene program. *Scientific reports*, *8*(1), p.15915.

Brown, M.S. and Goldstein, J.L., 2008. Selective versus total insulin resistance: a pathogenic paradox. *Cell metabolism*, *7*(2), pp.95-96.

Budanov, A.V. and Karin, M., 2008. p53 target genes Sestrin1 and Sestrin2 connect genotoxic stress and mTOR signaling.*Cell*, *134*(3), pp.451-460.

Budanov, A.V., Shoshani, T., Faerman, A., Zelin, E., Kamer, I., Kalinski, H., Gorodin, S., Fishman, A., Chajut, A., Einat, p. and Skaliter, R., 2002. Identification of a novel stress-responsive gene Hi95 involved in regulation of cell viability.*Oncogene*, *21*(39), p.6017.

Buller, C., Loberg, R.D., Fan, M.H., Zhu, Q., Park, J.L., Vesely, E., Inoki, K., Guan, K. and Brosius, F.C., 2008. A GSK-3, TSC2, mTOR Pathway Regulates Glucose Uptake and GLUT1 Glucose Transporter Expression. *American Journal of Physiology-Cell Physiology*.
Buller, C.L., 2010. Role of GLUT1 in the Mammalian Target of Rapamycin Pathway: Mechanisms of Regulation.

Caballero, B., Finer, N. and Wurtman, R.J., 1988. Plasma amino acids and insulin levels in obesity: response to carbohydrate intake and tryptophan supplements. *Metabolism*, *37*(7), pp.672-676.

Chantranupong, L., Wolfson, R.L., Orozco, J.M., Saxton, R.A., Scaria, S.M., Bar-Peled, L., Spooner, E., Isasa, M., Gygi, S.p. and Sabatini, D.M., 2014. The Sestrins interact with GATOR2 to negatively regulate the amino-acid-sensing pathway upstream of mTORC1. *Cell reports*, *9*(1), pp.1-8.

Chen, T., Ni, Y., Ma, X., Bao, Y., Liu, J., Huang, F., Hu, C., Xie, G., Zhao, A., Jia, W. and Jia, W., 2016. Branched-chain and aromatic amino acid profiles and diabetes risk in Chinese populations. *Scientific reports*, *6*, p.20594.

Cheng, Q., Beltran, V.D., Chan, S.M., Brown, J.R., Bevington, A. and Herbert, T.p., 2016. System-L amino acid transporters play a key role in pancreatic β-cell signalling and function.*Journal of molecular endocrinology*, *56*(3), pp.175-187.

Cheng, S.W., Fryer, L.G., Carling, D. and Shepherd, p.R., 2004. Thr2446 is a novel mammalian target of rapamycin (mTOR) phosphorylation site regulated by nutrient status.*Journal of Biological Chemistry*, *279*(16), pp.15719-15722.

Chhabra, N., 2012. Insulin Biosynthesis, Secretion, and Action [on-line]. Available at: http://www.namrata.co/insulin-biosynthesis-secretion-and-action/ [Accessed 01 Nov 2018]

Cho, N.H., Shaw, J.E., Karuranga, S., Huang, Y., da Rocha Fernandes, J.D., Ohlrogge, A.W. and Malanda, B., 2018. IDF Diabetes Atlas: global estimates of diabetes prevalence for 2017 and projections for 2045. *Diabetes research and clinical practice*, *138*, pp.271-281.

Comas, M., Toshkov, I., Kuropatwinski, K.K., Chernova, O.B., Polinsky, A., Blagosklonny, M.V., Gudkov, A.V. and Antoch, M.p., 2012. New

nanoformulation of rapamycin Rapatar extends lifespan in homozygous p53−/− mice by delaying carcinogenesis. *Aging (Albany NY)*, *4*(10), p.715.

Cooper, S.T., Maxwell, A.L., Kizana, E., Ghoddusi, M., Hardeman, E.C., Alexander, I.E., Allen, D.G. and North, K.N., 2004. C2C12 co‐culture on a fibroblast substratum enables sustained survival of contractile, highly differentiated myotubes with peripheral nuclei and adult fast myosin expression. Cell motility and the cytoskeleton, 58(3), pp.200-211.

Copp, J., Manning, G. and Hunter, T., 2009. TORC-specific phosphorylation of mammalian target of rapamycin (mTOR): phospho-Ser2481 is a marker for intact mTOR signaling complex 2. *Cancer research*, *69*(5), pp.1821-1827.

Da Silva Xavier, G., 2018. The Cells of the Islets of Langerhans. Journal of clinical medicine, 7(3), p.54.

Dann, S.G., Selvaraj, A. and Thomas, G., 2007. mTOR Complex1–S6K1 signaling: at the crossroads of obesity, diabetes and cancer. *Trends in molecular medicine*, *13*(6), pp.252-259.

Deblon, N., Bourgoin, L., Veyrat-Durebex, C., Peyrou, M., Vinciguerra, M., Caillon, A., Maeder, C., Fournier, M., Montet, X., Rohner-Jeanrenaud, F. and Foti, M., 2012. Chronic mTOR inhibition by rapamycin induces muscle insulin resistance despite weight loss in rats. *British journal of pharmacology*, *165*(7), pp.2325-2340.

Depaoli, M.R., Hay, J.C., Graier, W.F. and Malli, R., 2019. The enigmatic ATP supply of the endoplasmic reticulum. Biological Reviews, 94(2), pp.610-628.

DeFronzo, R.A. and Tripathy, D., 2009. Skeletal muscle insulin resistance is the primary defect in type 2 diabetes. *Diabetes care*, *32*(suppl 2), pp.S157-S163.

Deldicque, L., Canedo, C.S., Horman, S., De Potter, I., Bertrand, L., Hue, L. and Francaux, M., 2008. Antagonistic effects of leucine and glutamine on the mTOR pathway in myogenic C 2 C 12 cells. *Amino acids*, *35*(1), pp.147-155.

Dohm, G. L., C. W. Elton, J. E. Friedman, P. F. Pilch, W. P. Pories, S. M. Atkinson, and J. F. Caro. 1991. Decreased expression of glucose transporter in muscle from insulin-resistant patients. Am. J. Physiol. 260:E459-E463.

Doisaki M, Katano Y, Nakano I, Hirooka Y, Itoh A, Ishigami M, Hayashi K, Goto H, Fujita Y, Kadota Y, *et al*. 2010. Regulation of hepatic branched-chain alpha-keto acid dehydrogenase kinase in a rat model for type 2 diabetes mellitus at different stages of the disease. Biochem Biophys Res Commun, 393:303–7

Doi, M., Yamaoka, I., Fukunaga, T. and Nakayama, M., 2003. Isoleucine, a potent plasma glucose-lowering amino acid, stimulates glucose uptake in

C2C12 myotubes. *Biochemical and biophysical research communications*, *312*(4), pp.1111-1117.

Dimitriadis, G., Mitrou, P., Lambadiari, V., Maratou, E. and Raptis, S.A., 2011. Insulin effects in muscle and adipose tissue. Diabetes research and clinical practice, 93, pp.S52-S59.

Duan, D., Sharma, p., Yang, J., Yue, Y., Dudus, L., Zhang, Y., Fisher, K.J. and Engelhardt, J.F., 1998. Circular intermediates of recombinant adeno-associated virus have defined structural characteristics responsible for long-term episomal persistence in muscle tissue. *Journal of virology*, *72*(11), pp.8568-8577.

Dumont FJ, Staruch MJ, Koprak SL, Melino MR, Sigal NH. 1990. Distinct mechanisms of suppression of murine T cell activation by the related macrolides FK-506 and rapamycin. J Immunol. 144:251–258.

Ellis, B.L., Hirsch, M.L., Barker, J.C., Connelly, J.p., Steininger, R.J. and Porteus, M.H., 2013. A survey of ex vivo/in vitro transduction efficiency of mammalian primary cells and cell lines with Nine natural adeno-associated virus (AAV1-9) and one engineered adeno-associated virus serotype.*Virology journal*, *10*(1), p.74.

Felig, p., 1970. Plasma Amino Acid Levels and Insulin Secretion in Obesity. *Laboratory Medicine*, *1*(9), pp.39-42.

Felig, p., Marliss, E. and Cahill Jr, G.F., 1969. Plasma amino acid levels and insulin secretion in obesity. *New England Journal of Medicine*, *281*(15), pp.811-816.

Falck Suzanne. 2017. Pancreas: Functions and possible problems [on-line]. Available at: https://www.medicalnewstoday.com/articles/10011.php [Accessed 24 July 2019]

Floegel, A., Stefan, N., Yu, Z., Mühlenbruch, K., Drogan, D., Joost, H.G., Fritsche, A., Häring, H.U., de Angelis, M.H., Peters, A. and Roden, M., 2013. Identification of serum metabolites associated with risk of type 2 diabetes using a targeted metabolomic approach. *Diabetes*, *62*(2), pp.639-648.

Foster, K.G. and Fingar, D.C., 2010. Mammalian target of rapamycin (mTOR): conducting the cellular signaling symphony. *Journal of Biological Chemistry*, *285*(19), pp.14071-14077.

Fraga, S., Serrao, M.p. and Soares-da-Silva, p., 2002. L-type amino acid transporters in two intestinal epithelial cell lines function as exchangers with neutral amino acids. *The Journal of nutrition*, *132*(4), pp.733-738.

Frias, M.A., Thoreen, C.C., Jaffe, J.D., Schroder, W., Sculley, T., Carr, S.A. and Sabatini, D.M., 2006. mSin1 is necessary for Akt/PKB phosphorylation, and its

isoforms define three distinct mTORC2s. *Current Biology*, *16*(18), pp.1865-1870.

Friedman, J.E., Dohm, G.L., Leggett-Frazier, N., Elton, C.W., Tapscott, E.B., Pories, W.P. and Caro, J.F., 1992. Restoration of insulin responsiveness in skeletal muscle of morbidly obese patients after weight loss. Effect on muscle glucose transport and glucose transporter GLUT4. The Journal of clinical investigation, 89(2), pp.701-705.

Fueger, P.T., Li, C.Y., Ayala, J.E., Shearer, J., Bracy, D.P., Charron, M.J., Rottman, J.N. and Wasserman, D.H., 2007. Glucose kinetics and exercise tolerance in mice lacking the GLUT4 glucose transporter. The Journal of physiology, 582(2), pp.801-812.

Gannon, N.p. and Vaughan, R.A., 2016. Leucine-induced anabolic-catabolism: two sides of the same coin. *Amino Acids*,*48*(2), pp.321-336.

Gannon, N.p., Schnuck, J.K. and Vaughan, R.A., 2018. BCAA Metabolism and Insulin Sensitivity–Dysregulated by Metabolic Status?. *Molecular nutrition & food research*, *62*(6), p.1700756.

Gao, N., Flynn, D.C., Zhang, Z., Zhong, X.S., Walker, V., Liu, K.J., Shi, X. and Jiang, B.H., 2004. G1 cell cycle progression and the expression of G1 cyclins are regulated by PI3K/Akt/mTOR/p70S6K1 signaling in human ovarian cancer cells. *American Journal of Physiology-Cell Physiology*, *287*(2), pp.C281-C291.

García-Martínez, J.M. and Alessi, D.R., 2008. mTOR complex 2 (mTORC2) controls hydrophobic motif phosphorylation and activation of serum-and glucocorticoid-induced protein kinase 1 (SGK1). *Biochemical Journal*, *416*(3), pp.375-385.

Ge, D., Han, L., Huang, S., Peng, N., Wang, p., Jiang, Z., Zhao, J., Su, L., Zhang, S., Zhang, Y. and Kung, H., 2014. Identification of a novel MTOR activator and discovery of a competing endogenous RNA regulating autophagy in vascular endothelial cells. *Autophagy*, *10*(6), pp.957-971.

Gibbs, E. M., Stock, J. L., McCoid, S. C., Stukenbrok, H. A., Pessin, J. E., Stevenson, R. W., Milici, A. J. & McNeish, J. D. (1995) J. Clin. Invest. 95, 1512–1518.

GO, V., DiMagno, E., Gardner, J., Reber, H., Scheele, G., Emanuel Lebenthal., 1993. The Pancreas: biology, pathobiology, and disease. 2nd ed. USA: Lippincott Williams & Wilkins.

Gonzalez, E., Flier, E., Molle, D., Accili, D. and McGraw, T.E., 2011. Hyperinsulinemia leads to uncoupled insulin regulation of the GLUT4 glucose

transporter and the FoxO1 transcription factor. *Proceedings of the National Academy of Sciences*, *108*(25), pp.10162-10167.

Good Food Eating. 2014. Insulin & Insulin Resistance [on-line]. Available at: http://goodfoodeating.com/6758/insulin-and-insulin-resistance/[Accessed 03 June 2016]

Gould, G.W. and Holman, G.D., 1993. The glucose transporter family: structure, function and tissue-specific expression. *Biochemical Journal*, *295*(Pt 2), p.329.

Groenewoud, M.J. and Zwartkruis, F.J., 2013. Rheb and mammalian target of rapamycin in mitochondrial homoeostasis. *Open biology*, *3*(12), p.130185.

Gropper, S.S. and Groff, L.J., 1999. *Advanced nutrition and human metabolism 3rd* Edition. Wadsworth

Guertin, D.A., Stevens, D.M., Thoreen, C.C., Burds, A.A., Kalaany, N.Y., Moffat, J., Brown, M., Fitzgerald, K.J. and Sabatini, D.M., 2006. Ablation in mice of the mTORC components raptor, rictor, or mLST8 reveals that mTORC2 is required for signaling to Akt-FOXO and PKCα, but not S6K1.*Developmental cell*, *11*(6), pp.859-871.

Guo, S., 2014. Insulin signaling, resistance, and metabolic syndrome: insights from mouse models into disease mechanisms. *Journal of Endocrinology*, *220*(2), pp.T1-T23.

Guridi, M., Kupr, B., Romanino, K., Lin, S., Falcetta, D., Tintignac, L. and Rüegg, M.A., 2016. Alterations to mTORC1 signaling in the skeletal muscle differentially affect whole-body metabolism. Skeletal muscle, 6(1), p.1.

Han, H.S., Kang, G., Kim, J.S., Choi, B.H. and Koo, S.H., 2016. Regulation of glucose metabolism from a liver-centric perspective. *Experimental & molecular medicine*, *48*(3), p.e218.

Hancock, C.R., Han, D.H., Chen, M., Terada, S., Yasuda, T., Wright, D.C. and Holloszy, J.O., 2008. High-fat diets cause insulin resistance despite an increase in muscle mitochondria. *Proceedings of the National Academy of Sciences*, *105*(22), pp.7815-7820.

Hara, K., Maruki, Y., Long, X., Yoshino, K.I., Oshiro, N., Hidayat, S., Tokunaga, C., Avruch, J. and Yonezawa, K., 2002. Raptor, a binding partner of target of rapamycin (TOR), mediates TOR action. *Cell*, *110*(2), pp.177-189.

Hardy, O.T., Czech, M.p. and Corvera, S., 2012. What causes the insulin resistance underlying obesity?. *Current opinion in endocrinology, diabetes, and obesity*, *19*(2), p.81.

Harris, R.A., Hawes, J.W., Popov, K.M., Zhao, Y., Shimomura, Y., Sato, J.,

Jaskiewicz, J. and Hurley, T.D., 1997. Studies on the regulation of the mitochondrial α-ketoacid dehydrogenase complexes and their kinases. Advances in enzyme regulation, 37, pp.271-293.

Heslin, M.J., Newman, E., Wolf, R.F., Pisters, p.W. and Brennan, M.F., 1992. Effect of hyperinsulinemia on whole body and skeletal muscle leucine carbon kinetics in humans. American Journal of Physiology-Endocrinology And Metabolism, 262(6), pp.E911-E918.

Holmes, B.F., Kurth-Kraczek, E.J. and Winder, W.W., 1999. Chronic activation of 5′-AMP-activated protein kinase increases GLUT-4, hexokinase, and glycogen in muscle. *Journal of applied physiology*, *87*(5), pp.1990-1995.

Houde, V.p., Brûlé, S., Festuccia, W.T., Blanchard, p.G., Bellmann, K., Deshaies, Y. and Marette, A., 2010. Chronic rapamycin treatment causes glucose intolerance and hyperlipidemia by upregulating hepatic gluconeogenesis and impairing lipid deposition in adipose tissue. *Diabetes*, *59*(6), pp.1338-1348.

Hu, H.J., Shi, Z.Y., Lin, X.L., Chen, S.M., Wang, Q.Y. and Tang, S.Y., 2015. Upregulation of Sestrin2 expression protects against macrophage apoptosis induced by oxidized low-density lipoprotein. *DNA and cell biology*, *34*(4), pp.296-302.

Huffman, K.M., Shah, S.H., Stevens, R.D., Bain, J.R., Muehlbauer, M., Slentz, C.A., Tanner, C.J., Kuchibhatla, M., Houmard, J.A., Newgard, C.B. and Kraus, W.E., 2009. Relationships between circulating metabolic intermediates and insulin action in overweight to obese, inactive men and women. *Diabetes care*.

Hutson, S.M., Sweatt, A.J. and LaNoue, K.F., 2005. Branched-chain amino acid metabolism: implications for establishing safe intakes. The Journal of nutrition, 135(6), pp.1557S-1564S.

Ichii, H., Inverardi, L., Pileggi, A., Molano, R.D., Cabrera, O., Caicedo, A., Messinger, S., Kuroda, Y., Berggren, p.O. and Ricordi, C., 2005. A novel method for the assessment of cellular composition and beta-cell viability in human islet preparations. American journal of transplantation, 5(7), pp.1635-1645.

IDF. Diabetes Atlas Eighth Edition. 2017. 8th ed.

Imai, H., Kaira, K., Oriuchi, N., Shimizu, K., Tominaga, H., Yanagitani, N., Sunaga, N., Ishizuka, T., Nagamori, S., Promchan, K. and Nakajima, T., 2010. Inhibition of L-type amino acid transporter 1 has antitumor activity in non-small cell lung cancer. *Anticancer research*, *30*(12), pp.4819-4828.

Inoki, K., Kim, J. and Guan, K.L., 2012. AMPK and mTOR in cellular energy homeostasis and drug targets. *Annual review of pharmacology and toxicology*, *52*, pp.381-400.

Inoki, K., Zhu, T. and Guan, K.L., 2003. TSC2 mediates cellular energy response to control cell growth and survival.*Cell*, *115*(5), pp.577-590.

Ionescu-Tirgoviste, C., Gagniuc, p.A., Gubceac, E., Mardare, L., Popescu, I., Dima, S. and Militaru, M., 2015. A 3D map of the islet routes throughout the healthy human pancreas.*Scientific reports*, *5*, p.14634.

Jacinto, E., Facchinetti, V., Liu, D., Soto, N., Wei, S., Jung, S.Y., Huang, Q., Qin, J. and Su, B., 2006. SIN1/MIP1 maintains rictor-mTOR complex integrity and regulates Akt phosphorylation and substrate specificity. *Cell*, *127*(1), pp.125-137.

Jacinto, E., Loewith, R., Schmidt, A., Lin, S., Rüegg, M.A., Hall, A. and Hall, M.N., 2004. Mammalian TOR complex 2 controls the actin cytoskeleton and is rapamycin insensitive. *Nature cell biology*, *6*(11), p.1122.

Jaiswal, N., Maurya, C.K., Venkateswarlu, K., Sukanya, P., Srivastava, A.K., Narender, T. and Tamrakar, A.K., 2012. 4-Hydroxyisoleucine stimulates glucose uptake by increasing surface GLUT4 level in skeletal muscle cells via phosphatidylinositol-3-kinase-dependent pathway. European journal of nutrition, 51(7), pp.893-898.

Jeganathan, S., Abdullahi, A., Zargar, S., Maeda, N., Riddell, M.C. and Adegoke, O.A., 2014. Amino acid-induced impairment of insulin sensitivity in healthy and obese rats is reversible. *Physiological reports*, *2*(7).

Jensen, J., Rustad, p.I., Kolnes, A.J. and Lai, Y.C., 2011. The role of skeletal muscle glycogen breakdown for regulation of insulin sensitivity by exercise. *Frontiers in physiology*, *2*, p.112.

Johnson, M.R., Behmoaras, J., Bottolo, L., Krishnan, M.L., Pernhorst, K., Santoscoy, p.L.M., Rossetti, T., Speed, D., Srivastava, p.K., Chadeau-Hyam, M. and Hajji, N., 2015. Systems genetics identifies Sestrin 3 as a regulator of a proconvulsant gene network in human epileptic hippocampus.*Nature communications*, *6*, p.6031.

Kahn, B.B. and Flier, J.S., 2000. Obesity and insulin resistance. *The Journal of clinical investigation*, *106*(4), pp.473-481.

Kanai, F., Ito, K., Todaka, M., Hayashi, H., Kamohara, S., Ishii, K., Okada, T., Hazeki, O., Ui, M. and Ebina, Y., 1993. Insulin-stimulated GLUT4 translocation is relevant to the phosphorylation of IRS-1 and the activity of PI3

kinase. *Biochemical and biophysical research communications*, *195*(2), pp.762-768

Kanazawa, T., Taneike, I., Akaishi, R., Yoshizawa, F., Furuya, N., Fujimura, S. and Kadowaki, M., 2004. Amino acids and insulin control autophagic proteolysis through different signaling pathways in relation to mTOR in isolated rat hepatocytes. *Journal of Biological Chemistry*, *279*(9), pp.8452-8459.

Karakikes, I., Hadri, L., Rapti, K., Ladage, D., Ishikawa, K., Tilemann, L., Yi, G.H., Morel, C., Gwathmey, J.K., Zsebo, K. and Weber, T., 2012. Concomitant intravenous nitroglycerin with intracoronary delivery of AAV1. SERCA2a enhances gene transfer in porcine hearts. *Molecular Therapy*, *20*(3), pp.565-571.

Khamzina, L., Veilleux, A., Bergeron, S. and Marette, A., 2005. Increased activation of the mammalian target of rapamycin pathway in liver and skeletal muscle of obese rats: possible involvement in obesity-linked insulin resistance.*Endocrinology*, *146*(3), pp.1473-1481.

Khorami, S.A.H., Movahedi, A. and Sokhini, A.M.M., 2015. Review Article; PI3K/Akt pathway in modulating glucose homeostasis and its alteration in Diabetes. *Annals of Medical and Biomedical Sciences*, *1*(2).

Kim, D.H., Sarbassov, D.D., Ali, S.M., King, J.E., Latek, R.R., Erdjument-Bromage, H., Tempst, p. and Sabatini, D.M., 2002. mTOR interacts with raptor to form a nutrient-sensitive complex that signals to the cell growth machinery. *Cell*, *110*(2), pp.163-175.

Kim, D.K., Kanai, Y., Choi, H.W., Tangtrongsup, S., Chairoungdua, A., Babu, E., Tachampa, K., Anzai, N., Iribe, Y. and Endou, H., 2002. Characterization of the system L amino acid transporter in T24 human bladder carcinoma cells.*Biochimica et Biophysica Acta (BBA)-Biomembranes*,*1565*(1), pp.112-122.

Kim, E., 2009. Mechanisms of amino acid sensing in mTOR signaling pathway. *Nutrition research and practice*, *3*(1), pp.64-71.

Kim, S.G., Buel, G.R. and Blenis, J., 2013. Nutrient regulation of the mTOR complex 1 signaling pathway. Molecules and cells, 35(6), pp.463-473.

Kim, J.S., Ro, S.H., Kim, M., Park, H.W., Semple, I.A., Park, H., Cho, U.S., Wang, W., Guan, K.L., Karin, M. and Lee, J.H., 2015. Sestrin2 inhibits mTORC1 through modulation of GATOR complexes. *Scientific reports*, *5*, p.9502.

Kimball, S.R., 2001. Regulation of translation initiation by amino acids in eukaryotic cells. In *Signaling Pathways for Translation* (pp. 155-184). Springer,

Berlin, Heidelberg.

King, P.A., Horton, E.D., Hirshman, M.F. and Horton, E.S., 1992. Insulin resistance in obese Zucker rat (fa/fa) skeletal muscle is associated with a failure of glucose transporter translocation. *The Journal of clinical investigation*, 90(4), pp.1568-1575.

Kislinger, T., Gramolini, A.O., Pan, Y., Rahman, K., MacLennan, D.H. and Emili, A., 2005. Proteome dynamics during C2C12 myoblast differentiation. Molecular & Cellular Proteomics, 4(7), pp.887-901.

Kleinert, M., Liao, Y.H., Nelson, J.L., Bernard, J.R., Wang, W. and Ivy, J.L., 2011. An amino acid mixture enhances insulin-stimulated glucose uptake in isolated rat epitrochlearis muscle.*Journal of Applied Physiology*, *111*(1), pp.163-169.

Kotliar, N. and Pilch, P.F., 1992. Expression of the glucose transporter isoform GLUT 4 is insufficient to confer insulin-regulatable hexose uptake to cultured muscle cells. Molecular Endocrinology, 6(3), pp.337-345.

Kurebayashi, Y., Nagai, S., Ikejiri, A., Ohtani, M., Ichiyama, K., Baba, Y., Yamada, T., Egami, S., Hoshii, T., Hirao, A. and Matsuda, S., 2012. PI3K-Akt-mTORC1-S6K1/2 axis controls Th17 differentiation by regulating Gfi1 expression and nuclear translocation of RORγ. *Cell reports*, *1*(4), pp.360-373.

Kurth-Kraczek, E.J., Hirshman, M.F., Goodyear, L.J. and Winder, W.W., 1999. 5'AMP-activated protein kinase activation causes GLUT4 translocation in skeletal muscle. *Diabetes*, *48*(8), pp.1667-1671.

Kuzuya T, Katano Y, Nakano I, Hirooka Y, Itoh A, Ishigami M, Hayashi K, Honda T, Goto H, Fujita Y, *et al*. 2008. Regulation of branched-chain amino acid catabolism in rat models for spontaneous type 2 diabetes mellitus. Biochem Biophys Res Commun, 373:94–8

Laplante, M. and Sabatini, D.M., 2012. mTOR signaling in growth control and disease. *Cell*, *149*(2), pp.274-293.

Lee, J.H., Budanov, A.V. and Karin, M., 2013. Sestrins orchestrate cellular metabolism to attenuate aging. *Cell metabolism*, *18*(6), pp.792-801.

Lee, J.H., Budanov, A.V., Talukdar, S., Park, E.J., Park, H.L., Park, H.W., Bandyopadhyay, G., Li, N., Aghajan, M., Jang, I. and Wolfe, A.M., 2012. Maintenance of metabolic homeostasis by Sestrin2 and Sestrin3. *Cell metabolism*, *16*(3), pp.311-321.

Leontieva, O.V., Paszkiewicz, G., Demidenko, Z.N. and Blagosklonny, M.V., 2013. Resveratrol potentiates rapamycin to prevent hyperinsulinemia and obesity in male mice on high fat diet. *Cell death & disease*, *4*(1), p.e472.

Li, X., Wang, X., Liu, R., Ma, Y., Guo, H., Hao, L., Yao, p., Liu, L., Sun, X., He, K. and Cao, W., 2013. Chronic leucine supplementation increases body weight

and insulin sensitivity in rats on high-fat diet likely by promoting insulin signaling in insulin-target tissues. *Molecular nutrition & food research*,*57*(6), pp.1067-1079.

Liu, H., Liu, R., Xiong, Y., Li, X., Wang, X., Ma, Y., Guo, H., Hao, L., Yao, p., Liu, L. and Wang, D., 2014. Leucine facilitates the insulin-stimulated glucose uptake and insulin signaling in skeletal muscle cells: involving mTORC1 and mTORC2. *Amino acids*, *46*(8), pp.1971-1979.

Liu, R., Li, H., Fan, W., Jin, Q., Chao, T., Wu, Y., Huang, J., Hao, L. and Yang, X., 2017. Leucine supplementation differently modulates branched-Chain amino acid catabolism, mitochondrial function and metabolic profiles at the different stage of insulin resistance in rats on high-fat diet. *Nutrients*,*9*(6), p.565.

Long, X., Lin, Y., Ortiz-Vega, S., Yonezawa, K. and Avruch, J., 2005. Rheb binds and regulates the mTOR kinase. *Current Biology*, *15*(8), pp.702-713.

Lorain, S., Gross, D.A., Goyenvalle, A., Danos, O., Davoust, J. and Garcia, L., 2008. Transient immunomodulation allows repeated injections of AAV1 and correction of muscular dystrophy in multiple muscles. *Molecular Therapy*, *16*(3), pp.541-547.

Lowell, B.B., Shulman, G.I., (2005) Mitochondrial dysfunction and type 2 diabetes. *Science* 307:384 –387.

Lu, J., Xie, G., Jia, W. and Jia, W., 2013. Insulin resistance and the metabolism of branched-chain amino acids. Frontiers of medicine, 7(1), pp.53-59.

Lund, S., Holman, G.D., Schmitz, O. and Pedersen, O., 1995. Contraction stimulates translocation of glucose transporter GLUT4 in skeletal muscle through a mechanism distinct from that of insulin. *Proceedings of the National Academy of Sciences*, *92*(13), pp.5817-5821.

Luzi, L., Castellino, p. and DeFronzo, R.A., 1996. Insulin and hyperaminoacidemia regulate by a different mechanism leucine turnover and oxidation in obesity. *American Journal of Physiology-Endocrinology And Metabolism*, *270*(2), pp.E273-E281.

Lynch, C.J., Fox, H.L., Vary, T.C., Jefferson, L.S. and Kimball, S.R., 2000. Regulation of amino acid–sensitive TOR signaling by leucine analogues in adipocytes. *Journal of cellular biochemistry*, *77*(2), pp.234-251.

Macotela, Y., Emanuelli, B., Bång, A.M., Espinoza, D.O., Boucher, J., Beebe, K., Gall, W. and Kahn, C.R., 2011. Dietary leucine-an environmental modifier of insulin resistance acting on multiple levels of metabolism. *PloS one*, *6*(6), p.e21187.

Martel RR, Klicius J, Galet S. 1977. Inhibition of the immune response by rapamycin, a new antifungal antibiotic. Can J Physiol Pharmacol. 55:48–51.

May, R.C., Kelly, R.A. and Mitch, W.E., 1987. Mechanisms for defects in muscle protein metabolism in rats with chronic uremia. Influence of metabolic acidosis. The Journal of clinical investigation, 79(4), pp.1099-1103.

McCormack, S.E., Shaham, O., McCarthy, M.A., Deik, A.A., Wang, T.J., Gerszten, R.E., Clish, C.B., Mootha, V.K., Grinspoon, S.K. and Fleischman, A., 2013. Circulating branched-chain amino acid concentrations are associated with obesity and future insulin resistance in children and adolescents. *Pediatric obesity*, *8*(1), pp.52-61.

Meng, Z.X., Li, S., Wang, L., Ko, H.J., Lee, Y., Jung, D.Y., Okutsu, M., Yan, Z., Kim, J.K. and Lin, J.D., 2013. Baf60c drives glycolytic metabolism in the muscle and improves systemic glucose homeostasis through Deptor-mediated Akt activation. *Nature medicine*, *19*(5), p.640.

Meshkani, R. and Adeli, K., 2009. Hepatic insulin resistance, metabolic syndrome and cardiovascular disease. Clinical biochemistry, 42(13-14), pp.1331-1346.

Moghei, M., Tavajohi-Fini, P., Beatty, B. and Adegoke, O.A., 2016. Ketoisocaproic acid, a metabolite of leucine, suppresses insulin-stimulated glucose transport in skeletal muscle cells in a BCAT2-dependent manner. American Journal of Physiology-Cell Physiology, 311(3), pp.C518-C527.

Morato, p.N., Lollo, p.C.B., Moura, C.S., Batista, T.M., Carneiro, E.M. and Amaya-Farfan, J., 2013. A dipeptide and an amino acid present in whey protein hydrolysate increase translocation of GLUT-4 to the plasma membrane in Wistar rats. *Food chemistry*, *139*(1-4), pp.853-859.

Moran, J.L., Li, Y., Hill, A.A., Mounts, W.M. and Miller, C.P., 2002. Gene expression changes during mouse skeletal myoblast differentiation revealed by transcriptional profiling. Physiological genomics, 10(2), pp.103-111.

Morino ,K., Petersen, K.F., and Shulman, G.I., (2006) Molecular mechanisms of insulin resistance in humans and their potential links with mitochondrial dysfunction. *Diabetes* 55:S9 –S15.

Naylor, S.L. and Shows, T.B., 1980. Branched-chain aminotransferase deficiency in Chinese hamster cells complemented by two independent genes on human chromosomes 12 and 19. *Somatic cell genetics*, *6*(5), pp.641-652.

Nedachi, T. and Kanzaki, M., 2006. Regulation of glucose transporters by insulin and extracellular glucose in C 2 C 12 myotubes. *American Journal of Physiology-Endocrinology and Metabolism*, *291*(4), pp.E817-E828.

Newgard, C.B., An, J., Bain, J.R., Muehlbauer, M.J., Stevens, R.D., Lien, L.F.,

Haqq, A.M., Shah, S.H., Arlotto, M., Slentz, C.A. and Rochon, J., 2009. A branched-chain amino acid-related metabolic signature that differentiates obese and lean humans and contributes to insulin resistance. *Cell metabolism*, *9*(4), pp.311-326.

Nishitani, S., Matsumura, T., Fujitani, S., Sonaka, I., Miura, Y. and Yagasaki, K., 2002. Leucine promotes glucose uptake in skeletal muscles of rats. *Biochemical and biophysical research communications*, *299*(5), pp.693-696.

Nishitani, S., Takehana, K., Fujitani, S. and Sonaka, I., 2005. Branched-chain amino acids improve glucose metabolism in rats with liver cirrhosis. *American Journal of Physiology-Gastrointestinal and Liver Physiology*, *288*(6), pp.G1292-G1300.

Nogueira, V., Park, Y., Chen, C.C., Xu, p.Z., Chen, M.L., Tonic, I., Unterman, T. and Hay, N., 2008. Akt determines replicative senescence and oxidative or oncogenic premature senescence and sensitizes cells to oxidative apoptosis.*Cancer cell*, *14*(6), pp.458-470.

Ouwens, D.M., Withers, D.J., Alessi, D.R. and Shepherd, p.R., 1999. Mammalian target of rapamycin is a direct target for protein kinase B: identification of a convergence point for opposing effects of insulin and amino-acid deficiency on protein translation. *Biochemical Journal*,*344*(2), pp.427-431.

Palomeque, J., Chemaly, E.R., Colosi, p., Wellman, J.A., Zhou, S., Del Monte, F. and Hajjar, R.J., 2007. Efficiency of eight different AAV serotypes in transducing rat myocardium in vivo. *Gene therapy*, *14*(13), p.989.

Parmigiani, A., Nourbakhsh, A., Ding, B., Wang, W., Kim, Y.C., Akopiants, K., Guan, K.L., Karin, M. and Budanov, A.V., 2014. Sestrins inhibit mTORC1 kinase activation through the GATOR complex. *Cell reports*, *9*(4), pp.1281-1291.

Peng, M., Yin, N. and Li, M.O., 2014. Sestrins function as guanine nucleotide dissociation inhibitors for Rag GTPases to control mTORC1 signaling. *Cell*, *159*(1), pp.122-133.

Peng, N., Meng, N., Wang, S., Zhao, F., Zhao, J., Su, L., Zhang, S., Zhang, Y., Zhao, B. and Miao, J., 2014. An activator of mTOR inhibits oxLDL-induced autophagy and apoptosis in vascular endothelial cells and restricts atherosclerosis in apolipoprotein E-/-mice. *Scientific reports*, *4*.

Pereira, M.J., Palming, J., Rizell, M., Aureliano, M., Carvalho, E., Svensson, M.K. and Eriksson, J.W., 2012. mTOR inhibition with rapamycin causes impaired insulin signalling and glucose uptake in human subcutaneous and omental adipocytes. Molecular and cellular endocrinology,355(1), pp.96-105.

Petersen, K.F. and Shulman, G.I., 2006. Etiology of insulin resistance. *The*

American journal of medicine, *119*(5), pp.S10-S16.

Peterson, R.T., Beal, p.A., Comb, M.J. and Schreiber, S.L., 2000. FKBP12-rapamycin-associated protein (FRAP) autophosphorylates at serine 2481 under translationally repressive conditions. *Journal of Biological Chemistry*,*275*(10), pp.7416-7423.

Peyrollier, k., Hajduch, E., Blair, A. S., Russell, H.Y.D.E. and Hundal, H.S., 2000. L-leucine availability regulates phosphatidylinositol 3-kinase, p70 S6 kinase and glycogen synthase kinase-3 activity in L6 muscle cells: evidence for the involvement of the mammalian target of rapamycin (mTOR) pathway in the L-leucine-induced up-regulation of system A amino acid transport. *Biochemical Journal*, *350*(2), pp.361-368.

Phung, T.L., Ziv, K., Dabydeen, D., Eyiah-Mensah, G., Riveros, M., Perruzzi, C., Sun, J., Monahan-Earley, R.A., Shiojima, I., Nagy, J.A. and Lin, M.I., 2006. Pathological angiogenesis is induced by sustained Akt signaling and inhibited by rapamycin. *Cancer cell*, *10*(2), pp.159-170.

Pietiläinen, K.H., Naukkarinen, J., Rissanen, A., Saharinen, J., Ellonen, p., Keränen, H., Suomalainen, A., Götz, A., Suortti, T., Yki-Järvinen, H. and Orešič, M., 2008. Global transcript profiles of fat in monozygotic twins discordant for BMI: pathways behind acquired obesity. PLoS medicine, 5(3), p.e51.

Ploug, T., Van Deurs, B., Ai, H., Cushman, S.W. and Ralston, E., 1998. Analysis of GLUT4 distribution in whole skeletal muscle fibers: identification of distinct storage compartments that are recruited by insulin and muscle contractions. *The Journal of cell biology*, *142*(6), pp.1429-1446.

Pópulo, H., Lopes, J.M. and Soares, p., 2012. The mTOR signalling pathway in human cancer. *International journal of molecular sciences*, *13*(2), pp.1886-1918.

Rachdi, L., Balcazar, N., Osorio-Duque, F., Elghazi, L., Weiss, A., Gould, A., Chang-Chen, K.J., Gambello, M.J. and Bernal-Mizrachi, E., 2008. Disruption of Tsc2 in pancreatic β cells induces β cell mass expansion and improved glucose tolerance in a TORC1-dependent manner. *Proceedings of the National Academy of Sciences*, *105*(27), pp.9250-9255.

Rawat, A.K., Korthikunta, V., Gautam, S., Pal, S., Tadigoppula, N., Tamrakar, A.K. and Srivastava, A.K., 2014. 4-Hydroxyisoleucine improves insulin resistance by promoting mitochondrial biogenesis and act through AMPK and Akt dependent pathway. *Fitoterapia*, *99*, pp.307-317.

Redpath, N.T., Foulstone, E.J. and Proud, C.G., 1996. Regulation of translation elongation factor-2 by insulin via a rapamycin-sensitive signalling pathway. *The EMBO journal*,*15*(9), pp.2291-2297.

Renguet, E., Ginion, A., Gélinas, R., Bultot, L., Auquier, J., Robillard Frayne, I., Daneault, C., Vanoverschelde, J.L., Des Rosiers, C., Hue, L. and Horman, S., 2017. Metabolism and acetylation contribute to leucine-mediated inhibition of cardiac glucose uptake. *American Journal of Physiology-Heart and Circulatory Physiology*, *313*(2), pp.H432-H445.

Richter, E.A. and Hargreaves, M., 2013. Exercise, GLUT4, and skeletal muscle glucose uptake. Physiological reviews, 93(3), pp.993-1017.

Rietman, A., Schwarz, J., Tomé, D., Kok, F.J. and Mensink, M., 2014. High dietary protein intake, reducing or eliciting insulin resistance?. *European journal of clinical nutrition*, *68*(9), p.973.

Rietman, A., 2015. Effect of dietary protein on lipid and glucose metabolism: implications for metabolic health. Wageningen University.

Röder, p.V., Wu, B., Liu, Y. and Han, W., 2016. Pancreatic regulation of glucose homeostasis. Experimental & molecular medicine, 48(3), p.e219.

Rodríguez-Lázaro, D. and Hernández, M. (2013). Introduction to the Real-time PCR In Real-Time PCR in Food Science: Current Technology and Applications. D. Rodriguez-Lazaro, ed. (Norfolk, UK: Caister Academic Press). ISBN: 978-1-908230-15-7.

Rosenthal, J., Angel, A. and Farkas, J., 1974. Metabolic fate of leucine: a significant sterol precursor in adipose tissue and muscle. *American Journal of Physiology--Legacy Content*, *226*(2), pp.411-418.

Ryder, J.W., Chibalin, A.V. and Zierath, J.R., 2001. Intracellular mechanisms underlying increases in glucose uptake in response to insulin or exercise in skeletal muscle. *Acta physiologica Scandinavica*, *171*(3), pp.249-257.

Sadiq, F., Hazlerigg, D.G. and Lomax, M.A., 2007. Amino acids and insulin act additively to regulate components of the ubiquitin-proteasome pathway in C2C12 myotubes. *BMC molecular biology*, *8*(1), p.23.

Sancak, Y., Thoreen, C.C., Peterson, T.R., Lindquist, R.A., Kang, S.A., Spooner, E., Carr, S.A. and Sabatini, D.M., 2007. PRAS40 is an insulin-regulated inhibitor of the mTORC1 protein kinase. *Molecular cell*, *25*(6), pp.903-915.

Sanli, T., Linher-Melville, K., Tsakiridis, T. and Singh, G., 2012. Sestrin2 modulates AMPK subunit expression and its response to ionizing radiation in breast cancer cells. *PloS one*,*7*(2), p.e32035.

Saha, A.K., Xu, X.J., Lawson, E., Deoliveira, R., Brandon, A.E., Kraegen, E.W. and Ruderman, N.B., 2010. Downregulation of AMPK accompanies leucine-and

glucose-induced increases in protein synthesis and insulin resistance in rat skeletal muscle. Diabetes, 59(10), pp.2426-2434.

Sarbassov, D.D., Ali, S.M., Kim, D.H., Guertin, D.A., Latek, R.R., Erdjument-Bromage, H., Tempst, p. and Sabatini, D.M., 2004. Rictor, a novel binding partner of mTOR, defines a rapamycin-insensitive and raptor-independent pathway that regulates the cytoskeleton. *Current biology*, *14*(14), pp.1296-1302.

Sarbassov, D.D., Ali, S.M., Sengupta, S., Sheen, J.H., Hsu, p.p., Bagley, A.F., Markhard, A.L. and Sabatini, D.M., 2006. Prolonged rapamycin treatment inhibits mTORC2 assembly and Akt/PKB. *Molecular cell*, *22*(2), pp.159-168.

Sarbassov, D.D., Guertin, D.A., Ali, S.M. and Sabatini, D.M., 2005. Phosphorylation and regulation of Akt/PKB by the rictor-mTOR complex. *Science*, *307*(5712), pp.1098-1101.

Schnuck, J.K., Sunderland, K.L., Gannon, N.p., Kuennen, M.R. and Vaughan, R.A., 2016. Leucine stimulates PPARβ/δ-dependent mitochondrial biogenesis and oxidative metabolism with enhanced GLUT4 content and glucose uptake in myotubes. *Biochimie*, *128*, pp.1-7.

Sehgal SN, Baker H, Vézina C. 1975 Rapamycin (AY-22,989), a new antifungal antibiotic. II. Fermentation, isolation and characterization. J Antibiot (Tokyo) 28:727–732. doi: 10.7164/antibiotics.28.727.

Sekiguchi, T., Hirose, E., Nakashima, N., Ii, M. and Nishimoto, T., 2001. Novel G proteins, Rag C and Rag D, interact with GTP-binding proteins, Rag A and Rag B. *Journal of Biological Chemistry*, *276*(10), pp.7246-7257.

Shackelford, D.B. and Shaw, R.J., 2009. The LKB1–AMPK pathway: metabolism and growth control in tumour suppression. *Nature Reviews Cancer*, *9*(8), p.563.

Shah, S.H., Crosslin, D.R., Haynes, C.S., Nelson, S., Turer, C.B., Stevens, R.D., Muehlbauer, M.J., Wenner, B.R., Bain, J.R., Laferrere, B. and Gorroochurn, p., 2012. Branched-chain amino acid levels are associated with improvement in insulin resistance with weight loss. *Diabetologia*, *55*(2), pp.321-330.

Shaham, O., Wei, R., Wang, T.J., Ricciardi, C., Lewis, G.D., Vasan, R.S., Carr, S.A., Thadhani, R., Gerszten, R.E. and Mootha, V.K., 2008. Metabolic profiling of the human response to a glucose challenge reveals distinct axes of insulin sensitivity. *Molecular systems biology*, *4*(1), p.214.

She, p., Reid, T.M., Bronson, S.K., Vary, T.C., Hajnal, A., Lynch, C.J. and Hutson, S.M., 2007A. Disruption of BCATm in mice leads to increased energy expenditure associated with the activation of a futile protein turnover cycle.Cell metabolism, 6(3), pp.181-194.

She, p., Van Horn, C., Reid, T., Hutson, S.M., Cooney, R.N. and Lynch, C.J., 2007B. Obesity-related elevations in plasma leucine are associated with alterations in enzymes involved in branched-chain amino acid metabolism.American Journal of Physiology-Endocrinology and Metabolism, 293(6), pp.E1552-E1563.

Shigeyama, Y., Kobayashi, T., Kido, Y., Hashimoto, N., Asahara, S.I., Matsuda, T., Takeda, A., Inoue, T., Shibutani, Y., Koyanagi, M. and Uchida, T., 2008. Biphasic response of pancreatic β-cell mass to ablation of tuberous sclerosis complex 2 in mice. *Molecular and cellular biology*, *28*(9), pp.2971-2979.

Shimomura, Y., Murakami, T., Nakai, N., Nagasaki, M. and Harris, R.A., 2004. Exercise promotes BCAA catabolism: effects of BCAA supplementation on skeletal muscle during exercise. *The Journal of nutrition*, *134*(6), pp.1583S-1587S.

Sipula, I.J., Brown, N.F. and Perdomo, G., 2006. Rapamycin-mediated inhibition of mammalian target of rapamycin in skeletal muscle cells reduces glucose utilization and increases fatty acid oxidation. *Metabolism*, *55*(12), pp.1637-1644.

Suryawan, A., Hawes, J.W., Harris, R.A., Shimomura, Y., Jenkins, A.E. and Hutson, S.M., 1998. A molecular model of human branched-chain amino acid metabolism. The American journal of clinical nutrition, 68(1), pp.72-81.

Taborsky Jr, G.J., 2010. The physiology of glucagon.

Tai, E.S., Tan, M.L.S., Stevens, R.D., Low, Y.L., Muehlbauer, M.J., Goh, D.L.M., Ilkayeva, O.R., Wenner, B.R., Bain, J.R., Lee, J.J.M. and Lim, S.C., 2010. Insulin resistance is associated with a metabolic profile of altered protein metabolism in Chinese and Asian-Indian men. Diabetologia, 53(4), pp.757-767.

Tee, A.R., Manning, B.D., Roux, p.p., Cantley, L.C. and Blenis, J., 2003. Tuberous sclerosis complex gene products, Tuberin and Hamartin, control mTOR signaling by acting as a GTPase-activating protein complex toward Rheb. *Current biology*, *13*(15), pp.1259-1268.

Tischler, M.E. and Goldberg, A.L., 1980. Leucine degradation and release of glutamine and alanine by adipose tissue. *Journal of Biological Chemistry*, *255*(17), pp.8074-8081.

Tom, A. and Nair, K.S., 2006. Assessment of branched-chain amino acid status and potential for biomarkers. The Journal of nutrition, 136(1), pp.324S-330S.

Tortorella, L.L. and Pilch, P.F., 2002. C2C12 myocytes lack an insulin-responsive vesicular compartment despite dexamethasone-induced GLUT4 expression. American Journal of Physiology-Endocrinology and Metabolism,

283(3), pp.E514-E524.

Tremblay, F. and Marette, A., 2001. Amino acid and insulin signaling via the mTOR/p70 S6 kinase pathway A negative feedback mechanism leading to insulin resistance in skeletal muscle cells. *Journal of Biological Chemistry*, *276*(41), pp.38052-38060.

Tremblay, F., Brûlé, S., Um, S.H., Li, Y., Masuda, K., Roden, M., Sun, X.J., Krebs, M., Polakiewicz, R.D., Thomas, G. and Marette, A., 2007b. Identification of IRS-1 Ser-1101 as a target of S6K1 in nutrient-and obesity-induced insulin resistance.*Proceedings of the National Academy of Sciences*, *104*(35), pp.14056-14061.

Tremblay, F., Gagnon, A., Veilleux, A., Sorisky, A. and Marette, A., 2005a. Activation of the mammalian target of rapamycin pathway acutely inhibits insulin signaling to Akt and glucose transport in 3T3-L1 and human adipocytes. *Endocrinology*, *146*(3), pp.1328-1337.

Tremblay, F., Krebs, M., Dombrowski, L., Brehm, A., Bernroider, E., Roth, E., Nowotny, p., Waldhäusl, W., Marette, A. and Roden, M., 2005b. Overactivation of S6 kinase 1 as a cause of human insulin resistance during increased amino acid availability. *Diabetes*, *54*(9), pp.2674-2684.

Tremblay, F., Lavigne, C., Jacques, H. and Marette, A., 2007a. Role of dietary proteins and amino acids in the pathogenesis of insulin resistance. *Annu. Rev. Nutr.*, *27*, pp.293-310.

Tzatsos, A. and Kandror, K.V., 2006. Nutrients suppress phosphatidylinositol 3-kinase/Akt signaling via raptor-dependent mTOR-mediated insulin receptor substrate 1 phosphorylation. *Molecular and cellular biology*, *26*(1), pp.63-76.

Ueyama, A., Yaworsky, K.L., Wang, Q., Ebina, Y. and Klip, A., 1999. GLUT-4myc ectopic expression in L6 myoblasts generates a GLUT-4-specific pool conferring insulin sensitivity. *American Journal of Physiology-Endocrinology And Metabolism*, *277*(3), pp.E572-E578.

Um, S.H., D'Alessio, D. and Thomas, G., 2006. Nutrient overload, insulin resistance, and ribosomal protein S6 kinase 1, S6K1. *Cell metabolism*, *3*(6), pp.393-402.

Um, S.H., Frigerio, F., Watanabe, M., Picard, F., Joaquin, M., Sticker, M., Fumagalli, S., Allegrini, p.R., Kozma, S.C., Auwerx, J. and Thomas, G., 2004. Absence of S6K1 protects against age-and diet-induced obesity while enhancing insulin sensitivity. *Nature*, *431*(7005), p.200.

Vander Haar, E., Lee, S.I., Bandhakavi, S., Griffin, T.J. and Kim, D.H., 2007.

Insulin signalling to mTOR mediated by the Akt/PKB substrate PRAS40. *Nature cell biology*, *9*(3), p.316.

Vaughan, R.A., Garcia-Smith, R., Gannon, N.P., Bisoffi, M., Trujillo, K.A. and Conn, C.A., 2013. Leucine treatment enhances oxidative capacity through complete carbohydrate oxidation and increased mitochondrial density in skeletal muscle cells. Amino acids, 45(4), pp.901-911.

Vergès, B. and Cariou, B., 2015. mTOR inhibitors and diabetes. Diabetes Research and Clinical Practice, 110(2), pp.101-108.

Vigene Biosciences. Product Manual for AAV systems. 2016 [on-line]. Available at: https://www.vigenebio.com/uploads/AAVUserManual.pdf [Accessed 15 Dec 2018]

Wallace, T.M., Levy, J.C. and Matthews, D.R., 2004. Use and abuse of HOMA modeling. *Diabetes care*, *27*(6), pp.1487-1495.

Wang, D., Zhong, L., Nahid, M.A. and Gao, G., 2014. The potential of adeno-associated viral vectors for gene delivery to muscle tissue. *Expert opinion on drug delivery*, *11*(3), pp.345-364.

Wang, Q. and Holst, J., 2015. L-type amino acid transport and cancer: targeting the mTORC1 pathway to inhibit neoplasia.*American journal of cancer research*, *5*(4), p.1281.

Wang, T.J., Larson, M.G., Vasan, R.S., Cheng, S., Rhee, E.p., McCabe, E., Lewis, G.D., Fox, C.S., Jacques, p.F., Fernandez, C. and O'Donnell, C.J., 2011. Metabolite profiles and the risk of developing diabetes. Nature medicine, 17(4), pp.448-453.

Wang, X., Hu, Z., Hu, J., Du, J. and Mitch, W.E., 2006. Insulin resistance accelerates muscle protein degradation: activation of the ubiquitin-proteasome pathway by defects in muscle cell signaling. *Endocrinology*, *147*(9), pp.4160-4168.

Wang, X., Li, M., Gao, Y., Gao, J., Yang, W., Liang, H., Ji, Q., Li, Y., Liu, H., Huang, J. and Cheng, T., 2016. Rheb1-mTORC1 maintains macrophage differentiation and phagocytosis in mice. *Experimental cell research*, *344*(2), pp.219-228.

Watanabe-Asano, T., Kuma, A. and Mizushima, N., 2014. Cycloheximide inhibits starvation-induced autophagy through mTORC1 activation.Biochemical and biophysical research communications, 445(2), pp.334-339.

Werner, E.D., Lee, J., Hansen, L., Yuan, M. and Shoelson, S.E., 2004. Insulin resistance due to phosphorylation of insulin receptor substrate-1 at serine

302. *Journal of Biological Chemistry*, *279*(34), pp.35298-35305.

White, P.J. and Newgard, C.B., 2019. Branched-chain amino acids in disease. Science, 363(6427), pp.582-583.

WHO. 2018. Diabetes [on-line]. Available at: http://www.who.int/diabetes/en/ [Accessed 15 Nov 2017]

Wieman, H.L., Wofford, J.A. and Rathmell, J.C., 2007. Cytokine stimulation promotes glucose uptake via phosphatidylinositol-3 kinase/Akt regulation of Glut1 activity and trafficking. Molecular biology of the cell, 18(4), pp.1437-1446.

Wolfson, R.L., Chantranupong, L., Saxton, R.A., Shen, K., Scaria, S.M., Cantor, J.R. and Sabatini, D.M., 2016. Sestrin2 is a leucine sensor for the mTORC1 pathway. *Science*,*351*(6268), pp.43-48.

Wolfe, R.R., 2017. Branched-chain amino acids and muscle protein synthesis in humans: myth or reality?. Journal of the International Society of Sports Nutrition, 14(1), p.30.

Wood, I.S. and Trayhurn, P., 2003. Glucose transporters (GLUT and SGLT): expanded families of sugar transport proteins. British journal of nutrition, 89(1), pp.3-9.

Wu, K., Tian, R., Huang, J., Yang, Y., Dai, J., Jiang, R. and Zhang, L., 2018. Metformin alleviated endotoxemia-induced acute lung injury via restoring AMPK-dependent suppression of mTOR. *Chemico-biological interactions*.

Würtz, p., Mäkinen, V.p., Soininen, p., Kangas, A.J., Tukiainen, T., Kettunen, J., Savolainen, M.J., Tammelin, T., Viikari, J.S., Rönnemaa, T. and Kähönen, M., 2012. Metabolic signatures of insulin resistance in 7,098 young adults. *Diabetes*, p.DB_111355.

Xiao, F., Huang, Z., Li, H., Yu, J., Wang, C., Chen, S., Meng, Q., Cheng, Y., Gao, X., Li, J. and Liu, Y., 2011. Leucine deprivation increases hepatic insulin sensitivity via GCN2/mTOR/S6K1 and AMPK pathways. *Diabetes*, p.DB_101246.

Yamauchi, K., Sakurai, H., Kimura, T., Wiriyasermkul, p., Nagamori, S., Kanai, Y. and Kohno, N., 2009. System L amino acid transporter inhibitor enhances anti-tumor activity of cisplatin in a head and neck squamous cell carcinoma cell line.*Cancer letters*, *276*(1), pp.95-101.

Yang, Q. and Guan, K.L., 2007. Expanding mTOR signaling.*Cell research*, *17*(8), p.666.

Yap, A., Nishiumi, S., Yoshida, K.I. and Ashida, H., 2007. Rat L6 myotubes as an in vitro model system to study GLUT4-dependent glucose uptake stimulated by inositol derivatives. *Cytotechnology*, *55*(2), pp.103-108.

Ye, J., 2013. Mechanisms of insulin resistance in obesity. *Frontiers of medicine*, 7(1), pp.14-24.

Yoneyama, Y., Inamitsu, T., Chida, K., Iemura, S.I., Natsume, T., Maeda, T., Hakuno, F. and Takahashi, S.I., 2018. Serine phosphorylation by mTORC1 promotes IRS-1 degradation through SCFβ-TRCP E3 ubiquitin ligase. iScience, 5, pp.1-18.

Yoshizawa, F., 2012. New therapeutic strategy for amino acid medicine: notable functions of branched chain amino acids as biological regulators. *Journal of pharmacological sciences*,*118*(2), pp.149-155.

You, J.S., Anderson, G.B., Dooley, M.S. and Hornberger, T.A., 2015. The role of mTOR signaling in the regulation of protein synthesis and muscle mass during immobilization in mice. Disease models & mechanisms, 8(9), pp.1059-1069.

Zhang, Y., Gao, X., Saucedo, L.J., Ru, B., Edgar, B.A. and Pan, D., 2003. Rheb is a direct target of the tuberous sclerosis tumour suppressor proteins. *Nature cell biology*, *5*(6), p.578.

Zinzalla, V., Stracka, D., Oppliger, W. and Hall, M.N., 2011. Activation of mTORC2 by association with the ribosome. *Cell*, *144*(5), pp.757-768.

Zisman, A., Peroni, O.D., Abel, E.D., Michael, M.D., Mauvais-Jarvis, F., Lowell, B.B., Wojtaszewski, J.F., Hirshman, M.F., Virkamaki, A., Goodyear, L.J. and Kahn, C.R., 2000. Targeted disruption of the glucose transporter 4 selectively in muscle causes insulin resistance and glucose intolerance. Nature medicine, 6(8), p.924.

CHAPTER 9: APPENDIXES

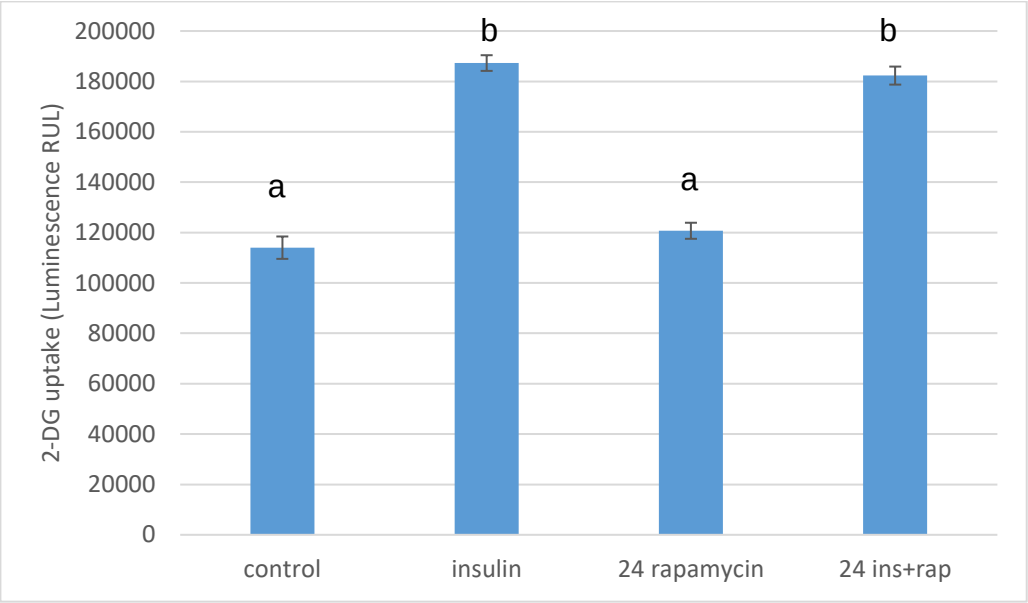


Figure 9.1 Effects of rapamycin (24h) +/- insulin on glucose uptake in L6 myotubes.

Differentiated L6 myotubes were pre-treated with or without rapamycin (100nM) for 24h and then incubated with insulin as noted for 1h before measurement of 2-DG uptake. Results are mean± SEM for n=6 wells for each treatment group. $p<0.001$ for one-way ANOVA. Means with the same letter are not different ($p>0.05$ for Bonferroni), whereas those with different letters are significantly different ($p<0.05$ for Bonferroni)

Repeat BCH experiments

These results were consistent with the BCH (glucose uptake+ western blotting) results in chapter 4 (Figure 4.16,17,18, 20, 21)

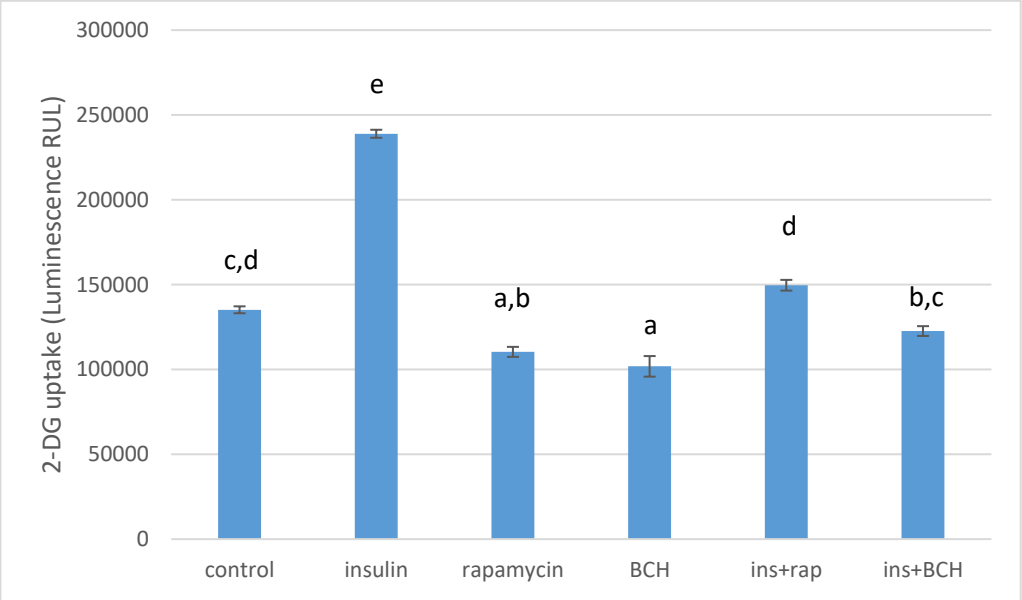
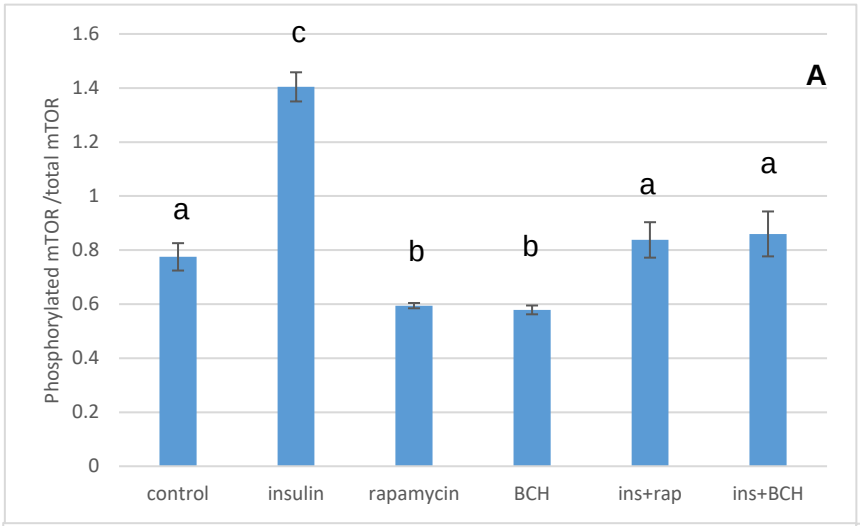
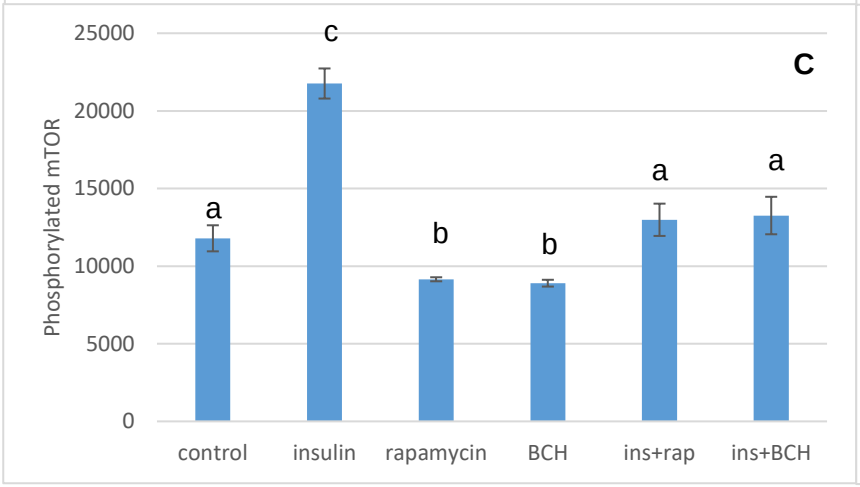


Figure 9.2 Effects of 4h rapamycin or BCH +/- insulin on glucose uptake in L6 myotubes.

Differentiated L6 myotubes were pre-treated with or without rapamycin (100nM) or BCH (25nM) for 4h and then incubated with insulin as noted for 1h before measurement of 2-DG uptake. Results are mean± SEM for n=4 wells for each treatment group. $p<0.001$ for one-way ANOVA. Means with the same letter are not different ($p>0.05$ for Bonferroni), whereas those with different letters are significantly different ($p<0.05$ for Bonferroni)



B	Control	Insulin	Rapamycin	BCH	I+R	I+B
Phosphorylated mTOR(Ser2448)						
Total mTOR						



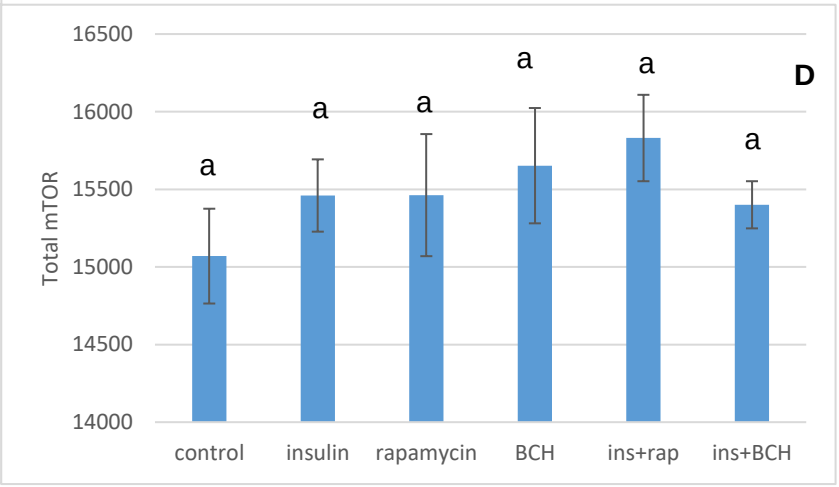


Figure 9.3 Effects of 4h rapamycin or BCH +/- 1h insulin on mTOR western blot in L6 myotubes.

Differentiated L6 myotubes were pre-treated with or without rapamycin (100nM) or BCH (25mM) for 4h and then incubated with insulin as noted for 1h. Representative western blot analysis and quantifications of A) ratio mTOR, B) western blot C) phosphorylated mTOR and D) total mTOR. Results are mean± SEM for n=3 wells for each treatment group. I+R: Ins+Rap I+B: Ins+BCH $p<0.001$ for A and C; $p=0.616$ (D) (one-way ANOVA). Means with the same letter are not different ($p>0.05$ for Bonferroni), whereas those with different letters are significantly different ($p<0.05$ for Bonferroni)

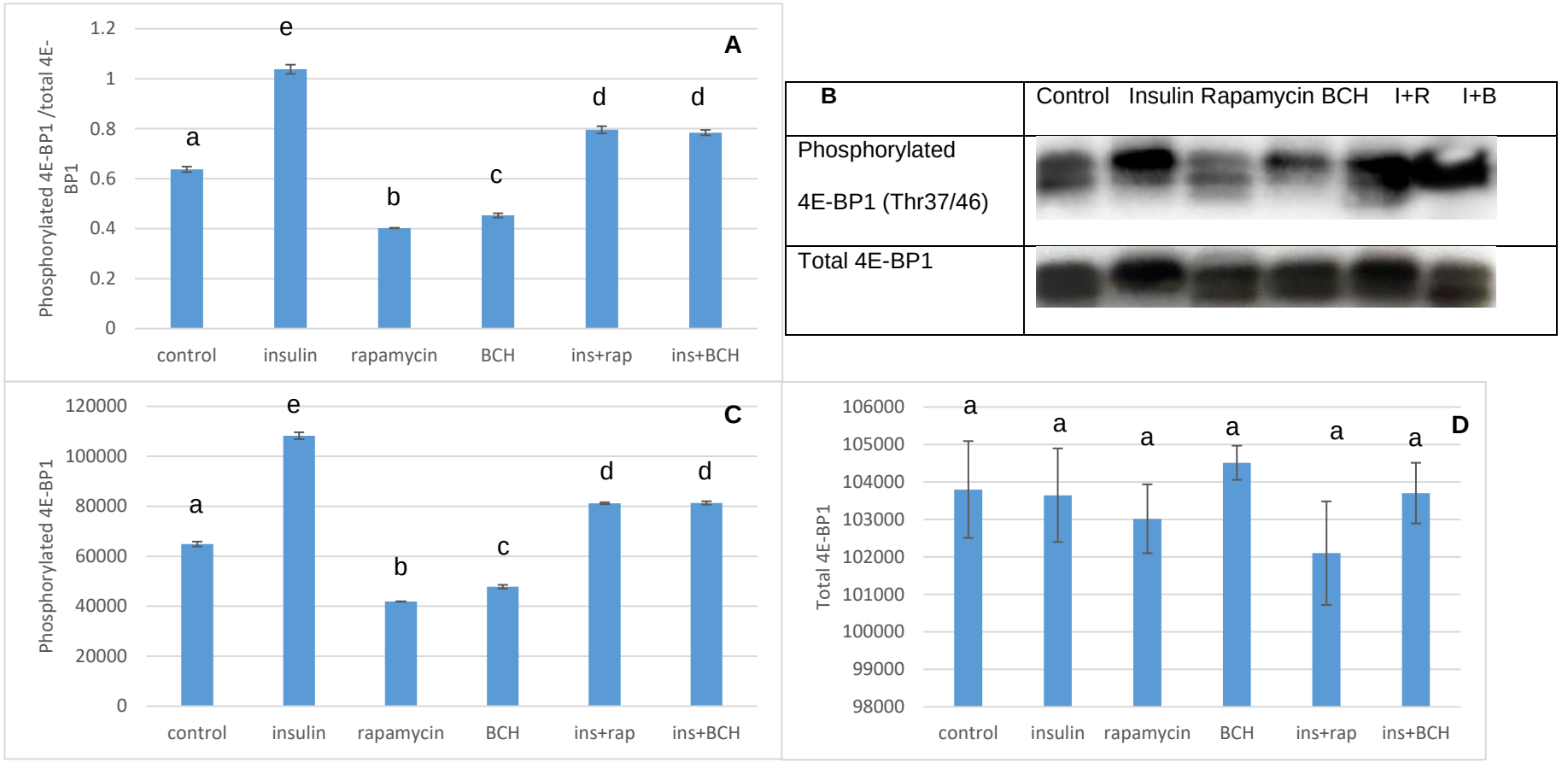
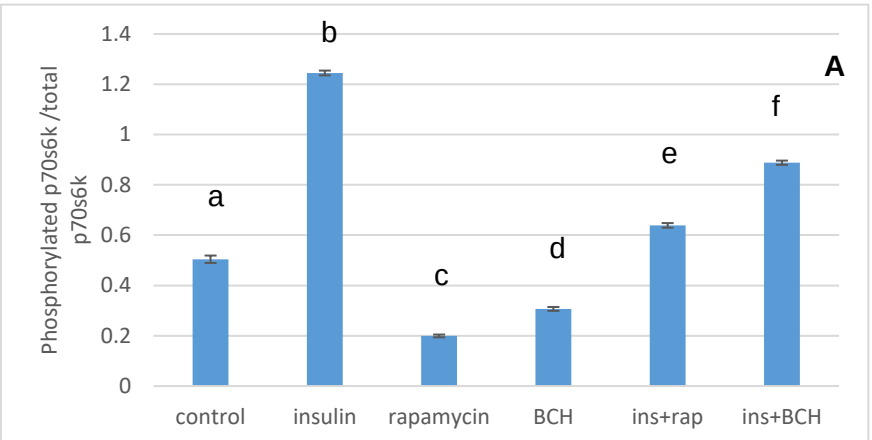
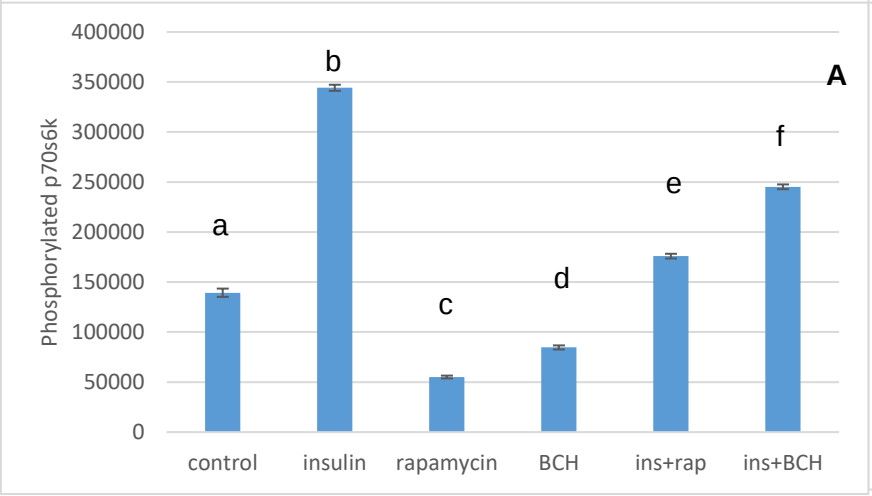


Figure 9.4 Effects of 4h rapamycin or BCH +/- 1h insulin on 4E-BP1 western blot in L6 myotubes.

Differentiated L6 myotubes were pre-treated with or without rapamycin (100nM) or BCH (25mM) for 4h and then incubated with insulin as noted for 1h. Representative western blot analysis and quantifications of A) ratio 4E-BP1, B) western blot C) phosphorylated 4E-BP1 and D) total 4E-BP1 Results are mean± SEM for n=3 wells for each treatment group. I+R: Ins+Rap I+B: Ins+BCH $p<0.001$ for A and C, $p=0.708$ (D) (one-way ANOVA). Means with the same letter are not different ($p>0.05$ for Bonferroni), whereas those with different letters are significantly different ($p<0.05$ for Bonferroni)



B	Control Insulin Rapamycin BCH I+R I+B
Phosphorylated p70S6K(Thr 389)	
Total p70S6K	



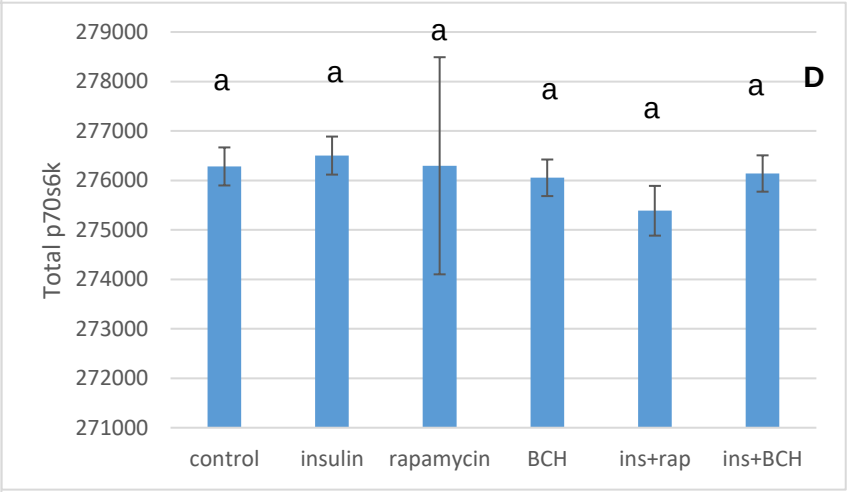
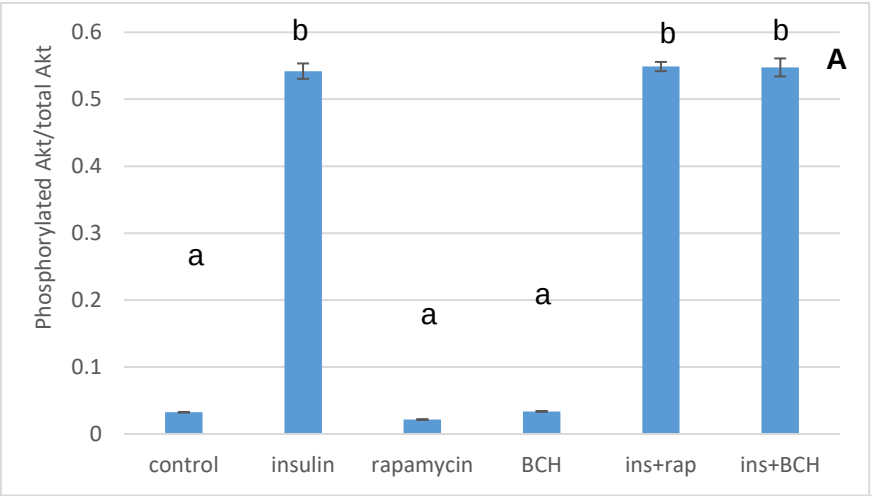
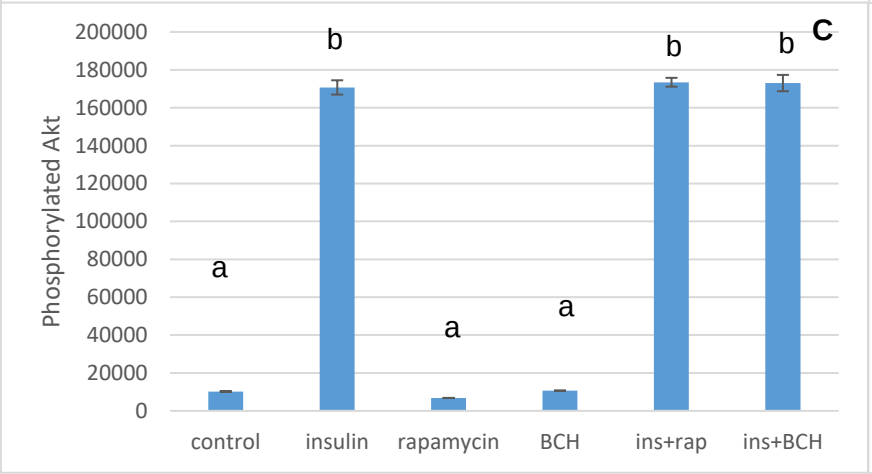


Figure 9.5 Effects of 4h rapamycin or BCH +/- 1h insulin on p70S6K western blot in L6 myotubes.

Differentiated L6 myotubes were pre-treated with or without rapamycin (100nM) or BCH (25nM) for 4h and then incubated with insulin as noted for 1h. Representative western blot analysis and quantifications of A) ratio p70S6K, B) western blot C) phosphorylated p70S6K and D) total p70S6K. Results are mean± SEM for n=3 wells for each treatment group. I+R: Ins+Rap I+B: Ins+BCH $p<0.001$ for A and C, $p=0.973$ (D) (one-way ANOVA). Means with the same letter are not different ($p>0.05$ for Bonferroni), whereas those with different letters are significantly different ($p<0.05$ for Bonferroni).



B	Control Insulin Rapamycin BCH I+R I+B
Phosphorylated Akt Ser473	
Total Akt	



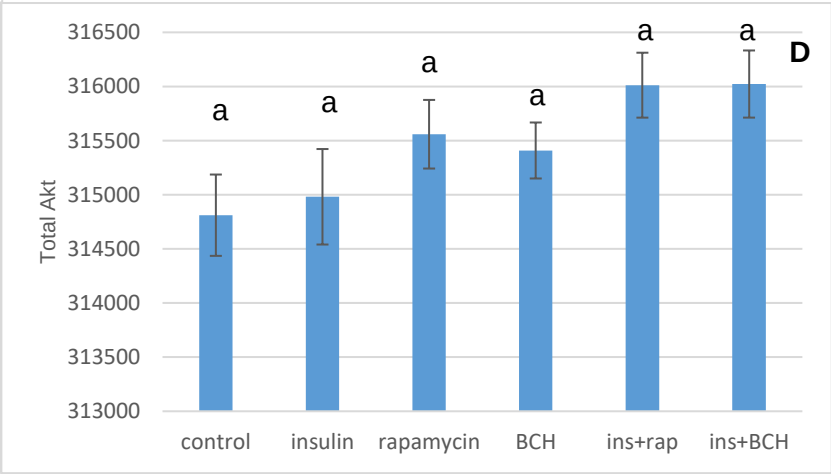


Figure 9.6 Effects of 4h rapamycin or BCH +/- 1h insulin on Akt western blot in L6 myotubes.

Differentiated L6 myotubes were pre-treated with or without rapamycin (100nM) or BCH (25nM) for 4h and then incubated with insulin as noted for 1h. Representative western blot analysis and quantifications of A) ratio Akt, B) western blot C) phosphorylated Akt and D) total Akt. Results are mean± SEM for n=3 wells for each treatment group. I+R: Ins+Rap I+B: Ins+BCH $p<0.001$ for A and C; $p=0.118$ (D) (one-way ANOVA). Means with the same letter are not different ($p>0.05$ for Bonferroni), whereas those with different letters are significantly different ($p<0.05$ for Bonferroni).

Repeat leucine experiments

These results were consistent with the leucine (glucose uptake+ western blotting) results in chapter 5 (Figure 5.2-10)

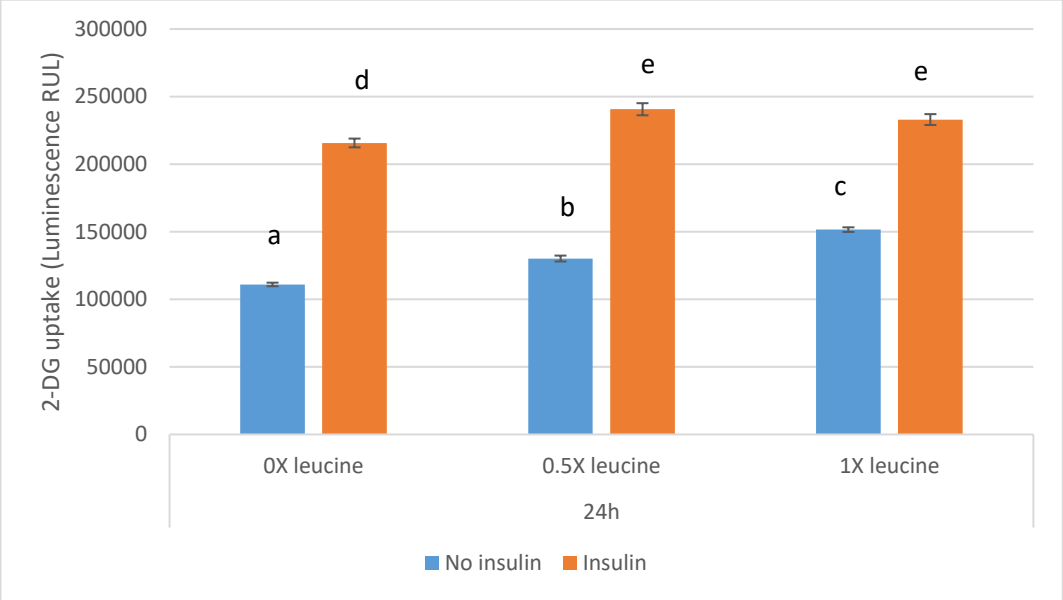


Figure 9.7 Effects of 24 hours treatment with different concentrations of leucine +/- 1 hour insulin on glucose uptake in L6 myotubes

Differentiated L6 myotubes were pre-treated with or without different leucine concentrations (0x, 0.5x,1x) for 24h and then incubated with insulin as noted or equivalent volume of vehicle control for 1h before measurement of 2-DG uptake. Results are mean± SEM for n=6 wells for each treatment group. $p<0.001$ (insulin x leucine). Means with the same letter are not different ($p>0.05$ for Bonferroni), whereas those with different letters are significantly different ($p<0.05$ for Bonferroni)

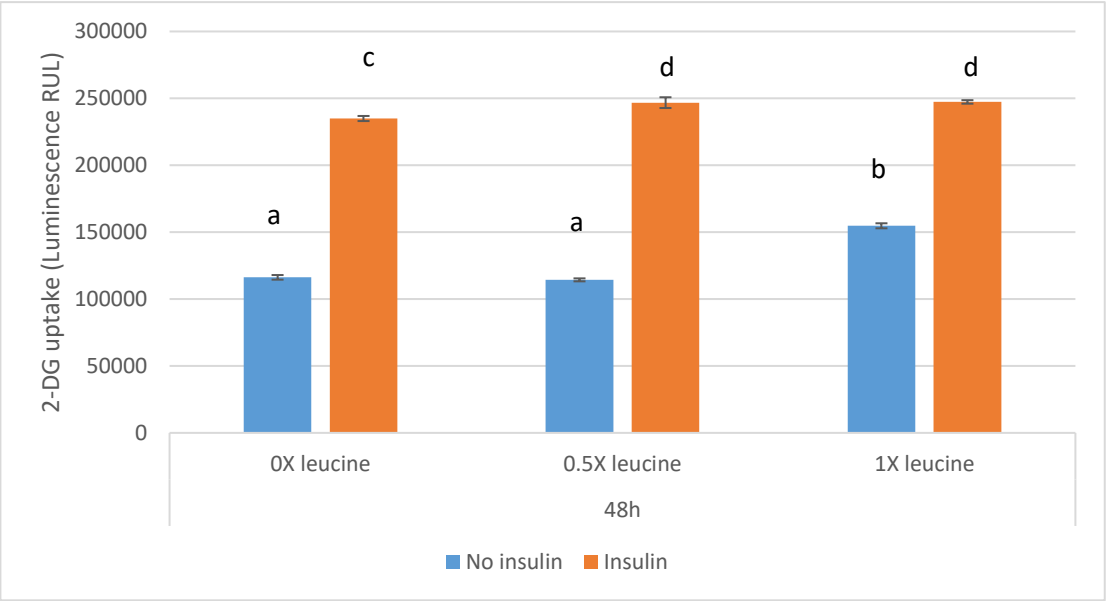
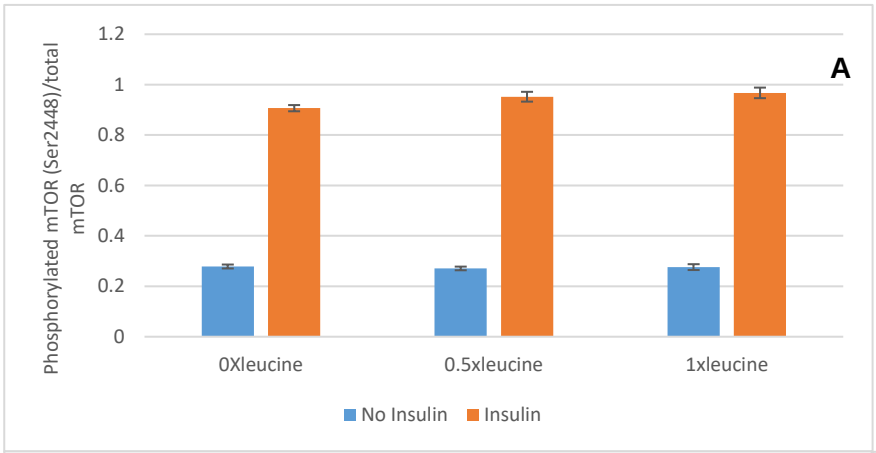
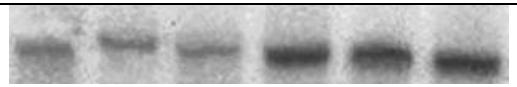
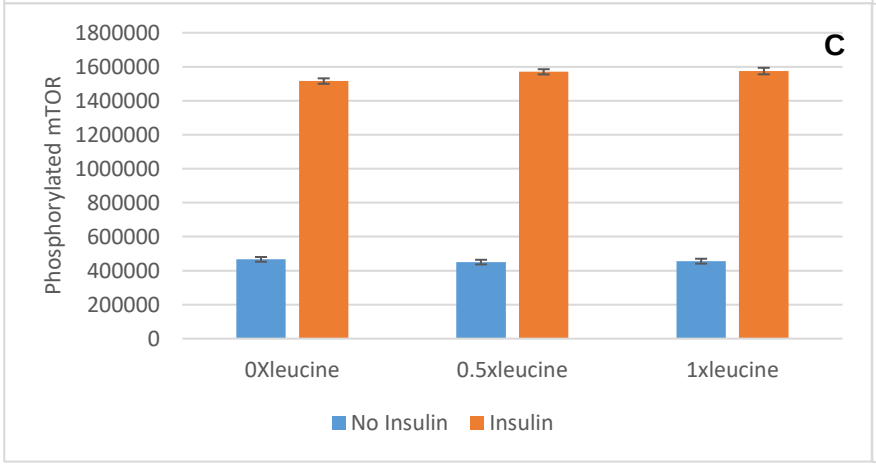


Figure 9.8 Effects of 48 hours treatment with different concentrations of leucine +/- 1 hour insulin on glucose uptake in L6 myotubes

Differentiated L6 myotubes were pre-treated with or without different leucine concentrations (0x, 0.5x,1x) for 48h and then incubated with insulin as noted or equivalent volume of vehicle control for 1h before measurement of 2-DG uptake. Results are mean± SEM for n=6 wells for each treatment group. $p<0.001$ insulin x leucine. Means with the same letter are not different ($p>0.05$ for Bonferroni), whereas those with different letters are significantly different ($p<0.05$ for Bonferroni)



24h B	0leu 0.5leu 1leu 0 ins x leu 0.5 ins x leu 1 ins x leu
Phosphorylated mTOR (Ser2448)	
Total mTOR	



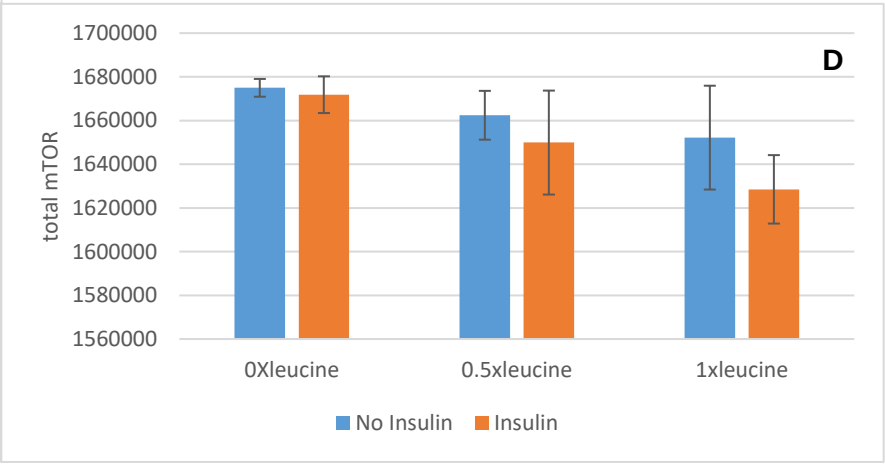
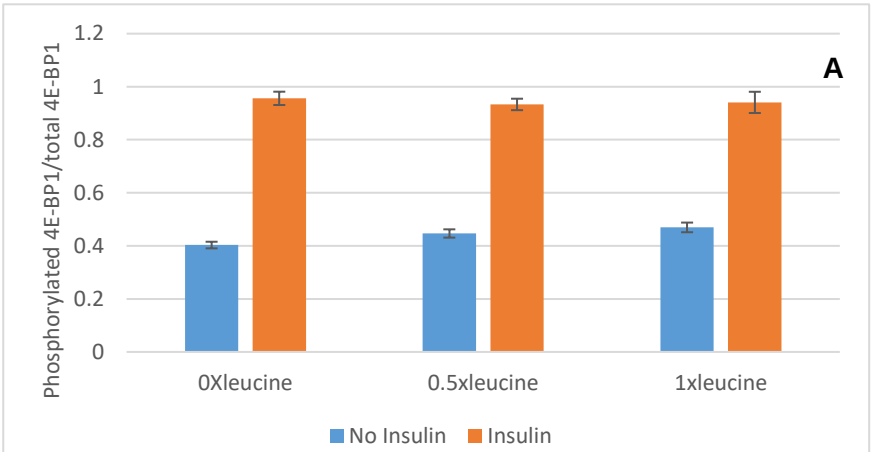
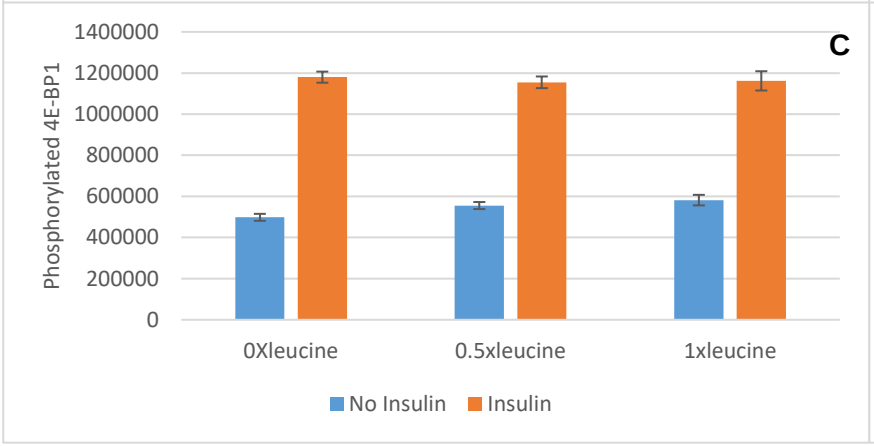


Figure 9.9 Effects of 24 hours treatment with different concentrations of leucine +/- 1 hour insulin on mTOR activity in L6 myotubes

Differentiated L6 myotubes were pre-treated with or without different leucine concentrations (0x, 0.5x,1x) for 24h, and then incubated with insulin as noted for 1h or equivalent volume of vehicle control. A) phospho/ total mTOR ratio, B) example western blots, C) phosphorylated mTOR and D) total mTOR. Results are mean± SEM for n=3 wells for each treatment group. A: $p<0.001$ for insulin only C: $p<0.001$ for insulin only; D: $p=0.822$, insulin x leucine; $p=0.344$, insulin; $p=0.17$, leucine.



24h B	0leu 0.5leu 1leu 0 ins x leu 0.5 ins x leu 1 ins x leu
Phosphorylated 4E-BP1	
Total 4E-BP1	



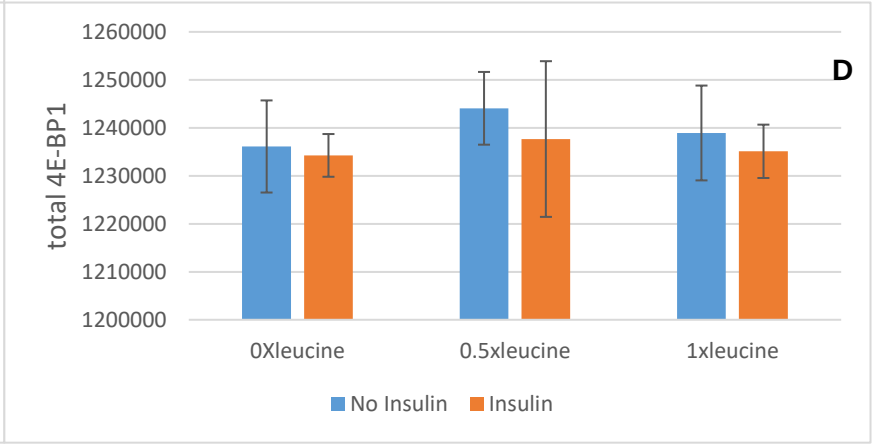
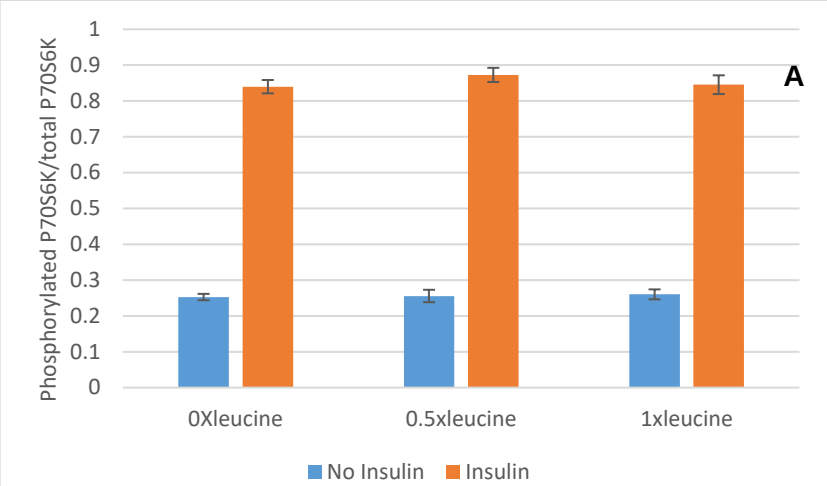
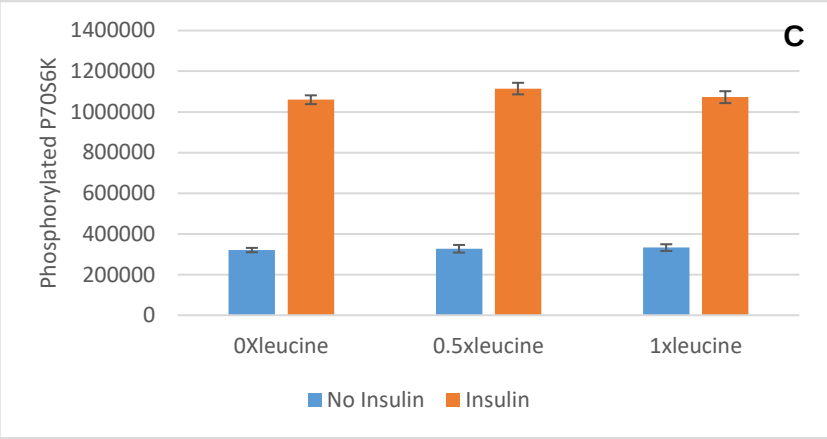


Figure 9.10 Effects of 24 hours treatment with different concentrations of leucine +/- 1 hour insulin on 4E-BP1 activity in L6 myotubes

Differentiated L6 myotubes were pre-treated with or without different leucine concentrations (0x, 0.5x,1x) for 24h and then incubated with insulin as noted for 1h or equivalent volume of vehicle control. A) phospho/ total 4E-BP1 ratio, B) example western blots C) phosphorylated 4E-BP1 and D) total 4E-BP1. Results are mean± SEM for n=3 wells for each treatment group. A: $p<0.001$ for insulin only, C: $p<0.001$ for insulin only; D: $p=0.973$, insulin x leucine; $p=0.838$, leucine; $p=0.619$, insulin



24h B	0leu 0.5leu 1leu 0 ins x leu 0.5 ins x leu 1 ins x leu
Phosphorylated P70s6k	
Total P70s6k	



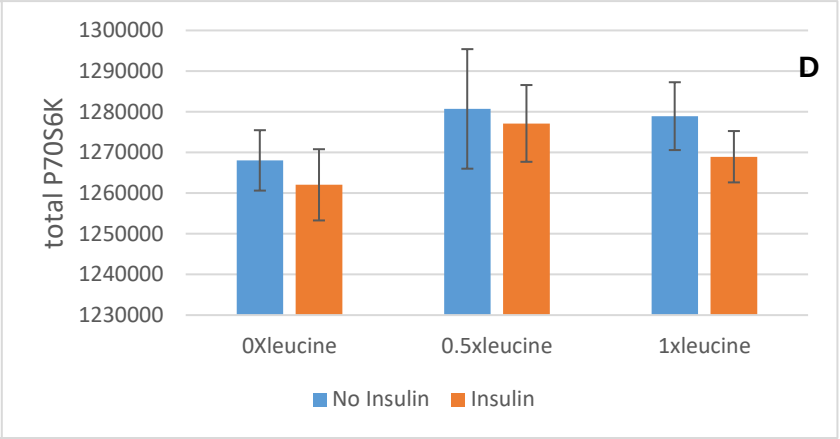
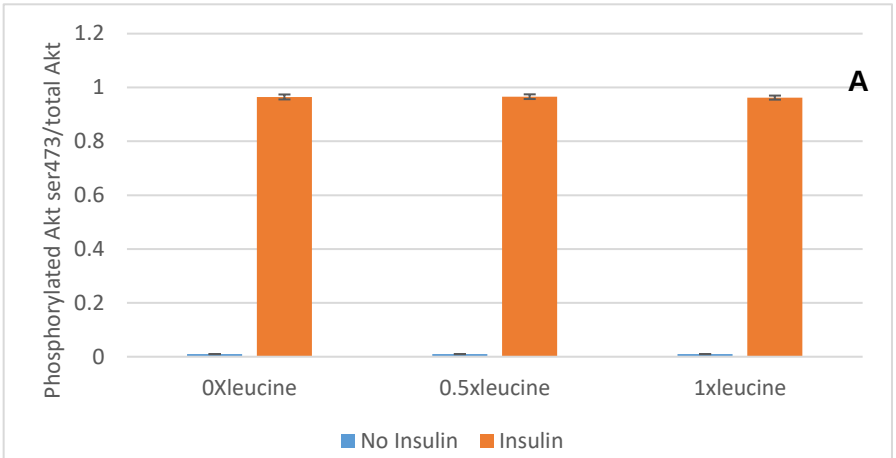
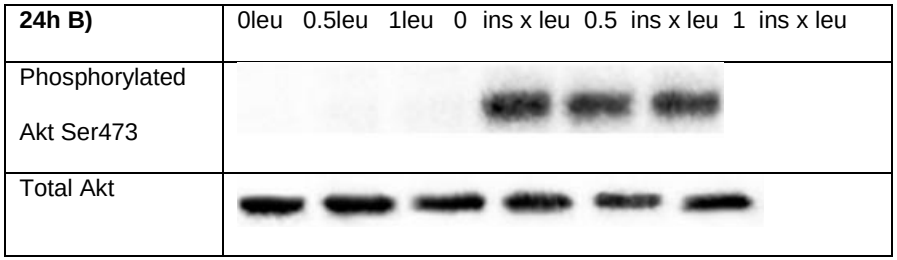
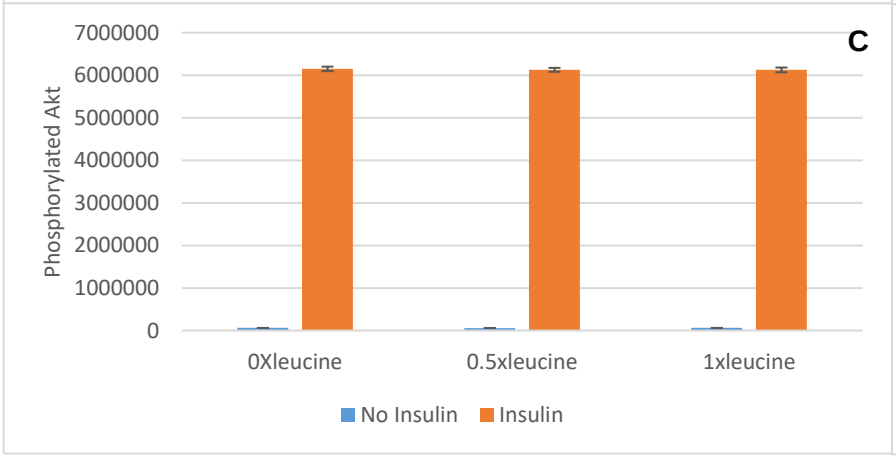


Figure 9.11 Effects of 24 hours treatment with different concentrations of leucine +/- 1 hour insulin on p70S6K activity in L6 myotubes

Differentiated L6 myotubes were pre-treated with or without different leucine concentrations (0x, 0.5x,1x) for 24h and then incubated with insulin as noted for 1h or equivalent volume of vehicle control. A) phospho/ total p70S6K ratio, B) example western blots C) phosphorylated p70S6K and D) total p70S6K. Results are mean± SEM for n=3 wells for each treatment group. A: $p<0.001$ for insulin only, C: $p<0.001$ for insulin only, D: $p=0.944$, insulin x leucine; $p=0.369$, leucine; $p=0.419$, insulin







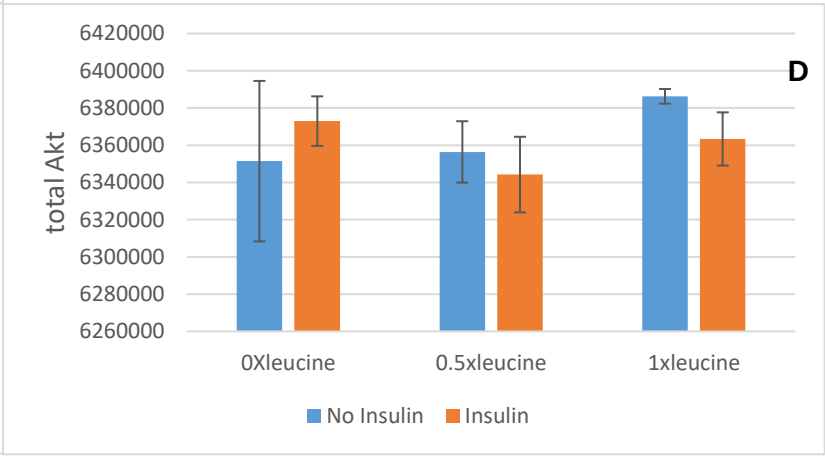
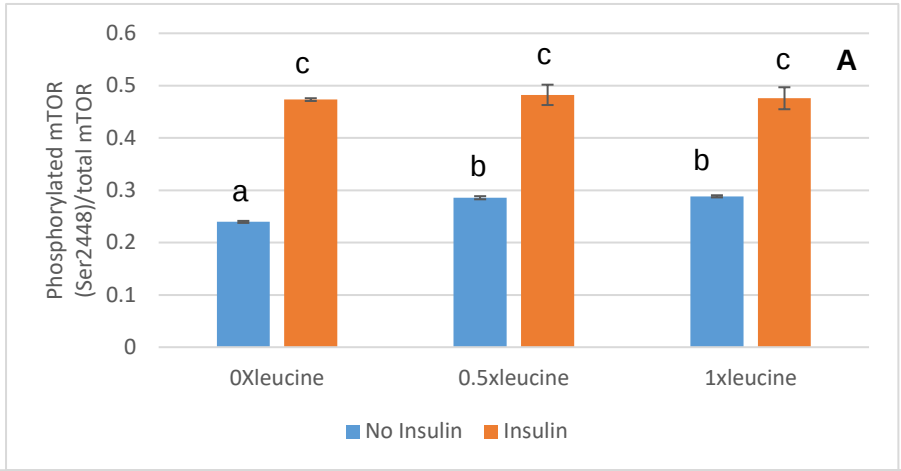
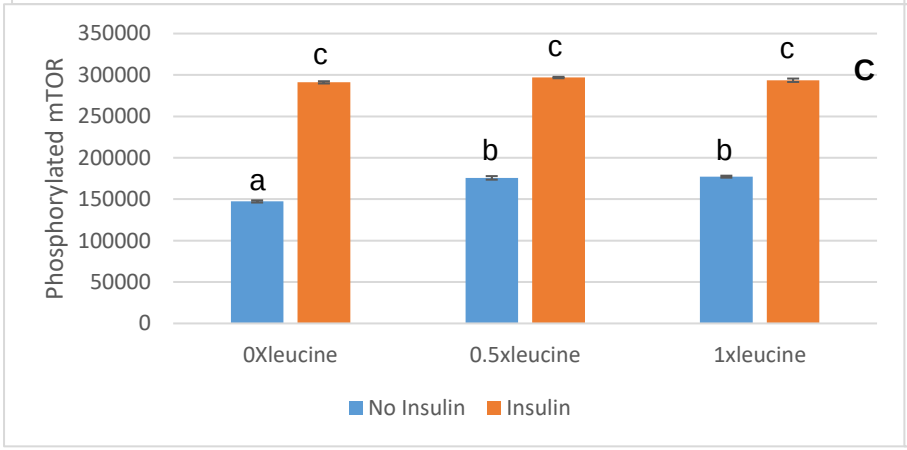


Figure 9.12 Effects of 24 hours treatment with different concentrations of leucine +/- 1 hour insulin on Akt activity in L6 myotubes

Differentiated L6 myotubes were pre-treated with or without different leucine concentrations (0x, 0.5x,1x) for 24h and then incubated with insulin as noted for 1h or equivalent volume of vehicle control. A) phospho/ total Akt ratio, B) example western blots C) phosphorylated Akt and D) total Akt. Results are mean± SEM for n=3 wells for each treatment group. A: $p<0.001$ for insulin only C: $p<0.001$ for insulin only; D: $p=0.592$, insulin x leucine; $p=0.558$, leucine; $p=0.807$, insulin



48h B	0leu 0.5leu 1leu 0 ins x leu 0.5 ins x leu 1 ins x leu
Phosphorylated mTOR (Ser2448)	
Total mTOR	



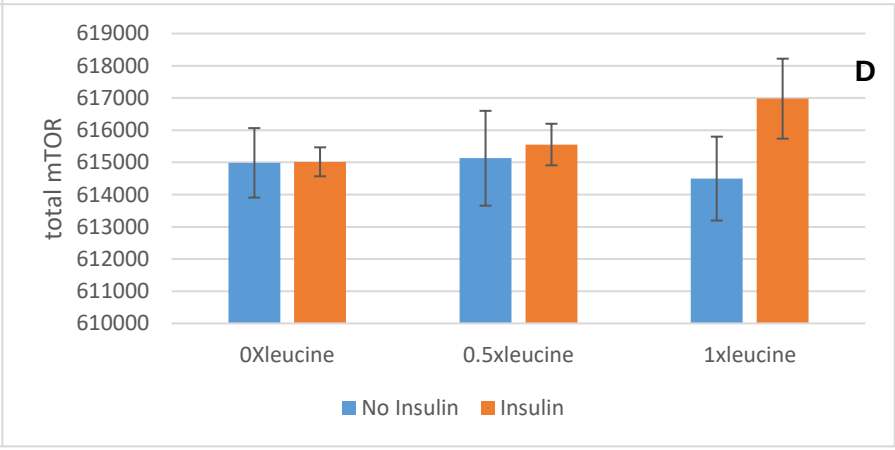
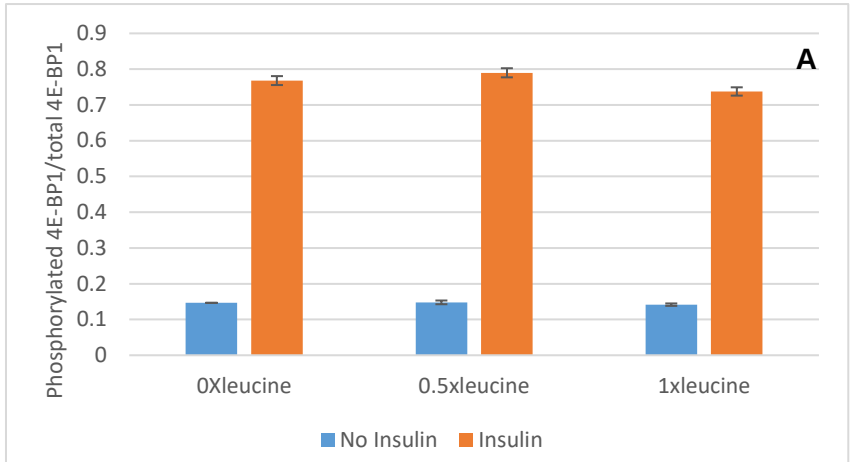
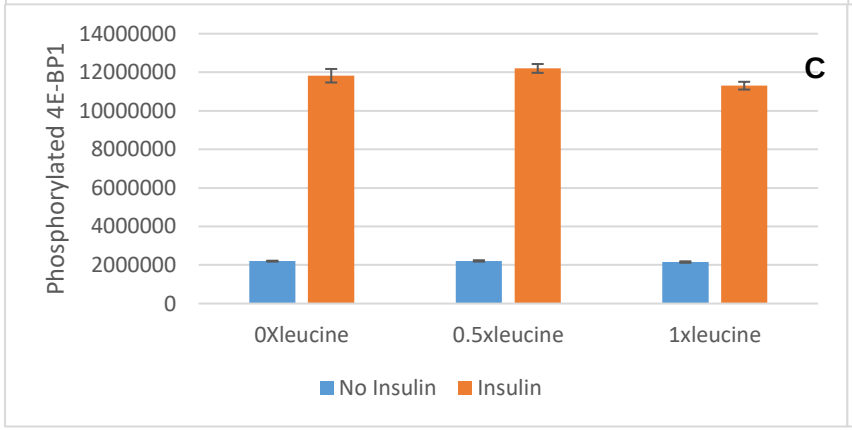


Figure 9.13 Effects of 48 hours treatment with different concentrations of leucine +/- 1 hour insulin on mTOR activity in L6 myotubes

Differentiated L6 myotubes were pre-treated with or without different leucine concentrations (0x, 0.5x,1x) for 48h and then incubated with insulin as noted for 1h or equivalent volume of vehicle control. A) phospho/ total mTOR ratio, B) example western blots C) phosphorylated mTOR and D) total mTOR. Results are mean± SEM for n=3 wells for each treatment group. A: $p<0.001$ insulin x leucine; C: $p<0.001$ insulin x leucine; D: $p=0.506$ insulin x leucine; $p=0.801$, leucine; $p=0.294$, insulin. Means with the same letter are not different ($p>0.05$ for Bonferroni), whereas those with different letters are significantly different ($p<0.05$ for Bonferroni)



48h B	0leu	0.5leu	1leu	0 ins x leu	0.5 ins x leu	1 ins x leu
Phosphorylated 4E-BP1 (Thr37/46)						
Total 4E-BP1						



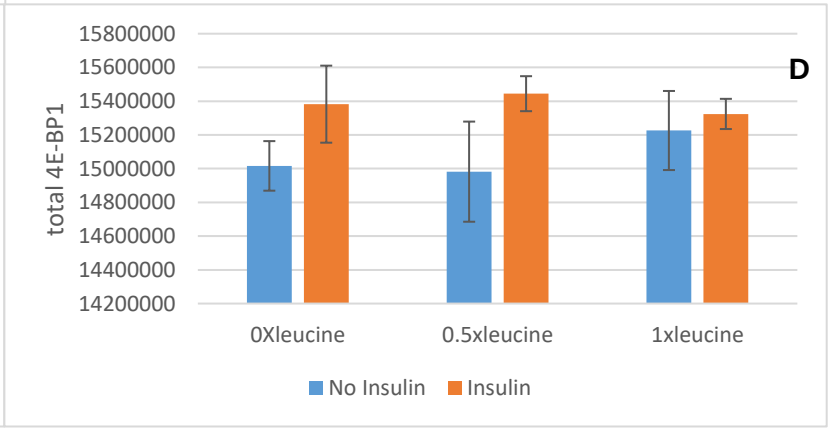
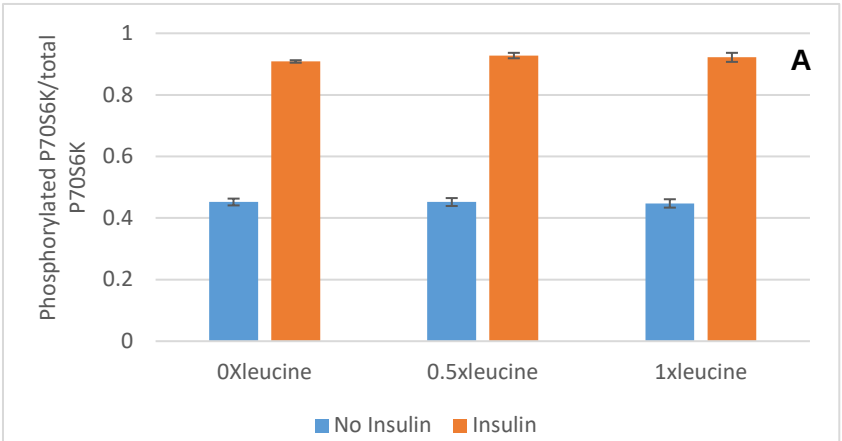
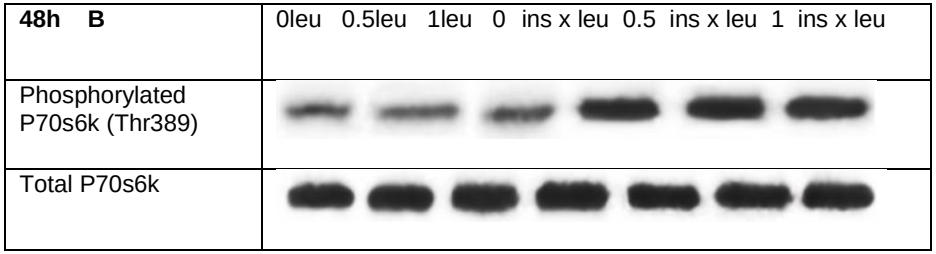
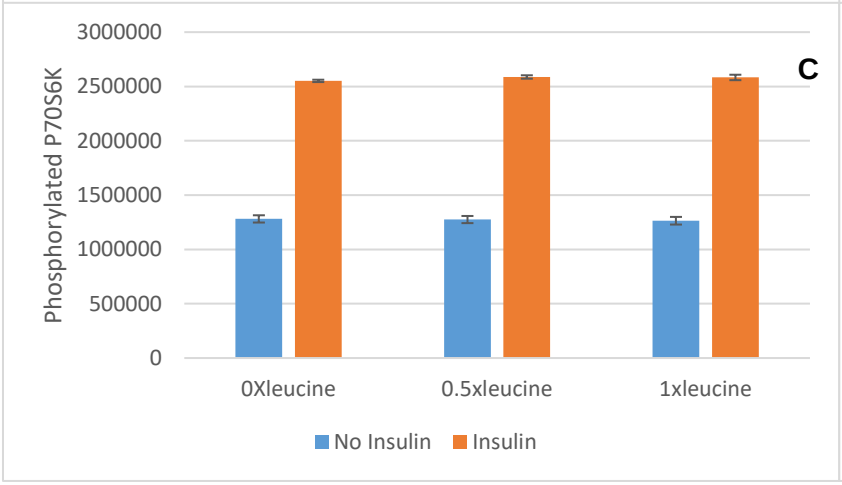


Figure 9.14 Effects of 48 hours treatment with different concentrations of leucine +/- 1 hour insulin on 4E-BP1 activity in L6 myotubes

Differentiated L6 myotubes were pre-treated with or without different leucine concentrations (0x, 0.5x,1x) for 48h and then incubated with insulin as noted for 1h or equivalent volume of vehicle control. A) phospho/ total 4E-BP1 ratio, B) example western blots C) phosphorylated 4E-BP1 and D) total 4E-BP1. Results are mean± SEM for n=3 wells for each treatment group. A: $p<0.001$ for insulin only, $p=0.022$ for leucine only C: $p<0.001$ for insulin only; D: $p=0.646$, insulin x leucine; $p=0.921$, leucine; $p=0.0.08$, insulin.







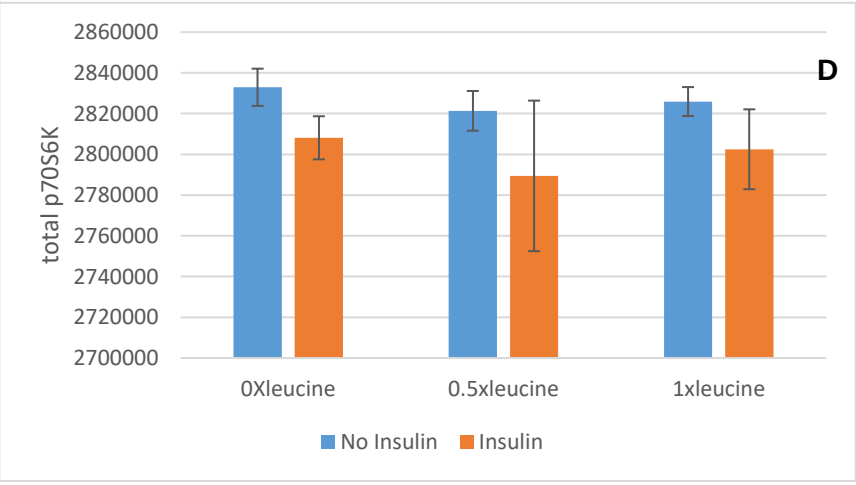
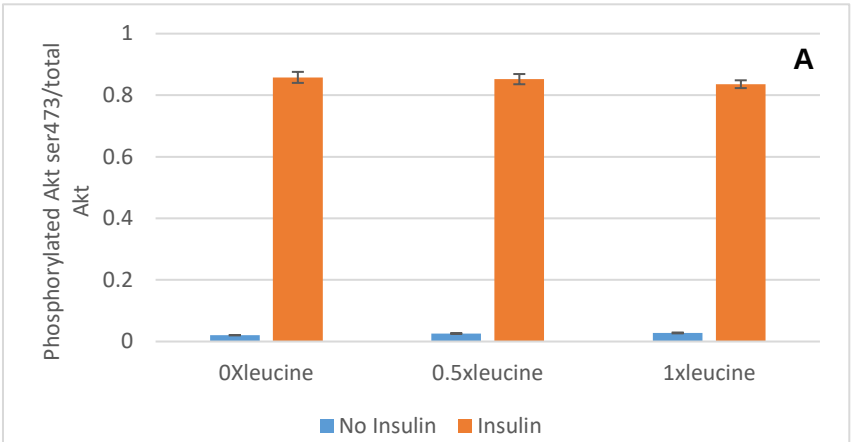
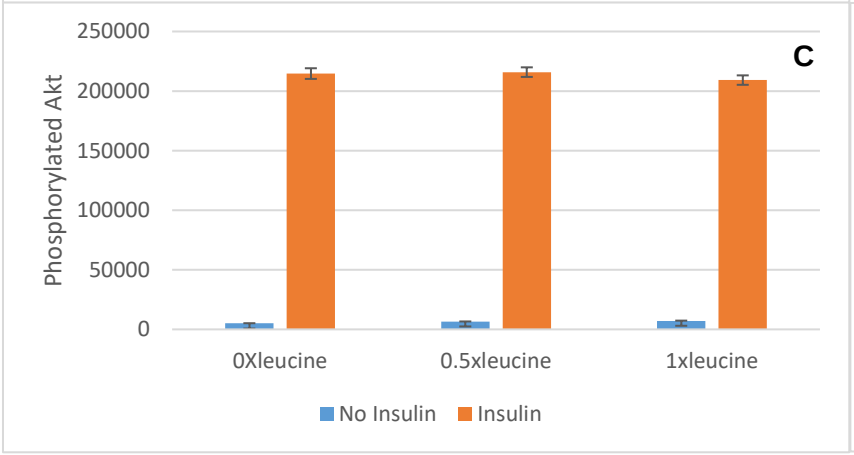


Figure 9.15 Effects of 48 hours treatment with different concentrations of leucine +/- 1 hour insulin on p70S6K activity in L6 myotubes

Differentiated L6 myotubes were pre-treated with or without different leucine concentrations (0x, 0.5x,1x) medium for 48h and then incubated with insulin as noted for 1h or equivalent volume of vehicle control. A) phospho/ total p70S6K ratio, B) example western blots C) phosphorylated p70S6K and D) total p70S6K. Results are mean± SEM for n=3 wells for each treatment group. A: $p<0.001$ for insulin only C: $p<0.001$ for insulin only; D: $p=0.971$, insulin x leucine; $p=0.724$, leucine; $p=0.105$, insulin



48h B)	0leu 0.5leu 1leu 0 ins x leu 0.5 ins x leu 1 ins x leu
Phosphorylated Akt Ser473	
Total Akt	



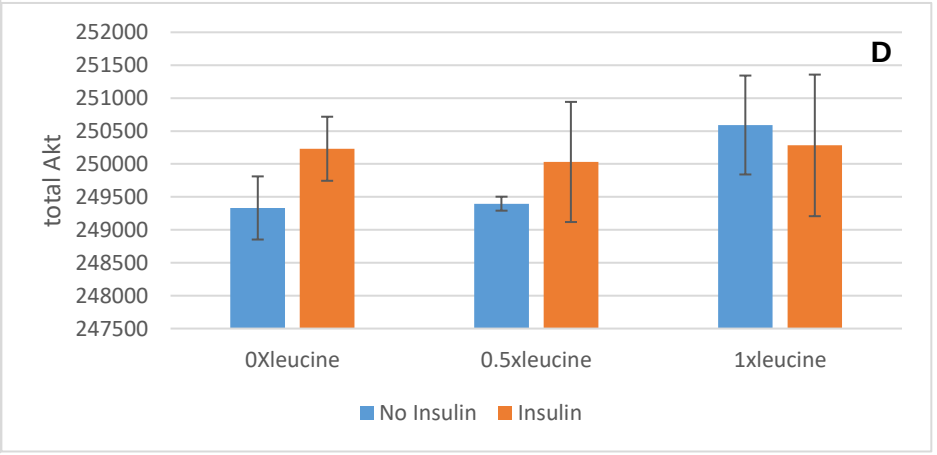


Figure 9.16 Effects of 48 hours treatment with different concentrations of leucine +/- 1 hour insulin on Akt activity in L6 myotubes

Differentiated L6 myotubes were pre-treated with or without different leucine concentrations (0x, 0.5x,1x) for 48h and then incubated with insulin as noted for 1h or equivalent volume of vehicle control. A) phospho/ total Akt ratio, B) example western blots C) phosphorylated Akt and D) total Akt. Results are mean± SEM for n=3 wells for each treatment group. A: $p<0.001$ for insulin only C: $p<0.001$ for insulin only; D: $p=0.679$, insulin x leucine; $p=0.549$, leucine; $p=0.496$, insulin

The repeat experiments of BCAA 24/48 and C2C12 glucose uptake 24/48 are not very consistent with previous results.

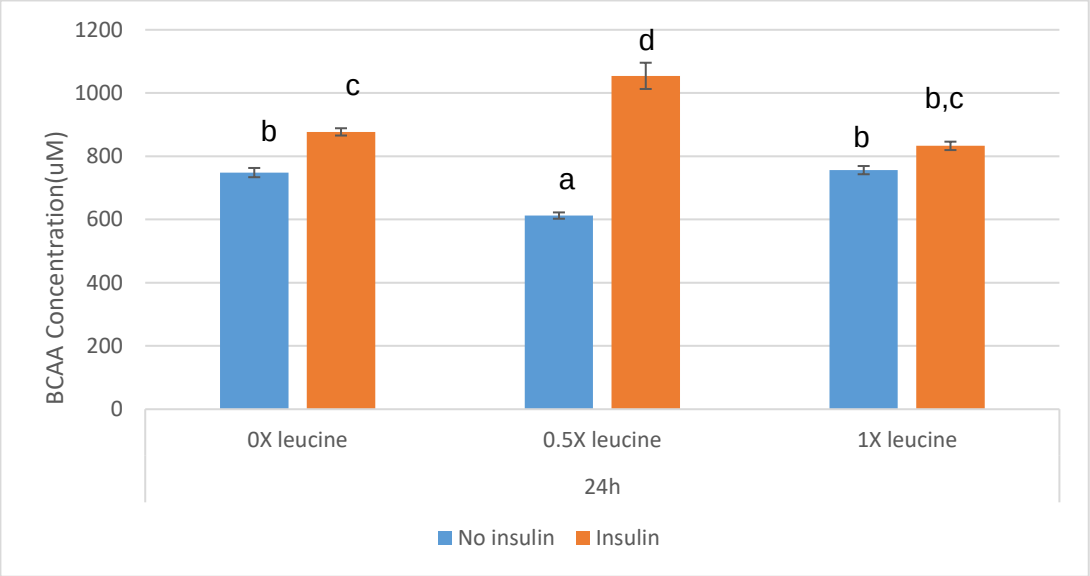


Figure 9.17 Effects of 24 hours treatment with different concentrations of leucine +/- 1 hour insulin on intracellular BCAA concentrations in L6 myotubes

Differentiated L6 myotubes were pre-treated with or without different leucine concentrations (0x, 0.5x,1x) for 24h and then incubated with insulin as noted or equivalent volume of vehicle control for 1h before measurement of intracellular BCAA concentrations. Results are mean± SEM for n=3 wells for each treatment group. $p<0.001$ insulin x leucine. Means with the same letter are not different ($p>0.05$ for Bonferroni), whereas those with different letters are significantly different ($p<0.05$ for Bonferroni)

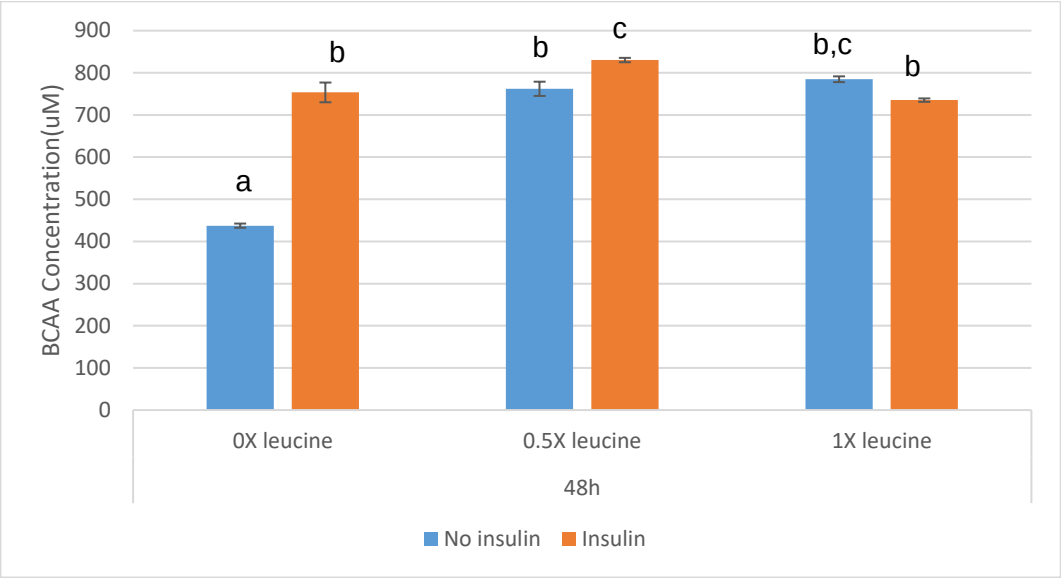


Figure 9.18 Effects of 48 hours treatment with different concentrations of leucine +/- 1 hour insulin on intracellular BCAA concentrations in L6 myotubes

Differentiated L6 myotubes were pre-treated with or without different leucine concentrations (0x, 0.5x,1x) for 48h and then incubated with insulin as noted or equivalent volume of vehicle control for 1h before measurement of intracellular BCAA concentrations. Results are mean± SEM for n=3 wells for each treatment group. $p<0.001$ insulin x leucine. Means with the same letter are not different ($p>0.05$ for Bonferroni), whereas those with different letters are significantly different ($p<0.05$ for Bonferroni)

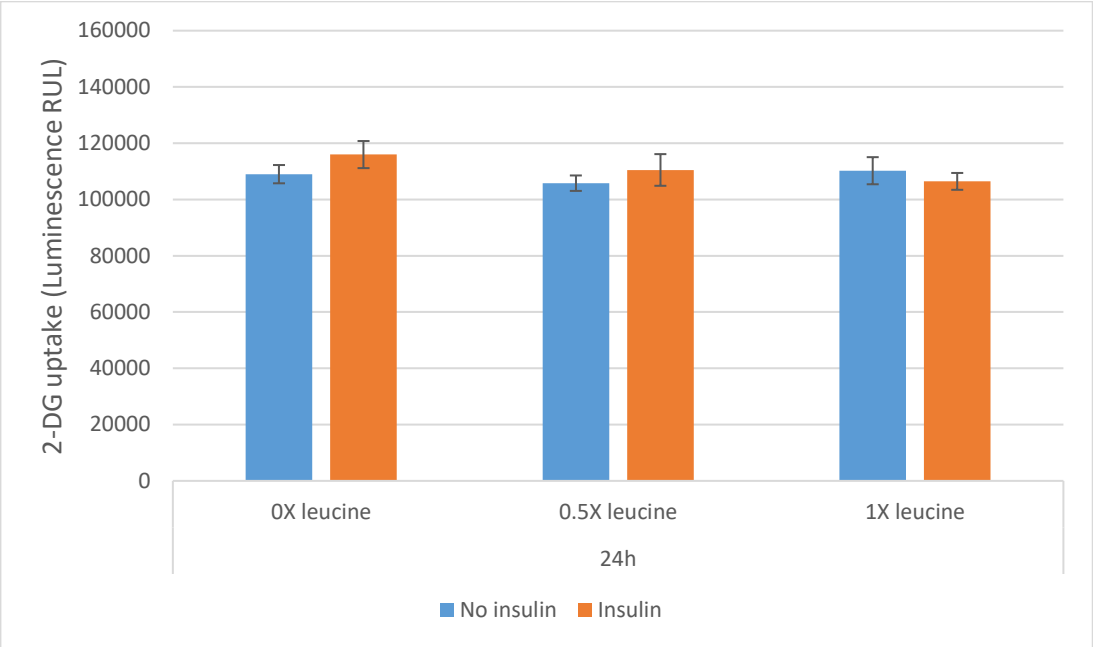


Figure 9.19 Effects of 24 hours treatment with different concentrations of leucine +/- 1 hour insulin on glucose uptake in C2C12 myotubes

Differentiated C2C12 myotubes were pre-treated with or without different leucine concentrations (0x, 0.5x,1x) for 24h and then incubated with insulin as noted or equivalent volume of vehicle control for 1h before measurement of 2-DG uptake. Results are mean± SEM for n=6 wells for each treatment group. p=0.395, insulin x leucine; p=0496, leucine; p=0.439, insulin

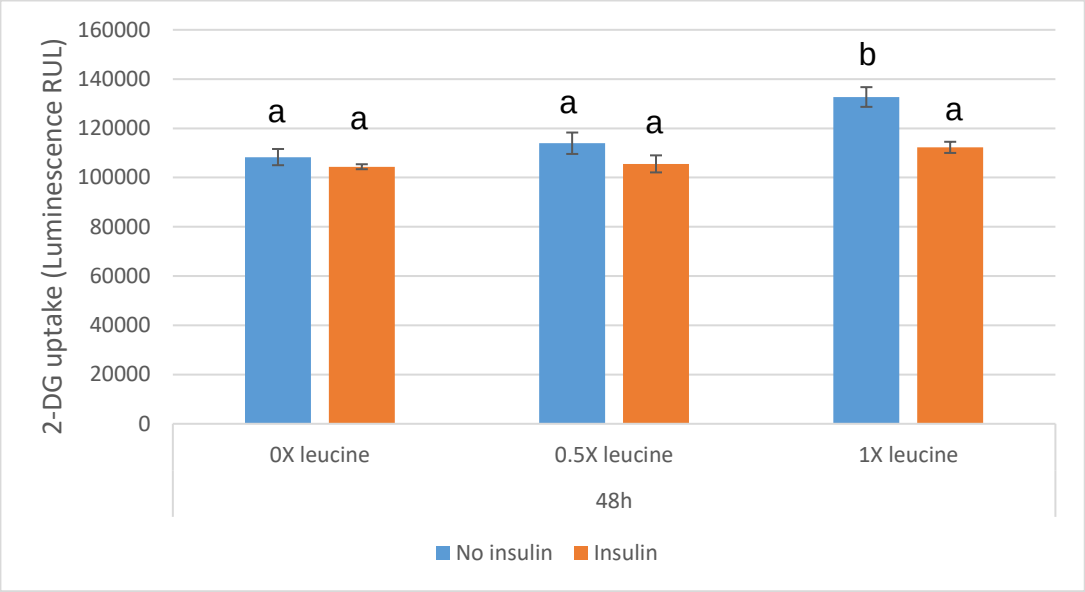


Figure 9.20 Effects of 48 hours treatment with different concentrations of leucine +/- 1 hour insulin on glucose uptake in C2C12 myotubes

Differentiated C2C12 myotubes were pre-treated with or without different leucine concentrations (0x, 0.5x, 1x) for 48h and then incubated with insulin as noted or equivalent volume of vehicle control for 1h before measurement of 2-DG uptake. Results are mean± SEM for n=6 wells for each treatment group. p=0.045 insulin x leucine. Means with the same letter are not different (p>0.05 for Bonferroni), whereas those with different letters are significantly different (p<0.05 for Bonferroni)